

A004844

15
AFFDL-TR-72-83

Volume II

PREDICTION OF SIX-DEGREE-OF-FREEDOM STORE SEPARATION TRAJECTORIES AT SPEEDS UP TO THE CRITICAL SPEED

Volume II - Users Manual for the Computer Programs

NIELSEN ENGINEERING & RESEARCH, INC.

// TR-37 vol 2

TECHNICAL REPORT AFFDL-TR-72-83, VOLUME II

OCTOBER 1974

Approved for public release; distribution unlimited.

AE AIR FORCE FLIGHT DYNAMICS LABORATORY
AIR FORCE SYSTEMS COMMAND
WRIGHT-PATTERSON AIR FORCE BASE, OHIO 45433

NOTICE

When Government drawings, specifications, or other data are used for any purpose other than in connection with a definitely related Government procurement operation, the United States Government thereby incurs no responsibility nor any obligation whatsoever; and the fact that the Government may have formulated, furnished, or in any way supplied the said drawings, specifications, or other data, is not to be regarded by implication or otherwise as in any manner licensing the holder or any other person or corporation, or conveying any rights or permission to manufacture, use, or sell any patented invention that may in any way be related thereto.

Copies of this report should not be returned unless return is required by security considerations, contractual obligations, or notice on a specific document.

PREDICTION OF SIX-DEGREE-OF-FREEDOM
STORE SEPARATION TRAJECTORIES AT
SPEEDS UP TO THE
CRITICAL SPEED

Volume II - Users Manual for the
Computer Programs

Frederick K. Goodwin
Marnix F. E. Dillenius

Approved for public release; distribution unlimited.

FOREWORD

This report, "Prediction of Six-Degree-of-Freedom Store Separation Trajectories at Speeds up to the Critical Speed," describes a combined theoretical-experimental program directed toward developing a computer program for predicting the trajectory of an external store separated from an aircraft of the fighter-bomber type at speeds up to the critical speed. Volume I, "Theoretical Methods and Comparisons with Experiment," describes the theoretical approach and presents extensive comparisons with experimental data. This volume, Volume II - "Users Manual for the Computer Programs," presents detailed instructions on the use of the computer programs.

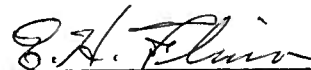
The work was carried out by Nielsen Engineering & Research, Inc., 510 Clyde Avenue, Mountain View, California 94043, under Contract No. F33615-71-C-1116. The contract was initiated under Project 8219, Task 821902, of the Air Force Flight Dynamics Laboratory. The Air Force Project Engineer on the contract was Jerry E. Jenkins, AFFDL/FGC. The report number assigned by Nielsen Engineering & Research, Inc. is NEAR TR 41.

The authors wish to thank Mr. Jenkins for his assistance during the course of the investigation. The computer program card decks are available upon request from Mr. Jenkins. His address is AFFDL/FGC, Wright-Patterson AFB, Ohio, 45433.

The work documented in this report was started on December 11, 1970 and was effectively concluded with the submission of this report. The report was submitted by the authors in June 1972.

This technical report has been reviewed and is approved for publication
FOR THE COMMANDER


JERRY E. JENKINS
Project Engineer
Flight Control Division


E. H. FLINN, Chief
Control Criteria Branch
Flight Control Division

ABSTRACT

Detailed instructions are presented for using two computer programs which calculate the six-degree-of-freedom trajectories of external stores which are separated from fighter-bomber type aircraft at speeds up to the critical speed. Single and multiple store configurations can be handled by the programs. The first program calculates the source distributions which represent the volume distributions of the fuselage, store(s), and ejector rack if one is present. The second program uses a lifting surface theory to determine a vorticity distribution which represents the wing and pylon loading and calculates the trajectory of the ejected store. This report describes the two programs, presents instructions for preparing input for the programs, describes the output from each program, and presents sample cases.

TABLE OF CONTENTS

<u>Section</u>	<u>Page No.</u>
1. INTRODUCTION	1
2. GENERAL DESCRIPTION OF THE USE OF THE PROGRAMS	3
2.1 Source Distribution Program	3
2.2 Trajectory Program	4
2.2.1 Input section	4
2.2.2 Vortex-lattice section	6
2.2.3 Trajectory section	6
3. SOURCE DISTRIBUTION PROGRAM	8
3.1 General Description of Program	8
3.2 Input Data	9
3.2.1 Input format	9
3.2.2 Sample input data	11
3.3 Output from the Program	14
4. SIX-DEGREE-OF-FREEDOM TRAJECTORY PROGRAM	15
4.1 General Description of Program	15
4.2 Input Data	19
4.2.1 Input format	19
4.2.2 Sample input data	35
4.3 Output from the Program	40
4.3.1 Sample trajectory - case 1	40
4.3.2 Sample trajectory - case 2	43
5. PROGRAM RUNNING TIMES	43
TABLES I AND II	45
FIGURES 1 THROUGH 23	48
APPENDIX I - DETAILS OF SOURCE DISTRIBUTION PROGRAM	127
APPENDIX II - DETAILS OF TRAJECTORY PROGRAM	137
REFERENCES	246

LIST OF ILLUSTRATIONS

<u>Figure</u>	<u>Page No.</u>
1. Listing of source-distribution program.	48
2. General flow chart of source distribution program	50
3. Source distribution program input format.	51
4. Sample input data for source distribution program.	52
5. Wind-tunnel models used in sample calculations.	53
6. Ogive-cylinder store source distribution output.	58
7. Fuselage source distribution output.	59
8. Small boattail store source distribution output.	60
9. Triple ejector rack source distribution output.	61
10. Listing of six-degree-of-freedom trajectory program.	62
11. General flow chart of trajectory program.	83
12. Trajectory program input format.	86
13. Specification of wing location relative to fuselage nose and incidence angle.	93
14. Example wing.	94
15. Variables describing and locating pylon, input data item number 17.	95
16. Configuration for sample trajectory number 1.	96
17. Input data for sample trajectory calculation number 1.	97
18. Configuration for sample trajectory number 2.	99
19. Input data for sample trajectory calculation number 2.	100
20. Trajectory program output for sample case 1.	102
21. Coordinate systems fixed in separated store and used in forces and moment calculation.	113
22. Coordinate systems used in trajectory calculation.	114
23. Trajectory program output for sample case 2.	115

LIST OF SYMBOLS

a_{\max}	maximum store body radius
c	local wing chord
c_{d_c}	section drag coefficient of a circular cylinder normal to airstream
C_A	axial-force coefficient, axial force/ $q_{\infty_s} S_R$
C_ℓ	rolling-moment coefficient, rolling moment/ $q_{\infty_s} S_R \ell_R$
C_m	pitching-moment coefficient, pitching moment/ $q_{\infty_s} S_R \ell_R$
C_n	yawing-moment coefficient, yawing moment/ $q_{\infty_s} S_R \ell_R$
C_N	normal-force coefficient, normal force/ $q_{\infty_s} S_R$
C_Y	side-force coefficient, side force/ $q_{\infty_s} S_R$
d	maximum diameter of store
I_{xx}, I_{yy}, I_{zz}	moments of inertia about x, y, z axes of figure 21; taken about store moment center
ℓ	store length
ℓ_R	reference length; store maximum diameter, d
M_∞	aircraft free-stream Mach number
p, q, r	rotational velocities about x, y, z axes of figure 21; positive as shown in figure 22
q_∞	free-stream dynamic pressure; $1/2 \rho_\infty V_\infty^2$
q_{∞_s}	ejected store free-stream dynamic pressure; $1/2 \rho_\infty V_{\infty_s}^2$
Q	strength of a point source
Q^*	$Q/4\pi \ell^2 V_\infty$
r	body radius
s	semispan of wing

S_R	reference area taken equal to body frontal area, πa_{\max}^2
t	time
U_s, V_s, W_s	total velocities as seen by store, positive in x_s, y_s, z_s
V_∞	aircraft free-stream velocity
V_{∞_s}	separated store free-stream velocity
x, y, z	coordinate system in compressible space
x', y', z'	coordinate system in incompressible space
x_B, y_B, z_B	coordinate system fixed in fuselage with the origin at nose, see figure 13
x_ℓ, z_ℓ	coordinate system fixed in local airfoil section of twisted wing, see figure 15(b), with x_ℓ lying along chord line
x_s, y_s, z_s	coordinate system in compressible space fixed in separated store with origin at store nose (fig. 21)
x_w, y_w, z_w	coordinate system fixed in wing with origin at root-chord leading edge, see figure 14
α_ℓ	local angle of attack due to wing twist and camber
Γ	strength of a horseshoe vortex
θ	local slope of wing thickness envelope
ξ, η, ζ	inertial coordinate system fixed in fuselage nose, positive forward along longitudinal axis, positive laterally to the right, and positive vertically downward respectively, see figure 22
ρ_∞	free-stream mass density
Ψ, θ, ϕ	store yaw, pitch and roll angles specifying angular orientation of store x, y, z coordinate system relative to ξ, η, ζ inertial system, see figure 22

PREDICTION OF SIX-DEGREE-OF-FREEDOM STORE SEPARATION
TRAJECTORIES AT SPEEDS UP TO THE CRITICAL SPEED

Volume II - Users Manual for the
Computer Program

1. INTRODUCTION

The purpose of this volume of the report is to describe and present instructions for using the two computer programs developed in conjunction with the theoretical work presented in Volume I, reference 1. The programs as described in this report have been run on both the CDC 6600 and Univac 1108 computers. The programs should run with very little, if any, modification on other computers with large enough memory capacity. The largest of the two programs requires approximately 110,000 octal words of core storage. No tapes, drums, or disks are used by either program. All input to the programs is from cards and all output is printed.

The two programs are

- (1) Source distribution program
- (2) Six-degree-of-freedom trajectory program

The source-distribution program is used to obtain source-sink distributions to represent the fuselage, rack, and store volumes. The trajectory program uses these source-sink distributions and additional information to first determine the vorticity distribution which represents the wing-pylon loading including interference of the fuselage, rack, and stores and then to calculate the store trajectory.

The next sections of this report will describe in more detail the general use of the programs and then present instructions for preparing the input data and interpreting the output. Details of the two programs are contained in two appendices.

The method of describing the aircraft components, the aircraft operational parameters, and the dynamical characteristics of the stores are of importance. The various parameters which are included in the computer program are

Wing Panels

Thickness distribution: Specified at large number of chordwise locations and at the same number of spanwise locations as used in the vortex lattice which represents the wing as a lifting surface.

Mean camber surface: May have both twist and camber.

Leading-edge shape: Represented by straight line segments of differing sweep.

Trailing-edge shape: Also represented by straight line segments of differing sweep.

Taper: Controlled by shape of leading and trailing edges.

Dihedral: Variable across wing panel.

Fuselage

Shape: Body of revolution.

Pylon

Thickness distribution: Same method of description as for wing panel.

Mean camber surface: Planar.

Orientation: Vertical and streamwise.

Leading-edge shape: Straight but can be swept.

Trailing-edge shape: Straight but can be swept.

Taper: Uniform taper.

Tip: Parallel to pylon root chord.

Number: One pylon per wing panel.

Rack

Shape: Body of revolution.

Stores

Shape: Body of revolution.

Number of stores: Ten, either singly or in MER or TER configurations.

Attached orientation: Initial pitch angle arbitrary, initial yaw angle zero.

Empennage: Planar or cruciform empennage.

Initial roll orientation: Arbitrary.

Power: Unpowered.

Airplane Operating Characteristics

Flight path: Straight but not necessarily horizontal.

Flight velocity: Constant.

Density: Constant.

Angle of attack: Constant.

Yaw angle: Zero.

Store Inertial Characteristics

Moments of inertia: Constant.

Products of inertia: Constant.

Center of gravity position: Not necessarily on store longitudinal axis.

Store Ejection Conditions

Initial velocity: In vertical plane normal to store longitudinal axis.

Initial pitching velocity: Arbitrary.

Initial yawing velocity: Zero.

Initial rolling velocity: Zero.

2. GENERAL DESCRIPTION OF THE USE OF THE PROGRAMS

The computer program which has been written to calculate the trajectory of a store separated from an aircraft consists of two programs, an axisymmetric source distribution program and a trajectory program. The calculation of the source distributions to represent the various axisymmetric bodies has been kept separate for two reasons. First, a number of runs may have to be made with the program to obtain a source distribution which adequately reproduces the shape of the body. The second reason is that once the source distribution is obtained for a specific Mach number it need not be recalculated since for a given body shape the distribution is only a function of Mach number.

2.1 Source Distribution Program

For a given aircraft-stores combination and Mach number, source distributions must be obtained for the fuselage, each different store shape, and the ejection rack if one is present. The actual shape of each body, made dimensionless by the length, must be approximated by a body of

revolution and specified by a series of segmented polynomials. If the body has a blunt base, the wake must be modeled by extending the body until it closes. If compressibility is to be accounted for in the vortex lattice and trajectory calculations, that is, the Mach number, M_∞ , is not to be specified as zero, then source distributions must be obtained for each Mach number of interest. The program determines the equivalent incompressible body by applying the transformation given by equation (1) of reference 1. The compressibility correction stretches the body by $1/\sqrt{1 - M_\infty^2}$. In the trajectory calculation an aircraft velocity must be specified. This need not be consistent with the Mach number so that for low flight speeds the Mach number zero shapes can be used. The program calculates and prints the source locations and strengths. These quantities are used as input data to the trajectory program.

2.2 Trajectory Program

After the source distributions which represent the volume distributions of the fuselage, all of the stores, and the rack, if one is present, have been determined the trajectory program is ready to be run. This program consists of three main sections. The first section reads in the input data and calculates quantities from these data, the second section solves for the vorticity distribution which represents the wing-pylon loading, and the third section calculates the trajectory.

2.2.1 Input section

The input section of the program reads in the following information

- (1) Aircraft flight conditions
- (2) Indices specifying what aircraft components are present
- (3) Fuselage data
- (4) Wing data
- (5) Pylon data
- (6) Rack data
- (7) Store data

The aircraft flight conditions, item (1) above, which can be varied are the angle of attack, flight path angle, Mach number, free-stream air density, and flight velocity. The Mach number must be consistent with that used to calculate the source distributions.

Item (2) consists of four indices. The first three specify whether or not the fuselage, pylon, and rack are present and the fourth specifies the number of stores. The program in its present form will handle a maximum of ten stores. This limit is imposed by dimension statements in the program and could be changed.

The fuselage input data consist of the length, maximum radius, and source distribution.

The wing input data locate the wing relative to the fuselage, including its incidence, and supply information required to lay out the vorticity and thickness distributions. The data also include the twist and camber distribution and the slope distribution of the thickness envelope. The wing leading and trailing edges can have breaks in sweep. The wing dihedral angle does not have to be constant over the semispan.

Similarly, the pylon input data locate the pylon from which the store is to be separated and provide information required to lay out the vorticity and thickness distributions. The pylon is located laterally relative to the fuselage centerline and longitudinally relative to the leading edge of the local wing chord. The data also include the slope distribution of the thickness envelope. The pylon cannot have twist or camber. The leading and trailing edges can be swept at constant but different sweep angles.

The rack, if one is present, is located immediately below the pylon. The input data for the rack locate its nose relative to the local wing chord and specify its incidence relative to the wing root chord. In addition, the rack length, maximum radius, and source distribution are input.

Data are input for each store present on the aircraft which assigns a store number and specifies a shape number, the length, and the maximum radius. Each store is located by specifying its lateral position relative to the wing root chord and the longitudinal and vertical position of the store nose relative to the wing chord immediately above the store. The incidence of the store relative to the wing root chord is also specified. A source distribution is input for each different store shape. Data should be input for all stores close enough to the store being separated to affect its trajectory. The separated store must be under the fuselage centerline or to the left of this line as seen by the pilot. For store-to-store

interference calculations, the program does not assume that the same stores exist to the right. Thus data must be input for stores on that side if they are close enough to affect the trajectory. The vortex-lattice calculation requires left to right symmetry. Thus, for this calculation the program ignores all stores input to the right of the fuselage centerline and assumes all stores input on the left side exist on the right.

2.2.2 Vortex-lattice section

The second main section of the program calculates the wing-pylon vorticity distribution. This is done using equations (6) and (7) of section 4.2.2 of reference 1. Before performing this calculation all of the aircraft components are located relative to the fuselage and then the entire configuration is transformed into an equivalent incompressible one using equation (1) of reference 1. The coefficient matrix is then calculated and the right-hand side is determined. Finally, the strengths of the vortices are calculated by solving the set of simultaneous equations.

2.2.3 Trajectory section

The third and last main section of the trajectory program is the trajectory calculation which consists of the following steps

- (1) Input additional information to describe separated store
- (2) Input empennage data if store has one
- (3) Initialize for trajectory calculation
- (4) Calculate aerodynamic forces and moments
- (5) Calculate accelerations and rates of change of orientation angles
- (6) Integrate equations of motion
- (7) Repeat steps (4), (5), and (6) to end of trajectory

The additional data describing the store to be separated include indices specifying which store is to be separated, the number of segments the body is to be broken into for the force calculation, the flow separation location, and whether the store has an empennage. Also, the store mass and inertia characteristics are read in along with the location of the point about which the aerodynamic moments are to be calculated. This is the point about which the moments and products of inertia were calculated. The location of the store center of mass relative to this point is also specified as are the store axial-force coefficient and the value of the crossflow-drag coefficient to be used in the viscous crossflow force and moment calculation.

Three other indices are input which pertain to options included in the computer program. Provision has been made to include or exclude the damping terms in the velocity field calculation. Also, for stores with empennages, rolling moment may or may not be included in the acceleration determination. The third option pertains to the calculation of free-flight trajectories as opposed to captive-store trajectories as obtained in the wind tunnel. In wind-tunnel captive-store testing it is customary to change the store pitch and yaw angles to account for translational motion only while measuring the aerodynamic forces and moments. This changes its position in the nonuniform flow field. Provision has been made in the computer program to simulate this.

For a store with an empennage, additional quantities must be specified. These data are an index indicating whether the empennage is planar or cruciform, the tail-fin semispan, the average body radius in the tail-fin region, the initial roll orientation of the fins, and the lift-curve slope of the fins alone. In addition the axial position at which the forces are assumed to act must be specified.

In the trajectory initialization certain store separation conditions are specified. These are an initial translational velocity in the vertical plane containing the store longitudinal axis and an initial pitching velocity. The store axial and lateral velocities and yawing and rolling rotational velocities are initially zero.

The integration of the equations of motion is done by a standard numerical integration technique with the aerodynamic forces and moments calculated at each point required by the integration scheme. The calculation of the nonuniform velocity field and the resulting forces and moments is described in section 5 of reference 1.

For a given aircraft-store combination and Mach number, it can be seen that a series of trajectories can be run with only minor changes to the input data deck. For example, the aircraft angle of attack can be varied by changing one number on one card as can the aircraft flight path angle. The altitude can be varied by changing the free-stream density and possibly the free-stream velocity to account for changes in the speed of sound. Among other things easily varied are the store mass and inertia properties, center of gravity location, and ejection conditions.

Provision has also been made for restarting a trajectory. This is accomplished by changing one card which specifies the initial and final times and adding two cards specifying the current values of the dependent variables. These are tabulated in the output at each integration step.

3. SOURCE DISTRIBUTION PROGRAM

The purpose of this program is to calculate the source-sink distributions which are required to represent the volume distributions of the fuselage, rack, and stores. The actual body shapes must be approximated by bodies of revolution. The program consists of the main program and two subroutines called SHAPE and INVERS. A listing of the program is presented in figure 1 and a flow chart in figure 2.

The program listing in figure 1 is specifically for the CDC 6600 computer. To run the program on other machines such as the Univac 1108 the three unsequenced statements following sequence number SORAL 34 in the main program may have to be removed or changed.

3.1 General Description of Program

The flow chart of figure 2 shows that the first function that the program performs is to read in all the required input data and to print it out. Next the locations at which sources are to be placed are determined. The location of the first source is specified by the input data as is the distance between sources in terms of a fraction of the local body radius. Thus the location of each successive source is determined from the location of the previous one and the radius at that point. Subroutine SHAPE calculates the radius and local surface slope from the equations describing the body. The program in its present form will handle up to 100 sources. If it tries to lay out more than this number a message indicating this is printed and the calculation is terminated.

The program next determines the body radius and surface slope at the points on the body where the surface boundary condition is to be imposed. This is discussed in sections 4.1.2 of reference 2. The points are located axially midway between two adjacent sources. One location, which is just forward of the location at which the body first reaches its maximum thickness, is eliminated. Thus, the surface boundary condition is imposed at $(N-2)$ locations where N is the number of sources.

The next part of the program calculates the coefficient matrix and the right-hand side of the set of simultaneous equations to be solved for the source strengths. Equations (19) through (21) of reference 2 are used. Following this, subroutine INVERS is called to solve for the source strengths.

The last section of the program takes the source distribution just determined and calculates the shape of the body represented by it. This shape should be compared with the known shape and if the representation is inaccurate a new source distribution should be tried. This will be discussed further in section 3.2.1.

The shape given by the source distribution is obtained from the equation for the stream function, ψ^* , equation (14) of reference 2. Since one of the boundary conditions imposed is that the nose is a stagnation point the body shape will be given by the $\psi^* = 0$ line.

A detailed description of the main program and the two subroutines is presented in Appendix I.

3.2 Input Data

3.2.1 Input format

The format of the input data for the source distribution program is shown in figure 3. Three lines of information are shown for each item. The first line gives the program variable names. The second line shows the card column fields into which the data are to be punched, and the third line shows the FORTRAN format type. Data punched in I format are right justified in the field, whereas data in F format can be punched anywhere in the field. A decimal point should be included in F-type data.

Item number 1 is an index NCARDS which indicates how many cards of information are to follow to identify the run, item number 2. The value of NCARDS must be one or greater.

Item number 2 is a set of NCARDS cards containing hollerith information which may start and end anywhere on the card. The cards are reproduced in the output just as they are read in.

Item number 3 consists of one card with one index, NSECT, and the Mach number, FMACH. The index NSECT specifies the number of segmented polynomials being used to represent the body. The maximum value of NSECT is seven, that is,

$$1 \leq \text{NSECT} \leq 7$$

The next two items, items number 4 and 5, of input data are associated with the polynomials used to describe the body shape and the wake. The polynomial programmed in subroutine SHAPE is

$$\frac{r}{\ell} = c_1 + c_7 \sqrt{c_2 \left(\frac{x}{\ell}\right)^2 + c_3 \left(\frac{x}{\ell}\right) + c_4} + c_5 \left(\frac{x}{\ell}\right) + c_6 \left(\frac{x}{\ell}\right)^2 \quad (1)$$

where c_1 through c_7 are the coefficients, r is the local body radius, and ℓ is the body length. The source distributions must be calculated for shapes which are made dimensionless by the body length since the trajectory program is written assuming this to be the case. This length is the length of the body and does not include the additional length due to the addition of a wake.

The polynomials are for the actual body, not the equivalent $M_\infty = 0$ body. The equivalent incompressible body is determined by the program. The transformation given by equation (1) of reference 1 is applied to the actual shape. This transformation is

$$x' = \frac{x}{\sqrt{1 - M_\infty^2}}, \quad y' = y, \quad z' = z \quad (2)$$

Therefore the body is lengthened by a factor $1/\sqrt{1 - M_\infty^2}$.

As was mentioned previously, items number 4 and 5 on figure 3 are input data associated with the polynomials specifying the shape of the actual axisymmetric body. Item 4 consists of one card which contains the NSECT values of the end points of the polynomials describing the shape. The decimal point can be placed anywhere in the ten-column field.

Item number 5 on figure 3 is a set of NSECT cards specifying the values of the coefficients of the polynomials, equation (1). All seven coefficients are input even though many of them may be zero.

Item number 6 on figure 3 is the last card of input data. The eight quantities are

XSFSST	value of x/ℓ at which the first source is to be placed
XSLST	value of x/ℓ beyond which no source is to be placed

PERCR	fraction of the local body radius between sources
XRMAX	value of x/ℓ at which maximum radius or thickness is first reached
XINIT	initial value of x/ℓ at which body radius is to be calculated from source distribution
XFINAL	final value of x/ℓ at which body radius is to be calculated from source distribution
DELX	increment between points at which body radius is to be calculated from source distribution
RMAX	maximum value of r/ℓ of actual body

The first four quantities are used in calculating the source distribution. The values of XSFST and PERCR are important in obtaining a good representation of the body shape. The location of the first source, XSFST, controls how well the nose of the body is modeled. A value of 0.001 or 0.002 has been found to be satisfactory. If the value is too large, the nose will generally be blunter than desired. The correct value of PERCR is found by trial and error. A procedure which has been found to work quite well is to make a calculation with $PERCR = 1.0$. If the shape generated by the resulting source distribution is not adequate, that is, too large in diameter or contains ripples of undesirable magnitude, then PERCR should be decreased. If an excellent fit is obtained a larger value of PERCR should be tried. From the standpoint of computation time during the trajectory calculation, the number of sources should be minimized.

The value of XSLST must be at least 0.005 less than the length of the body. For blunt-based bodies which are extended to model a wake, the value must be at least 0.005 less than the x/ℓ of the end of the wake. The quantity XRMAX is self-explanatory.

The last four quantities on the last card pertain to the calculation of the shape represented by the source distribution. This shape is to be compared with the known body shape to determine the accuracy of the source distribution. Hence, a sufficiently small value of DELX should be used so that details of the calculated shape can be seen.

3.2.2 Sample input data

Four sets of sample input data for the source distribution program are shown in figure 4. These are data used to calculate source distributions to model the volume distributions of the various bodies used in the wind-

tunnel tests performed in conjunction with the present work. The various components of the wind-tunnel model are shown in figure 5.

Referring to figures 3 and 5(d), first consider the input data for the ogive-cylinder store shown in figure 4(a). The first card contains NCARDS, which is 2, and the next two cards are these two cards of identifying information. The next card contains NSECT and FMACH. The body, including its wake, is to be represented by three polynomials, NSECT = 3, of the type given by equation (1). The Mach number, FMACH, is 0.4. Examining figure 5(d) it is seen that the nose is an ogive 1.5 inches long so that it ends at (ℓ is the store length)

$$\frac{x}{\ell} = \frac{1.5}{6.375} = 0.2353$$

The cylindrical section ends at $x/\ell = 1.0$. To model the wake let us use the same shape as the nose. Therefore, the wake terminates at $x/\ell = 1.2353$. The end points of these three polynomials are contained on the next card, card 5 of figure 4(a).

The next three cards contain the coefficients of the polynomials for the three sections (see eq. (1)). The nose section is a circular arc so that when the following boundary conditions are imposed

$$\begin{aligned} \frac{x}{\ell} = 0 & & \frac{r}{\ell} = 0 \\ \frac{x}{\ell} = 0.2353 & & \frac{r}{\ell} = \frac{0.375}{6.375} = 0.05882 \\ \frac{x}{\ell} = 0.2353 & & \frac{dr}{dx} = 0 \end{aligned}$$

the equation of a circle gives

$$\frac{r}{\ell} = -0.4413 + \sqrt{-\left(\frac{x}{\ell}\right)^2 + 0.4706 \frac{x}{\ell} + 0.1947} \quad (3)$$

The cylindrical section runs from $x/\ell = 0.2353$ to $x/\ell = 1.0$ and in this region

$$\frac{r}{\ell} = 0.05882 \quad (4)$$

The wake is also a circular arc. By imposing the following three boundary conditions

$$\frac{x}{\ell} = 1.0 \qquad \frac{r}{\ell} = 0.05882$$

$$\frac{x}{\ell} = 1.0 \qquad \frac{dr}{dx} = 0$$

$$\frac{x}{\ell} = 1.2353 \qquad \frac{r}{\ell} = 0$$

we obtain

$$\frac{r}{\ell} = -0.4413 + \sqrt{-\left(\frac{x}{\ell}\right)^2 + 2.0 \frac{x}{\ell} - 0.7499} \qquad (5)$$

Equations (3), (4), and (5) are the three polynomials describing the shape of the store and the coefficients are contained in cards 6 through 8 of figure 4(a).

The last card of figure 4(a) contains the remaining input data. The first number, XSFST, specifies that the first source is to be located at $x/\ell = 0.002$. The second number, XSLST, indicates that no source is to be placed behind $x/\ell = 1.23$ and the third number, PERCR, requires that the source spacing be 0.7 times the local value of r/ℓ . The fourth quantity on this card, XRMAX, specifies that the maximum body radius is first reached at $x/\ell = 0.2353$. The next three quantities specify the values of x/ℓ at which the body radius is to be calculated from the source distribution. The first value of x/ℓ , XINIT, is 0.01, the last value, XFINAL, is 1.23, and the interval between points, DELX, is 0.02. The last quantity on this card, RMAX, is the maximum value of r/ℓ for the store, 0.05882.

The remaining three sets of input data shown in figure 4 are for the fuselage, figure 5(a), the small boattail store, figure 5(e), and the TER rack, figure 5(c). The fuselage is represented by a circular arc nose, a cylindrical centerbody, and a circular arc afterbody which is allowed to close aft of the actual base of the fuselage in order to model the wake.

Table I presents the coordinates of the small boattail store. Examination of figure 4(c) shows that this body is approximated by a series of circular arcs except for the short cylindrical section at the base of the body. The wake is again modeled by a circular arc.

The TER rack shown in figure 5(c) can be approximated by a body of revolution to which are attached three short pylons. In the present programs the pylons are not accounted for and a source distribution is used to model the body of revolution. The input data of figure 4(d) shows that the nose is approximated by an ellipse, the center section by a cylinder, and the aft end by a circular arc. Again, this aft section is extended until it closes in order to model the wake.

3.3 Output from the Program

The output data from the source distribution program for the four sets of input data shown in figure 4 are presented in figures 6 through 9. Figure 6 is the output for the ogive-cylinder store; figure 7, the output for the fuselage; figure 8, the output for the small boattail store; and figure 9, the output for the triple ejector rack.

Part (a) of each figure is page 1 of the output. This page tabulates most of the input data. Page 2 of the output, part (b) of each figure, tabulates the x/l locations at which the sources were placed along with the values of r/l and dr/dx calculated from the input polynomials at these values of x/l .

Page 3 of the output, part (c) of each figure, specifies the number of sources, the Mach number, the values of x/l at which the sources are located, and also the dimensionless incompressible source strengths. These are tabulated in the format in which they are to be punched (6E12.4) for input into the trajectory programs. They are not punched in the order shown. The values of x/l are first punched and then beginning on a new card the values of Q are punched.

Page 4 of the output, part (d) of each figure, lists the shape calculated from the source distribution. Tabulated as a function of x/l is the calculated r/l . This radius distribution should be compared with that given by the polynomials used to represent the body. If the two shapes do not agree to the desired accuracy, then the location of the first source and the source spacing should be varied in order to attempt to improve the representation.

4. SIX-DEGREE-OF-FREEDOM TRAJECTORY PROGRAM

The six-degree-of-freedom trajectory program uses the source distributions, calculated as described in the preceding section, as input data. In addition other data are input describing the various components of the aircraft and locating them with respect to each other as well as data describing the aircraft flight conditions. The vorticity distribution representing the wing-pylon loading is next determined and following this additional data describing the separated store are read in and the trajectory calculation performed.

The program just described consists of a main program and 32 subroutines. Table II lists these subroutines in alphabetical order and gives a one-sentence description of what each subroutine does. A listing of the six-degree-of-freedom trajectory program and its 32 subroutines is presented in figure 10 and a general flow chart of the main program in figure 11. The program listing in figure 10 is specifically for the CDC 6600 computer. To run it on other machines such as the Univac 1108 the three unsequenced cards following sequence number 6DA01124 in the main program may have to be removed or changed. A detailed description of the program and subroutines, including the equations programmed, is presented in Appendix II.

4.1 General Description of Program

The computer program integrates the six-degree-of-freedom equations of motion, which are derived in Appendix II of reference 1, in the manner described in section 6 of that reference. The aerodynamic forces and moments are calculated by the methods presented in section 5 of that report.

A general flow chart of the program is presented in figure 11. Page 1 of the flow chart, figure 11(a), is the input section of the program. Constants are defined and heading information is read and printed. The aircraft flight conditions are input as are indices specifying what aircraft components are present. If the fuselage is present the fuselage data are read in and printed.

The next steps in the program read in the data required to model the wing. The data locating the wing and specifying its incidence relative to the fuselage are first read and then subroutine WVLIN is called. This

routine reads in the data required to lay out the vortex lattice which will represent the loaded wing and lays out the lattice. In addition it reads in the twist and camber distribution at the vortex lattice control points. The last wing input data is the thickness distribution. These data are read in by subroutine WTHIN.

A check is made in the program to determine whether or not a pylon is present. If it is, data describing the pylon are read and subroutines PVLIN and PTHIN are called to read in the data required to lay out the pylon vortex lattice and thickness distribution. Following this the pylon is located in the fuselage coordinate system.

The next two steps in the program call subroutines VLOUT and THOUT which output the vortex lattice and thickness distribution data. The vortex strengths are calculated and tabulated later.

One of the optional aircraft components is the ejection rack. If one is present the next steps in the program input all of the data describing and locating the rack. The input data locate the rack relative to the local wing chord. Calculations are made which locate it in both the wing and fuselage coordinate system.

Provision has been made for not including any stores in the input data. This has been done so that the program can be used to determine the coordinates of the points at which the wing twist and camber distribution must be input. The next step in the program checks to see if there are any stores and if there are none the store input section of the program is bypassed. If there are stores, subroutine STRIO is called to read in and print all of the store data. These data consist of the locations and incidences of all the stores and a source distribution for each different shape. After all of these data are input, each store is located in the fuselage coordinate system.

Boxes 2 through 5 of the left-hand column of figure 11(b) are associated with the calculation of the vorticity distribution to represent the wing-pylon loading. The equations used to solve for the vorticity distribution are equations (6) and (7) of section 4.2.2 of reference 1. The first step is to call subroutine VLCOEF which calculates the coefficient matrix, that is, the coefficients multiplying the unknown vortex strengths, Γ_n , in equations (6) and (7). The next step is to call

subroutine VLRHS which calculates the right-hand side of this set of simultaneous equations. The resulting set of equations are then solved by calling subroutine INVERS. Subroutine VSTOUT is called to output the resulting vortex strengths, control point coordinates, and interference velocities at these points. If there are no stores present this ends the calculation and the program returns to the beginning to read another set of input data.

If stores are present the program continues and reads in the additional data required to describe the store to be separated and performs the initialization for the trajectory calculation. The remainder of the flow chart of figure 11(b) shows this part of the programs. First the additional data describing the store are read in. These data consist of, among other things, the mass and inertia characteristics, polynomials defining the body shape, and center of gravity location. The next step is to calculate other quantities from these data.

If the store to be separated has an empennage the data required to describe the empennage are input and subroutine EMPINI is called to initialize for the empennage force and moment calculation.

Provision is made in the program for prescribing initial vertical and pitching velocities relative to the parent aircraft. These are next read in and then the initial values of the 12 dependent variables in the trajectory calculation are computed. These are

- (1) The three coordinates of the store center of moments relative to the fuselage nose.
- (2) The three translational velocity components of the store center of moments relative to the fuselage.
- (3) The three store rotational velocities.
- (4) The three angles giving the store orientation relative to the fuselage.

Reference positions of the store nose, center of moments, and base are next calculated and the initial and final trajectory times, as well as a guess at the integration interval, are input. If the initial time is not zero, then the trajectory is being restarted from a previous run and the current values of the 12 dependent variables obtained from that run are

read in. The last step in the initialization is to initialize subroutine ADAMS, the integration routine.

The last page of the flow chart, figure 11(c), is the integration loop of the program. The first steps are to calculate the aerodynamic forces and moments acting on the body and the empennage, if one is present, of the separated store. The body forces and moments are determined by the methods described in section 5.2 of reference 1. The empennage forces and moments are determined as discussed in section 5.3 and Appendix I of that reference.

One of the options in the computer program is to calculate a wind-tunnel captive-store trajectory as opposed to a free-flight trajectory. It is customary in the wind tunnel to change the store orientation relative to the parent aircraft while measuring the forces and moments in order to approximately account for the store translational motion relative to the aircraft. The computer program also does this during the force and moment calculation. Thus, if a captive store trajectory is being calculated, the next step in the program is to put the store back to its correct orientation and call subroutine DIRCOS in order to calculate the free-flight direction cosines between the store body coordinate system and the inertial coordinate system which is fixed in the fuselage.

The next series of steps determines the store translational and rotational accelerations. This involves solving the set of six simultaneous equations given by equations (II-16) through (II-18) and (II-41) through (II-43) of Appendix II of reference 1 making use of the relationships given in section 6.1 of that reference. The coefficient matrix is first calculated and then the right-hand sides are determined. Subroutine INVERS is called to solve the set of six equations for the accelerations. The rates of change of the orientation angles are next determined from equation (II-1) of Appendix II of reference 1.

A check is next made to see if output is to be printed at the end of an integration step. If output is not required the integration continues by calling subroutine ADAMS. If it is required, subroutine OUTPUT is called. Upon return from this subroutine a check is made to see if the time is equal to the final time which was read in and if so, the trajectory is stopped and control returns to the beginning to read in a new set of data. If it is not, the integration is continued.

4.2 Input Data

4.2.1 Input format

The format for the input data for the trajectory program is shown in figure 12. Three lines of information are shown for each item. The first line gives the program variable names, the second line shows the card column fields into which the data are to be punched, and the third line shows the FORTRAN format type. Data punched in I and E formats are right justified in the fields whereas data in F format can be punched anywhere in the field. A decimal point should be included in both E- and F-type data.

Item number 1 is an index NCARDS which indicates how many cards of information are to follow to identify the run, item number 2. The value of NCARDS must be one or greater.

Item number 2 is a set of NCARDS cards containing hollerith information identifying the run and may start and end anywhere on the card. The cards are reproduced in the output just as they are read in.

Item number 3 consists of one card and contains the following information:

ALFAC	fuselage angle of attack, degrees
GAMF	fuselage flight path angle, degrees
FMACH	Mach number
RHO	air density at flight altitude, slugs per cubic foot
VINF	aircraft free-stream velocity, feet per second

The aircraft is assumed to be flying in a straight line; however, it can be climbing or diving. For climbing flight, GAMF is positive. The Mach number, FMACH, is used in the compressibility correction. For low flight velocities where compressibility can be ignored, it can be input as zero. FMACH should be the same as that used in calculating the source distributions to be input later.

Item number 4 contains four indices which specify what aircraft components are present. They are

NFU fuselage? NFU = 0, no
 NFU = 1, yes

NPY pylon? NPY = 0, no
 NPY = 1, yes

NRACK rack? NRACK = 0, no
 NRACK = 1, yes

NSTRS number of stores; $0 \leq \text{NSTRS} \leq 10$

Provision has been made for omitting the fuselage since for trajectories of stores dropped from near the wing tip the fuselage probably has a negligible influence. For cases with no fuselage the reference coordinate system is fixed at the wing root-chord leading edge and ALFAC and GAMF of item 3 should be the wing angle of attack and flight path angle, respectively. If a rack is present, NRACK = 1, the pylon to which it is attached must also be present, NPY = 1. The number of stores can be zero. This allows the input data deck through item 25 to be checked out without running a trajectory. In addition the program can also be used as an aid in determining the points on the wing and pylon at which the slopes of the camberline and the thickness distribution are to be input.

Item number 5 consists of two quantities which are

FLTHC length of actual fuselage, feet

FRMAX maximum fuselage radius, feet

This item and the next three are omitted if NFU = 0.

Items number 6, 7, and 8 are data specifying the source distribution for the equivalent incompressible fuselage as calculated by the source distribution program. Item number 6, NFSOR, specifies the number of sources. This number is printed at the top of page 3 of the source distribution output, see for example figure 7(c). Item 7, the FXL array, and item 8, the FSOR array, are the locations, x/ℓ , and the dimensionless strengths, Q^* , of the NFSOR sources, respectively. These quantities are also printed on page 3 of the source distribution program output, see for example figure 7(c). Item 7 contains all of the x/ℓ 's punched six to a card except for the last card which will contain less if NFSOR is not a multiple of 6. Item 8 begins on a new card and contains the Q^* 's.

Item number 9 contains three parameters which specify the wing location relative to the fuselage nose and the incidence of the root chord relative to the fuselage longitudinal axis. These three parameters are shown pictorially in figure 13 and are

XBWOC	x_B	location of the wing root-chord leading edge, feet
ZBWO	z_B	location of the wing root-chord leading edge, feet
WIC		incidence angle of wing root chord measured relative to fuselage axis, degrees

The wing root chord is the chord obtained by extending the exposed wing panel to the fuselage x_B , z_B plane of symmetry. All three quantities are measured on the actual, not the equivalent incompressible, configuration. The compressibility correction is made in the program. In the example of figure 13, XBWOC and ZBWO are negative and WIC is positive. If the wing were below the fuselage axis, ZBWO would be positive.

Item number 10 contains two quantities which are

CRW	length of wing root chord, feet
SSPAN	wing semispan, feet

Both quantities are input as positive quantities.

Items 11 and 12 are input data describing the left wing panel which are used to lay out the wing vortex lattice. The quantities are

NCW	number of vortices in a chordwise row on wing
MSW	number of vortices in a spanwise row on wing; also number of thickness strips in a spanwise row on wing; $MSW \leq 30$
I	wing vortex trailing leg number; $I = 1$ to $MSW+1$
Y(I)	y_w location of I^{th} trailing leg on the left wing panel, feet (zero when $I = 1$, negative for all other I 's since on left panel; measured in wing planform plane)
PSIWLE(I)	leading-edge sweep of wing section to the right of the I^{th} trailing leg, degrees; positive swept back (measured in wing planform plane)
PSIWTE(I)	trailing-edge sweep of wing section to the right of the I^{th} trailing leg, degrees; positive swept back (measured in wing planform plane)
PHID(I)	dihedral angle of wing section to the right of the I^{th} trailing leg, degrees; positive up

Based on these input data, the wing is divided chordwise and spanwise into trapezoidal shaped elemental panels and one horseshoe vortex placed on each panel. All the NCW panels in a chordwise row have equal chords and spans, the spans being determined by the $Y(I)$'s. The horseshoe vortex is made up of three vortex lines; a bound vortex which is swept to coincide with the quarter chord of the panel and two trailing vortex legs which lie along the edges of the panel and extend to infinity behind the wing.

The question arises as to the values to use for NCW and MSW. This is discussed to some extent in section 4.3.2 of reference 2 where it is shown that as the vertical distance from the wing to the points at which the velocity field is to be calculated decreases additional chordwise vortices must be added in order to accurately calculate the velocities. A procedure which can be used is to locate the initial position of the axis of the store whose trajectory is to be calculated relative to the wing in terms of a fraction of the local wing chord, that is, the chord immediately above the store, and use the following table.

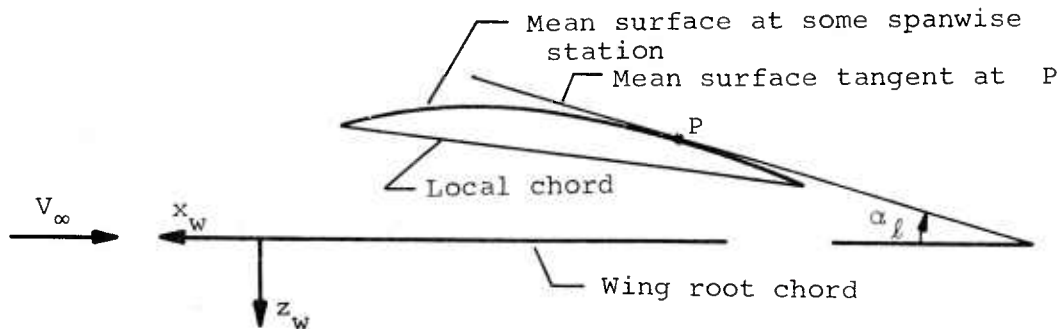
z/c	NCW
0.10	10
.15	8
.20	6
.25	4

The number of vortices in a spanwise row is controlled to some extent by the wing. A vortex trailing leg must coincide with the root chord and each break in leading-edge sweep angle, trailing-edge sweep angle, and dihedral angle, and if a pylon is present, a trailing leg must coincide with the spanwise location of the pylon. One must also coincide with the wing tip. Consider the example wing of figure 14. There is a break in trailing-edge sweep at $y_w/s = -0.2$, a break in leading-edge sweep at -0.4 , a pylon at -0.6 , and a break in dihedral at -0.7 . To place a trailing leg at each of these positions plus the wing tip and the root chord requires five vortices across the semispan. This is the minimum number which can be used for this wing and may or may not be sufficient. Experience with the program has shown that in some cases five vortices in a spanwise row has given good results.

edge. If $NUNI = 0$, data for all chordwise rows must be input starting nearest the root chord and working outboard. Data for each row start on a new card (omit if $NTAC = 0$)

The vortex lattice control points are at the midspan of the three-quarter chord line of each elemental panel laid out by NCW , MSW , and the $Y(I)$'s of items 11 and 12.

The values of $ALPHAL(J)$ are obtained as follows. Consider the following sketch



which shows the cambered and twisted section of the lifting surface at some spanwise station for zero wing angle of attack. At the control point P, a tangent to the surface is constructed, which makes an angle α_l with the root chord (the x_w axis). The positive sense of α_l is shown. The input value required is $ALPHAL(J) = \tan \alpha_l$. For wings which have the same camber distribution at all spanwise stations and no twist, $NUNI = 1$, data are only input for the row of control points closest to the root chord. The program assigns these values to all other rows.

The two indices of item number 15 are associated with the specification of the wing thickness distribution. They are

- $NCWS$ number of thickness panels in a chordwise row on the wing;
 $(NCWS * MSW) \leq 400$
- $NUNIS$ if wing has a similar thickness distribution at all spanwise stations, $NUNIS = 1$; if not, $NUNIS = 0$

The thickness panels are also trapezoidal in shape. The span of each chordwise strip is the same as the corresponding row of horseshoe vortices. Each of these chordwise strips is divided into $NCWS$ equal chord panels.

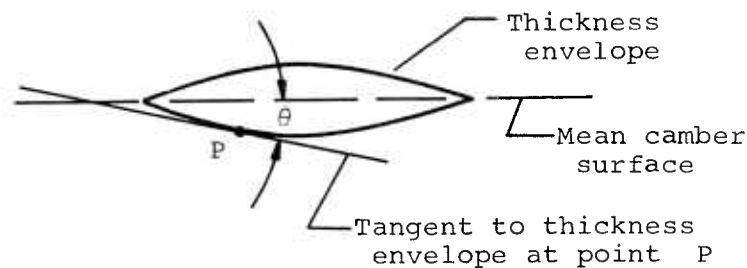
Considerably more thickness panels should be used in a chordwise row than were vortices. Experience with the program has shown 16 to 20 thickness panels usually to be sufficient. Again, this can only be checked by varying the number and examining the resulting store load distributions and the minimum number, consistent with the desired accuracy, should be used to minimize the trajectory calculation time.

The data contained in item number 16 are

THETAL(J) slope of the wing thickness distribution at the centers of the thickness panels. If NUNIS = 1 only data for the chordwise row adjacent to the root chord are input. The first value is for the panel at the leading edge. If NUNIS = 0, data for all chordwise rows must be input starting at the root chord and working outboard. Data for each row start on a new card.

Note that the values of the thickness slopes are input for the center of each panel, that is, the midspan of the 50-percent chord. Also, for wings with similar distributions at all spanwise station, NUNIS = 1, data are only input for the row of panels adjacent to the root chord. The program assigns these values to all other rows.

The values of THETAL(J) are obtained as follows. Consider the following sketch



which shows the thickness envelope at a spanwise station where the slopes are to be determined. At a point P at which the slope is required, a tangent to the surface of the thickness envelope is constructed which makes an angle θ with the line connecting the leading and trailing edges of the envelope. The input value required is THETAL(J) = $\tan \theta$. Forward of the point of maximum thickness θ is positive and aft of this point it is negative.

The next five items of input data, items 17 through 21, are associated with the pylon if one is present, $NPY = 1$. Item number 17 consists of one card and contains the following quantities

IP	index of the y_w location of the pylon. This must be one of the $Y(I)$'s read in for the wing vortex lattice
PSIPLE	sweep angle of the pylon leading edge in the wing coordinate system, degrees. Positive sweep is swept back.
PSIPTE	sweep angle of the pylon trailing edge in the wing coordinate system, degrees. Positive sweep is swept back.
CRP	length of pylon root chord, feet
H	height of pylon measured from wing chordal plane, feet
XPLE	location of pylon root chord leading edge measured from local wing chord leading edge, feet (negative behind)

The pylon location can be under the fuselage, $IP = 1$, or at one of the wing vortex trailing leg locations outboard of the wing fuselage juncture. The remaining five items are shown in figure 15 for the two cases.

The next two items of input data are associated with the vortex lattice which represents the pylon loading. Item number 18 is one card and contains

NCP	number of vortices in a chordwise row on the pylon; $(NCP * MSP) \leq 30$
MSP	number of vortices in a spanwise row on pylon; also number of thickness strips in a spanwise row on the pylon; $MSP \leq 4$

For a typical pylon, two or three vortices in a spanwise row are sufficient, $MSP = 2$ or 3 . The number chordwise, NCP , depends on the length of the pylon root chord. The chordwise dimensions of the trapezoidal shaped area elements on the pylon should be approximately the same as those on the wing immediately above the pylon. That is, the local wing chord length divided by NCW of item 11 should be approximately equal to the pylon root chord length divided by NCP .

The program is limited to 100 vortices on the wing-pylon combination. Thus

$$NCW * MSP + NCP * MSP \leq 100$$

Item number 19 consists of a deck of MSP+1 cards which contain the following information

K	pylon vortex trailing leg number; K = 1 to MSP+1
Z(K)	z location of the K th trailing leg, feet; measured from local wing chord

The first trailing leg should be placed on the pylon root chord and the last on the tip chord. The remaining trailing legs should be equally spaced between these two. For a pylon located under the fuselage, figure 15(a), Z(1) should be the z_w location of the pylon root chord, the bottom of the fuselage, and Z(MSP+1) should equal Z(1) + H. For a pylon under the wing, Z(1) = 0 and Z(MSP+1) = H.

Items 20 and 21 provide data required in order to model the pylon thickness distribution. The data are

NCPS	number of thickness panels in a chordwise row on the pylon; (NCPS*MSP) \leq 180
NUNIP	if pylon has a similar thickness distribution at all spanwise stations, NUNIP = 1; if not, NUNIP = 0
THETPL(J)	slope of the pylon thickness distribution at the centers of the thickness panels. If NUNIP = 1 only data for the chordwise row adjacent to the root chord are input. The first value is for the panel at the leading edge. If NUNIP = 0, data for all chordwise rows must be input starting at the root chord and working outboard. Data for each row start on a new card.

These data are prepared in the same manner as were the corresponding data for the wing thickness, items 15 and 16.

The next four items of input data locate and describe the ejection rack if one is present, NRACK of item 4 is equal to one. If NRACK = 0 these four items are bypassed. If a rack is present the preceding data for the pylon must have been input since the program has been written assuming that if there is a rack there also is a pylon. The rack data to be input only model the body of the rack. No provision has been made in the program for modeling the short pylons on which the stores are mounted.

Item number 22 is one card and contains the following information

RLTHC	length of rack, feet
RRMAX	maximum rack radius, feet
XRNC	x/ℓ location of rack nose measured from local wing chord leading edge, feet; positive ahead
ZRN	z/ℓ location of rack nose measured from local wing chord leading edge, feet; positive below
RIC	rack incidence angle measured relative to wing root chord, degrees; positive nose up

Items number 23, 24, and 25 are data specifying the source distribution for the equivalent incompressible rack as calculated by the source distribution program.

NRSOR	number of rack sources; $NRSOR \leq 100$
RXL(J)	incompressible (x/ℓ) 's of the rack sources
RSOR(J)	incompressible dimensionless rack source strengths

Item number 23, NRSOR, specifies the number of sources. This number is printed at the top of page 3 of the source distribution output, see for example figure 9(c). Item 24, the RXL array, and item 25, the RSOR array, are the locations, x/ℓ , and the dimensionless strengths, Q^* , of the NRSOR sources, respectively. These quantities are also printed on page 3 of the source distribution program output, see for example figure 9(c). Item 24 contains all of the x/ℓ 's punched six to a card except for the last card which will contain less if NRSOR is not a multiple of 6. Item 25 begins on a new card and contains the Q^* 's.

If no stores are present, NSTRS of item 4 is equal to zero, this concludes the input data deck. If NSTRS is not zero, then the next five items of input data describe all stores present on the aircraft including the store to be separated. The store to be separated must be under the fuselage centerline or to the left of this line as seen by the pilot. Data should be input for all stores which are close enough to affect the trajectory including those under the right wing panel.

Item number 26 is a deck of NSTRS cards which contain the following information.

NUMSTR(J)	store number; different for each store and ≤ 99
NSHAPE(J)	shape number of store; ≤ 99
SLTHC(J)	length of store, feet
SRMAX(J)	maximum radius of store, feet
XSNC(J)	x_ℓ location of store nose measured from wing chord leading edge immediately above store, feet; positive ahead
YSN(J)	y_w location of store nose measured from wing root chord, feet; positive to the right
ZSN(J)	z_ℓ location of store nose measured from wing chord leading edge immediately above store, feet; positive below
SIC(J)	store incidence angle measured relative to wing root chord, degrees; positive nose up

The numbers of the stores do not have to be consecutive and can have any value from 1 to 99. The same applies to the shape numbers except that more than one store can have the same shape number. For example, for a MER grouping of six identical stores, different store numbers would be assigned to each store but they would all have the same shape number.

Item number 27 is one card which contains

NSHPT	total number of shapes for which store source distributions are to be input; equal to the number of different values of NSHAPE(J)
-------	---

Items 28, 29, and 30 are the source distribution data for a particular store shape. These three items are repeated in sequence for each different shape. The data are

MSHAPE	shape number of store represented by the following source distribution; equal to one of the values of NSHAPE(J)
MSOR	number of sources for this store shape; $MSOR \leq 100$
DUMX(J)	incompressible (x/ℓ) 's of the store sources
DUMQ(J)	incompressible dimensionless store source strengths

The quantity MSHAPE must have the same value as one of the shape numbers read into the NSHAPE(J) array, item 26. The remaining quantities specify the source distribution for the equivalent incompressible store as calculated by the source distribution program. The quantity MSOR specifies the number of sources. This number is printed at the top of page 3 of the source distribution output, see for example figure 6(c). Item 29, the DUMX array, and item 30, the DUMQ array, are the locations, x/ℓ , and the dimensionless strengths, Q^* , of the MSOR sources, respectively. These quantities are also printed on page 3 of the source distribution program output, see for example figure 6(c). Item 29 contains all of the x/ℓ 's punched six to a card except for the last card which will contain less if MSOR is not a multiple of 6. Item 30 begins on a new card and contains the Q^* 's. The quantity MSOR and the DUMX and DUMQ arrays are temporary storage for the source distribution. Immediately after reading in all data for one distribution these data are transferred to other arrays for each store with this shape.

The remainder of the input data deck is additional data required to describe the store being separated and other data required for the force and moment and trajectory calculations.

Item number 31 is one card which contains eight indices. They are

NEJECT	number of the store being separated
NSEG	number of equal length segments the body is to be broken into for the force calculation; $NSEG \leq 40$
NSEGXO	number of body segments to the flow separation location
NGAM	trajectory to simulate wind-tunnel captive-store trajectory? NGAM = 0, no NGAM = 1, yes
NPOLY	number of polynomials specifying store shape; $1 \leq NPOLY \leq 7$
NROLL	rolling moment to be calculated? NROLL = 0, no NROLL = 1, yes
NEMP	empennage present? NEMP = 0, no NEMP = 1, yes
NDAMP	damping to be included in force calculation? NDAMP = 0, no NDAMP = 1, yes

The index NEJECT must be one of the store numbers that was read into the NUMSTR array through item 26.

In the store body force and moment calculation, the body is divided into NSEG equal length segments. Experience in using the program has shown that 20 body segments, NSEG = 20, usually yields sufficiently accurate forces and moments. This can only be checked for a specific case by varying NSEG and comparing results. To minimize calculation time NSEG should be kept as small as possible.

No definite rules for the selection of a value of NSEGXO can be given. For stores with cylindrical afterbodies NSEGXO should probably be input as NSEG. For stores with boattailed afterbodies NSEGXO should probably be less than NSEG. A further discussion is given in sections 6.2 and 8.2 of reference 2. In that discussion the work of Hopkins (ref. 3) is mentioned. In this work he correlated, for bodies of revolution in uniform flow, the maximum extent of applicability of potential flow as a function of the location of the maximum negative rate of change of body cross-sectional area. From that reference

$$\frac{x_o}{\ell} = 0.378 + 0.527 \frac{x_1}{\ell}$$

where x_o/ℓ is the location on the body where potential flow is no longer applicable and viscous forces are important and x_1/ℓ is the location on the body of the maximum negative rate of change of cross-sectional area (ℓ is the body length). Whether or not this correlation applies to non-uniform flow is not known but it can be used in estimating the value of NSEGXO.

The index NGAM is included as input solely for the purpose of allowing the program to be used to compare with captive store data obtained in the wind tunnel. Since the wind tunnel cannot produce a flow where the store sees a free-stream velocity coming from a different direction than that seen by the parent aircraft the captive store case must be handled differently by the computer program.

The number of polynomials specifying the store shape, NPOLY, is the number required to specify the shape from the store nose to its base. These polynomials are used in the force and moment calculation and, hence, do not have to model the wake in the manner done in the source distribution

calculation. The polynomials are of the same form, however, and are given by equation (1).

The next index, NROLL, indicates whether or not the rolling moment for a store with an empennage is to be calculated. NEMP specifies whether there is an empennage. The last index, NDAMP, is used by the program to determine whether or not aerodynamic damping in pitch, yaw, and roll is to be included in the force and moment calculation.

Item number 32 is one card and specifies the store mass and inertia characteristics. The quantities are

SMASS	store mass, slugs
FIXX	I_{xx} moment of inertia, slug-ft ²
FIYY	I_{yy} moment of inertia, slug-ft ²
FIZZ	I_{zz} moment of inertia, slug-ft ²
FIYZ	I_{yz} product of inertia, slug-ft ²
FIXZ	I_{xz} product of inertia, slug-ft ²
FIXY	I_{xy} product of inertia, slug-ft ²

The equations defining the moments and products of inertia are given by equation (II-36) of Appendix II of reference 1.

The one card of item number 33 contains

XMOM	location along store axis about which the pitching and yawing moments are to be taken, negative behind nose, feet; same point about which moments of inertia are taken
XBAR	x location of store c.g. measured from moment center, feet; positive forward
YBAR	y location of store c.g. measured from store axis, feet; positive to the right
ZBAR	z location of store c.g. measured from store axis, feet; positive below

The next two items of input, items 34 and 35 describe the shape of the ejected store. The quantities contained on the cards are

XEND(J)	x/l of end points of polynomials specifying shape of ejected store, NPOLY values
COEF(J,K)	coefficients of polynomials specifying shape

These data are the same data input as items 4 and 5 to the source distribution, see figure 3, with one exception. This exception is that the shape is only required in the range $0 \leq x/\ell \leq 1$ since no load is carried by the wake which was modeled in obtaining the source distribution. The preparation of these data is described in section 3.2.1.

Item number 36 contains two quantities which are

CA	store axial-force coefficient; reference area is store maximum cross-sectional area
CDC	crossflow-drag coefficient

The store axial-force coefficient is not calculated by the computer program so it is required input. The crossflow-drag coefficient is used in the viscous crossflow force and moment calculation which is used in place of the slender-body calculation behind the assumed separation location. It is defined as the section drag coefficient of a circular cylinder normal to the airstream. That is,

$$CDC = c_{d_c} = \frac{\text{drag per unit length}}{q_\infty (2r)}$$

where q_∞ is the free-stream dynamic pressure and r is the cylinder radius. The value commonly used for this parameter is 1.2.

The next two items of input data are included in the input data deck if an empennage is present, NEMP = 1 in item 31. Item 37 contains

IPLNR	IPLNR = 0, cruciform empennage IPLNR = 1, planar empennage
MSF	number of spanwise control points on each fin; <u>must</u> be odd and $5 \leq MSF \leq 11$.

It should be noted that MSF must be odd and in the range $5 \leq MSF \leq 11$. For the store shown in figure 5(d) MSF = 5 has been found to give accurate results. The larger the fin span to body radius ratio, the more points required.

The next card, item number 38, contains

XTAIL	x location at which empennage forces are to act measured from store nose, feet; negative number
RADAV	average store body radius in empennage region, feet; positive number

FINSS	tail fin semispan, measured from body longitudinal axis, feet; positive number
PHIROL	initial fin orientation, degrees; $0 \leq \text{PHIROL} \leq 90$; PHIROL = 0 if fins vertical and horizontal
CLALPH	lift-curve slope of two exposed panels joined together, per radian; reference area is store maximum cross-sectional area

The location at which the empennage forces are assumed to act, XTAIL, is arbitrary. A good position to use is the quarter chord of the mean aerodynamic chord of the exposed panels. The lift-curve slope, CLALPH, can be estimated using reference 4.

Item number 39 is one card which contains the initial velocities of the store relative to the parent aircraft such as might exist at the end of the ejection stroke of a store released from a pylon or rack. The two quantities are

VZERO	store downward ejection velocity perpendicular to store longitudinal axis, ft/sec
VAR(5)	store initial pitching rate, q , radians/sec

At the beginning of the trajectory, the end of the stroke, the store is oriented such that its y -axis is parallel to the y_B fuselage axis shown in figure 13. Thus the x,z store plane is parallel to the x_B,z_B fuselage plane and the initial translational velocity of the store, VZERO, is in the x,z store plane perpendicular to the store x -axis. The initial pitching rate of the store, q or VAR(5), is about the store y -axis positive nose up.

The next card, item number 40, contains three times. They are

DTIME	integration interval, seconds
TIMEI	initial time, seconds
TIMEF	final time, seconds

The first, DTIME, is an initial guess at the integration interval to be used in the integration subroutine. Experience in using the program has shown that 0.05 or 0.10 seconds is a good value to use. The initial time, TIMEI, must be input as 0.0 unless a trajectory is to be restarted using the last page of output from a previous run to obtain the initial conditions. Then, TIMEI should be given the value that appears on that page of output.

The final time, TIMEF, is the time from ejection at which the trajectory calculation is to be terminated. Except for very unusual trajectories, a value of 0.5 to 0.7 seconds is normally sufficient for the store to clear the aircraft.

If TIMEI and TIMEF are both input as zero, no trajectory calculation will be performed. However, the store load distributions and forces and moments will be calculated with the store in its initial position. This feature can be useful in checking out the entire input data deck prior to running a trajectory or for studying store loadings at specific points.

The last item of input, item number 41, is input only if a trajectory is being restarted, TIMEI \neq 0. This item consists of two cards with VAR(1) through VAR(8) on the first card and VAR(9) through VAR(12) on the second. The following table gives the notation used to identify VAR(1) through VAR(12) on the trajectory program output which will be discussed in section 4.3.

<u>Program Notation</u>	<u>Output Notation</u>
VAR(1)	DXF, ft/sec
VAR(2)	DYF, ft/sec
VAR(3)	DZF, ft/sec
VAR(4)	P, radians/sec
VAR(5)	Q, radians/sec
VAR(6)	R, radians/sec
VAR(7)	XF of XMOM, ft.
VAR(8)	YF of XMOM, ft.
VAR(9)	ZF of XMOM, ft.
VAR(10)	PSI, degrees
VAR(11)	THETA, degrees
VAR(12)	PHI, degrees

4.2.2 Sample input data

Sample input data decks for two cases will now be presented. Both cases will utilize the wind-tunnel model components shown in figure 5 except that they have been scaled up by a factor of twenty in order to approximate a full-scale aircraft and stores.

The configuration for the first example is shown in figure 16. It consists of the wing-fuselage combination shown in figure 5(a) with the pylon of figure 5(b) at the one-third semispan position of the left wing panel. The store being ejected is below this pylon and is that shown in figure 5(d). Its initial position is one radius below the carriage position. The cruciform fins are rolled 45° from the vertical and horizontal. Grouped under the fuselage are three of the stores shown in figure 5(e). They are positioned as they would be if the pylon and rack shown in figures 5(b) and 5(c) were present. The store which may exist under the right wing panel has not been included since it is so far removed from the store being ejected that it would not influence the trajectory.

The input data deck for this case is tabulated in figure 17. The item numbers indicated on the figure correspond to those of figure 12. The first item on figure 17 is item number 1 which contains the value of NCARDS, in this case 13. This is followed by item number 2, which consists of these 13 cards of identifying information.

Item number 3 specifies the aircraft flight conditions. The angle of attack is 4.0 degrees, the flight path angle is 0.0 degrees, and the Mach number is 0.4. The free-stream air density is 0.0020482 slugs per cubic foot which corresponds to a flight altitude of 5,000 feet. The flight velocity is 440.7 feet per second.

The aircraft components which are present are specified by item 4. There is a fuselage; there is a pylon; there is no rack; and there are 4 stores.

Items 5 through 8 are the fuselage input data. Item 5 contains the fuselage length and maximum radius as shown in figure 16. Items 6, 7, and 8 contain the source distribution representing the fuselage volume. These data were obtained from figure 7(c).

The next seven items are the wing input data. Item 9 gives the position of the wing root chord leading edge and wing incidence relative to the fuselage and item 10 specifies the root chord length and the semispan. These quantities are shown in figure 16. Items 11 and 12 are data required by the program to lay out the vortex lattice. There are to be 8 vortices in each chordwise row and 5 of these rows across the semispan.

This requires that the spanwise locations on the left wing panel of six trailing legs and the sweep and dihedral angles to the right of these points be specified. These data are contained on the six cards of item 12. Note that one trailing leg coincides with the pylon location, $y = -6.66667$. Item 13 indicates that the wing has neither twist nor camber, and thus item 14 of figure 12 is omitted from the input data deck. Items 15 and 16 specify the wing thickness distribution. The two indices on item 15 indicate that 16 thickness panels are to be placed in a chordwise row and that the wing has a similar thickness distribution at all spanwise stations. Consequently, item 16 consists of two cards with the 16 values of the slope of the thickness distribution. The airfoil section specification is shown in figure 5(a).

Since there is a pylon, items 17 through 21 are input and contain the pylon data. The pylon is the one shown in figure 5(b), except that it has been scaled up by a factor of 20. Item 17 of the input data specifies that the pylon is located below vortex trailing leg number 3, the leading- and trailing-edge sweep angles are 0.0 degrees, the root chord length is 3.33333 feet, the height is 1.652 feet, and the leading edge is 3.046 feet behind the local wing chord leading edge (see fig. 16). Items 18 and 19 are the pylon vortex lattice data. There are to be two vortices in a chordwise row and two of these rows spanwise. The three trailing leg locations are given by item 19. Items 20 and 21 specify the pylon thickness distribution. There are to be 60 thickness panels in a chordwise row and the thickness distribution is similar at all spanwise stations. The large number of panels chordwise is necessitated by the thickness distribution of the pylon shown in figure 5(b). Since the pylon is a flat plate with a radius on the leading and trailing edges, a large number of panels is required if any leading-edge and trailing-edge detail is to be included. This is shown by the thickness envelope slope data of item 21. Sixty equal chord panels in a chordwise row only places four panels on each of the two radii.

Since there is no ejection rack in the case shown in figure 16, items 22 through 25 are omitted from the input data deck.

Item 26 begins the store data. One card is input for each store shown in figure 16. The wing store is assigned store number 10 and the TER group 20, 21, and 22, 20 being the bottom store, 21 the left shoulder

store, and 22 the right shoulder store. The wing store is assigned shape number 2 and the TER stores, shape number 5. With the exception of the incidence angle of the stores, which is 0.0, the information required to prepare the remaining data in item 26 are shown in figure 16. The trajectory to be calculated is for the wing store and is to be started with the store one radius below the carriage position. The data for this store locate it in this position. Since two different shape numbers were assigned in item 26, two different source distributions are to be input. This is indicated in item 27. Items 28, 29, and 30, which are the source distributions, are input twice. The first set of data is for shape 2 and is obtained from the source distribution program output which was presented in figure 6(c). The data for shape 5 are from figure 8(c).

Item 31 contains eight indices which indicate the following. Store number 10, NEJECT = 10, is the store being separated and the body is to be broken into 20 segments, NSEG = 20, for the force and moment calculation with flow separation occurring at the base of the store, NSEGX0 = 20. In addition, a free-flight trajectory is to be calculated, NGAM = 0; two polynomials are to be input describing the body shape, NPOLY = 2; rolling moment is to be calculated, NROLL = 1; the store has an empennage, NEMP = 1; and aerodynamic damping is to be included, NDAMP = 1.

Item 32 contains the mass and inertia characteristics of the separated store. The particular numbers used in this example have been assigned and have not been determined by specifying a density distribution of the store and performing the required integrations. Item 33 specifies that the inertia characteristics are assumed to have been calculated about a point 5.3125 feet behind the store nose and that the store center of gravity is not offset from this point.

Items 34 and 35 contain the end points and coefficients of the polynomials describing the store shape. These data are the same as those used in the source distribution calculation for this shape except that a polynomial for the wake is not required since the load distributions are not calculated on the wake. The last end point could have been 1.0 rather than 1.1 as shown.

The store axial force coefficient, 0.4, and crossflow drag coefficient, 0.0, are input in item 36. A crossflow drag coefficient is not used in this example since flow separation is not assumed to occur ahead of the store base.

Items 37 and 38 are data describing the store empennage. Item 37 specifies a cruciform empennage and five control points on each tail panel. Item 38 indicates that the empennage forces act 9.376 feet behind the store nose, the body radius in the fin region is 0.625 feet, the fin semispan is 1.45833 feet, the initial fin orientation is 45° from the vertical and horizontal, and the lift-curve slope is 3.22. The fin details are obtained from figure 5(d) and scaled up by a factor of 20.

Item 39 specifies an initial downward translational velocity of the store of 10 feet per second and an initial pitching rate velocity of 0.0.

The last card of input, item 40, provides a guess at the integration interval and the initial and final times. Since the initial time is 0.0, item 41 is not included.

Input data have been prepared for a second sample trajectory calculation. The configuration is shown in figure 18. It is made up of the model components shown in figure 5 which again have been scaled up by a factor of 20. In this case there is a pylon with a TER under the fuselage centerline. The bottom store on the rack is being ejected with its initial position one radius below the carriage position. In this case there is a store under each wing panel since they will each have an equal effect on the trajectory.

The input data deck for this case is listed in figure 19. An item-by-item description of this deck will not be given. With the detailed description which was given for the deck of figure 17, the program user should be able to understand the preparation of the deck of figure 19. The major differences are

- (1) The pylon is under the fuselage.
- (2) There is a TER on the pylon.
- (3) There is a store under the right wing panel.
- (4) The separated store does not have an empennage.

4.3 Output from the Program

4.3.1 Sample trajectory - case 1

Figure 20 presents the output from the trajectory program for sample case 1, the configuration of figure 16, and the data deck of figure 17.

The first three pages of output are self-explanatory since they tabulate input data for the flight conditions, fuselage, wing, and pylon. The fourth page of output, figure 20(d), tabulates the coordinates of the wing and pylon vortex-lattice control points along with the input values of the slope of the wing camberline at these points. The x, y, z coordinates are in the wing coordinate system, see figure 14, whose origin is at the leading edge of the wing root chord. These points are in the wing chordal plane. Thus, for wings with dihedral, the z -coordinate will not be zero. The next page of output, figure 20(e), tabulates the input values of the slopes of the thickness distribution for all chordwise rows on both the wing and pylon. Figure 20(f) lists the input data describing the four stores present.

Page 7 of the output, figure 20(g), is another page of output pertaining to the wing-pylon vortex lattice. The x, y, z coordinates are the same as those tabulated in figure 20(d). The next three columns, $U/VINF$, $V/VINF$, and $W/VINF$, are the sums of the dimensionless perturbation velocities in the x , y , and z directions, respectively, induced at the control points by all of the other aircraft components. These include fuselage, rack, and stores as well as wing thickness on pylon and pylon thickness on wing. $VINF$ is the free-stream velocity. The last column tabulates the strengths of the horseshoe vortices divided by the free-stream velocity, $\Gamma/VINF$, which were determined by solving the set of simultaneous equations given by equation (6) and (7) of reference 1.

Page 8 of the output, figure 20(h), indicates the number of the store separated and tabulates the additional data which were read in to describe this store.

The last three parts of figure 20, parts i, j, and k, are output for three points in the trajectory, the first point, an intermediate point, and the point at which the trajectory is terminated. The complete output from the program will contain a page like this for each integration step, in this case every 0.05 seconds.

At the top of each page is the trajectory time in seconds. Following this, the forces and moments are tabulated, components as well as totals, and then the body load distributions and the velocity distributions along the store axis from which these load distributions were calculated. The load distributions are the sums of those due to buoyancy, slender body, and viscous crossflow. The velocity field calculation is discussed in detail in section 5.1 of reference 1 and the force and moment calculation in sections 5.2 and 5.3.

The following table relates the program output variables to the x_s, y_s, z_s coordinate system and positive directions shown in figure 21.

<u>Program Notation</u>	<u>Notation of Figure 21</u>
CN	C_N
CY	C_Y
CLM	C_m
CLN	C_n
CLL	C_ℓ
X, FT	x_s , feet
X/L	x_s/ℓ_s
DCN/DX	dC_N/dx_s , per foot
DCY/DX	dC_Y/dx_s , per foot
U/VS	U_s/V_{∞_s}
V/VS	V_s/V_{∞_s}
W/VS	W_s/V_{∞_s}

As the store pitches, yaws, and rolls during the trajectory, the x_s, y_s, z_s coordinate system pitches, yaws, and rolls with it. The velocities and forces are always calculated in this coordinate system.

The remaining quantities tabulated on each page of trajectory output specify the store location, orientation, velocities, and accelerations relative to the parent aircraft at that particular time. Before discussing these quantities, the coordinate systems must be mentioned. Figure 21 shows another coordinate system, x, y , and z , which is fixed in the store

and moves with the store as it yaws, pitches, and rolls. The origin of this system is fixed at the store moment center. This coordinate system is also shown in figure 22 along with another system, ξ, η, ζ . This latter system is an inertial coordinate system whose origin is fixed in the fuselage nose and is parallel to the x_B, y_B, z_B system of figure 13. At any point in time, the two coordinate systems are orientated with respect to each other by a system of angles. The system of angles are those shown in figure 22 and consist of three rotations in the yaw, Ψ , pitch, Θ , and roll, Φ sequence. The positive sense of the three store rotational velocities about the x, y, z axes are also shown in the figure.

Following the load and velocity distribution output on, for example, figure 20(j), the location of the store in the fuselage, or inertial, coordinate system is tabulated. The location of the store nose, NOSE, moment center, XMOM, and base, BASE, are tabulated relative to the fuselage nose and also relative to the position of the store at time $t = 0$. In this tabulation XF is x_B of figure 13 or ξ of figure 22. Likewise, YF is y_B or η and ZF is z_B or ζ .

The next output are the translational velocities and accelerations of the store relative to the moving aircraft. For example,

$$DXF = \frac{dx_B}{dt} \text{ or } \frac{d\xi}{dt}, \text{ ft/sec}$$

$$D2XF = \frac{d^2x_B}{dt^2} \text{ or } \frac{d^2\xi}{dt^2}, \text{ ft/sec}^2$$

Next the rotational velocities shown in figure 22 are listed as are the rotational accelerations. The notation is

$$P = p, \text{ radians/sec}$$

$$Q = q, \text{ radians/sec}$$

$$R = r, \text{ radians/sec}$$

$$PDOT = \frac{dp}{dt}, \text{ radians/sec}^2$$

$$QDOT = \frac{dq}{dt}, \text{ radians/sec}^2$$

$$RDOT = \frac{dr}{dt}, \text{ radians/sec}^2$$

The last output printed at each integration step are the values of the three orientation angles shown in figure 22 and their time rates of change. The notation is

$$\text{PSI} = \Psi, \text{ deg.}$$

$$\text{THETA} = \Theta, \text{ deg.}$$

$$\text{PHI} = \Phi, \text{ deg.}$$

$$\text{DPSI} = \frac{d\Psi}{dt}, \text{ radians/sec}$$

$$\text{DTHETA} = \frac{d\Theta}{dt}, \text{ radians/sec}$$

$$\text{DPHI} = \frac{d\Phi}{dt}, \text{ radians/sec}$$

4.3.2 Sample trajectory - case 2

The output for the second sample trajectory are presented in figure 22. This case was shown in figure 18 with the input data deck listed in figure 19. The output is basically in the same format as that shown in figure 20 for case 1 with one exception. An additional page of output is printed which tabulates the rack input data.

5. PROGRAM RUNNING TIMES

The programs described in this report have been run on both the Univac 1108 and the CDC 6600. Because of machine differences, the running times vary from one machine to the other. As a consequence, only an approximate running time for each of the two programs can be given. On any machine comparable to the previously mentioned, the source distribution program should take 3 to 5 seconds per distribution.

The running time of the trajectory program is a function of a number of additional factors, some of which are

- (a) Number of sources required to represent the bodies
- (b) Number of stores present
- (c) Number of vortices used in vorticity distribution
- (d) Number of thickness panels on wing and pylon
- (e) Number of body segments and tail fin control points used in force and moment calculation

(f) Integration interval

(g) Real time duration of trajectory

With the exception of (f) above, all of the other things should be kept to a minimum. The integration routine used in the program selects the integration interval to be used based on accuracy requirements which are incorporated in the program. In arriving at this interval, it uses the guess which was input. For the program to run with the largest interval, too large a guess is better than too small. For the two sample trajectories which were presented, the running times were 2 to 3 minutes on the CDC 6600 and 7 to 8 minutes on the Univac 1108.

TABLE I
SMALL BOATTAIL STORE COORDINATES

Station, inches	Radius, inches
0	0
0.112	0.067
0.212	0.108
0.312	0.139
0.412	0.161
0.512	0.180
0.612	0.195
0.712	0.209
0.812	0.222
0.912	0.232
1.012	0.241
1.112	0.248
1.212	0.254
1.312	0.258
1.412	0.262
1.512	0.265
1.612	0.266
1.712	0.267
1.812	0.267
1.912	0.268
2.312	0.268
2.412	0.266
2.512	0.264
2.612	0.259
2.712	0.254
2.812	0.248
2.912	0.241
3.012	0.234
3.173	0.222
3.812	0.175
4.430	0.175

TABLE II
SUBROUTINES USED IN SIX-DEGREE-OF-FREEDOM TRAJECTORY PROGRAM

<u>Subroutine Name</u>	<u>Function</u>
ADAMS	Numerical integration routine to integrate differential equations
CEL1	Calculates complete elliptic integral of the first kind
CEL2	Calculates complete elliptic integral of the second kind
DIRCOS	Calculates direction cosines between inertial and store body coordinate systems
ELI1	Calculates generalized elliptic integral of the first kind
ELI2	Calculates generalized elliptic integral of the second kind
EMPFOR	Calculates store empennage forces and moments
EMPINI	Initializes for empennage force and moment calculation
FORCE	Calculates the store-body forces and moments
INFWW	Calculates velocities induced at a field point by a horseshoe vortex
INTOST	Transforms a vector with components in the inertial coordinate system to one with component in the store body coordinate system
INVERS	Solves a system of simultaneous linear algebraic equations
OUTPUT	Prints forces, moments, load distributions, and trajectory data at the end of each integration step
PTHIN	Reads in pylon thickness data and lays out thickness strips
PVLIN	Reads in pylon vortex-lattice data and lays out vortices
SHAPE	Calculates radius and surface slope at a point on separated store from input polynomials
SIMSON	Performs a Simpson rule integration

TABLE II (conc.)

<u>Subroutine Name</u>	<u>Function</u>
SOROUT	Prints an input source distribution
STRIO	Reads in and prints out data for all stores present
STTOIN	Transforms a vector with components in the store body coordinate system to one with components in the inertial coordinate system
THOUT	Prints wing and pylon surface slopes
THPVEL	Calculates velocities induced at a field point by the pylon thickness distribution
THWVEL	Calculate velocities induced at a field point by the wing thickness distribution
VELFLD	Calculates velocities induced at a field point by all aircraft components
VELOC	Calculates velocities at a field point of an axisymmetric body
VLCOEF	Calculates coefficient matrix of set of equations to be solved for wing-pylon vorticity distribution
VLIVEL	Calculates velocities induced at a field point by wing-pylon vorticity distribution and calls THWVEL and THPVEL
VLOUT	Prints vortex lattice control point coordinates and input twist and camber distribution
VLRRHS	Calculates right-hand side of set of equations to be solved for wing-pylon vorticity distribution
VSTOUT	Prints interference velocities at vortex-lattice control points and vortex strengths
WTHIN	Reads in wing thickness data and lays out thickness strips
WVLIN	Reads in wing vortex-lattice data and lays out vortices


```

IF (NBB,LT,NSORC) NAA=NAA+1
DO 102 J=1,NAA
  NBB=6*(J-1)+1
  NCENB=5
  IF (NC,GT,NSORC) NCENB=NC
  WRITE (6,731) (X(N),NENB,NC)
  102 WRITE (6,732) (X(N),NENB,NC)
C
C CALCULATE BODY SHAPE FROM SOURCE DISTRIBUTION
C
X=XINIT
EPS=5.0E-07
WRITE (6,701)
WRITE (6,719)
J=0
55 RERMAX
  J=J+1
  M=1
  52 PSI=R/R+0.5
  AMX=X(K)
  51 PSI=PSI-G(K)*(1.0*X/M/SORT(X*M*R*R))
  TEM=1
  IF (ABS(PSI),LE,EPS) GO TO 54
  IF (PSI,LT,0.0) RER=RMX/(2.0*(M-1))
  IF (PSI,GT,0.0) RER=RMX/(2.0*(M-1))
  IF (X,LT,0.0001) GO TO 54
  IF (X,LT,1.20) GO TO 52
  54 X(J)=1.20 GO TO 52
  R(J)=R/BETA
  IF (J,EQ,7) GO TO 200
  53 X=DEL
  IF (X,GT,NAL) 55,55,56
  56 IF (J,EQ,0) GO TO 4
  200 WRITE (6,728) (X(N),N=1,J)
  WRITE (6,729) (R(N),N=1,J)
  J=J
  J=J
  IF (J,GT,7) 4,53,53
  END
C
C SUBROUTINE TO SOLVE SIMULTANEOUS EQUATIONS
C
SUBROUTINE INVER(A,NSYS,N,NMAX,MMAX)
DIMENSION A(NMAX,MMAX),X(150)
5 SIGN=1.0
  NPT=N+1
  NPLSY=N+NSYS
  DO 14 I=1,NMI
    IP1=I+1
    MAX=1
    AMAX=ABS(A(I,I))
    DO 10 K=IPI,N
      AKMAX=ABS(A(K,I))
      IF (AKMAX,LE,AMAX) GO TO 10
      MAX=K
      AMAX=AKMAX
    10 CONTINUE
    IF (AMAX,LT,1.0E-12) GO TO 16
    IF (MAX,EQ,I) GO TO 12
    DO 11 L=I,NPLSY
      TEM=A(I,L)
      A(I,L)=A(MAX,L)
      A(L,I)=TEM
      SIGN=-SIGN
    11 CONTINUE
    DO 14 J=IPI,N
      IF (A(J,I)) 30,14,30
  12
  14

```

```

30 CONST=A(J,I)/A(I,I)
  DO 13 L=1,NPLSY
    A(J,L)=A(J,L)+A(I,L)*CONST
  13 CONTINUE
  DEL=0.0
  TEM=1.0
  DO 15 I=1,N
    IF (A(I,I)) 15,16,15
  15 TEM=TEMP*A(I,I)
    DET=SIGN*TEMP
    DET=SIGN*TEMP
    GO TO 18
  16 WRITE(6,100)
  100 FORMAT(5X,'BMMATRIX IS SINGULAR')
  STOP
  DO 21 I=NPI,NPLSY
    DO 20 K=1,N
      X(K)=X(K,I)
      IF (K,EQ,N) GO TO 20
      J=J+1
      X(K)=X(K)-A(K,J)*X(J)
      IF (J,NE,N) GO TO 19
    20 X(K)=X(K)/A(K,K)
    DO 21 J=1,N
      21 A(J,I)=X(J)
    RETURN
  END
C
C SUBROUTINE TO CALCULATE SHAPE
C
SUBROUTINE SHAPE (X,NB,XE,C,R,DRDX)
DIMENSION XE(7),C(7,7)
DO 1 K=1,NS
  XL=XE(K)
  J=K
  IF (X,LE,XL) GO TO 2
  1 CONTINUE
  2 R=C(J,I)+X*C(J,5)+X*X*C(J,6)
  ARG=X*X*C(J,2)+X*C(J,3)+C(J,4)
  DRDX=C(J,5)+2.0*X*C(J,6)
  IF (ARG,LE,0.0) RETURN
  R=R+80RT(ARG)*C(J,7)
  DRDX=DRDX+(2.0*X*C(J,2)+C(J,3))/(2.0*80RT(ARG))*C(J,7)
  RETURN
  END
30A3 1
30A3 2
30A3 3
30A3 4
30A3 5
30A3 6
30A3 7
30A3 8
30A3 9
30A3 10
30A3 11
30A3 12
30A3 13
30A3 14
30A3 15
30A3 16
30A3 17

```

(b) Page 2.

Figure 1.- Concluded.

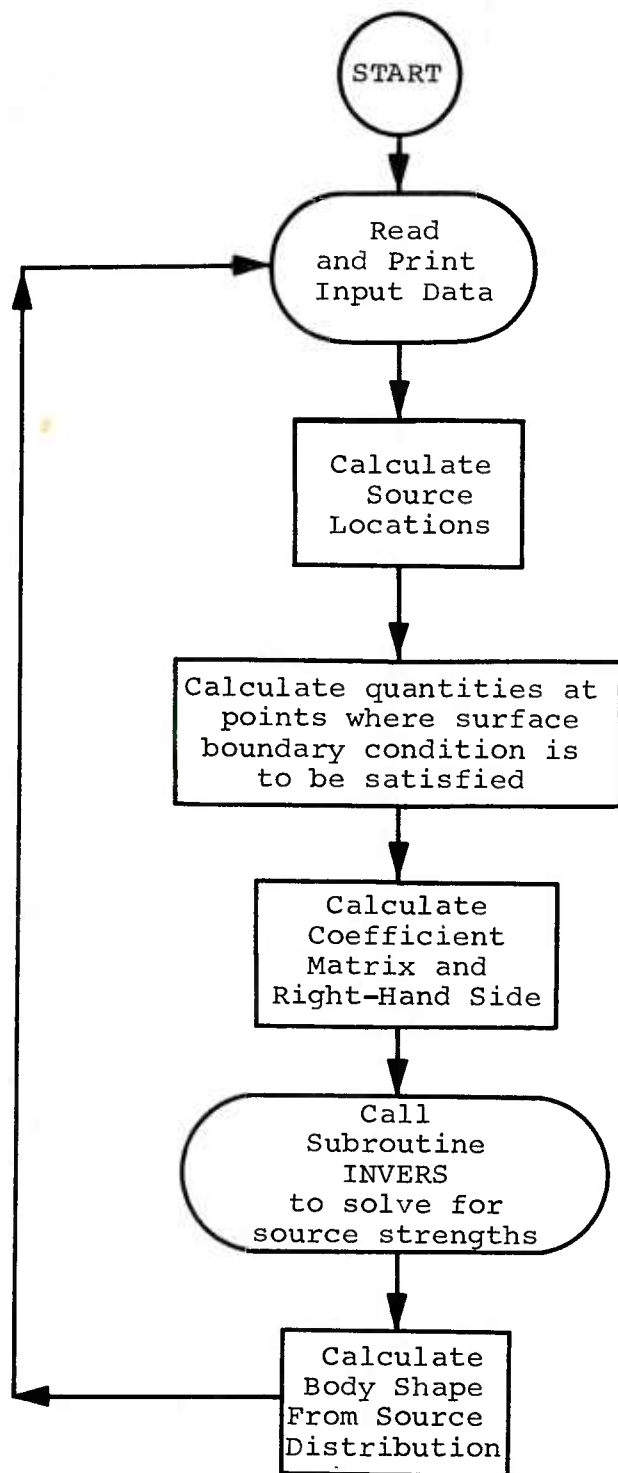


Figure 2.- General flow chart of source distribution program.

Item No. 1 (1 card)

Variable	NCARDS
Card Column	5
Format Type	I

Item No. 2 (NCARDS cards)

Variable	Q	80
Card Column		
Format Type	A	

Item No. 3 (1 card)

Variable	NSECT	FMACH
Card Column	5	15
Format Type	I	F

Item No. 4 (1 card)

Variable	XEND(1)	XEND(2)	...	XEND(NSECT)			
Card Column	10	20	30	40	50	60	70
Format Type	F	F	F	F	F	F	F

Item No. 5 (J = 1 to NSECT; NSECT cards)

Variable	COEF(J,1)	COEF(J,2)	COEF(J,3)	COEF(J,4)	COEF(J,5)	COEF(J,6)	COEF(J,7)
Card Column	10	20	30	40	50	60	70
Format Type	F	F	F	F	F	F	F

Item No. 6 (1 card)

Variable	XSFST	XSLST	PERCR	XRMAX	XINIT	XFINAL	DELX	RMAX
Card Column	10	20	30	40	50	60	70	80
Format Type	F	F	F	F	F	F	F	F

Figure 3.- Source distribution program input format.

2
OGIVE-CYLINDER STORE WITH WAKE MODELED WITH SAME SHAPE AS NOSE
CALCULATION FOR MACH NUMBER OF 0.4

3 0.4
0.2353 1.0 1.2353
-0.4413 -1.0 0.4706 0.1947 1.0
0.05882
-0.4413 -1.0 2.0 -0.7499 1.0
0.002 1.23 0.7 0.2353 0.01 1.23 0.02 0.05882

(a) Ogive-cylinder store.

2
FUSELAGE WITH WAKE MODELED BY CONTINUATION OF AFTERBODY
CALCULATION FOR MACH NUMBER OF 0.4

3 0.4
0.32 0.7534 1.1752
-1.0975 -1.0 0.64 1.2045 1.0
0.0457
-1.9237 -1.0 1.5068 3.3109 1.0
0.002 1.17 1.0 0.32 0.01 1.17 0.02 0.0457

(b) Fuselage.

2
SMALL BOATTAIL STORE WITH CIRCULAR ARC USED TO MODEL WAKE
CALCULATION FOR MACH NUMBER OF 0.4

7 0.4
0.0478 0.1381 0.3187 0.7162 0.8363 1.0 1.05
-0.20198 -1.19048 0.27490 0.04080 1.0
-0.37945 -1.19048 0.40120 0.14655 1.0
-70.50828 -1.19048 12.394484975.93318 1.0
-1.98790 -1.19048 1.09634 3.96180 1.0
1.00320 -1.19048 1.99121 0.10092 -1.0
0.03700
-0.02172 -1.19048 2.38095 -1.18702 1.0
0.002 1.045 0.7 0.4316 0.01 1.03 0.02 0.0605

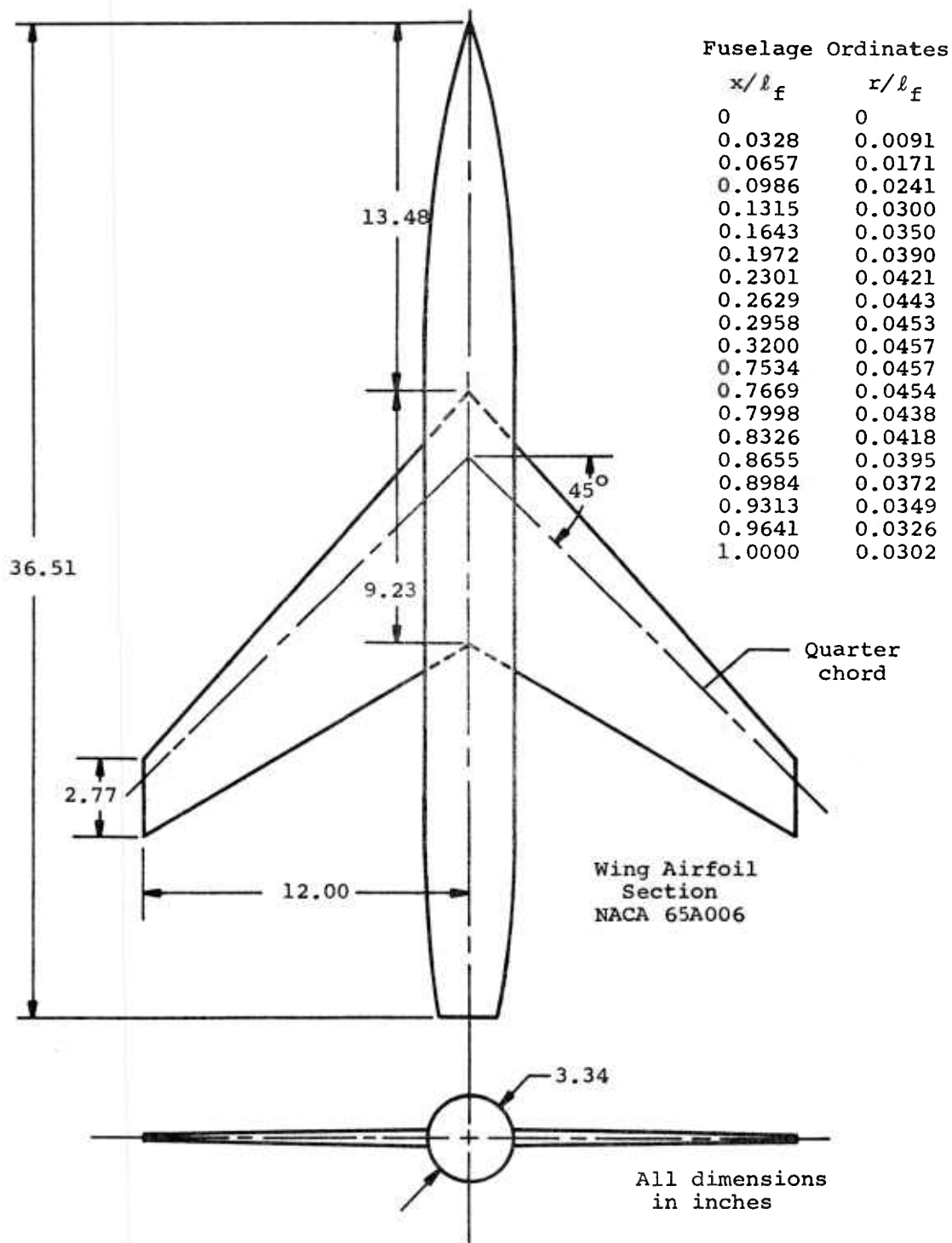
(c) Small boattail store.

2
TRIPLE EJECTION RACK WITH WAKE MODELED BY CONTINUATION OF AFTERBODY
CALCULATION FOR MACH NUMBER OF 0.4

3 0.4
0.24424 0.89195 1.02936
-0.05421 0.02648 1.0
0.05687
-0.13691 -1.0 1.7839 -0.75802 1.0
0.002 1.02 0.6 0.24424 0.01 1.01 0.02 0.05687

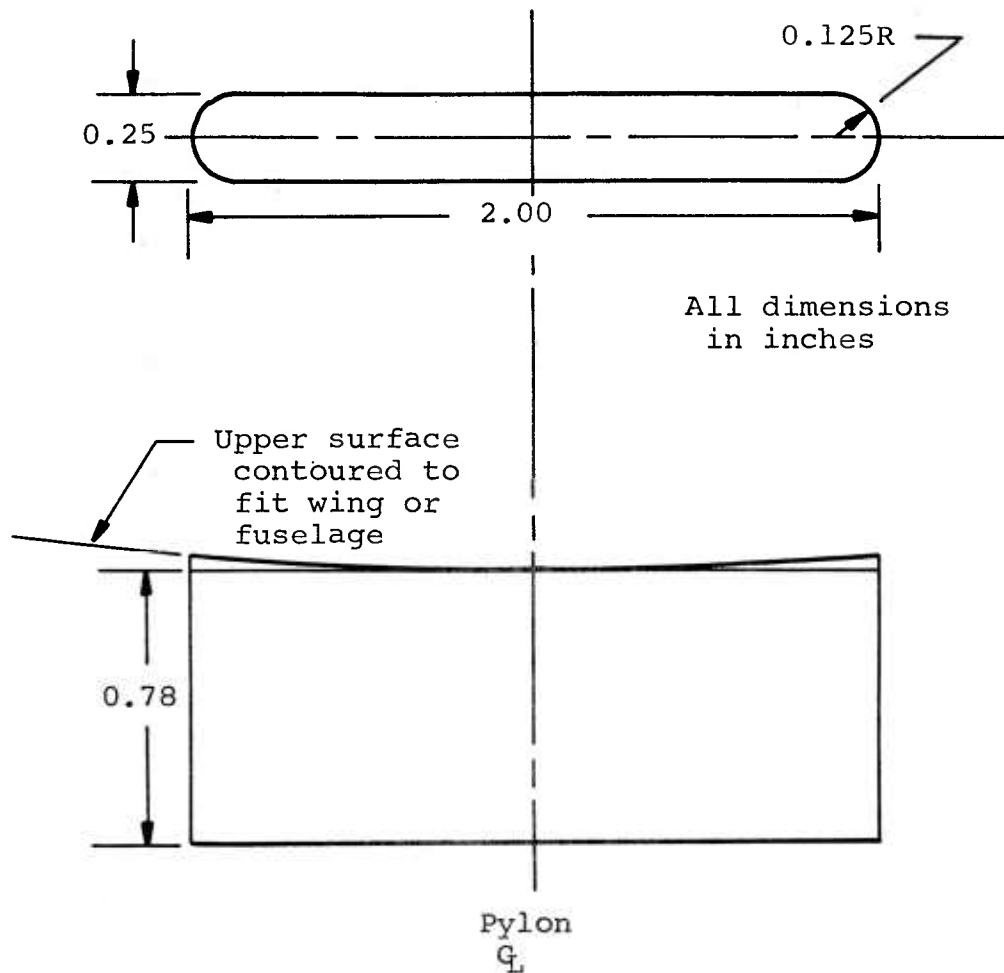
(d) Triple ejection rack.

Figure 4.- Sample input data for source distribution program.



(a) Wing-fuselage combination.

Figure 5.- Wind-tunnel models used in sample calculations.

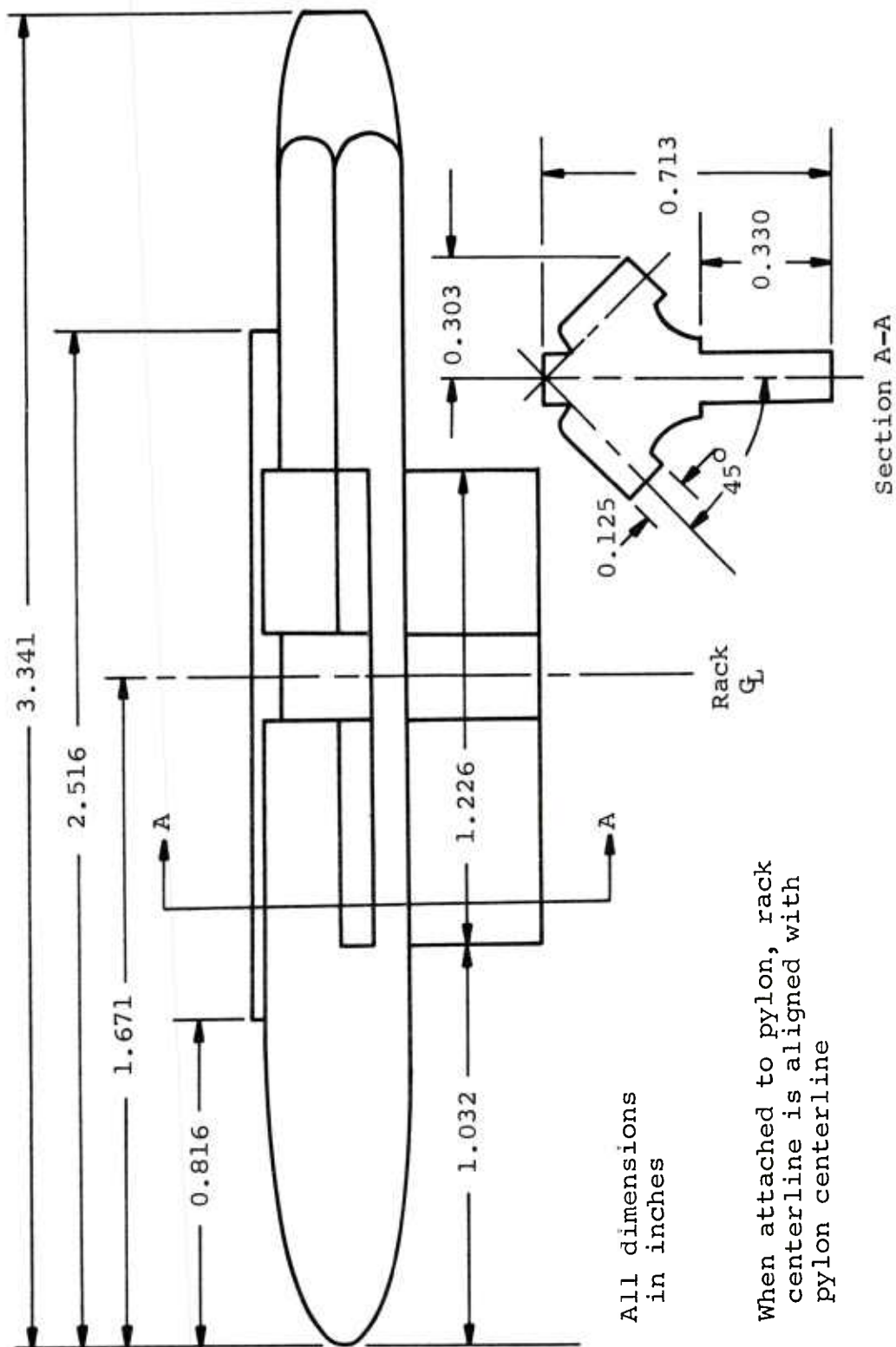


For wing pylons, pylon centerline located at 40% wing chord.

For fuselage pylon, pylon centerline located 19.43 inches aft of fuselage nose.

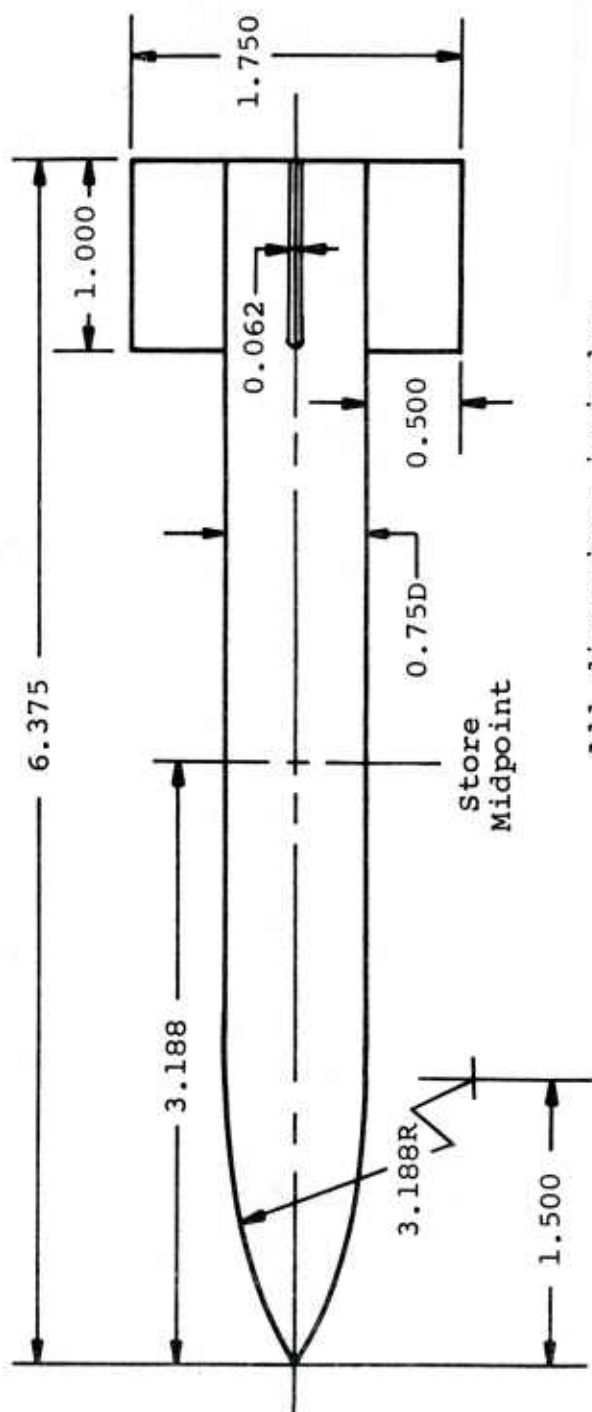
(b) Pylon used with single store and TER rack.

Figure 5.- Continued.



(c) Details of TER rack.

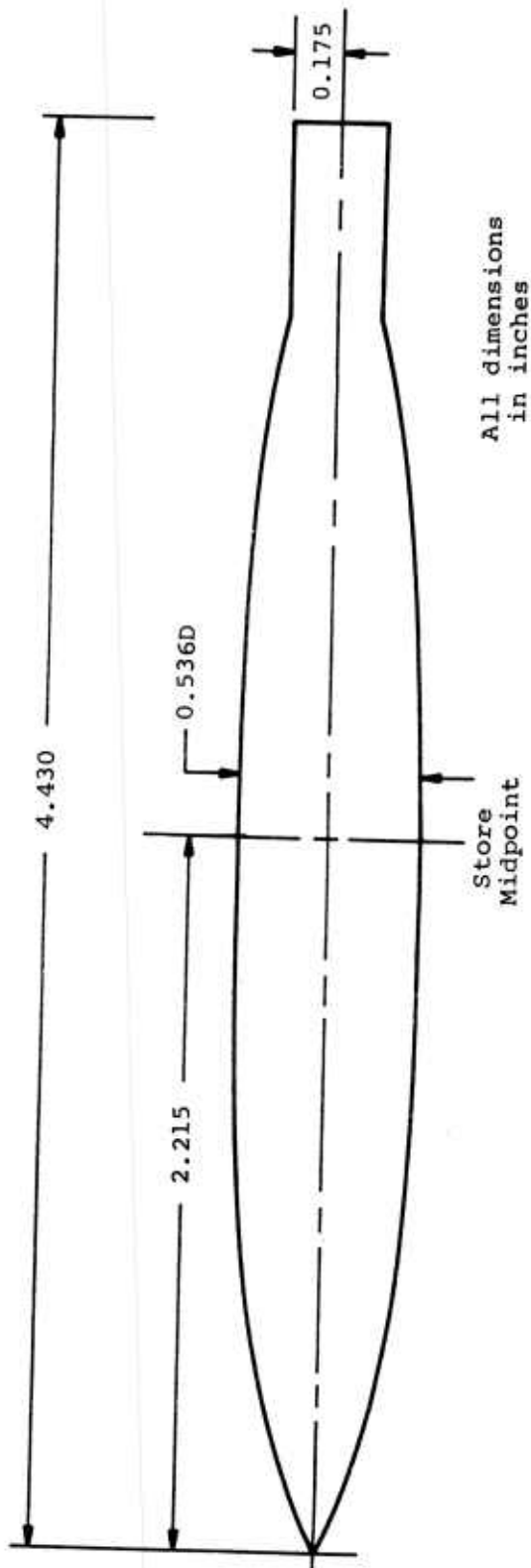
Figure 5.- Continued.



All dimensions in inches.

(d) Ogive-cylinder store with rectangular cruciform fins.

Figure 5.- Continued.



Store midpoint aligned with suspension centerline
on TER rack when in carriage position.

(e) Small boattail store.

Figure 5.- Concluded.

FOR THIS CASE THERE ARE 51 SOURCES

INCOMPRESSIBLE SOURCE DISTRIBUTION FOR EACH NUMBER

X/L	2.0000-03	2.8473-03	3.5132-03	4.6705-03	5.2109-03	6.2721-03
0	4.8513-06	-4.3213-06	2.4420-06	-7.1044-07	1.2030-08	1.0483-06
X/L	1.1000-02	1.4620-02	1.9400-02	2.4061-02	3.3810-02	4.5910-02
0	2.5749-05	4.3291-06	7.8030-06	1.3010-05	2.3010-05	3.7407-05
X/L	5.7099-02	7.4405-02	9.5145-02	1.1909-01	1.4904-01	1.8104-01
0	5.9534-05	8.9502-05	1.2214-04	1.5482-04	1.2020-04	2.0261-04
X/L	2.1781-01	2.5531-01	2.9305-01	3.3079-01	3.6852-01	4.0620-01
0	-5.0470-05	-1.1398-04	1.1594-04	-1.2468-04	1.2050-04	-1.2020-04
X/L	4.4400-01	4.8173-01	5.1947-01	5.5721-01	5.9494-01	6.3268-01
0	1.2144-04	-1.2260-04	1.2145-04	-1.2235-04	1.2211-04	-1.2213-04
X/L	6.7042-01	7.0615-01	7.4389-01	7.8263-01	8.2130-01	8.5910-01
0	1.2235-04	-1.2188-04	1.2265-04	-1.2149-04	1.2130-04	-1.2063-04
X/L	9.3457-01	9.7231-01	1.0100-01	1.0477-01	1.0840-01	1.1204-01
0	1.2450-04	-1.1674-04	1.1595-04	1.1480-04	-1.1327-04	1.1271-04
X/L	1.1711-00	1.1459-00	1.1697-00	1.1084-00	1.2023-00	1.2127-00
0	-1.7495-04	-1.3912-04	-9.3587-05	-5.4285-05	-2.4460-05	-1.2350-05
X/L	1.2200-00	1.2250-00	1.2284-00			
0	-1.0227-05	4.6640-06	-1.1713-05			

(c) Page 3.

SHAPE CALCULATED FROM SOURCE DISTRIBUTION

X/L	0.1000	0.3000	0.5000	0.7000	0.9000	1.1000	1.3000
R/L	0.0597	0.1499	0.2332	0.3079	0.3724	0.4291	0.4762
X/L	1.5000	1.7000	1.9000	2.1000	2.3000	2.5000	2.7000
R/L	0.3152	0.5474	0.5715	0.5858	0.5908	0.5944	0.5969
X/L	2.9000	3.1000	3.3000	3.5000	3.7000	3.9000	4.1000
R/L	0.5866	0.5908	0.5894	0.5884	0.5894	0.5904	0.5946
X/L	4.5000	4.5000	4.7000	4.9000	5.1000	5.3000	5.5000
R/L	0.5869	0.5904	0.5906	0.5892	0.5891	0.5906	0.5905
X/L	5.7000	5.9000	6.1000	6.3000	6.5000	6.7000	6.9000
R/L	0.5891	0.5895	0.5908	0.5901	0.5884	0.5899	0.5908
X/L	7.1000	7.3000	7.5000	7.7000	7.9000	8.1000	8.3000
R/L	0.5896	0.5889	0.5902	0.5908	0.5893	0.5904	0.5905
X/L	8.5000	8.7000	8.9000	9.1000	9.3000	9.5000	9.7000
R/L	0.5905	0.5891	0.5893	0.5908	0.5902	0.5884	0.5896
X/L	9.9000	1.0100	1.0300	1.0500	1.0700	1.0900	1.1100
R/L	0.5911	0.5889	0.5806	0.5846	0.5845	0.5841	0.5847
X/L	1.1300	1.1500	1.1700	1.1900	1.2100	1.2300	1.2500
R/L	0.5862	0.5802	0.2932	0.2177	0.1344	0.0460	

(d) Page 4.

OGIVE-CYLINDER STORE WITH WAKE MODELED WITH SAME SHAPE AS HOSE
CALCULATION FOR EACH NUMBER OF 0.4

X/L OF END POINT OF EACH SECTION OF BODY

SECTION	1	2	3
X/L	2.2550	1.0000	1.2350

COEFFICIENTS OF POLYNOMIAL DESCRIBING EACH SECTION

SECTION	C1	C2	C3	C4	C5	C6	C7
1	-44130	-1.00000	4.7060	1.9470	0.0000	0.0000	1.0000
2	0.05882	0.00000	0.0000	0.0000	0.0000	0.0000	0.0000
3	-44130	-1.00000	2.00000	-1.74990	0.0000	0.0000	1.0000

FIRST SOURCE AT X/L = 0.0200
SOURCE SPACING IS .70000 TIMES LOCAL INCOMPRESSIBLE R/L

(a) Page 1.

SOURCE LOCATIONS AND BODY RADIUS AND SURFACE SLOPE AT THESE LOCATIONS

X/L	0.0200	0.0265	0.0351	0.0467	0.0621	0.0827	0.1101
R/L	0.0101	0.0135	0.0180	0.0241	0.0321	0.0426	0.0564
DR/X	52746	52559	52310	51978	51537	50953	50184
X/L	0.1463	0.1940	0.2566	0.3381	0.4432	0.5770	0.7449
R/L	0.0744	0.0976	0.1270	0.1638	0.2086	0.2617	0.3220
DR/X	49176	47865	46176	44025	41324	37992	33963
X/L	0.9515	1.1999	1.4904	1.8194	2.1781	2.5531	2.9305
R/L	0.3672	0.4529	0.5127	0.5591	0.5846	0.5882	0.5862
DR/X	29197	23698	17511	10732	0.5500	0.0000	0.0000
X/L	3.3079	3.6852	4.0626	4.4400	4.8173	5.1947	5.5721
R/L	0.5882	0.5882	0.5882	0.5882	0.5882	0.5882	0.5882
DR/X	0.0000	0.0000	0.0000	0.0000	0.0000	0.0000	0.0000
X/L	5.9494	6.3268	6.7042	7.0815	7.4569	7.8363	8.2136
R/L	0.5882	0.5882	0.5882	0.5882	0.5882	0.5882	0.5882
DR/X	0.0000	0.0000	0.0000	0.0000	0.0000	0.0000	0.0000
X/L	8.5910	8.9684	9.3457	9.7231	1.01005	1.04770	1.08397
R/L	0.5882	0.5882	0.5882	0.5882	0.5870	0.5852	0.58170
DR/X	0.0000	0.0000	0.0000	0.0000	-0.02009	-0.09583	-1.17032
X/L	1.11713	1.14593	1.16969	1.18838	1.20247	1.21272	1.21948
R/L	0.4469	0.3703	0.2913	0.2196	0.1598	0.10762	0.06762
DR/X	-24092	-30509	-36072	-40664	-44277	-47000	-48979
X/L	1.22499	1.22841					
R/L	0.0533	0.0359					
DR/X	-50376	-51341					

(b) Page 2.

Figure 6.- Ogive-cylinder store source distribution output.

FOR THIS CASE THERE ARE NO SOURCES

INCOMPRESSIBLE SOURCE DISTRIBUTION FOR EACH NUMBER 440

X/L	2.0000-03	2.5300-03	3.2000-03	4.0000-03	5.1200-03	6.1000-03
u	0.0353-06	-5.4782-06	3.5395-06	-2.1783-06	1.6162-06	-6.6496-07
X/L	8.1831-03	1.0337-02	1.3040-02	1.6450-02	2.0729-02	2.6072-02
u	1.0445-06	3.1040-07	1.3737-06	1.6004-06	2.1400-06	2.8260-06
X/L	3.2730-02	4.0933-02	5.1142-02	6.3097-02	7.8000-02	9.7224-02
u	6.6430-06	9.9387-06	1.4413-05	2.1403-05	3.0000-05	4.0582-05
X/L	1.1902-01	1.4458-01	1.7400-01	2.0777-01	2.4415-01	2.8372-01
u	5.2073-05	6.2487-05	6.8767-05	7.2400-05	7.3261-05	7.4004-05
X/L	3.2500-04	3.6696-04	4.0885-04	4.5073-04	4.9262-04	5.3450-04
u	-7.6629-07	-1.2700-05	9.9914-06	-1.1501-05	1.0717-05	-1.1060-05
X/L	5.7393-01	6.1827-01	6.6018-01	7.0204-01	7.4393-01	7.8581-01
u	1.1063-05	-1.0703-05	1.1553-05	-9.8993-06	1.6490-05	-1.3206-05
X/L	8.2745-01	8.6805-01	9.0887-01	9.4920-01	9.8973-01	1.0070-01
u	-3.1426-05	-4.5538-05	-5.3833-05	-5.6492-05	-5.3967-05	-4.8229-05
X/L	1.0338-00	1.0573-00	1.0776-00	1.0944-00	1.1094-00	1.1215-00
u	-4.0372-05	-3.2497-05	-2.4705-05	-1.8652-05	-1.3021-05	-9.7400-06
X/L	1.1316-00	1.1599-00	1.1467-00	1.1524-00	1.1564-00	1.1603-00
u	-5.9456-06	-5.1103-06	-1.9394-06	-3.3003-06	7.1284-07	-3.6450-06
X/L	1.1632-00	1.1656-00	1.1675-00	1.1690-00	1.1690-00	1.1690-00
u	3.4910-06	-6.0077-06	6.0040-06	-9.4139-06		

(c) Page 3.

SHAPE CALCULATED FROM SOURCE DISTRIBUTION

X/L	0.1000	0.3000	0.5000	0.7000	0.9000	1.1000
R/L	0.0404	0.0910	0.1363	0.1839	0.2263	0.2651
X/L	1.5000	1.7000	1.9000	2.1000	2.3000	2.5000
R/L	0.3325	0.3606	0.3854	0.4068	0.4253	0.4409
X/L	2.9000	3.1000	3.3000	3.5000	3.7000	3.9000
R/L	0.4579	0.4612	0.4628	0.4630	0.4628	0.4624
X/L	4.3000	4.5000	4.7000	4.9000	5.1000	5.3000
R/L	0.4630	0.4628	0.4624	0.4620	0.4616	0.4612
X/L	5.7000	5.9000	6.1000	6.3000	6.5000	6.7000
R/L	0.4626	0.4620	0.4616	0.4612	0.4608	0.4604
X/L	7.1000	7.3000	7.5000	7.7000	7.9000	8.1000
R/L	0.4624	0.4620	0.4616	0.4612	0.4608	0.4604
X/L	8.5000	8.7000	8.9000	9.1000	9.3000	9.5000
R/L	0.4620	0.4616	0.4612	0.4608	0.4604	0.4600
X/L	9.9000	1.01000	1.03000	1.05000	1.07000	1.09000
R/L	0.4616	0.4612	0.4608	0.4604	0.4600	0.4596
X/L	1.13000	1.15000	1.17000	1.19000	1.21000	1.23000
R/L	0.4612	0.4608	0.4604	0.4600	0.4596	0.4592

(d) Page 4.

FUSELAGE WITH WAKE MODELED BY CONTINUATION OF AFTERBODY
CALCULATION FOR EACH NUMBER OF 0.4

X/L OF LND POINT OF EACH SECTION OF BODY

SECTION	1	2	3
X/L	3.2000	7.5340	1.1750

COEFFICIENTS OF POLYNOMIAL DESCRIBING EACH SECTION

SECTION	C1	C2	C3	C4	C5	C6	C7
1	-1.00750	-1.00000	6.40000	1.20450	0.00000	0.00000	1.00000
2	0.04570	0.00000	0.00000	0.00000	0.00000	0.00000	0.00000
3	-1.92370	-1.00000	1.50680	3.31090	0.00000	0.00000	1.00000

FIRST SOURCE AT X/L = 0.0200
SOURCE SPACING IS 1.0000 TIMES LOCAL INCOMPRESSIBLE R/L

(a) Page 1.

SOURCE LOCATIONS AND BODY RADIUS AND SURFACE SLOPE AT THESE LOCATIONS

X/L	0.0200	0.0253	0.0320	0.0405	0.0512	0.0647	0.0818
R/L	0.0058	0.0073	0.0093	0.0117	0.0148	0.0186	0.0235
DN/R/L	0.28907	0.28907	0.28841	0.28758	0.28652	0.28519	0.28351
X/L	0.1034	0.1305	0.1646	0.2073	0.2607	0.3273	0.4099
R/L	0.0296	0.0372	0.0466	0.0583	0.0727	0.0902	0.1113
DN/R/L	0.28139	0.27874	0.27541	0.27124	0.26605	0.25962	0.25167
X/L	0.5119	0.6370	0.7891	0.9722	1.1902	1.4458	1.7406
R/L	0.1364	0.1660	0.1999	0.2378	0.2789	0.3234	0.3634
DN/R/L	0.24192	0.23005	0.21575	0.19868	0.17859	0.15528	0.12872
X/L	2.0737	2.4415	2.8372	3.2508	3.6896	4.0885	4.5073
R/L	0.4014	0.4318	0.4512	0.4570	0.4570	0.4570	0.4570
DN/R/L	0.09901	0.06649	0.03175	0.00000	0.00000	0.00000	0.00000
X/L	4.9262	5.3450	5.7639	6.1827	6.6016	7.0204	7.4393
R/L	0.4570	0.4570	0.4570	0.4570	0.4570	0.4570	0.4570
DN/R/L	0.00000	0.00000	0.00000	0.00000	0.00000	0.00000	0.00000
X/L	7.0581	8.2745	8.6805	9.0887	9.4920	9.8973	1.0070
R/L	0.4583	0.4440	0.4235	0.3971	0.3652	0.3299	0.2930
DN/R/L	-0.1646	-0.3782	-0.5831	-0.7816	-0.9685	-1.1414	-1.2963
X/L	1.03382	1.05731	1.07757	1.09483	1.10937	1.12152	1.13159
R/L	0.2563	0.2210	0.1863	0.1587	0.1346	0.1098	0.0804
DN/R/L	-1.1385	-1.5819	-1.6658	-1.7603	-1.8378	-1.9027	-1.9507
X/L	1.13987	1.14666	1.15218	1.15607	1.16030	1.16324	1.16560
R/L	0.0740	0.0603	0.0490	0.0396	0.0320	0.0258	0.0207
DN/R/L	-2.0013	-2.0379	-2.0677	-2.0920	-2.1117	-2.1276	-2.1404
X/L	1.16750	1.16903	1.16903	1.16903	1.16903	1.16903	1.16903
R/L	0.0167	0.0134	0.0105	0.0096	0.0086	0.0076	0.0066
DN/R/L	-2.1508	-2.1591					

(b) Page 2.

Figure 7.- Fuselage source distribution output.

FOR THIS CASE THERE ARE 44 SOURCELOC

SMALL BOATTAILED STORE WITH CIRCULAR ARC USED TO MODEL WAKE
CALCULATION FOR MACH NUMBER OF 0.4

X/L OF END POINT OF EACH SECTION OF BODY

SECTION X/L	1	2	3	4	5	6	7
	.04780	.13810	.31870	.71620	.85550	1.00000	1.05000

COEFFICIENTS OF POLYNOMIAL DESCRIBING EACH SECTION

SECTION	C1	C2	C3	C4	C5	C6	C7
1	-.02198	-1.19048	.27490	.04060	.00000	.00000	1.00000
2	-.37945	-1.19048	.40120	.14655	.00000	.00000	1.00000
3	-70.50828	-1.19048	12.39448	975.43317	.00000	.00000	1.00000
4	-1.98790	-1.19048	1.09634	3.96186	.00000	.00000	1.00000
5	1.00320	-1.19048	1.99121	.10092	.00000	.00000	-1.00000
6	.03700	.00000	.00000	.00000	.00000	.00000	.00000
7	-.02172	-1.19048	2.38095	-1.18702	.00000	.00000	1.00000

FIRST SOURCE AT X/L = .00200
SOURCE SPACING IS .70000 TIMES LOCAL INCOMPRESSIBLE R/L

(a) Page 1.

SOURCE LOCATIONS AND BODY RADIUS AND SURFACE SLOPE AT THESE LOCATIONS

X/L	R/L	DR/UX	X/L	R/L	DR/UX	X/L	R/L	DR/UX	X/L	R/L	DR/UX	X/L	R/L	DR/UX	X/L	R/L	DR/UX
.00200	.00287	.00411	.00586	.00834	.01101	.01602	.01602	.01602	.01602	.01602	.01602	.01602	.01602	.01602	.01602	.01602	.01602
.00135	.00193	.00274	.00366	.00541	.00750	.01025	.01025	.01025	.01025	.01025	.01025	.01025	.01025	.01025	.01025	.01025	.01025
.00427	.00572	.00753	.01038	.01489	.02094	.02904	.02904	.02904	.02904	.02904	.02904	.02904	.02904	.02904	.02904	.02904	.02904
.02319	.03201	.04354	.05815	.07598	.09719	.12159	.12159	.12159	.12159	.12159	.12159	.12159	.12159	.12159	.12159	.12159	.12159
.01374	.01797	.02277	.02780	.03306	.03804	.04213	.04213	.04213	.04213	.04213	.04213	.04213	.04213	.04213	.04213	.04213	.04213
.00918	.01167	.01456	.01782	.02142	.02536	.02954	.02954	.02954	.02954	.02954	.02954	.02954	.02954	.02954	.02954	.02954	.02954
.14862	.17742	.20779	.23980	.27354	.30909	.34653	.34653	.34653	.34653	.34653	.34653	.34653	.34653	.34653	.34653	.34653	.34653
.04488	.04753	.04990	.05259	.05541	.05836	.06120	.06120	.06120	.06120	.06120	.06120	.06120	.06120	.06120	.06120	.06120	.06120
.08553	.08484	.08433	.08378	.08321	.08261	.08201	.08201	.08201	.08201	.08201	.08201	.08201	.08201	.08201	.08201	.08201	.08201
.38580	.42644	.46791	.50958	.55081	.59097	.62948	.62948	.62948	.62948	.62948	.62948	.62948	.62948	.62948	.62948	.62948	.62948
.00335	.00463	.00645	.00827	.01020	.01220	.01427	.01427	.01427	.01427	.01427	.01427	.01427	.01427	.01427	.01427	.01427	.01427
.04333	.01973	-.00432	-.02849	-.05246	-.07567	-.09842	-.09842	-.09842	-.09842	-.09842	-.09842	-.09842	-.09842	-.09842	-.09842	-.09842	-.09842
.60584	.69965	.73065	.75881	.78492	.80970	.83372	.83372	.83372	.83372	.83372	.83372	.83372	.83372	.83372	.83372	.83372	.83372
.05270	.04831	.04390	.04070	.03862	.03743	.03700	.03700	.03700	.03700	.03700	.03700	.03700	.03700	.03700	.03700	.03700	.03700
-.11982	-.13984	-.13112	-.09585	-.06342	-.03279	-.00319	-.00319	-.00319	-.00319	-.00319	-.00319	-.00319	-.00319	-.00319	-.00319	-.00319	-.00319
.85746	.88119	.90493	.92867	.95241	.97614	.99988	.99988	.99988	.99988	.99988	.99988	.99988	.99988	.99988	.99988	.99988	.99988
.03700	.03700	.03700	.03700	.03700	.03700	.03700	.03700	.03700	.03700	.03700	.03700	.03700	.03700	.03700	.03700	.03700	.03700
.00000	.00000	.00000	.00000	.00000	.00000	.00000	.00000	.00000	.00000	.00000	.00000	.00000	.00000	.00000	.00000	.00000	.00000
1.02362	1.04355																
.03106	.01281																
-.53288	-1.50162																

(b) Page 2.

INCOMPRESSIBLE SOURCE DISTRIBUTION, FOR MACH NUMBER .40

X/L	2.0000-03	2.8092-03	4.1068-03	5.8023-03	8.3099-03	1.1610-02
0	3.8930-06	-2.9405-06	1.8989-06	5.6064-07	2.6280-06	9.7913-06
X/L	1.6619-02	2.3192-02	4.3538-02	4.3538-02	5.0100-02	7.4981-02
0	9.7339-06	1.8419-05	3.2418-05	5.3611-05	5.6472-05	9.3560-05
X/L	9.7189-02	1.2159-01	1.4962-01	1.7742-01	2.0179-01	2.3040-01
0	8.9716-05	9.5860-05	-5.8060-05	1.3457-04	-2.0497-04	1.2904-04
X/L	2.7354-01	3.0909-01	3.4853-01	3.8580-01	4.2644-01	4.6701-01
0	1.0512-05	1.3060-04	9.0154-05	-2.6121-05	1.2754-04	-1.0093-04
X/L	5.0958-01	5.5081-01	5.9097-01	6.2994-01	6.6584-01	6.9965-01
0	6.5806-05	-1.7406-04	3.1092-05	-2.3365-04	4.9012-05	-2.8651-04
X/L	7.3065-01	7.5881-01	7.8492-01	8.0970-01	8.3372-01	8.5740-01
0	8.2015-05	-2.0799-04	1.6071-04	-2.1183-04	2.2493-04	-2.1059-04
X/L	8.8119-01	9.0493-01	9.2867-01	9.5241-01	9.7614-01	9.9988-01
0	2.1369-04	-2.0999-04	2.1380-04	-2.0582-04	1.9470-04	2.2062-05
X/L	1.0230-00	1.0435-00				
0	-4.1387-04	1.8404-05				

(c) Page 3.

SHAPE CALCULATED FROM SOURCE DISTRIBUTION

X/L	.01000	.03000	.05000	.07000	.09000	.11000	.13000
R/L	.00709	.01725	.02523	.03152	.03660	.04050	.04322
X/L	.15000	.17000	.19000	.21000	.23000	.25000	.27000
R/L	.04496	.04682	.04845	.05004	.05170	.05347	.05511
X/L	.29000	.31000	.33000	.35000	.37000	.39000	.41000
R/L	.05672	.05840	.06003	.06159	.06316	.06471	.06624
X/L	.43000	.45000	.47000	.49000	.51000	.53000	.55000
R/L	.06437	.06467	.06497	.06529	.06560	.06591	.06622
X/L	.57000	.59000	.61000	.63000	.65000	.67000	.69000
R/L	.06103	.05972	.05840	.05619	.05394	.05181	.04980
X/L	.71000	.73000	.75000	.77000	.79000	.81000	.83000
R/L	.04605	.04328	.04103	.03858	.03606	.03354	.03100
X/L	.85000	.87000	.89000	.91000	.93000	.95000	.97000
R/L	.03639	.03580	.03542	.03505	.03467	.03429	.03391
X/L	.99000	1.01000	1.03000				
R/L	.03654	.03439	.02493				

(d) Page 4.

Figure 8.- Small boattail store source distribution output.

FOR THIS CASE THERE ARE 39 SOURCES

TRK RACK WITH WAKE MODELED BY CONTINUATION OF AFTERBODY
CALCULATION FOR MACH NUMBER OF 0.4

X/L OF LNU POINT OF EACH SECTION OF BODY

SECTION 1 2 3
X/L .24424 .89195 1.02936

COEFFICIENTS OF POLYNOMIAL DESCRIBING EACH SECTION

SECTION	C1	C2	C3	C4	C5	C6	C7
1	.00000	-.05421	.02648	.00000	.00000	.00000	1.00000
2	.05687	.00000	.00000	.00000	.00000	.00000	.00000
3	-.13691	-1.00000	1.78390	-.75802	.00000	.00000	1.00000

FIRST SOURCE AT X/L= .00200
SOURCE SPACING IS .60000 TIMES LOCAL INCOMPRESSIBLE X/L

(a) Page 1.

SOURCE LOCATIONS AND BODY RADIUS AND SURFACE SLOPE AT THESE LOCATIONS

X/L	R/L	UR/UX	X/L	R/L	UR/UX	X/L	R/L	UR/UX	X/L	R/L	UR/UX
.00200	.00599	.01268	.02290	.03612	.05249	.07185	.08522	.10162	.11866	.13595	.15377
.00726	.01252	.01822	.02494	.02976	.03582	.04228	.04896	.05582	.06288	.06994	.07699
1.80815	1.03151	.68828	.49910	.37909	.29513	.23197	.18448	.14548	.11866	.09401	.07185
.09401	.11866	.14548	.17408	.20404	.23488	.26613	.29800	.33037	.36324	.39661	.43048
.04484	.04877	.05201	.05447	.05609	.05682	.05667	.05567	.05377	.05122	.04804	.04428
.18104	.13957	.10293	.06982	.03885	.00892	.00000	.00000	.00000	.00000	.00000	.00000
.29740	.32867	.35995	.39122	.42249	.45377	.48504	.51631	.54759	.57886	.61013	.64141
.05687	.05687	.05687	.05687	.05687	.05687	.05687	.05687	.05687	.05687	.05687	.05687
.00000	.00000	.00000	.00000	.00000	.00000	.00000	.00000	.00000	.00000	.00000	.00000
.51631	.54759	.57886	.61013	.64141	.67268	.70395	.73523	.76650	.79777	.82905	.86032
.05687	.05687	.05687	.05687	.05687	.05687	.05687	.05687	.05687	.05687	.05687	.05687
.00000	.00000	.00000	.00000	.00000	.00000	.00000	.00000	.00000	.00000	.00000	.00000
.73523	.76650	.79777	.82905	.86032	.89159	.92287	.95414	.98541	.01668	.04795	.07922
.05687	.05687	.05687	.05687	.05687	.05687	.05687	.05687	.05687	.05687	.05687	.05687
.00000	.00000	.00000	.00000	.00000	.00000	.00000	.00000	.00000	.00000	.00000	.00000
.95278	.97867	.99869	1.01235	.02484	.01494	.00404	.00000	.00000	.00000	.00000	.00000
.04709	.03639	.02484	.01494	.00404	.00000	.00000	.00000	.00000	.00000	.00000	.00000
-.33062	-.50042	-.65990	-.79283								

(b) Page 2.

Figure 9.- Triple ejector rack source distribution output.

INCOMPRESSIBLE SOURCE DISTRIBUTION FOR MACH NUMBER .40

X/L	2.0000-03	5.9337-03	1.2479-02	2.2699-02	3.6119-02	5.2403-02
0	-5.6644-07	2.0447-05	5.2145-05	6.6002-05	8.0062-05	8.4621-05
X/L	7.1853-02	9.4000-02	1.1060-01	1.4584-01	1.7400-01	2.0404-01
0	9.2691-05	9.0897-05	8.2019-05	7.5763-05	1.7033-05	1.2030-04
X/L	2.3484-01	2.6613-01	2.9740-01	3.2867-01	3.5995-01	3.9122-01
0	-1.1844-04	5.3628-05	-5.1306-05	4.5147-05	-4.4240-05	4.7384-05
X/L	4.2249-01	4.5377-01	4.8504-01	5.1631-01	5.4759-01	5.7886-01
0	-4.7663-05	4.6662-05	-4.7357-05	4.7119-05	-4.7123-05	4.7384-05
X/L	6.1013-01	6.4141-01	6.7268-01	7.0395-01	7.3523-01	7.6650-01
0	-4.6877-05	4.7641-05	-4.6504-05	4.8151-05	-4.5770-05	4.9387-05
X/L	7.9777-01	8.2905-01	8.6032-01	8.9159-01	9.2287-01	9.5414-01
0	-4.4021-05	5.8037-05	-7.4667-05	2.8150-04	-2.9120-04	-3.0630-04
X/L	9.7867-01	9.9869-01	1.0123+00			
0	-2.1453-04	-7.9127-05	-4.6523-05			

(c) Page 3.

SHAPE CALCULATED FROM SOURCE DISTRIBUTION

X/L	0.1000	0.3000	0.5000	0.7000	0.9000	1.1000	1.3000
R/L	0.01622	0.02738	0.03452	0.03984	0.04412	0.04754	0.05029
X/L	0.15000	0.17000	0.19000	0.21000	0.23000	0.25000	0.27000
R/L	0.05248	0.05420	0.05558	0.05659	0.05706	0.05712	0.05715
X/L	0.29000	0.31000	0.33000	0.35000	0.37000	0.39000	0.41000
R/L	0.05715	0.05712	0.05715	0.05715	0.05712	0.05713	0.05715
X/L	0.43000	0.45000	0.47000	0.49000	0.51000	0.53000	0.55000
R/L	0.05712	0.05712	0.05715	0.05712	0.05712	0.05715	0.05713
X/L	0.57000	0.59000	0.61000	0.63000	0.65000	0.67000	0.69000
R/L	0.05712	0.05715	0.05715	0.05715	0.05712	0.05715	0.05712
X/L	0.71000	0.73000	0.75000	0.77000	0.79000	0.81000	0.83000
R/L	0.05715	0.05715	0.05712	0.05715	0.05715	0.05712	0.05713
X/L	0.85000	0.87000	0.89000	0.91000	0.93000	0.95000	0.97000
R/L	0.05715	0.05715	0.05704	0.05602	0.05314	0.04801	0.04044
X/L	0.99000	1.01000					
R/L	0.03030	0.01699					

(d) Page 4.


```

C      READ(5,701) NFU,NPY,NKALK,NSTRS
C
C      INPUT FUSELAGE DATA
C
C      IF (NFU.EQ.0) GO TO 10
C      READ(5,706) FLTHC,FRMAX
C      WRITE(6,708) FLTHC,FRMAX
C      WRITE(6,709) FLTHC,FRMAX
C      FLTHI=FLTHC/BETA
C      FLTHI=FLTHI*FLTHI
C      READ(5,701) NFESOR
C      READ(5,710) (FSOR(N),N=1,NFESOR)
C      WRITE(6,711) (FSOR(N),N=1,NFESOR)
C      CALL SOROUT (NFESOR,FXL,FSOR)
C      DO 2 NE1,NFESOR
C      FXL(N)=FLTHI*FXL(N)
C      2 FSOR(N)=FLTHI*FSOR(N)
C
C      INPUT WING DATA
C
C      10 READ(5,706) XBWOC,ZBWO,WIC
C      XBWOI=XBWOC/BETA
C      WII=FUNA(WIC)
C      WICR=WIC/HAD
C      WICR=COS(WICR)
C      SWICR=SIN(WICR)
C      WIIR=WI/RAU
C      ALFWIR=FAIR*WIIR
C      CWIIR=COS(WIIR)
C      SWIIR=SIN(WIIR)
C      WRITE(6,712)
C      WRITE(6,713) XBWOC,ZBWO,WIC
C      CALL WVLIN (ALPHAL,CRWI,ALPHL1,CHLOCL,TANPHI,SUMY,
C      1YLOC,SWPC,SWPV,PHI,SINPHI,COSPHI,SWPVV,SW,PVZ,PCX,PTLX,
C      2PTLY,PTLZ)
C      CALL WTHIN (THETAL,DELTX,CHLOCLB,SWPCS,XRC,CHLOCL,Z1,TANPHI,
C      1FACTOR)
C      DO 12 NE1,MS
C      SINWS(N)=SIN(ATAN(SWPCS(N)))
C      12 COSWS(N)=COS(ATAN(SWPCS(N)))
C
C      INPUT PYLON DATA
C
C      IF (NPY.EQ.0) GO TO 18
C      CALL PVLIN (Z,CRPI,SWPPLI,SWPPTI,XPLEI,XP,YP,ZP,SUMZ,SWPCP,
C      1SWPV,SP,PVPX,PVPY,PVPZ,PCPX)
C      CALL PTHIN (THETPL,DELTPX,CRPI,Z,SWPPLI,SWPPTI,SWPPCS,XPRC,
C      1XP,FACTOR)
C      DO 15 NE1,MPS
C      SINSPS(N)=SIN(ATAN(SWPPCS(N)))
C      15 COSSPS(N)=COS(ATAN(SWPPCS(N)))
C      XPC=XP*BETA
C      ZP=ZP*Z(1)
C      XBPO=XBWOC*XPC*CWICR*ZP*SWICR
C      XBPOT=XBPO/BETA
C      YBPO=YP
C      ZBPO=ZBWO*ZP*CWICR-XPC*SWICR
C      GO TO 20
C      18 MP1=M
C      NCP=M
C      MSP=0
C      NP=0
C      NCP=0
C      MP=0
C      NP=0
C      OUTPUT VORTEX LATTICE CONTROL POINT COORDINATES AND TWIST AND
C      CAMBER DISTRIBUTION
C
C      20 CALL VLOUT (X,NCM,PCX,BETA,PVZ,ALPHAL,NPY,MP1,MPP,ICP,PCPY,PVPY,SLA01214
C      1,PVPZ)
C      60A01182
C      60A01183
C      60A01184
C      60A01185
C      60A01186
C      60A01187
C      60A01188
C      60A01189
C      60A01190
C      60A01191
C      60A01192
C      60A01193
C      60A01194
C      60A01195
C      60A01196
C      60A01197
C      60A01198
C      60A01199
C      60A01200
C      60A01201
C      60A01202
C      60A01203
C      60A01204
C      60A01205
C      60A01206
C      60A01207
C      60A01208
C      60A01209
C      60A01210
C      60A01211
C      60A01212
C      60A01213
C
C      20 CALL VLOUT (X,NCM,PCX,BETA,PVZ,ALPHAL,NPY,MP1,MPP,ICP,PCPY,PVPY,SLA01214
C      1,PVPZ)
C      60A01215
C      60A01216
C      60A01217
C      60A01218
C      60A01219
C      60A01220
C      60A01221
C      60A01222
C      60A01223
C      60A01224
C      60A01225
C      60A01226
C      60A01227
C      60A01228
C      60A01229
C      60A01230
C      60A01231
C      60A01232
C      60A01233
C      60A01234
C      60A01235
C      60A01236
C      60A01237
C      60A01238
C      60A01239
C      60A01240
C      60A01241
C      60A01242
C      60A01243
C      60A01244
C      60A01245
C      60A01246
C      60A01247
C      60A01248
C      60A01249
C      60A01250
C      60A01251
C      60A01252
C      60A01253
C      60A01254
C      60A01255
C      60A01256
C      60A01257
C      60A01258
C      60A01259
C      60A01260
C      60A01261
C      60A01262
C      60A01263
C      60A01264
C      60A01265
C      60A01266
C      60A01267
C      60A01268
C      60A01269
C      60A01270
C      60A01271
C      60A01272
C      60A01273
C      60A01274
C      60A01275
C      60A01276
C      60A01277
C      60A01278
C      60A01279
C      60A01280
C      60A01281
C      60A01282
C      60A01283
C      60A01284
C      60A01285
C
C      OUTPUT THICKNESS DISTRIBUTION
C
C      CALL THOUT (WS,THETAL,BETA,NCWS,NP,MP1,MPP,ICP,PCPY,PVPY,SLA01214
C      1,PVPZ)
C      60A01286
C      60A01287
C      60A01288
C      60A01289
C      60A01290
C      60A01291
C      60A01292
C      60A01293
C      60A01294
C      60A01295
C      60A01296
C      60A01297
C      60A01298
C      60A01299
C      60A01300
C      60A01301
C      60A01302
C      60A01303
C      60A01304
C      60A01305
C      60A01306
C      60A01307
C      60A01308
C      60A01309
C      60A01310
C      60A01311
C      60A01312
C      60A01313
C      60A01314
C      60A01315
C      60A01316
C      60A01317
C      60A01318
C      60A01319
C      60A01320
C      60A01321
C      60A01322
C      60A01323
C      60A01324
C      60A01325
C      60A01326
C      60A01327
C      60A01328
C      60A01329
C      60A01330
C      60A01331
C      60A01332
C      60A01333
C      60A01334
C      60A01335
C      60A01336
C      60A01337
C      60A01338
C      60A01339
C      60A01340
C      60A01341
C      60A01342
C      60A01343
C      60A01344
C      60A01345
C      60A01346
C      60A01347
C      60A01348
C      60A01349
C      60A01350
C      60A01351
C      60A01352
C      60A01353
C      60A01354
C      60A01355
C      60A01356
C      60A01357
C      60A01358
C      60A01359
C      60A01360
C      60A01361
C      60A01362
C      60A01363
C      60A01364
C      60A01365
C      60A01366
C      60A01367
C      60A01368
C      60A01369
C      60A01370
C      60A01371
C      60A01372
C      60A01373
C      60A01374
C      60A01375
C      60A01376
C      60A01377
C      60A01378
C      60A01379
C      60A01380
C      60A01381
C      60A01382
C      60A01383
C      60A01384
C      60A01385
C      60A01386
C      60A01387
C      60A01388
C      60A01389
C      60A01390
C      60A01391
C      60A01392
C      60A01393
C      60A01394
C      60A01395
C      60A01396
C      60A01397
C      60A01398
C      60A01399
C      60A01400
C      60A01401
C      60A01402
C      60A01403
C      60A01404
C      60A01405
C      60A01406
C      60A01407
C      60A01408
C      60A01409
C      60A01410
C      60A01411
C      60A01412
C      60A01413
C      60A01414
C      60A01415
C      60A01416
C      60A01417
C      60A01418
C      60A01419
C      60A01420
C      60A01421
C      60A01422
C      60A01423
C      60A01424
C      60A01425
C      60A01426
C      60A01427
C      60A01428
C      60A01429
C      60A01430
C      60A01431
C      60A01432
C      60A01433
C      60A01434
C      60A01435
C      60A01436
C      60A01437
C      60A01438
C      60A01439
C      60A01440
C      60A01441
C      60A01442
C      60A01443
C      60A01444
C      60A01445
C      60A01446
C      60A01447
C      60A01448
C      60A01449
C      60A01450
C      60A01451
C      60A01452
C      60A01453
C      60A01454
C      60A01455
C      60A01456
C      60A01457
C      60A01458
C      60A01459
C      60A01460
C      60A01461
C      60A01462
C      60A01463
C      60A01464
C      60A01465
C      60A01466
C      60A01467
C      60A01468
C      60A01469
C      60A01470
C      60A01471
C      60A01472
C      60A01473
C      60A01474
C      60A01475
C      60A01476
C      60A01477
C      60A01478
C      60A01479
C      60A01480
C      60A01481
C      60A01482
C      60A01483
C      60A01484
C      60A01485
C      60A01486
C      60A01487
C      60A01488
C      60A01489
C      60A01490
C      60A01491
C      60A01492
C      60A01493
C      60A01494
C      60A01495
C      60A01496
C      60A01497
C      60A01498
C      60A01499
C      60A01500
C      60A01501
C      60A01502
C      60A01503
C      60A01504
C      60A01505
C      60A01506
C      60A01507
C      60A01508
C      60A01509
C      60A01510
C      60A01511
C      60A01512
C      60A01513
C      60A01514
C      60A01515
C      60A01516
C      60A01517
C      60A01518
C      60A01519
C      60A01520
C      60A01521
C      60A01522
C      60A01523
C      60A01524
C      60A01525
C      60A01526
C      60A01527
C      60A01528
C      60A01529
C      60A01530
C      60A01531
C      60A01532
C      60A01533
C      60A01534
C      60A01535
C      60A01536
C      60A01537
C      60A01538
C      60A01539
C      60A01540
C      60A01541
C      60A01542
C      60A01543
C      60A01544
C      60A01545
C      60A01546
C      60A01547
C      60A01548
C      60A01549
C      60A01550
C      60A01551
C      60A01552
C      60A01553
C      60A01554
C      60A01555
C      60A01556
C      60A01557
C      60A01558
C      60A01559
C      60A01560
C      60A01561
C      60A01562
C      60A01563
C      60A01564
C      60A01565
C      60A01566
C      60A01567
C      60A01568
C      60A01569
C      60A01570
C      60A01571
C      60A01572
C      60A01573
C      60A01574
C      60A01575
C      60A01576
C      60A01577
C      60A01578
C      60A01579
C      60A01580
C      60A01581
C      60A01582
C      60A01583
C      60A01584
C      60A01585
C      60A01586
C      60A01587
C      60A01588
C      60A01589
C      60A01590
C      60A01591
C      60A01592
C      60A01593
C      60A01594
C      60A01595
C      60A01596
C      60A01597
C      60A01598
C      60A01599
C      60A01600
C      60A01601
C      60A01602
C      60A01603
C      60A01604
C      60A01605
C      60A01606
C      60A01607
C      60A01608
C      60A01609
C      60A01610
C      60A01611
C      60A01612
C      60A01613
C      60A01614
C      60A01615
C      60A01616
C      60A01617
C      60A01618
C      60A01619
C      60A01620
C      60A01621
C      60A01622
C      60A01623
C      60A01624
C      60A01625
C      60A01626
C      60A01627
C      60A01628
C      60A01629
C      60A01630
C      60A01631
C      60A01632
C      60A01633
C      60A01634
C      60A01635
C      60A01636
C      60A01637
C      60A01638
C      60A01639
C      60A01640
C      60A01641
C      60A01642
C      60A01643
C      60A01644
C      60A01645
C      60A01646
C      60A01647
C      60A01648
C      60A01649
C      60A01650
C      60A01651
C      60A01652
C      60A01653
C      60A01654
C      60A01655
C      60A01656
C      60A01657
C      60A01658
C      60A01659
C      60A01660
C      60A01661
C      60A01662
C      60A01663
C      60A01664
C      60A01665
C      60A01666
C      60A01667
C      60A01668
C      60A01669
C      60A01670
C      60A01671
C      60A01672
C      60A01673
C      60A01674
C      60A01675
C      60A01676
C      60A01677
C      60A01678
C      60A01679
C      60A01680
C      60A01681
C      60A01682
C      60A01683
C      60A01684
C      60A01685
C      60A01686
C      60A01687
C      60A01688
C      60A01689
C      60A01690
C      60A01691
C      60A01692
C      60A01693
C      60A01694
C      60A01695
C      60A01696
C      60A01697
C      60A01698
C      60A01699
C      60A01700
C      60A01701
C      60A01702
C      60A01703
C      60A01704
C      60A01705
C      60A01706
C      60A01707
C      60A01708
C      60A01709
C      60A01710
C      60A01711
C      60A01712
C      60A01713
C      60A01714
C      60A01715
C      60A01716
C      60A01717
C      60A01718
C      60A01719
C      60A01720
C      60A01721
C      60A01722
C      60A01723
C      60A01724
C      60A01725
C      60A01726
C      60A01727
C      60A01728
C      60A01729
C      60A01730
C      60A01731
C      60A01732
C      60A01733
C      60A01734
C      60A01735
C      60A01736
C      60A01737
C      60A01738
C      60A01739
C      60A01740
C      60A01741
C      60A01742
C      60A01743
C      60A01744
C      60A01745
C      60A01746
C      60A01747
C      60A01748
C      60A01749
C      60A01750
C      60A01751
C      60A01752
C      60A01753
C      60A01754
C      60A01755
C      60A01756
C      60A01757
C      60A01758
C      60A01759
C      60A01760
C      60A01761
C      60A01762
C      60A01763
C      60A01764
C      60A01765
C      60A01766
C      60A01767
C      60A01768
C      60A01769
C      60A01770
C      60A01771
C      60A01772
C      60A01773
C      60A01774
C      60A01775
C      60A01776
C      60A01777
C      60A01778
C      60A01779
C      60A01780
C      60A01781
C      60A01782
C      60A01783
C      60A01784
C      60A01785
C      60A01786
C      60A01787
C      60A01788
C      60A01789
C      60A01790
C      60A01791
C      60A01792
C      60A01793
C      60A01794
C      60A01795
C      60A01796
C      60A01797
C      60A01798
C      60A01799
C      60A01800
C      60A01801
C      60A01802
C      60A01803
C      60A01804
C      60A01805
C      60A01806
C      60A01807
C      60A01808
C      60A01809
C      60A01810
C      60A01811
C      60A01812
C      60A01813
C      60A01814
C      60A01815
C      60A01816
C      60A01817
C      60A01818
C      60A01819
C      60A01820
C      60A01821
C      60A01822
C      60A01823
C      60A01824
C      60A01825
C      60A01826
C      60A01827
C      60A01828
C      60A01829
C      60A01830
C      60A01831
C      60A01832
C      60A01833
C      60A01834
C      60A01835
C      60A01836
C      60A01837
C      60A01838
C      60A01839
C      60A01840
C      60A01841
C      60A01842
C      60A01843
C      60A01844
C      60A01845
C      60A01846
C      60A01847
C      60A01848
C      60A01849
C      60A01850
C      60A01851
C      60A01852
C      60A01853
C      60A01854
C      60A01855
C      60A01856
C      60A01857
C      60A01858
C      60A01859
C      60A01860
C      60A01861
C      60A01862
C      60A01863
C      60A01864
C      60A01865
C      60A01866
C      60A01867
C      60A01868
C      60A01869
C      60A01870
C      60A01871
C      60A01872
C      60A01873
C      60A01874
C      60A01875
C      60A01876
C      60A01877
C      60A01878
C      60A01879
C      60A01880
C      60A01881
C      60A01882
C      60A01883
C      60A01884
C      60A01885
C      60A01886
C      60A01887
C      60A01888
C      60A01889
C      60A01890
C      60A01891
C      60A01892
C      60A01893
C      60A01894
C      60A01895
C      60A01896
C      60A01897
C      60A01898
C      60A01899
C      60A01900
C      60A01901
C      60A01902
C      60A01903
C      60A01904
C      60A01905
C      60A01906
C      60A01907
C      60A01908
C      60A01909
C      60A01910
C      60A01911
C      60A01912
C      60A01913
C      60A01914
C      60A01915
C      60A01916
C      60A01917
C      60A01918
C      60A01919
C      60A01920
C      60A01921
C      60A01922
C      60A01923
C      60A01924
C      60A01925
C      60A01926
C      60A01927
C      60A01928
C      60A01929
C      60A01930
C      60A01931
C      60A01932
C      60A01933
C      60A01934
C      60A01935
C      60A01936
C      60A01937
C      60A01938
C      60A01939
C      60A01940
C      60A01941
C      60A01942
C      60A01943
C      60A01944
C      60A01945
C      60A01946
C      60A01947
C      60A01948
C      60A01949
C      60A01950
C      60A01951
C      60A01952
C      60A01953
C      60A01954
C      60A01955
C      60A01956
C      60A01957
C      60A01958
C      60A01959
C      60A01960
C      60A01961
C      60A01962
C      60A01963
C      60A01964
C      60A01965
C      60A01966
C      60A01967
C      60A01968
C      60A01969
C      60A01970
C      60A01971
C      60A01972
C      60A01973
C      60A01974
C      60A01975
C      60A01976
C      60A01977
C      60A01978
C      60A01979
C      60A01980
C      60A01981
C      60A01982
C      60A01983
C      60A01984
C      60A01985
C      60A01986
C      60A01987
C      60A01988
C      60A01989
C      60A01990
C      60A01991
C      60A01992
C      60A01993
C      60A01994
C      60A01995
C      60A01996
C      60A01997
C      60A01998
C      60A01999
C      60A02000
C      60A02001
C      60A02002
C      60A02003
C      60A02004
C      60A02005
C      60A02006
C      60A02007
C      60A02008
C      60A02009
C      60A02010
C      60A02011
C      60A02012
C      60A02013
C      60A02014
C      60A02015
C      60A02016
C      60A02017
C      60A02018
C      60A02019
C      60A02020
C      60A02021
C      60A02022
C      60A02023
C      60A02024
C      60A02025
C      60A02026
C      60A02027
C      60A02028
C      60A02029
C      60A02030
C      60A02031
C      60A02032
C      60A02033
C      60A02034
C      60A02035
C      60A02036
C      60A02037
C      60A02038
C      60A02039
C      60A02040
C      60A02041
C      60A02042
C      60A02043
C      60A02044
C      60A02045
C      60A02046
C      60A02047
C      60A02048
C      60A02049
C      60A02050
C      60A02051
C      60A02052
C      60A02053
C      60A02054
C      60A02055
C      60A02056
C      60A02057
C      60A02058
C      60A02059
C      60A02060
C      60A02061
C      60A02062
C      60A02063
C      60A02064
C      60A02065
C      60A02066
C      60A02067
C      60A02068
C      60A02069
C      60A02070
C      60A02071
C      60A02072
C      60A02073
C      60A02074
C      60A02075
C      60A02076
C      60A02077
C      60A02078
C      60A02079
C      60A02080
C      60A02081
C      60A02082
C      60A02083
C      60A02084
C      60A02085
C      60A02086
C      60A02087
C      60A02088
C      60A02089
C      60A02090
C      60A02091
C      60A02092
C      60A02093
C      60A02094
C      60A02095
C      60A02096
C      60A02097
C      60A02098
C      60A02099
C      60A02100
C      60A02101
C      60A02102
C      60A02103
C      60A02104
C      60A02105
C      60A02106
C      60A02107
C      60A02108
C      60A02109
C      60A02110
C      60A02111
C      60A02112
C      60A02113
C      60A02114
C      60A02115
C      60A02116
C      60A02117
C      60
```

```

C
NN=MMP+1
IF (IP.EQ.1) NN=M+1
MM=NN-1
DO 40 N=1,MM
40 FVN(N,NN)=CIR(N)
CALL INVS (FVN,1,MM,100,101)
DO 41 N=1,MM
41 CIR(N)=FVN(N,NN)
IF (IP.NE.1) GO TO 43
DO 42 N=MPI,MMP
42 CIR(N)=0
43 CONTINUE
C
C OUTPUT INTERFERENCE VELOCITIES AND VORTEX STRENGTHS
C
CALL VSTOUT (M,NCN,PCX,BETA,BETASQ,UEI,VEI,CIR,PVY,PVZ,NPY,NPI,
1,MMP,NCN,PCPX,PVY,PVZ)
IF (INSTRS.EQ.0) GO TO 1000
C
C INPUT ADDITIONAL INFORMATION REQUIRED TO DESCRIBE EJECTED STORE
C
READ (5,701) NEJECT,NSEG,NSEGQ,NGAM,NPOL,NROLL,NEMP,NDAMP
READ (5,706) SMAS,FIIX,FIY,FIZZ,FIY2,FIY2,FIY2,FIY2,FIY2,FIY2
WRITE (6,716) NEJECT
WRITE (6,718) SMAS,FIIX,FIY,FIY2,FIY2,FIY2,FIY2,FIY2,FIY2,FIY2
XMON=ABS(XMON)
DO 50 J=1,NPOLY
50 READ (5,706) (COEF(J,K),K=1,7)
WRITE (6,719)
DO 51 J=1,NPOLY
51 WRITE (6,720) J,XEND(J)
DO 52 J=1,NPOLY
52 WRITE (6,720) J,(COEF(J,K),K=1,7)
C
C DETERMINE GEOMETRIC PARAMETERS DESCRIBING STORE
C
DO 53 J=1,NSTRS
IF (NEJECT=NUMSTR(J)) 53,54,53
54 NEJSTR=J
53 CONTINUE
ESTLGC=SLTHC(NEJSTR)
ESTLGI=SLTHI(NEJSTR)
ESTRMX=SRMAX(NEJSTR)
SHEF=PI*ESTRMX**2
REF=2.0*ESTRMX
FSEG=NSEG
DELX=ESTLGC/FSEG
DELXI=ESTLGI/FSEG
DX=DELX/2.0
DXI=DELXI/2.0
EXSTI(1)=0.0
EXSTI(2)=0.0
NHSEG=2*NSEG+1
DO 55 J=2,NHSEG
55 EXSTI(J)=EXSTI(J-1)+DXI
EXSTI(J)=EXSTI(J-1)+DX
DO 56 J=2,NHSEG
56 XAX=EXSTI(J)*ESTLGC
CALL SHAPE (XAX,NPOLY,XEND,COEF,RK,LDRDX(J))
ERAD(J)=ESTLGC*RR
XSEG=SRMAX(NEJSTR)
XSEF=PI*XSEG**2
WRITE (6,722) XSEF
READ (5,706) C,CUC
WRITE (6,723) CA,CUC

```

(c) Page 3.

Figure 10.- Continued.

```

NHSEG=2*NSEG+1
NASYM=0
IF (ABS(XBAR).GT.1.0E-05) NASYM=1
IF (ABS(YBAR).GT.1.0E-05) NASYM=1
IF (ABS(ZBAR).GT.1.0E-05) NASYM=1
SAPG=SIGN(ALFACR+GAMF*QTR)
CAPG=SIGN(ALFACR+GAMF*QTR)
C
C INPUT EMPENNAGE DATA IF EMPENNAGE IS PRESENT
C
CNEM=0.0
CLMEM=0.0
CYEM=0.0
CLNEM=0.0
CLLEM=0.0
IF (NEMP.EQ.0) GO TO 57
READ (5,701) IPLNR,MSF
READ (5,706) XTAL,RADAV,FINSS,PHIROL,CLALPH
IF (IPLNR.EQ.1) WRITE (6,724)
IF (IPLNR.EQ.0) WRITE (6,725)
WRITE (6,726) XTAL,RADAV
WRITE (6,727) FINSS,PHIROL
WRITE (6,728) CLALPH
CALL EMPINI
C
C INITIALIZE FOR TRAJECTORY CALCULATION
C
57 VAR(11)=SSIBCR(NEJSTR)
VAR(12)=0.0
VAR(13)=0.0
READ (5,706) VZERO,VAR(5)
VAR(11)=VZERO*SSIBCR(NEJSTR)
VAR(12)=0.0
VAR(13)=VZERO*CSIBCR(NEJSTR)
VAR(14)=0.0
VAR(15)=0.0
VAR(16)=0.0
VAR(17)=XB50(NEJSTR)-XMON*CSIBCR(NEJSTR)
VAR(18)=YB50(NEJSTR)
VAR(19)=ZB50(NEJSTR)*XMON*SSIBCR(NEJSTR)
XNOSEI=XB50(NEJSTR)
YNOSEI=YB50(NEJSTR)
ZNOSEI=ZB50(NEJSTR)
XCGI=VAR(7)
YCGI=VAR(8)
ZCGI=VAR(9)
XBASEI=XNOSEI-SLTHC(NEJSTR)*CSIBCR(NEJSTR)
YBASEI=YNOSEI
ZBASEI=ZNOSEI+SLTHC(NEJSTR)*SSIBCR(NEJSTR)
READ (5,706) DTIME,TIMEI,TIMEF
NEG=12
DTIME=DTIME
TIME=TIMEI
IF (TIME.LE.0.0) GO TO 60
READ (5,706) VAR
DO 61 J=10,12
61 VAR(J)=DTR*VAR(J)
60 NDIFEG=1
CALL ADAMS (DTIME,DTIME,VAR,DVAR,NEG,NDIFEG,TIME)
NOUT=1
C
C CALCULATE AERODYNAMIC FORCES AND MOMENTS
C
62 CALL FORCE
IF (NEMP.EQ.1) CALL EMPFOK
IF (NGAM.EQ.1) CALL DIRCOS(VAR,U)
C
C CALCULATE ACCELERATIONS
C
C CALCULATE COEFFICIENT MATRIX
C
DO 70 J=1,6
DO 70 K=1,6

```



```

        ZPM=PVPZ(JC)-PVPZ(JVP)
        DO 262 I=1,2
        CALL INFMW(SWPVP(JVP),PHIP,XPM,YPM,ZPM,SP(JVP),FUP(I),FVP(I),FVP(I))
        IF(P(I))
            PHIP=PHIP
            SWPVP(JVP)=-SWPVP(JVP)
        262 CONTINUE
        FVN(JC,JV)=(FVP(I)+FVP(2))*COS(PHI(JC))-(FVP(I)+FVP(2))*SIN(PHI(JC))
        312 CONTINUE
        C
        C CONTROL POINTS ON PYLON, VORTICES ON WING
        C
        DO 412 JC=MP1,MMP
        JCP=JC-M
        DO 412 JV=1,M
        XPM=PCPX(JCP)-PVPX(JV)
        YPM(1)=PVPY(JCP)-PVT(JV)
        YPM(2)=PVPY(JCP)+PVT(JV)
        ZPM=PVPZ(JCP)-PVPZ(JV)
        DO 263 I=1,2
        CALL INFMW(SWPVP(JVP),PHI(JV),XPM,YPM(Z),ZPM,SW(JV),FUM(I),FVM(I),FVM(I))
        263 CONTINUE
        FVN(JC,JV)=-(FVM(1)+FVM(2))
        412 CONTINUE
        C
        C CONTROL POINTS ON PYLON, VORTICES ON PYLON
        C
        DO 512 JCP=MP1,MMP
        JCP=JC-M
        DO 512 JV=MP1,MMP
        JVP=JV-M
        XPM=PCPX(JCP)-PVPX(JVP)
        YPM(1)=PVPY(JCP)-PVPY(JVP)
        YPM(2)=PVPY(JCP)+PVPY(JVP)
        ZPM=PVPZ(JCP)-PVPZ(JVP)
        DO 264 I=1,2
        CALL INFMW(SWPVP(JVP),PHIP,XPM,YPM(Z),ZPM,SP(JVP),FUP(I),FVP(I),FVP(I))
        IF(P(I))
            PHIP=PHIP
            SWPVP(JVP)=-SWPVP(JVP)
        264 CONTINUE
        FVN(JC,JV)=-(FVP(1)+FVP(2))
        512 CONTINUE
        1103 RETURN
        END
    
```

(r) Page 18.

Figure 10.- Continued.

(s) page 19.

80

```

50 DO 51 NV=1,M
51 CIR(NV)=Z1.566371*(ALFAIR+ALPHIL(NV))*COSPHI(NV)+VEI(NV)*SINPHI(NV)
1V)=UEI(NV)*ALPHIL(NV)+WEI(NV))*COSPHI(NV)
IF (NPY.EQ.U.OR.IP.EQ.1) RETURN
DO 52 NV=M+1,MMP
52 CIR(NV)=Z1.566371*VEI(NV)
RETURN
END
60A30103
60A30104
60A30105
60A30106
60A30107
60A30108
60A30109
60A30110
60A30111

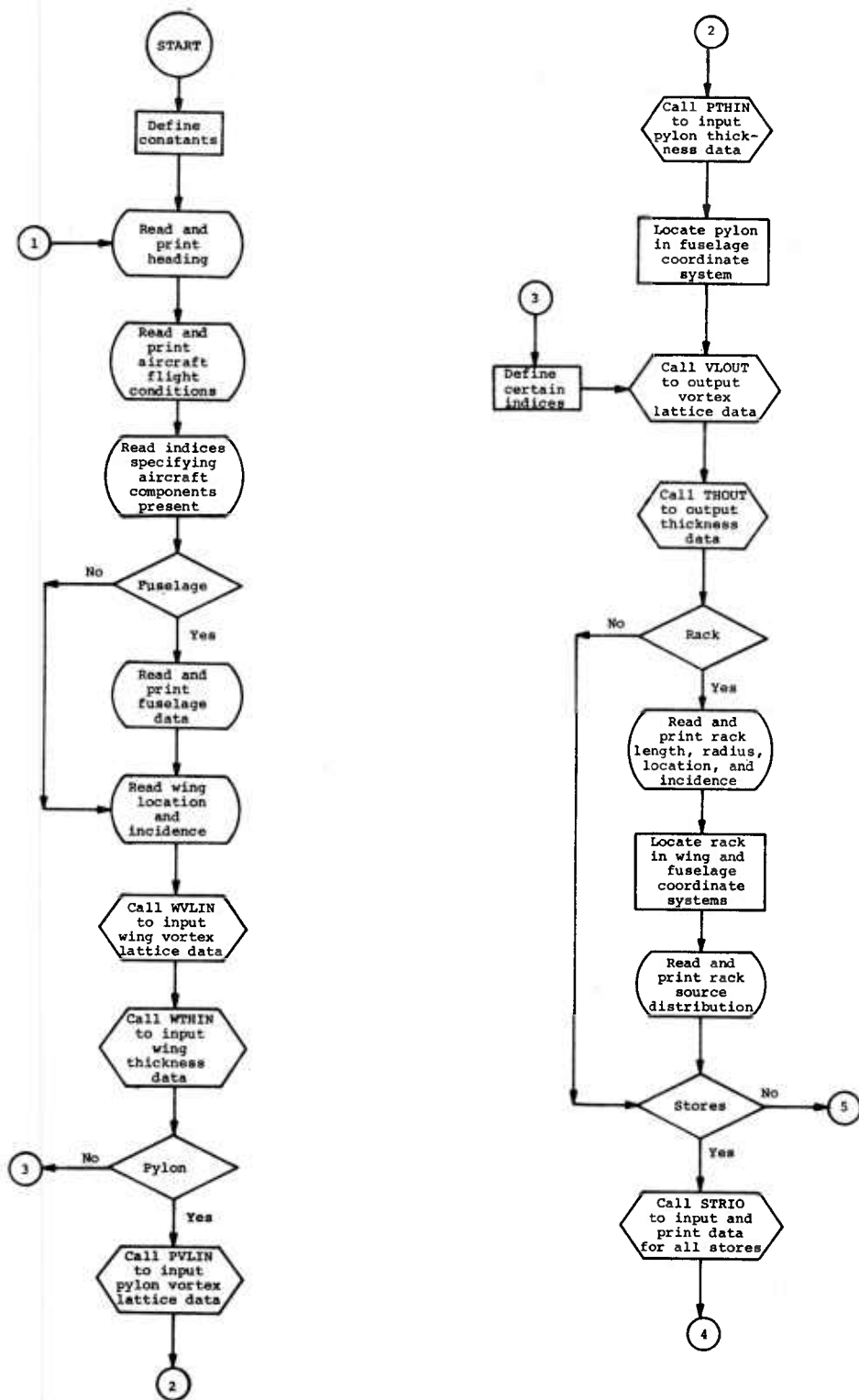
C SUBROUTINE TO OUTPUT INTERFERENCE VELOCITIES AND VORTEX STRENGTHS
C
C
C SUBROUTINE VSTOUT (M=NCW,PCX=BETA,BELASQ,UEI,VEI,WEI,CIR,PVY,PVZ,
INPY,MPI,MMP,NCP,PCPX,IPVY,IPVZ)
C
C DIMENSION PCX(1),PVY(1),PVZ(1),UEI(1),VEI(1),WEI(1),CIR(1),PCPX(1),PCPY(1),PVY(1),PVZ(1)
C
C 1*PVY(1),PVZ(1)
C
C 701 FORMAT(1H1,40X,'NO VORTEX LATTICE CONTROL POINT COORDINATES/3RX,
147HINTERFERENCE VELOCITIES INDUCED AT THESE POINTS/46X,27HCALCULATED/
22D VORTEX STRENGTHS/48X,24H(WING COORDINATE SYSTEM))
C
C
C WING
C
C 702 FORMAT(/10X,19H4ING CONTROL POINTS/17X,10HROW VORTEX/5X,5HX, FT,6X6DA31 13
1,5HY, FT,6X,5HZ, FT,6X,6HU/VINF,5X,6HV/VINF,5X,6HW/VINF,3X,10HGAMMA/DA31 14
2A/VINF)
C
C 703 FORMAT(15X,21S,3X,7F11.5)
C
C 704 FORMAT(/10X,20HPYLON CONTROL POINTS/17X,10HROW VORTEX/5X,5HX, FT,
16X,5HY, FT,6X,5HZ, FT,17X,6HV/VINF,14X,10HGAMMA/VINF)
C
C 705 FORMAT(15X,21S,3X,3F11.5,11X,F11.5,11X,F11.5)
C
C WRITE(6,701)
C
C WRITE(6,702)
C
C DO 1 J=1,M
C
C NROW=J-1)/NCW+1
C
C NVOR=J-NCW*(NROW-1)
C
C TRANSFORM TO COMPRESSIBLE SPACE
C
C
C PCXC=PCX(J)*BETA
C
C UUEI(UJ)/BETASQ
C
C VVEI(VJ)/BETA
C
C WVEI(WJ)/BETA
C
C C=CIR(UJ)/BETA
C
C 1 WRITE(6,703) NROW,NVOR,PCXC,PVY(UJ),PVZ(UJ),U,V,W,C
C
C IF (NPY.EQ.0) RETURN
C
C
C PYLON
C
C
C WRITE(6,704)
C
C DO 2 J=M+1,MMP
C
C NROW=J-M-1)/NCP+1
C
C NVOR=J-M-NCP*(NROW-1)
C
C JP=J-M
C
C TRANSFORM TO COMPRESSIBLE SPACE
C
C
C PCXC=PCX(JP)*BETA
C
C VVEI(VJ)/BETA
C
C C=CIR(UJ)/BETA
C
C 2 WRITE(6,705) NROW,NVOR,PCXC,PVY(UJ),PVZ(UJ),U,V,C
C
C RETURN
C
C END
60A30103
60A30104
60A30105
60A30106
60A30107
60A30108
60A30109
60A30110
60A30111

C SUBROUTINE TO INPUT WING THICKNESS DATA AND LAY OUT STRIPS
C
C
C SUBROUTINE ATHIN (THETAL,DELTX,CHLOCB,SWPCS,XRC,CHLOC,Z1,TANPHI,
IFACTOR)
C
C DIMENSION THETAL(1),DELTX(1),CHLOCB(1),SWPCS(1),XRC(1),CHLOC(1),
Z1(1),TANPHI(1),FACTOR(1)
C
C DIMENSION Y(31),PSIWLE(31),PSIWTE(31),PHIU(31),SWPWL(31),SWPWT(1),SHUA(31),
11,XLEL(31),ZLEL(31)
C
C COMMON /INDLX/ NCW,MSW,MN,IMAX,IP,NCP,MSW,MP,MPI,MMP,KMAX,NCW,C,MS,
INCP,MP,INSTRES,NPY,NRACK,NFU
C
C COMMON /CONST/ BETA,OTR,PHIP,TMUPI,HAD
C
C COMMON /WING/ CRW,SSPAN,SREF,SPAN,CAVE,Y,PSIWLE,PSIWTE,PHID,SWPWL,SWPWT,
1,SWPWT1,XLEL,ZLEL
C
C
C FORMAT STATEMENTS
C
C
C 701 FORMAT(10I5)
C
C 702 FORMAT(1F10.0)
C
C 703 FORMAT(/14X,15H THICKNESS PANELS ARE TO BE LAY OUT ON EACH WING/DA32 19
16 PANEL/20X,13,20H CHORDWISE ROWS WITH/13,12H IN EACH ROW/21X,43HTELA32 20
21E CHORDWISE ROWS COINCIDE WITH THOSE USED/21X,21HIN THE VORTEX LA32 21
STICE//)
C
C READ(5,701) NCW,NUNIS
C
C READ(5,702) IMAX,IP,NCP,MSW,MP,MPI,MMP,KMAX,NCW,C,MS,
INCP,MP,INSTRES,NPY,NRACK,NFU
C
C WRITE (6,703) MS,MSW,NCW
C
C IF (NUNIS.NE.0) GO TO 5
C
C MN=0
C
C DO 1 JNW=1,MS,NCW
C
C MN=MS*NCW
C
C 1 READ (5,702) (THETAL(J),J=JNW,MN)
C
C GO TO 10
C
C 5 READ (5,702)(THETAL(J),J=1,NCW)
C
C DO 6 J=2,MSW
C
C J=J-1)*NCW
C
C DO 6 K=1,NCW
C
C KK=J+K
C
C 6 THETAL(KK)=THETAL(K)
C
C DO 8120 J=1,MS
C
C 8120 THETAL(J)=THETAL(J)*BETA
C
C
C LAY-OUT SPANWISE STRIPS ON THE INCOMPRESSIBLE WING
C
C
C D=NCW
C
C DO 601 I=2,IMAX
C
C DELTX(I)=CHLOCB(I)/D
C
C DO 720 JWC=1,NCW
C
C JS=(I-2)*NCW+JWC
C
C A=JWC
C
C SWPCS(JS)=SWPWL(I)-((A-0.5)/D)*(SWPWL(I)-SWPWT(I))
C
C CUSSWP=COS(ATAN(SWPCS(JS)))
C
C XRC(JS)=XLEL(I)-((A-0.5)/D)*CHLOCB(I)-Y(I-1)*SWPCS(JS)
C
C Z1(JS)=ZLEL(I)-((Y(I)+Y(I-1))/2.0)*TANPHI(I)
C
C FACTOR(JS)=(THETAL(JS)*DELTX(I)+CUSSWP)/TMUPI
C
C 720 CONTINUE
C
C 601 CONTINUE
C
C RETURN
C
C END
60A32 1
60A32 2
60A32 3
60A32 4
60A32 5
60A32 6
60A32 7
60A32 8
60A32 9
60A32 10
60A32 11
60A32 12
60A32 13
60A32 14
60A32 15
60A32 16
60A32 17
60A32 18
60A32 19
60A32 20
60A32 21
60A32 22
60A32 23
60A32 24
60A32 25
60A32 26
60A32 27
60A32 28
60A32 29
60A32 30
60A32 31
60A32 32
60A32 33
60A32 34
60A32 35
60A32 36
60A32 37
60A32 38
60A32 39
60A32 40
60A32 41
60A32 42
60A32 43
60A32 44
60A32 45
60A32 46
60A32 47
60A32 48
60A32 49
60A32 50
60A32 51
60A32 52
60A32 53
60A32 54
60A32 55
60A32 56
60A32 57
60A32 58

```

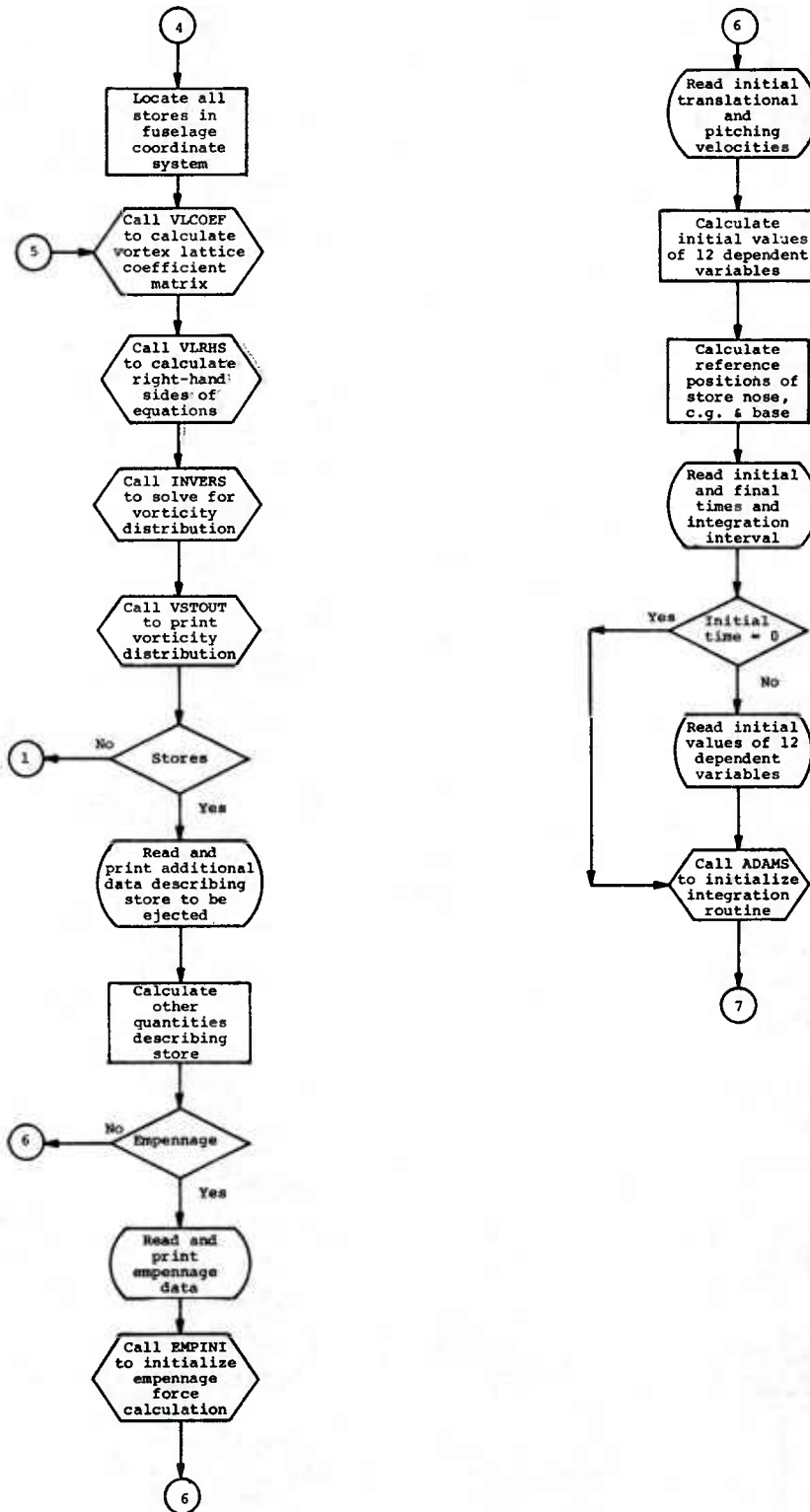
(t) Page 20.

Figure 10.- Continued.



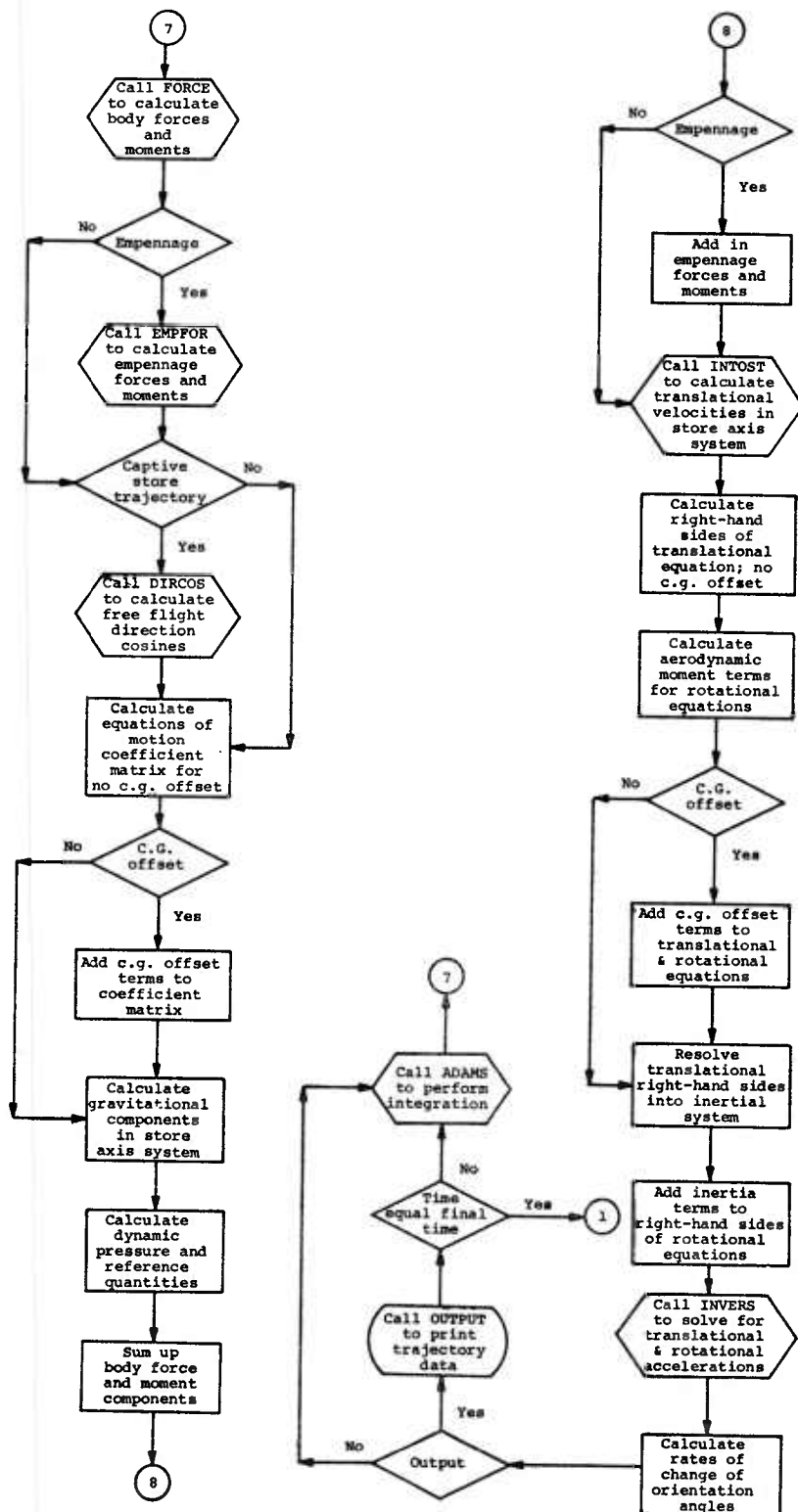
(a) Page 1.

Figure 11.- General flow chart of trajectory program.



(b) Page 2.

Figure 11.- Continued.



(c) Page 3.

Figure 11.- Concluded.

Item No. 1 (1 card)

Variable	NCARDS
Card Column	5
Format Type	I

Item No. 2 (NCARDS cards)

Variable	HEAD	
Card Column	1	80
Format Type	A	

Item No. 3 (1 card)

Variable	ALFAC	FMF	FMACH	RHO	VINF
Card Column	10	20	30	40	50
Format Type	F	F	F	F	F

Item No. 4 (1 card)

Variable	NFU	NPV	NBACK	NSTRS
Card Column	5	10	15	20
Format Type	I	I	I	I

Item No. 5 (1 card, omit if NFU = 0)

Variable	FLTHC	FMAX
Card Column	10	20
Format Type	F	F

Item No. 6 (1 card, omit if NFU = 0)

Variable	NFSOR
Card Column	5
Format Type	I

Item No. 7 (NFSOR values, six to a card. Omit if NFU = 0)

Variable	FXL(1)	FXL(2)	FXL(3)	FXL(NFSOR)
Card Column	12	24	36	48
Format Type	E	E	E	E
				60
				72
				E

(a) Page 1.

Figure 12.- Trajectory program input format.

Item No. 8 (NFSOR values, six to a card. Omit if NFU = 0)

Variable	FSOR(1)	FSOR(2)	...	FSOR(NFSOR)		
Card Column	12	24		48	60	72
Format Type	E	E	E	E	E	E

Item No. 9 (1 card)

Variable	XWOC	ZBWO	WIC
Card Column	10	20	30
Format Type	F	F	F

Item No. 10 (1 card)

Variable	CRW	SSPAN
Card Column	10	20
Format Type	F	F

Item No. 11 (1 card)

Variable	NCW	MSW
Card Column	5	10
Format Type	I	I

Item No. 12 (I = 1 to MSW+1; MSW+1 cards)

Variable	I	Y(I)	PSIWLE(I)	PSIWTE(I)	PHID(I)
Card Column	5	15	25	35	45
Format Type	I	F	F	F	F

Item No. 13 (1 card)

Variable	NTAC	NUNI
Card Column	5	10
Format Type	I	I

Item No. 14 (NCW values, eight to a card. Omit if NTAC = 0. One set of cards if NUNI = 1; MSW sets if NUNI = 0.

Variable	ALPHAL(1)	ALPHAL(2)	...	ALPHAL(NCW)		
Card Column	10	20	30	40	50	60
Format Type	F	F	F	F	F	F

(b) Page 2.

Figure 12.- Continued.

Item No. 15 (1 card)

Variable	NCWS	NUNIS
Card Column	5	10
Format Type	I	I

Item No. 16 (NCWS values, eight to a card. One set of cards if NUNIS = 1; NSW sets if NUNIS = 0.)

Variable	THETAL(1)	THETAL(2)	...	THETAL(NCWS)
Card Column	10	20	30	50
Format Type	F	F	F	F
				60
				70
				80
				F

Item No. 17 (1 card. Omit if NPY = 0.)

Variable	IP	PSIPLE	PSIPTE	CRP	H	XPLE
Card Column	5	15	25	35	45	55
Format Type	I	F	F	F	F	F

Item No. 18 (1 card. Omit if NPY = 0.)

Variable	NCP	MSP
Card Column	5	10
Format Type	I	I

Item No. 19 (K = 1 to MSP+1; MSP+1 cards. Omit if NPY = 0.)

Variable	K	Z(K)
Card Column	5	15
Format Type	I	F

Item No. 20 (1 card. Omit if NPY = 0.)

Variable	NCPS	NUNIP
Card Column	5	10
Format Type	I	I

Item No. 21 (NCPS values, eight to a card. Omit if NPY = 0. One set of cards if NUNIP = 1; MSP sets if NUNIP = 0.)

Variable	THETPL(1)	THETPL(2)	...	THETPL(NCPS)
Card Column	10	20	30	50
Format Type	F	F	F	F
				60
				70
				80
				F

(c) Page 3.

Figure 12.- Continued.

Item No. 22 (1 card. Omit if NRACK = 0.)

Variable	Card Column	Format Type	RLTHC	RRMAX	XRNC	ZRNN	RIC
	10		20	30	40	50	
	F		F	F	F	F	

Item No. 23 (1 card. Omit if NRACK = 0.)

Variable	Card Column	Format Type	NRSOR
	5		
	I		

Item No. 24 (NRSOR values, six to a card. Omit if NRACK = 0.)

Variable	Card Column	Format Type	RXL(1)	RXL(2)	...	RXL(NRSOR)
	12		24	36	48	60
	E		E	E	E	E
						72
						E

Item No. 25 (NRSOR values, six to a card. Omit if NRACK = 0.)

Variable	Card Column	Format Type	RSOR(1)	RSOR(2)	...	RSOR(NRSOR)
	12		24	36	48	60
	E		E	E	E	E
						72
						E

Note: If NSTRS = 0, this completes the input data. Since no stores are present, NSTRS = 0, a trajectory cannot be run.

Item No. 26 (J = 1 to NSTRS; NSTRS cards)

Variable	Card Column	Format Type	NUMSTR(J)	NSHAPE(J)	SLATC(J)	SRMAX(J)	XSNC(J)	YSN(J)	ZSN(J)	SIC(J)
	5		10	20	30	40	50	60	70	
	I		I	F	F	F	F	F	F	F

Item No. 27 (1 card)

Variable	Card Column	Format Type	NSHPT
	5		
	I		

(d) Page 4.

Figure 12.- Continued.

Item No. 28* (1 card)

Variable	MSOR
Card Column	5 10
Format Type	I I

Item No. 29* (MSOR values, six to a card)

Variable	DUMX(1)	DUMX(2)	...	DUMX(MSOR)	
Card Column	12	24	36	48	72
Format Type	E	E	E	E	E

Item No. 30* (MSOR values, six to a card)

Variable	DUMQ(1)	DUMQ(2)	...	DUMQ(MSOR)	
Card Column	12	24	36	48	72
Format Type	E	E	E	E	E

Item No. 31 (1 card)

Variable	NEJECT	NSEG	NSECKO	NGAM	NPOLY	NROLL	NEMP	NDAMP
Card Column	5	10	15	20	25	30	35	40
Format Type	I	I	I	I	I	I	I	I

Item No. 32 (1 card)

Variable	SMASS	FIXX	FIYY	FIZZ	FIYZ	FIXZ	FIYX
Card Column	10	20	30	40	50	60	70
Format Type	F	F	F	F	F	F	F

Item No. 33 (1 card)

Variable	XMOM	XBAR	YBAR	ZBAR
Card Column	10	20	30	40
Format Type	F	F	F	F

*If NSHPT > 1, repeat items 28 through 30, in sequence, NSHPT times.

(e) Page 5.

Figure 12.- Continued.

Item No. 34 (1 card)

Variable	XEND(1)	XEND(2)	...	XEND(NPOLY)			
Card Column	10	20	30	40	50	60	70
Format Type	F	F	F	F	F	F	F

Item No. 35 (J = 1 to NPOLY; NPOLY cards)

Variable	COEF(J,1)	COEF(J,2)	COEF(J,3)	COEF(J,4)	COEF(J,5)	COEF(J,6)	COEF(J,7)
Card Column	10	20	30	40	50	60	70
Format Type	F	F	F	F	F	F	F

Item No. 36 (1 card)

Variable	CA	CDC
Card Column	10	20
Format Type	F	F

Item No. 37 (1 card. Omit if NEMP = 0)

Variable	IPLNR	MSF
Card Column	5	10
Format Type	I	I

Item No. 38 (1 card. Omit if NEMP = 0)

Variable	XTAIL	RADAV	FINSS	PHIROL	CLALPH
Card Column	10	20	30	40	50
Format Type	F	F	F	F	F

Item No. 39 (1 card)

Variable	VZERO	VAR(5)
Card Column	10	20
Format Type	F	F

(f) Page 6.
Figure 12.- Continued.

Item No. 40 (1 card)

Variable	DTIME	TIMEI	TIMEF
Card Column	10	20	30
Format Type	F	F	F

Item No. 41 (2 cards. Omit if TIMEI = 0)

Variable	VAR(1)	VAR(2)	...	VAR(12)					
Card Column	10	20	30	40	50	60	70	80	
Format Type	F	F	F	F	F	F	F	F	

(g) Page 7.
Figure 12.- Concluded.

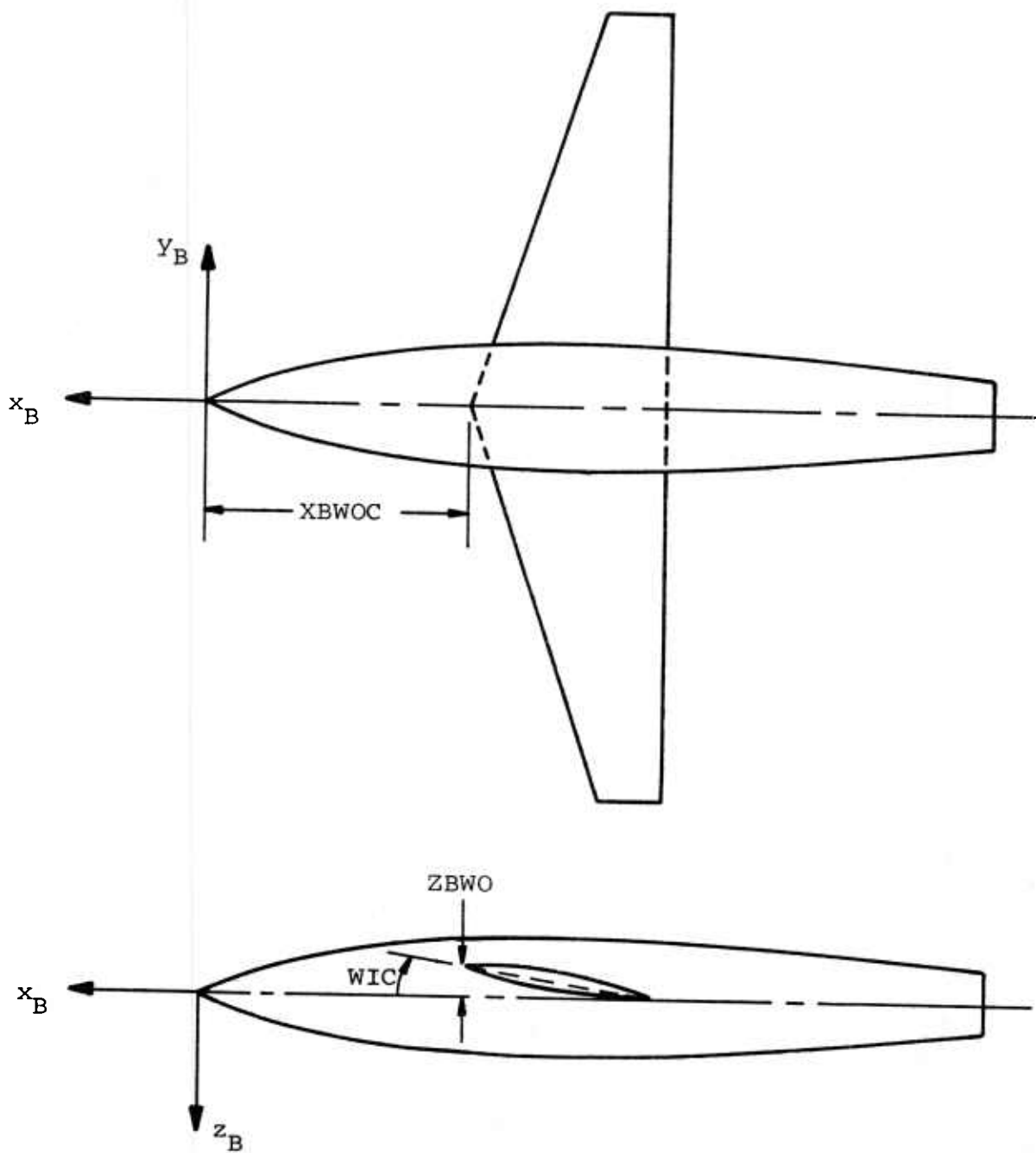


Figure 13.- Specification of wing location relative to fuselage nose and incidence angle.

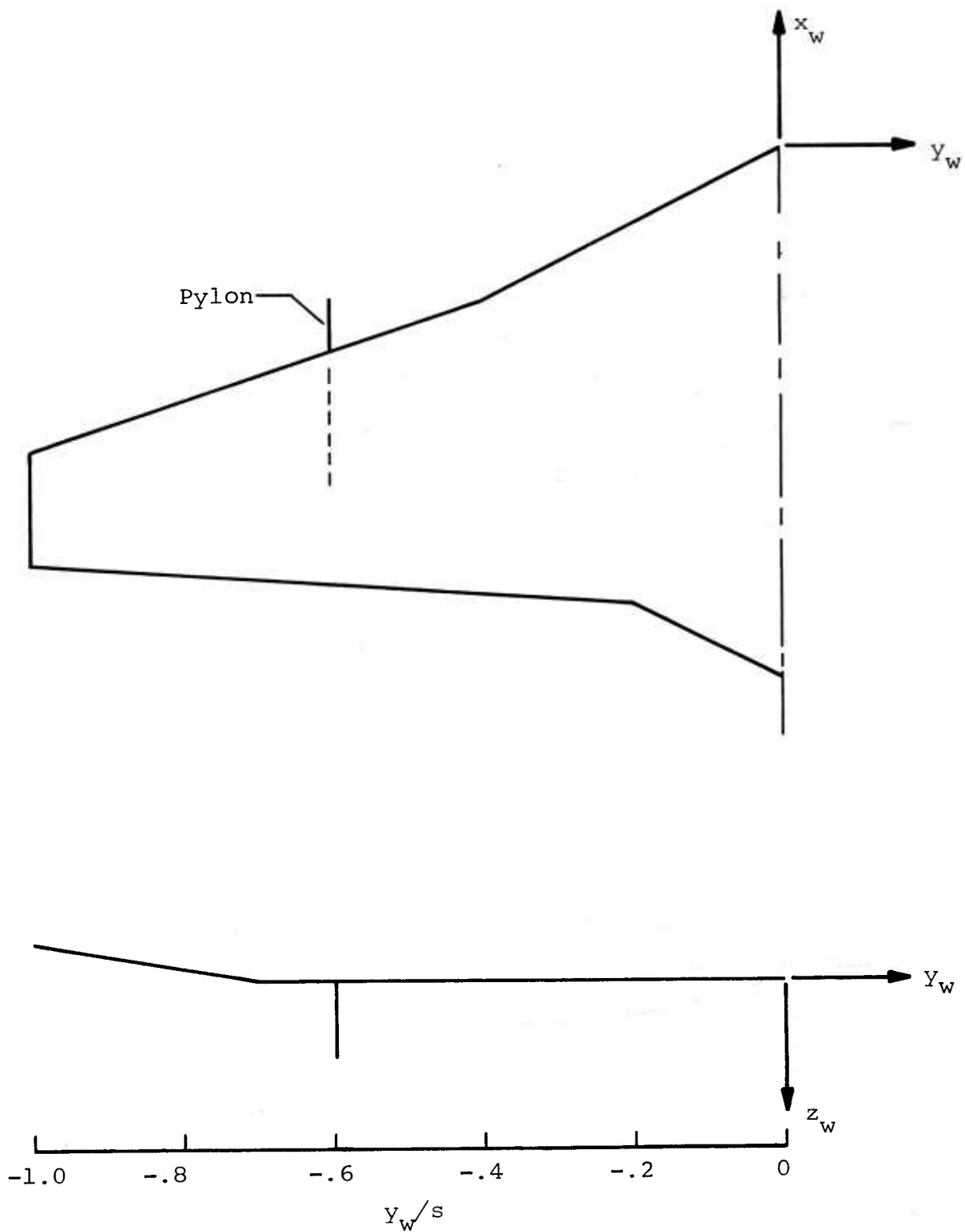
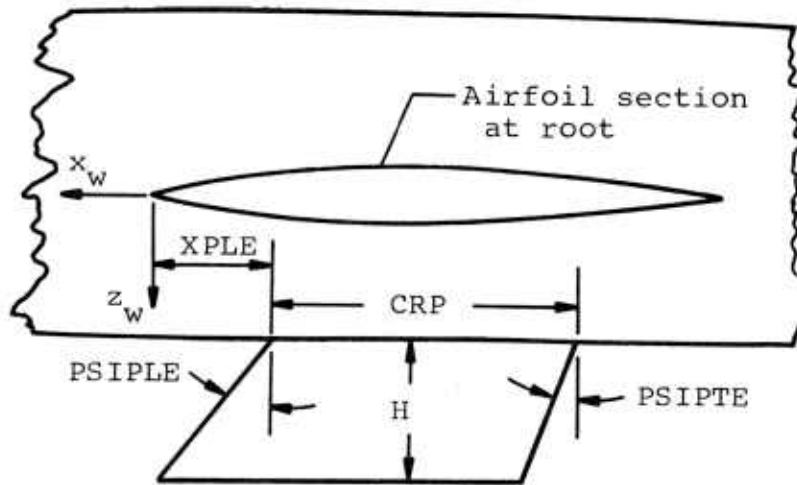
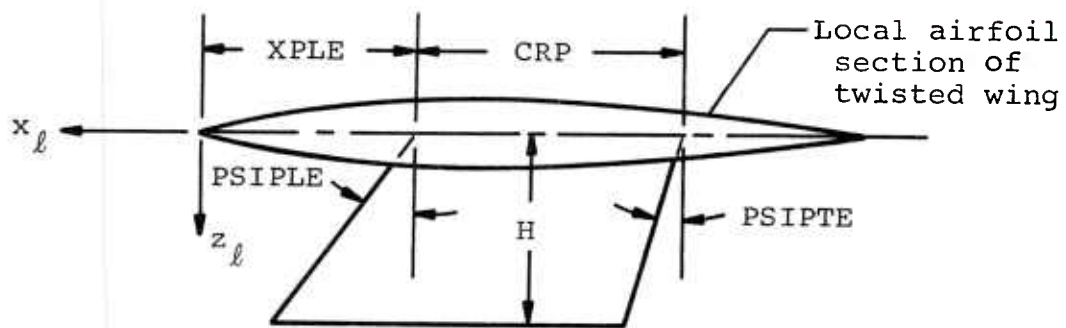


Figure 14.- Example wing.



(a) Pylon under fuselage centerline.



(b) Pylon under wing.

Figure 15.- Variables describing and locating pylon, input data item number 17.

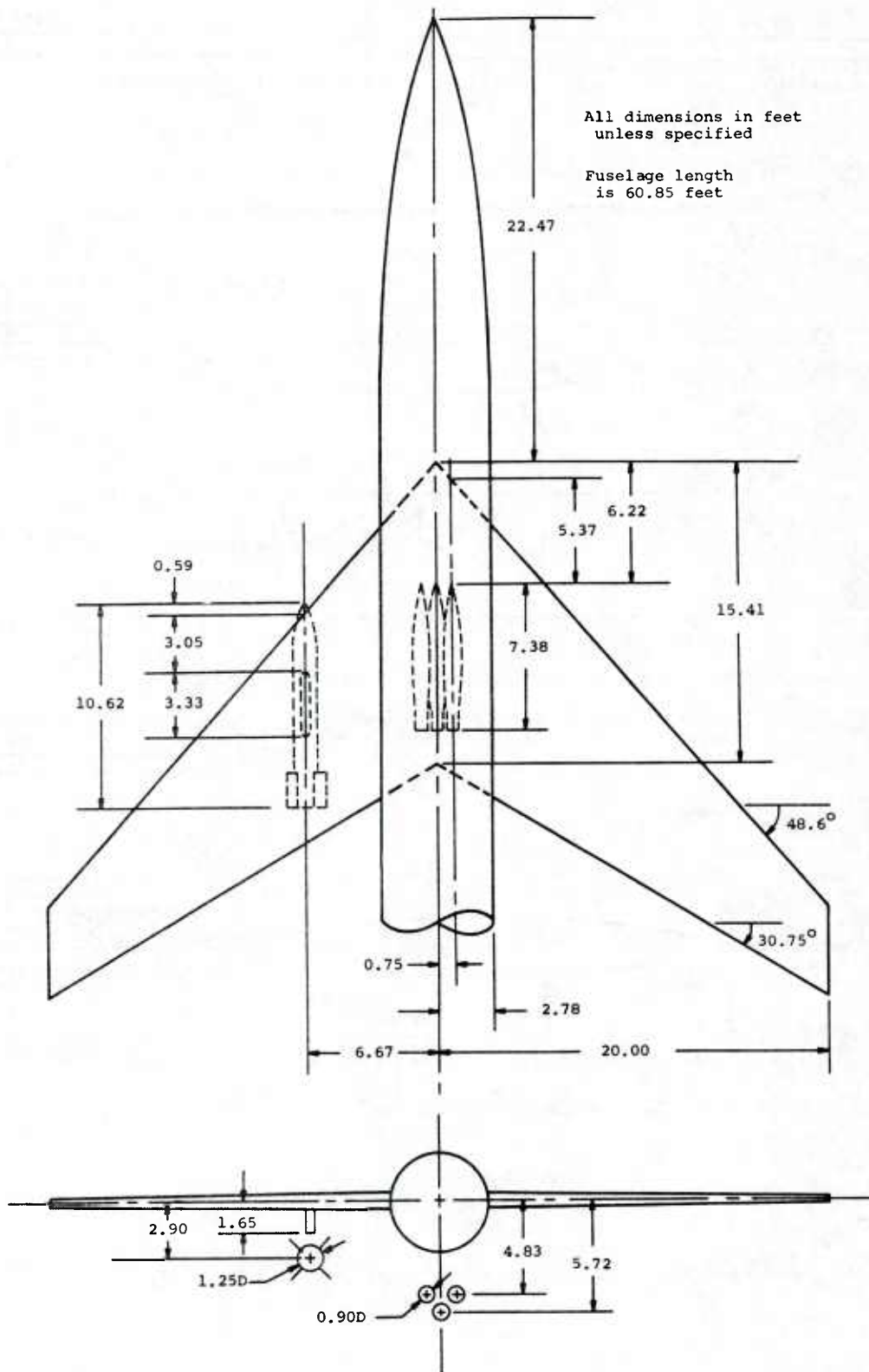


Figure 16.- Configuration for sample trajectory number 1.

13								1	
SAMPLE TRAJECTORY CALCULATION NUMBER 1									
AIRCRAFT AND STORES ARE SCALED UP VERSIONS OF MODELS USED IN EXPERIMENTAL									
PROGRAM CONDUCTED IN CONJUNCTION WITH THIS WORK									
MODELS SCALED UP BY A FACTOR OF 20 TO APPROXIMATE A FULL SCALE AIRCRAFT									
THERE IS A FINNED OGIVE-CYLINDER STORE ON A PYLON AT THE 1/3 SEMISPAN									
LOCATION OF THE LEFT WING PANEL									
THERE ARE ALSO THREE SMALL FINLESS BOATTAILED STORES GROUPED AS A TEP								2	
CLUSTER UNDER THE FUSELAGE									
THE STORE UNDER THE WING IS EJECTED WITH THE TRAJECTORY STARTING ONE									
RADIUS BELOW THE CARRIAGE POSITION									
IT IS A FREE-FLIGHT TRAJECTORY, NOT A CAPTIVE STORE TRAJECTORY									
ROLLING MOMENT IS CALCULATED									
DAMPING IS INCLUDED									
4.0	0.0	0.4	.0020482 440.7				3		
1	1	0	4						4
60.85	2.7834								5
58									6
2.0000-03	2.5300-03	3.2006-03	4.0487-03	5.1206-03	6.4745-03				
8.1831-03	1.0337-02	1.3048-02	1.6456-02	2.0729-02	2.6072-02				
3.2730-02	4.0993-02	5.1192-02	6.3697-02	7.8907-02	9.7224-02				
1.1902-01	1.4458-01	1.7406-01	2.0737-01	2.4415-01	2.8372-01				
3.2508-01	3.6696-01	4.0885-01	4.5073-01	4.9262-01	5.3450-01	7			
5.7639-01	6.1827-01	6.6016-01	7.0204-01	7.4393-01	7.8581-01				
8.2745-01	8.6805-01	9.0887-01	9.4326-01	9.7673-01	1.0070-00				
1.0538-00	1.0573-00	1.0776-00	1.0948-00	1.1094-00	1.1215-00				
1.1316-00	1.1399-00	1.1467-00	1.1522-00	1.1567-00	1.1603-00				
1.1632-00	1.1656-00	1.1675-00	1.1690-00						
6.0353-06	-5.4782-06	3.5398-06	-2.1785-06	1.6162-06	-6.6962-07				
1.0445-06	3.1040-07	1.3737-06	1.6004-06	2.8780-06	4.2266-06				
6.6436-06	9.9387-06	1.4813-05	2.1403-05	3.0083-05	4.0582-05				
5.2073-05	6.2487-05	6.8767-05	6.2946-05	7.3261-05	4.5069-06				
-7.6829-07	-1.2766-05	9.9914-06	-1.1501-05	1.0717-05	-1.1060-05	8			
1.1063-05	-1.0703-05	1.1555-05	-9.8993-06	1.6496-05	-1.3298-05				
-3.1426-05	-4.5538-05	-5.3635-05	-5.6492-05	-5.3967-05	-4.8229-05				
-4.0372-05	-3.2497-05	-2.4705-05	-1.8652-05	-1.3021-05	-9.7406-06				
-5.9456-06	-5.1105-06	-1.9394-06	-3.3603-06	7.1284-07	-3.6458-06				
3.4910-06	-6.0077-06	8.0640-06	-9.4139-06						
-22.406	0.0	0.0							9
15.412	20.0								10
8	5								11
1	0.0	0.0	0.0	0.0					
2	-3.33333	48.6	30.75	0.0					
3	-6.66667	48.6	30.75	0.0					
4	-10.00000	48.6	30.75	0.0					
5	-15.00000	48.6	30.75	0.0					
6	-20.00000	48.6	30.75	0.0					
0									13
16	1								15
.18074	.09400	.06400	.04400	.02800	.01955	-.00122	-.01341	16	
-.02561	-.03782	-.05005	-.06000	-.06600	-.06719	-.06719	-.06719		
3	0.0	0.0	3.33333	1.652	-3.046				17
2	2								18
1	0.0								19
2	0.826								
3	1.652								
60	1								
1.7406	.7502	.3536	.06686	0.0	0.0	0.0	0.0	20	
0.0	0.0	0.0	0.0	0.0	0.0	0.0	0.0	21	
0.0	0.0	0.0	0.0	0.0	0.0	0.0	0.0		
0.0	0.0	0.0	0.0	0.0	0.0	0.0	0.0		
0.0	0.0	0.0	0.0	0.0	0.0	0.0	0.0		
0.0	0.0	0.0	0.0	0.0	0.0	0.0	0.0		
0.0	0.0	0.0	0.0	0.0	0.0	0.0	0.0		
0.0	0.0	0.0	0.0	0.0	0.0	0.0	0.0		
0.0	0.0	0.0	0.0	0.0	0.0	0.0	0.0		
0.0	0.0	0.0	0.0	0.0	0.0	0.0	0.0		
0.0	0.0	0.0	0.0	0.0	0.0	0.0	0.0		
-.06686	-.3536	-.7502	-1.7406						
10	2	10.625	0.625	0.59333	-6.66667	2.902	0.0	26	
20	5	7.38333	0.44667	-6.22083	0.0	5.71666	0.0		
21	5	7.38333	0.44667	-5.37033	-0.75	4.83333	0.0		
22	5	7.38333	0.44667	-5.37033	0.75	4.83333	0.0		
2									27

(a) Page 1.

Figure 17.- Input data for sample trajectory calculation number 1.

						Item No.
2 51						28
2.0000-03	2.6473-03	3.5132-03	4.6705-03	6.2149-03	8.2721-03	29
1.1006-02	1.4626-02	1.9400-02	2.5661-02	3.3810-02	4.4316-02	
5.7099-02	7.4485-02	9.5145-02	1.1999-01	1.4904-01	1.8194-01	
2.1781-01	2.5531-01	2.9305-01	3.3079-01	3.6852-01	4.0626-01	
4.4400-01	4.8175-01	5.1947-01	5.5721-01	5.9494-01	6.3268-01	
6.7042-01	7.0815-01	7.4589-01	7.8363-01	8.2136-01	8.5910-01	
8.9084-01	9.3457-01	9.7231-01	1.0100-00	1.0477-00	1.0840-00	
1.1171-00	1.1459-00	1.1697-00	1.1884-00	1.2025-00	1.2127-00	
1.2200-00	1.2250-00	1.2284-00				
4.8513-06	-4.3215-06	2.4426-06	-7.1054-07	1.2638-06	1.0935-06	30
2.5749-06	4.3291-06	7.8030-06	1.3510-05	2.3018-05	3.7947-05	
5.9954-05	8.9502-05	1.2214-04	1.5482-04	1.2820-04	2.0261-04	
-5.0476-05	-1.1398-04	1.1594-04	-1.2468-04	1.2050-04	-1.2526-04	
1.2144-04	-1.2266-04	1.2185-04	-1.2235-04	1.2211-04	-1.2213-04	
1.2233-04	-1.2188-04	1.2265-04	-1.2149-04	1.2318-04	-1.2063-04	
1.2450-04	-1.1674-04	1.1695-04	1.1480-05	-1.1924-04	-1.7271-04	
-1.7495-04	-1.3912-04	-9.3587-05	-5.4285-05	-2.9966-05	-1.2530-05	
-1.0227-05	4.6640-06	-1.1713-05				
5 44						28
2.0000-03	2.8692-03	4.1068-03	5.8625-03	8.3399-03	1.1810-02	29
1.6019-02	2.3192-02	3.2007-02	4.3538-02	5.8146-02	7.5981-02	
9.7189-02	1.2159-01	1.4862-01	1.7742-01	2.0779-01	2.3980-01	
2.7554-01	3.0909-01	3.4655-01	3.8580-01	4.2644-01	4.6791-01	
5.0956-01	5.5081-01	5.9097-01	6.2948-01	6.6584-01	6.9965-01	
7.3065-01	7.5881-01	7.8492-01	8.0970-01	8.3372-01	8.5746-01	
8.8119-01	9.0493-01	9.2867-01	9.5241-01	9.7614-01	9.9988-01	
1.0236-00	1.0435-00					
3.8950-06	-2.9405-06	1.8989-06	5.6064-07	2.6288-06	4.7915-06	
9.7339-06	1.8419-05	3.2418-05	5.3617-05	5.6472-05	9.3568-05	30
8.9716-05	9.5866-05	-5.8866-05	1.3457-04	-2.0499-05	1.2904-04	
1.0512-05	1.3466-04	9.0154-05	-2.6121-05	1.2754-04	-1.0693-04	
6.5050-05	-1.7406-04	3.1092-05	-2.3365-04	4.9012-05	-2.8651-04	
8.2015-05	-2.0799-04	1.6671-04	-2.1783-04	2.2493-04	-2.1059-04	
2.1369-04	-2.0999-04	2.1386-04	-2.0582-04	1.9470-04	2.2062-05	
-4.1387-04	1.8464-05					
10 20 20 0 2 1 1 1						31
15.53	8.0	80.0	80.0	0.0	0.0	32
-5.3125	0.0	0.0	0.0			33
0.2353	1.1					34
-0.4415	-1.0	0.4706	0.1947		1.0	35
0.05862						36
0.4	0.0					37
0	5					38
-9.376	0.625	1.45833	45.0	3.22		39
10.0	0.0					40
0.05	0.0	0.6				

(b) Page 2.

Figure 17.- Concluded.

										Item No.
13										1
SAMPLE TRAJECTORY CALCULATION NUMBER 2										
AIRCRAFT AND STORES ARE SCALED UP VERSIONS OF MODELS USED IN EXPERIMENTAL PROGRAM CONDUCTED IN CONJUNCTION WITH THIS WORK										
MODELS SCALED UP BY A FACTOR OF 20 TO APPROXIMATE A FULL SCALE AIRCRAFT										
THERE IS A SMALL FINLESS BOATTAILED STORE AT THE 1/3 SEMISPAN LOCATION OF BOTH WING PANELS										2
THERE ALSO ARE THREE FINLESS OGIVE-CYLINDER STORES GROUPED ON A TIE-RACK/PYLON UNDER THE FUSELAGE										
THE BOTTOM STORE OF THE TIE GROUPING IS THE STORE EJECTED WITH THE TRAJECTORY STARTING ONE RADIUS BELOW THE CARRIAGE POSITION										
IT IS A FREE-FLIGHT TRAJECTORY, NOT A CAPTIVE STORE TRAJECTORY										
DAMPING IS INCLUDED										
THE AIRCRAFT IS DIVING AT A FLIGHT PATH ANGLE OF -30 DEGREES										
6.0	-30.0	0.4	.0020482 440.7							3
1	1	1	5							4
60.85	2.7834									5
50										6
2.0000-03	2.5300-03	3.2000-03	4.0487-03	5.1200-03	6.4745-03					7
8.1531-03	1.0337-02	1.3048-02	1.6450-02	2.0729-02	2.6072-02					
3.2730-02	4.0993-02	5.1192-02	6.3697-02	7.8907-02	9.7224-02					
1.1902-01	1.4456-01	1.7406-01	2.0737-01	2.4415-01	2.8372-01					
3.2500-01	3.6696-01	4.0885-01	4.5073-01	4.9262-01	5.3450-01					
5.7039-01	6.1827-01	6.6010-01	7.0204-01	7.4393-01	7.8581-01					
8.2745-01	8.6805-01	9.0887-01	9.4326-01	9.7673-01	1.0070-00					
1.0338-00	1.0573-00	1.0770-00	1.0948-00	1.1094-00	1.1215-00					8
1.1310-00	1.1399-00	1.1467-00	1.1522-00	1.1567-00	1.1603-00					
1.1632-00	1.1656-00	1.1675-00	1.1690-00							
6.0353-06	-5.4782-06	3.5398-06	-2.1785-06	1.6162-06	-6.6962-07					
1.0445-06	3.1040-07	1.3737-06	1.6004-06	2.8780-06	4.2266-06					
6.6430-06	9.9587-06	1.4813-05	2.1403-05	3.0083-05	4.0582-05					
5.2073-05	6.2487-05	6.8767-05	6.2940-05	7.3261-05	4.5069-06					
-7.6829-07	-1.2766-05	9.9914-06	-1.1501-05	1.0717-05	-1.1060-05					
1.1063-05	-1.0703-05	1.1555-05	-9.8993-06	1.6490-05	-1.3296-05					
-3.1420-05	-4.5538-05	-5.3835-05	-5.6492-05	-5.3967-05	-4.8229-05					
-4.0372-05	-3.2497-05	-2.4705-05	-1.8652-05	-1.3021-05	-9.7400-06					
-5.9450-06	-5.1105-06	-1.9394-06	-3.3603-06	7.1284-07	-3.6458-06					
3.4910-06	-6.0077-06	8.0640-06	-9.4139-06							9
-22.406	0.0	0.0								10
15.412	20.0									11
8	5									12
1	0.0	0.0	0.0	0.0						
2	-3.33333	48.6	30.75	0.0						
3	-6.66667	48.6	30.75	0.0						
4	-10.00000	48.6	30.75	0.0						
5	-15.00000	48.6	30.75	0.0						
6	-20.00000	48.6	30.75	0.0						
0										13
10	1									15
.10074	.09400	.06400	.04400	.02800	.01955	-.00122	-.01341			16
-.02501	-.03702	-.05005	-.06000	-.06600	-.06719	-.06719	-.06719			17
1	0.0	0.0	3.33333	1.652	-8.24583					18
2	2									19
1	2.7834									20
2	3.6094									21
3	4.4354									22
60	1									23
1.7400	.7502	.3536	.06686	0.0	0.0	0.0	0.0	0.0	0.0	24
0.0	0.0	0.0	0.0	0.0	0.0	0.0	0.0	0.0	0.0	
0.0	0.0	0.0	0.0	0.0	0.0	0.0	0.0	0.0	0.0	
0.0	0.0	0.0	0.0	0.0	0.0	0.0	0.0	0.0	0.0	
0.0	0.0	0.0	0.0	0.0	0.0	0.0	0.0	0.0	0.0	
0.0	0.0	0.0	0.0	0.0	0.0	0.0	0.0	0.0	0.0	
0.0	0.0	0.0	0.0	0.0	0.0	0.0	0.0	0.0	0.0	
0.0	0.0	0.0	0.0	0.0	0.0	0.0	0.0	0.0	0.0	
0.0	0.0	0.0	0.0	0.0	0.0	0.0	0.0	0.0	0.0	
0.0	0.0	0.0	0.0	0.0	0.0	0.0	0.0	0.0	0.0	
0.0	0.0	0.0	0.0	0.0	0.0	0.0	0.0	0.0	0.0	
0.0	0.0	0.0	0.0	0.0	0.0	0.0	0.0	0.0	0.0	
-.00606	-.3536	-.7502	-1.7400							25
5.50833	0.31667	-7.12833	4.75207	0.0						26

(a) Page 1.

Figure 19.- Input data for sample trajectory calculation number 2.

								Item No.
39								23
2.0000-03	5.9937-03	1.2679-02	2.2899-02	3.6119-02	5.2485-02			24
7.1853-02	9.4006-02	1.1860-01	1.4548-01	1.7408-01	2.0404-01			
2.3488-01	2.6013-01	2.9740-01	3.2867-01	3.5995-01	3.9122-01			
4.2449-01	4.5377-01	4.8504-01	5.1631-01	5.4759-01	5.7886-01			
6.1013-01	6.4141-01	6.7268-01	7.0395-01	7.3523-01	7.6650-01			
7.9777-01	8.2905-01	8.6032-01	8.9159-01	9.2287-01	9.5478-01			
9.7867-01	9.9869-01	1.0123-00						25
-5.6644-07	2.0447-05	5.2143-05	6.6002-05	8.0062-05	8.8621-05			
9.2091-05	9.0897-05	8.2019-05	7.5763-05	1.7835-05	1.2050-04			
-1.1040-04	5.3828-05	-5.1300-05	4.5747-05	-4.8280-05	4.6454-05			
-4.7069-05	4.6862-05	-4.7357-05	4.7119-05	-4.7125-05	4.7348-05			
-4.6877-05	4.7041-05	-4.6504-05	4.8151-05	-4.5770-05	4.9387-05			
-4.4521-05	5.8037-05	-7.4667-05	2.8150-04	-2.9120-04	-3.0856-04			26
-2.1453-04	-7.9127-05	-4.6523-05						
10	5	7.38333	0.44667	-1.0275	-6.66667	1.98612	0.0	
20	2	10.625	0.625	-4.6	0.0	6.52107	0.0	
21	2	10.625	0.625	-3.6172	-0.86667	4.96353	0.0	
22	2	10.625	0.625	-3.6172	0.86667	4.96333	0.0	
30	5	7.38333	0.44667	-1.0275	6.66667	1.98612	0.0	27
2								28
5 44								29
2.0000-03	2.8692-03	4.1068-03	5.8625-03	8.3399-03	1.1810-02			
1.6019-02	2.3192-02	3.2007-02	4.3538-02	5.8140-02	7.5981-02			
9.7189-02	1.2159-01	1.4862-01	1.7742-01	2.0779-01	2.3980-01			
2.7354-01	3.0909-01	3.4053-01	3.8580-01	4.2644-01	4.6791-01			
5.0958-01	5.5081-01	5.9097-01	6.2948-01	6.6584-01	6.9965-01			
7.3065-01	7.5881-01	7.8492-01	8.0970-01	8.3372-01	8.5746-01			30
8.8119-01	9.0493-01	9.2867-01	9.5241-01	9.7614-01	9.9988-01			
1.0230-00	1.0435-00							
3.8950-06	-2.9405-06	1.8989-06	5.6064-07	2.6288-06	4.7915-06			
9.7339-06	1.8419-05	3.2418-05	5.3617-05	5.6472-05	9.3568-05			
8.9710-05	9.5866-05	-5.8868-05	1.3457-04	-2.0499-05	1.2904-04			
1.0512-05	1.3466-04	9.0154-05	-2.6121-05	1.2754-04	-1.0693-04			28
6.5850-05	-1.7406-04	3.1092-05	-2.3365-04	4.9612-05	-2.8651-04			
8.2015-05	-2.0799-04	1.6871-04	-2.1783-04	2.2493-04	-2.1059-04			
2.1369-04	-2.0999-04	2.1388-04	-2.0582-04	1.9470-04	2.2662-05			
-4.1387-04	1.8464-05							
2 51								
2.0000-03	2.6473-03	3.5132-03	4.6705-03	6.2149-03	8.2721-03			30
1.1000-02	1.4626-02	1.9400-02	2.5661-02	3.3810-02	4.4316-02			
5.7099-02	7.4485-02	9.5145-02	1.1999-01	1.4904-01	1.8194-01			
2.1781-01	2.5531-01	2.9305-01	3.3079-01	3.6852-01	4.0626-01			
4.4400-01	4.8173-01	5.1947-01	5.5721-01	5.9494-01	6.3268-01			
6.7042-01	7.0815-01	7.4589-01	7.8363-01	8.2136-01	8.5910-01			
8.9684-01	9.3457-01	9.7231-01	1.0100-00	1.0477-00	1.0840-00			31
1.1171-00	1.1459-00	1.1697-00	1.1884-00	1.2025-00	1.2127-00			
1.2200-00	1.2250-00	1.2284-00						
4.8513-06	-4.3215-06	2.4420-06	-7.1054-07	1.2638-06	1.0935-06			
2.5749-06	4.3291-06	7.8030-06	1.3510-05	2.3018-05	3.7947-05			
5.9954-05	8.9502-05	1.2214-04	1.5482-04	1.2820-04	2.0261-04			
-5.0470-05	-1.1398-04	1.1594-04	-1.2468-04	1.2050-04	-1.2326-04			32
1.2144-04	-1.2266-04	1.2185-04	-1.2235-04	1.2211-04	-1.2213-04			
1.2233-04	-1.2188-04	1.2263-04	-1.2149-04	1.2318-04	-1.2063-04			
1.2450-04	-1.1674-04	1.1695-04	1.1480-05	-1.1924-04	-1.7271-04			
-1.7495-04	-1.3912-04	-9.3587-05	-5.4285-05	-2.9960-05	-1.2530-05			
-1.0227-05	4.6040-06	-1.1713-05						
20	20	20	0	2	0	0	1	33
15.53	8.0	80.0	80.0	80.0	0.0	0.0	0.0	34
-5.3125	0.0	0.0	0.0					35
0.2353	1.1							36
-0.4413	-1.0	0.4706	0.1947			1.0		37
0.03802								38
0.2	0.0							39
10.0	0.0							40
0.03	0.0	0.6						

(b) Page 2.

Figure 19.- Concluded.

SIX-DEGREE-OF-FREEDOM TRAJECTORY PROGRAM

SAMPLE TRAJECTORY CALCULATION NUMBER 1
 AIRCRAFT AND STORES ARE SCALED UP VERSIONS OF MODELS USED IN EXPERIMENTAL
 PROGRAM CONDUCTED IN CONJUNCTION WITH THIS WORK
 MODELS SCALED UP BY A FACTOR OF 20 TO APPROXIMATE A FULL SCALE AIRCRAFT
 THERE IS A FINNED CGIVE-CYLINDER STORE ON A FYLCA AT THE 1/3 SEMISPAN
 LOCATION OF THE LEFT WING PANEL
 THERE ARE ALSO THREE SMALL FINLESS BOATTIALED STORES GROUPED AS A TER
 CLUSTER UNDER THE FUSELAGE
 THE STORE UNDER THE WING IS EJECTED WITH THE TRAJECTORY STARTING ONE
 RADIUS BELOW THE CARRIAGE POSITION
 IT IS A FREE-FLIGHT TRAJECTORY, NOT A CAPTIVE STORE TRAJECTORY
 ROLLING MOMENT IS CALCULATED
 DAMPING IS INCLUDED

AIRCRAFT FLIGHT CONDITIONS
 ANGLE OF ATTACK = 4.00 DEGREES
 FLIGHT PATH ANGLE = 0.00 DEGREES
 MACH NUMBER = .40
 FREE STREAM MASS DENSITY = .0020462 SLUGS PER CUBIC FOOT
 FREE STREAM VELOCITY = 440.70 FEET PER SECOND

FUSELAGE INPUT DATA
 FUSELAGE LENGTH = 60.85000 FEET
 MAXIMUM RADIUS = 2.78340 FEET

INCOMPRESSIBLE SOURCE DISTRIBUTION

X/L	2.00000E-03	2.53000E-03	3.20060E-03	4.04870E-03	5.12060E-03	6.47450E-03	8.18310E-03	1.03370E-02
O*(K)	6.03530E-06	5.47820E-06	3.53980E-06	-2.17850E-06	1.61620E-06	-6.69620E-07	1.04450E-06	3.10400E-07
X/L	1.30480E-02	1.64560E-02	2.07290E-02	2.60720E-02	3.27300E-02	4.09930E-02	5.11920E-02	6.36970E-02
O*(K)	1.37370E-06	1.60040E-06	2.87800E-06	4.22660E-06	6.64360E-06	9.93870E-06	1.48130E-05	2.14030E-05
X/L	7.89070E-02	9.72240E-02	1.19020E-01	1.44580E-01	1.74060E-01	2.07370E-01	2.44150E-01	2.83720E-01
O*(K)	3.00830E-05	4.05820E-05	5.20730E-05	6.24870E-05	6.87670E-05	6.29460E-05	7.32610E-05	4.50690E-06
X/L	3.25080E-01	3.66960E-01	4.08850E-01	4.50730E-01	4.92620E-01	5.34500E-01	5.76390E-01	6.18270E-01
O*(K)	-7.68290E-07	-1.27660E-05	9.99140E-06	-1.15010E-05	1.07170E-05	-1.10600E-05	1.10630E-05	-1.07030E-05
X/L	6.60160E-01	7.02040E-01	7.43930E-01	7.85810E-01	8.27450E-01	8.68050E-01	9.06870E-01	9.43260E-01
O*(K)	1.15550E-05	-9.89930E-06	1.64960E-05	-1.32980E-05	3.14260E-05	-4.55380E-05	5.38350E-05	-5.64920E-05
X/L	9.76730E-01	1.00700E+00	1.03380E+00	1.05730E+00	1.07760E+00	1.09480E+00	1.10940E+00	1.12150E+00
O*(K)	-5.39670E-05	-4.82290E-05	-4.03720E-05	-3.24970E-05	-2.47050E-05	-1.86520E-05	-1.30210E-05	-9.74060E-06
X/L	1.13160E+00	1.13990E+00	1.14670E+00	1.15220E+00	1.15670E+00	1.16030E+00	1.16320E+00	1.16560E+00
O*(K)	-5.94580E-06	-5.11050E-06	-1.93940E-06	-3.36030E-06	7.12840E-07	-3.44580E-05	3.49100E-06	-6.00770E-06
X/L	1.16750E+00	1.16900E+00						
O*(K)	8.06400E-06	-9.41390E-06						

(a) Page 1.

Figure 20.- Trajectory program output for sample case 1.

WING INPUT DATA

LOCATION OF WING ROOT CHORD LEADING EDGE RELATIVE TO FUSELAGE NOSE
 XF = -22.4600 FEET
 ZF = 0.0000 FEET
 INCIDENCE ANGLE OF WING ROOT CHORD RELATIVE TO FUSELAGE AXIS
 IM = 0.00 DEGREES
 LENGTH OF WING ROOT CHORD
 CRM = 15.41200 FEET
 WING SEMISPAN
 SSPAN = 20.00000 FEET

40 VORTICES ARE TO BE LAID OUT ON EACH WING PANEL
 5 CHORDWISE ROWS WITH 8 IN EACH ROW

SPANWISE LOCATIONS OF TRAILING VORTEX LEGS AND SWEEP ANGLES AND
 DIHEDRAL ANGLE OF WING SECTION TO THE RIGHT

I	SPANWISE LOCATION FEET	LF SWEEP DEGREES	TE SWEEP DEGREES	DIHEDRAL DEGREES
1	0.00000	0.00000	0.00000	0.00000
2	-2.33333	48.60000	30.75000	0.00000
3	-6.66667	48.60000	30.75000	0.00000
4	-10.00000	48.60000	30.75000	0.00000
5	-15.00000	48.60000	30.75000	0.00000
6	-20.00000	48.60000	30.75000	0.00000

80 THICKNESS PANELS ARE TO BE LAID OUT ON EACH WING PANEL
 5 CHORDWISE ROWS WITH 16 IN EACH ROW
 THE CHORDWISE ROWS COINCIDE WITH THOSE USED
 IN THE VORTEX LATTICE

(b) Page 2.

Figure 20.- Continued.

PYLON INPUT DATA

LEADING EDGE OF PYLON ROOT CHORD IS AT X = -3.04600 FEET (MEASURED FROM LOCAL WING LEADING EDGE)
 SPANWISE LOCATION IS Y = -6.66667 FEET
 ROOTCHORD = 3.33333 FEET
 HEIGHT = 1.65200 FEET
 LEADING EDGE SWEEP ANGLE = 0.00000 DEGREES
 TRAILING EDGE SWEEP ANGLE = 0.00000 DEGREES

4 VORTICES ARE TO BE LAID OUT ON THE PYLON
 2 CHORDWISE ROWS WITH 2 IN EACH ROW

SPANWISE LOCATIONS OF TRAILING VORTEX LEGS

K	Z FEET
1	0.00000
2	.82600
3	1.65200

120 THICKNESS PANELS ARE TO BE LAID OUT ON THE PYLON
 2 CHORDWISE ROWS WITH 60 IN EACH ROW
 THE CHORDWISE ROWS COINCIDE WITH THOSE USED
 IN THE VORTEX LATTICE

(c) Page 3.

Figure 20.- Continued.

VORTEX LATTICE CONTROL POINT COORDINATES AND
INLET TWIST AND CAMBER DISTRIBUTION
AT THESE POINTS
(WING COORDINATE SYSTEM)

WING CONTROL POINTS		X, FT	Y, FT	Z, FT	SLOPE
ROW	VORTEX	-3.25106	-1.66667	0.00000	0.00000
		-5.06520	-1.66667	0.00000	0.00000
1	2	-6.87934	-1.66667	0.00000	0.00000
1	3	-8.69348	-1.66667	0.00000	0.00000
1	4	-10.50761	-1.66667	0.00000	0.00000
1	5	-12.32175	-1.66667	0.00000	0.00000
1	6	-14.13589	-1.66667	0.00000	0.00000
1	7	-15.95003	-1.66667	0.00000	0.00000
1	8	-17.76417	-1.66667	0.00000	0.00000
2	1	-6.86345	-5.00000	0.00000	0.00000
2	2	-8.45286	-5.00000	0.00000	0.00000
2	3	-10.04227	-5.00000	0.00000	0.00000
2	4	-11.63168	-5.00000	0.00000	0.00000
2	5	-13.22110	-5.00000	0.00000	0.00000
2	6	-14.81051	-5.00000	0.00000	0.00000
2	7	-16.39992	-5.00000	0.00000	0.00000
2	8	-17.98933	-5.00000	0.00000	0.00000
3	1	-10.47583	-8.33333	0.00000	0.00000
3	2	-11.84052	-8.33333	0.00000	0.00000
3	3	-13.20520	-8.33333	0.00000	0.00000
3	4	-14.56989	-8.33333	0.00000	0.00000
3	5	-15.93458	-8.33333	0.00000	0.00000
3	6	-17.29927	-8.33333	0.00000	0.00000
3	7	-18.66395	-8.33333	0.00000	0.00000
3	8	-20.02864	-8.33333	0.00000	0.00000
4	1	-14.99430	-12.50000	0.00000	0.00000
4	2	-16.07508	-12.50000	0.00000	0.00000
4	3	-17.15587	-12.50000	0.00000	0.00000
4	4	-18.24265	-12.50000	0.00000	0.00000
4	5	-19.32643	-12.50000	0.00000	0.00000
4	6	-20.41021	-12.50000	0.00000	0.00000
4	7	-21.49399	-12.50000	0.00000	0.00000
4	8	-22.57777	-12.50000	0.00000	0.00000
5	1	-20.40597	-17.50000	0.00000	0.00000
5	2	-21.15657	-17.50000	0.00000	0.00000
5	3	-21.90326	-17.50000	0.00000	0.00000
5	4	-22.64996	-17.50000	0.00000	0.00000
5	5	-23.39665	-17.50000	0.00000	0.00000
5	6	-24.14334	-17.50000	0.00000	0.00000
5	7	-24.89004	-17.50000	0.00000	0.00000
5	8	-25.63673	-17.50000	0.00000	0.00000

PYLON CONTROL POINTS		X, FT	Y, FT	Z, FT
ROW	VORTEX	-11.85785	-6.66667	.41300
		-13.52452	-6.66667	.41300
1	2	-11.85785	-6.66667	1.23900
2	2	-13.52452	-6.66667	1.23900

(d) Page 4.

Figure 20.- Continued.

STORE INPUT DATA

STORE NO	SHAPE NO	LENGTH FT	MAXIMUM RADIUS FT	STORE LOCATION RELATIVE TO LOCAL WING CHORD LEADING EDGE				INCIDENCE ANGLE DEG	
				X, FT	Y, FT	Z, FT			
10	2	10.62500	.62500	.59333	-6.66667	2.90200		0.00000	
20	5	7.38333	.44667	-6.22083	0.00000	5.71666		0.00000	
21	5	7.38333	.44667	-5.37033	-7.50000	4.83333		0.00000	
22	5	7.38333	.44667	-5.37033	.75000	4.83333		0.00000	

SOURCE DISTRIBUTION FOR SHAPE NO 2

INCOMPRESSIBLE SOURCE DISTRIBUTION

X/L	2.00000E-03	2.64730E-03	3.51320E-03	4.67050E-03	6.21490E-03	8.27210E-03	1.10050E-02	1.46260E-02
Q*(K)	4.85130E-06	4.32150E-06	2.44260E-06	7.10540E-07	1.26380E-06	1.09350E-06	2.57490E-06	4.32910E-06
X/L	1.94000E-02	2.56610E-02	3.38100E-02	4.43160E-02	5.76990E-02	7.44860E-02	9.51450E-02	1.19990E-01
Q*(K)	7.80300E-06	1.35100E-05	2.30180E-05	3.79470E-05	5.99540E-05	8.95020E-05	1.22140E-04	1.54820E-04
X/L	1.49040E-01	1.81940E-01	2.17810E-01	2.55310E-01	2.93050E-01	3.30790E-01	3.68520E-01	4.06260E-01
Q*(K)	1.28200E-04	2.02610E-04	5.04760E-05	1.13980E-04	1.15940E-04	1.24680E-04	1.20500E-04	1.23260E-04
X/L	4.44000E-01	4.81730E-01	5.19470E-01	5.457210E-01	5.94940E-01	6.32680E-01	6.70420E-01	7.08150E-01
Q*(K)	1.21440E-04	1.22660E-04	1.21850E-04	1.22350E-04	1.22110E-04	1.22130E-04	1.22330E-04	1.21880E-04
X/L	7.45890E-01	7.83630E-01	8.21360E-01	8.59100E-01	8.96840E-01	9.34570E-01	9.72310E-01	1.01000E+00
Q*(K)	1.22630E-04	1.21450E-04	1.23180E-04	1.20630E-04	1.24500E-04	1.16740E-04	1.16350E-04	1.14800E-05
X/L	1.04770E+00	1.08400E+00	1.11710E+00	1.14590E+00	1.16970E+00	1.18440E+00	1.20250E+00	1.21270E+00
Q*(K)	-1.19240E-04	-1.72710E-04	-1.74950E-04	-1.39120E-04	-9.35870E-05	-5.42850E-05	-2.99660E-05	-1.25300E-05
X/L	1.22000E+00	1.22500E+00	1.22840E+00					
Q*(K)	-1.02270E-05	4.66400E-06	-1.17130E-05					

SOURCE DISTRIBUTION FOR SHAPE NO 5

INCOMPRESSIBLE SOURCE DISTRIBUTION

X/L	2.00000E-03	2.86920E-03	4.10680E-03	5.86250E-03	8.33990E-03	1.18100E-02	1.66190E-02	2.31920E-02
Q*(K)	3.89500E-06	2.94050E-06	1.89890E-06	5.60640E-07	2.62880E-06	4.79150E-06	9.73390E-06	1.84190E-05
X/L	3.20070E-02	4.35380E-02	5.81460E-02	7.59810E-02	9.71890E-02	1.21590E-01	1.48620E-01	1.77420E-01
Q*(K)	3.24180E-05	5.36170E-05	5.64720E-05	9.35680E-05	8.97160E-05	9.58660E-05	5.88680E-05	1.34570E-04
X/L	2.07790E-01	2.33900E-01	2.73540E-01	3.09090E-01	3.46530E-01	3.85800E-01	4.26440E-01	4.67910E-01
Q*(K)	2.04990E-05	1.29040E-04	1.05120E-05	1.34660E-04	9.01540E-05	2.61210E-05	1.27540E-04	1.06930E-04
X/L	5.09580E-01	5.50810E-01	5.90970E-01	6.29480E-01	6.65840E-01	6.99650E-01	7.30650E-01	7.58810E-01
Q*(K)	6.58560E-05	-1.74060E-04	3.10920E-05	-2.33650E-04	4.96120E-05	-2.86510E-04	8.20150E-05	-2.07990E-04
X/L	7.84920E-01	8.09700E-01	8.33720E-01	8.57480E-01	8.81190E-01	9.04930E-01	9.28670E-01	9.52410E-01
Q*(K)	1.68710E-04	-2.17830E-04	2.24930E-04	-2.10590E-04	2.13690E-04	-2.05990E-04	2.13880E-04	-2.05620E-04
X/L	5.76140E-01	9.95860E-01	1.02360E+00	1.04350E+00				
Q*(K)	1.94700E-04	2.26620E-05	-4.13870E-04	1.84640E-05				

(F) Page 6.

Figure 20.- Continued.

VORTEX LATTICE CONTROL POINT COORDINATES
INTERFERENCE VELOCITIES INDUCED AT THESE POINTS
CALCULATED VORTEX STRENGTHS
(WING COORDINATE SYSTEM)

WING CONTROL POINTS		X, FT	Y, FT	Z, FT	U/VINF	V/VINF	W/VINF	GAMMA/VINF
ROW	VORTEX	-3.2510E	-1.66667	0.00000	.00222	.00059	-.00259	.46855
		-5.06520	-1.66667	0.00000	.00154	.00103	-.00418	.24799
		-6.87934	-1.66667	0.00000	.00120	.00162	-.00509	.18793
		-8.69348	-1.66667	0.00000	.00459	.00274	-.00339	.14525
		-10.50761	-1.66667	0.00000	.00674	.00290	.00024	.11146
		-12.32175	-1.66667	0.00000	.00557	.00162	.00386	.08888
		-14.13589	-1.66667	0.00000	.00314	.00016	.00352	.07134
		-15.95003	-1.66667	0.00000	.00130	.00145	.00314	.04854
		-17.76417	-1.66667	0.00000	.00285	.00328	-.00420	.53281
		-19.57831	-1.66667	0.00000	.00101	.00620	-.00568	.25502
		-21.39245	-1.66667	0.00000	.00506	.01178	-.00223	.17273
		-23.20659	-1.66667	0.00000	.01595	.00704	-.00301	.12221
		-25.02073	-1.66667	0.00000	.01336	.00619	.00410	.08794
		-26.83487	-1.66667	0.00000	.00135	.00676	.00540	.07498
		-28.64901	-1.66667	0.00000	.00225	.00277	.00513	.05885
		-30.46315	-1.66667	0.00000	.00209	.00383	.00787	.03257
		-32.27729	-1.66667	0.00000	.00710	.01254	-.00789	.51205
		-34.09143	-1.66667	0.00000	.01548	.00393	-.00271	.22712
		-35.90557	-1.66667	0.00000	.01315	.00785	.00314	.15060
		-37.71971	-1.66667	0.00000	.00230	.00977	.00486	.11711
		-39.53385	-1.66667	0.00000	.00193	.00477	.00413	.06482
		-41.34799	-1.66667	0.00000	.00314	.00448	.00608	.07045
		-43.16213	-1.66667	0.00000	.00082	.00536	.00838	.05096
		-44.97627	-1.66667	0.00000	.00294	.00454	.00729	.03584
		-46.79041	-1.66667	0.00000	.00241	.00154	.00852	.44449
		-48.60455	-1.66667	0.00000	.00195	.00202	.00077	.21136
		-50.41869	-1.66667	0.00000	.00143	.00236	.00098	.14839
		-52.23283	-1.66667	0.00000	.00084	.00255	.00112	.11350
		-54.04697	-1.66667	0.00000	.00023	.00254	.00115	.08896
		-55.86111	-1.66667	0.00000	.00031	.00233	.00107	.06919
		-57.67525	-1.66667	0.00000	.00067	.00199	.00192	.05119
		-59.48939	-1.66667	0.00000	.00086	.00161	.00075	.03196
		-61.30353	-1.66667	0.00000	.00018	.00079	.00020	.34461
		-63.11767	-1.66667	0.00000	.00009	.00078	.00020	.16329
		-64.93181	-1.66667	0.00000	.00001	.00075	.00019	.11374
		-66.74595	-1.66667	0.00000	.00005	.00071	.00018	.08573
		-68.56009	-1.66667	0.00000	.00011	.00066	.00017	.06557
		-70.37423	-1.66667	0.00000	.00015	.00061	.00016	.04828
		-72.18837	-1.66667	0.00000	.00000	.00056	.00014	.03503
		-74.00251	-1.66667	0.00000	.00020	.00051	.00013	.02101
		-75.81665	-1.66667	0.00000				
PYLON CONTROL POINTS		X, FT	Y, FT	Z, FT	J/JINF	GAMMA/JINF		
ROW	VORTEX	-11.85785	-6.66667	.41300	.04004	.03896		
		-13.52452	-6.66667	.41300	.04008	.00785		
		-15.19119	-6.66667	1.23900	.02832	.03588		
		-16.85785	-6.66667	1.23900	.02980	.01295		
		-18.52452	-6.66667	1.23900				
		-20.19119	-6.66667	1.23900				

(g) Page 7.

Figure 20.- Continued.

STORE NUMR 10 IS THE STORE EJECTED

ADDITIONAL INPUT FOR THIS STORE

STORE MASS = 15.52000 SLUGS

MOMENTS AND PRODUCTS OF INERTIA, SLUG - SQ FT

IXX = 8.00000

IYY = 80.00000

IZZ = 80.00000

IYZ = -0.00000

IXZ = -0.00000

IYX = -0.00000

STORE CMOMENT CENTER IS -5.31250 FEET BEHIND NOSE

STORE CENTER OF GRAVITY OFFSET FROM MOMENT CENTER, FEET

XBAR = -0.00000

YBAR = -0.00000

ZBAR = -0.00000

POLYNOMIALS SPECIFYING COMPRESSIBLE STORE SHAPE

X/L OF END OF EACH SECTION

SECTION	X/L	C1	C2	C3	C4	C5	C6	C7
1	.23530							
2	1.10000							
1		-.44130	-1.00000	.47060	.19470	-0.00000	-0.00000	1.00000
2		.05682	-0.00000	-0.00000	-0.00000	-0.00000	-0.00000	-0.00000

SEPARATION ASSUMED 10.62500 FEET FROM NOSE

AXIAL-FORCE COEFFICIENT IS .40000

CROSSFLCN-DRAG COEFFICIENT IS 0.00000

THIS STORE HAS A CRUCIFORM EMPENNAGE

THE EMPENNAGE FORCES ACT -5.37600 FEET BEHIND NOSE

THE AVERAGE BODY RADIUS IN THE EMPENNAGE REGION IS .62500 FEET

THE TAIL FIN SEMISPAN MEASURED FROM THE BODY AXIS IS 1.45833 FEET

THE FINS ARE INITIALLY ROLLED 45.00 DEGREES FROM THE VERTICAL AND HORIZONTAL

THE FIN LIFT-CURVE SLOPE IS 3.22000 PER RADIAN

(h) Page 8.

Figure 20.- Continued.

TIME = 0.0000 SECONDS

FORCE AND MOMENT COEFFICIENTS

	CN	CY	CLM	CLN	CLL
BUOYANCY	.00331	-.05182	-.11664	.05864	
SLENDER BODY	.15013	-.02781	.36065	-.20897	
CROSSFLOW	0.00000	0.00000	0.00000	0.00000	
EMPELLANCE	.48463	-.06976	-1.57544	.22676	.00341
TOTAL	.63807	-.04574	-1.31144	.07643	.00341

LOAD AND VELOCITY DISTRIBUTIONS

X, FT	X/L	CCN/DX	CCY/DX	U/V/S	H/V/S
.26563	.02500	.04912	-.02518	.97263	.06130
.79688	.07500	.07788	-.04730	.97254	.07594
1.32813	.12500	.05337	-.03917	.97312	.07028
1.85938	.17500	.00853	-.01347	.97434	.06449
2.39063	.22500	-.03650	.01586	.97630	.05863
2.92188	.27500	-.04169	.02301	.97962	.05277
3.45313	.32500	-.02090	.02327	.98550	.04817
3.98438	.37500	.01616	.02225	.99307	.04789
4.51563	.42500	.03565	.02107	.99864	.05174
5.04688	.47500	.03981	.01968	1.00165	.05684
5.57813	.52500	.04357	.01757	1.00320	.06234
6.10938	.57500	.04673	.01461	1.00323	.06843
6.64063	.62500	.03409	.01117	1.00057	.07422
7.17188	.67500	.00422	.00774	.99577	.07678
7.70313	.72500	-.00925	.00451	.99242	.07602
8.23438	.77500	-.00617	.00162	.99144	.07488
8.76563	.82500	-.00174	-.00083	.99057	.07440
9.29688	.87500	-.00009	-.00273	.98997	.07432
9.82813	.92500	-.00086	-.00398	.98918	.07429
10.35937	.97500	-.00313	-.00450	.98825	.07405

LOCATION OF STORE IN FUSELAGE COORDINATE SYSTEM, DIMENSIONS OF FEET

	XF	YF	ZF	DEL XF	DEL YF	DEL ZF
NOSE	-29.43452	-6.66667	2.90200	0.00000	0.00000	0.00000
XMOM	-34.74702	-6.66667	2.90200	0.00000	0.00000	0.00000
BASE	-40.05952	-6.66667	2.90200	0.00000	0.00000	0.00000

TRANSLATIONAL VELOCITIES AND ACCELERATIONS OF STORE IN FUSELAGE COORDINATE SYSTEM

	OXF	OYF	OZF	D2XF	D2YF	D2ZF
0.00000	0.00000	10.00000	-8.55424	-.72155	22.03029	

ROTATIONAL VELOCITIES AND ACCELERATIONS OF STORE IN STORE COORDINATE SYSTEM

	P	Q	R	POOT	QOOT	ROOT
0.00000	0.00000	0.00000	0.00000	.13068	-5.01997	.29257

STORE ANGULAR ORIENTATION IN FUSELAGE COORDINATE SYSTEM AND RATES OF CHANGE OF THESE ANGLES

	PSI	THETA	PHI	OPSI	OTHEA	OPHI
0.00000	0.00000	0.00000	0.00000	0.00000	0.00000	0.00000

(i) Page 9.

Figure 20.- Continued.

TIME = .33000 SECONDS

FORCE AND MOMENT COEFFICIENTS

	CN	CY	CLM	CLN	CLL
RUCYANCY	-.02861	.01105	.00637	.00578	
SLENDER BODY	-.07613	.00222	-.15164	-.02370	
CROSSFLOW	0.00000	0.00000	0.00000	0.00000	
EMBENNAGE	-.23144	.00735	.75237	-.02388	-.00005
TOTAL	-.33616	.02071	.60710	-.04180	-.00005

LOAD AND VELOCITY DISTRIBUTIONS

X, FT	Y/L	CCN/DX	DCY/CX	U/V/S	V/V/S	W/V/S
.26563	.02500	-.01387	-.00285	.59323	.00456	-.02155
.79688	.07500	-.02973	-.00504	.59366	-.00448	-.02272
1.32813	.12500	-.03254	-.00367	.59372	.00428	-.02387
1.85938	.17500	-.02529	-.00084	.59398	-.00397	-.02496
2.39063	.22500	-.01104	.00296	.59422	-.00355	-.02601
2.92188	.27500	-.00717	.00389	.59442	-.00306	-.02700
3.45313	.32500	-.00664	.00410	.59459	-.00252	-.02792
3.98438	.37500	-.00609	.00410	.59468	-.00197	-.02876
4.51563	.42500	-.00556	.00393	.59472	-.00144	-.02953
5.04688	.47500	-.00511	.00362	.59469	-.00094	-.03024
5.57813	.52500	-.00478	.00322	.59459	-.00048	-.03090
6.10938	.57500	-.00460	.00276	.59444	-.00008	-.03152
6.64063	.62500	-.00459	.00229	.59423	.00025	-.03212
7.17188	.67500	-.00473	.00183	.59398	.00052	-.03274
7.70313	.72500	-.00499	.00140	.59371	.00074	-.03338
8.23438	.77500	-.00533	.00103	.59344	.00090	-.03407
8.76563	.82500	-.00571	.00074	.59318	.00102	-.03480
9.29688	.87500	-.00609	.00052	.59296	.00110	-.03558
9.82813	.92500	-.00647	.00039	.59278	.00116	-.03642
10.35937	.97500	-.00684	.00036	.59264	.00121	-.03730

LOCATION OF STORE IN FUSELAGE COORDINATE SYSTEM, DIMENSIONS OF FEET

	XF	YF	ZF	DEL XF	DEL YF	DEL ZF
NOSE	-29.64944	-6.64122	7.75488	-.21492	.02545	4.85288
X40M	-34.91757	-6.69052	7.07147	-.17055	-.02385	4.16947
BASE	-40.18570	-6.73982	6.38807	-.12617	-.07315	3.48607

TRANSLATIONAL VELOCITIES AND ACCELERATIONS OF STORE IN FUSELAGE COORDINATE SYSTEM

	DXF	DYF	DZF	D2XF	D2YF	D2ZF
	-.68143	-.09959	18.62260	-.63350	.36865	36.86115

ROTATIONAL VELOCITIES AND ACCELERATIONS OF STORE IN STORE COORDINATE SYSTEM

P	Q	R	POOT	QOOT	ROOT
.00515	-.44903	.03813	-.00173	2.32617	-.15804

STORE ANGULAR ORIENTATION IN FUSELAGE COORDINATE SYSTEM AND RATES OF CHANGE OF THESE ANGLES

	PSI	THETA	PHI	DPSI	DTHETA	DPHI
	.53620	-7.39106	.04346	.03810	-.45986	.00025

TIME = .60000 SECONDS

FORCE AND MOMENT COEFFICIENTS

	CN	CY	CLM	CLN	CLL
BUOYANCY	.00684	-.00207	-.00138	.00035	
SLINDER BODY	-.01553	.00688	.03042	.00000	
CROSSFLOW	0.00000	0.00000	0.00000	0.00000	
EMPELLAGE	-.06458	.02773	.20595	-.07390	-.00003
TOTAL	-.07728	.02754	.11670	-.04314	-.00003

LOAD AND VELOCITY DISTRIBUTIONS

X, FT	X/L	CON/DX	DCY/DX	U/V/S	V/V/S	M/V/S
.25563	.02500	-.00826	.00282	.59685	.00456	-.01333
.79688	.07500	-.01517	.00512	.59683	.00446	-.01312
1.32813	.12500	-.01378	.00462	.59681	.00468	-.01291
1.85938	.17500	-.00725	.00263	.59678	.00430	-.01270
2.39063	.22500	-.00003	.00004	.59676	.00423	-.01249
2.92188	.27500	.00163	-.00048	.59673	.00416	-.01227
3.45313	.32500	.00163	-.00045	.59669	.00410	-.01206
3.98438	.37500	.00162	-.00043	.59665	.00404	-.01184
4.51563	.42500	.00159	-.00041	.59661	.00398	-.01163
5.04688	.47500	.00156	-.00040	.59656	.00393	-.01142
5.57813	.52500	.00152	-.00040	.59651	.00388	-.01121
6.10938	.57500	.00147	-.00040	.59646	.00382	-.01101
6.64063	.62500	.00143	-.00040	.59641	.00377	-.01092
7.17188	.67500	.00137	-.00041	.59636	.00372	-.01064
7.70313	.72500	.00132	-.00041	.59632	.00366	-.01046
8.23438	.77500	.00128	-.00041	.59628	.00361	-.01029
8.76563	.82500	.00123	-.00041	.59626	.00355	-.01012
9.29688	.87500	.00120	-.00040	.59624	.00350	-.00996
9.82813	.92500	.00118	-.00038	.59623	.00345	-.00980
10.35937	.97500	.00116	-.00036	.59623	.00340	-.00964

LOCATION OF STORE IN FUSELAGE COORDINATE SYSTEM, DIMENSIONS OF FEET

	RELATIVE TO FUSELAGE NOSE	RELATIVE TO INITIAL POSITION	
	XF YF ZF	DEL XF DEL YF DEL ZF	
NOSE	-30.13832	-6.64507 15.10681	.02160 12.20481
XWOM	-35.39700	-6.69036 14.35391	-.02369 11.45191
BASE	-40.65568	-6.73564 13.60101	-.06897 10.69901

TRANSLATIONAL VELOCITIES AND ACCELERATIONS OF STORE IN FUSELAGE COORDINATE SYSTEM

	RELATIVE TO FUSELAGE MOTION				
	DXF DYF DZF	D2XF D2YF D2ZF			
-3.39481	.10764	29.62998	-16.44409	.48567	31.51233

ROTATIONAL VELOCITIES AND ACCELERATIONS OF STORE IN STORE COORDINATE SYSTEM

	P Q R	PDOT QDOT RDOT		
.00478	.26324	-.04360	.45186	-.16543

STORE ANGULAR ORIENTATION IN FUSELAGE COORDINATE SYSTEM AND RATES OF CHANGE OF THESE ANGLES

	PSI THETA PHI	DPSI DTHETA DPHI			
.49334	-8.14753	.13647	-.04341	.26334	.01093

(k) Page 11.

Figure 20.- Concluded.

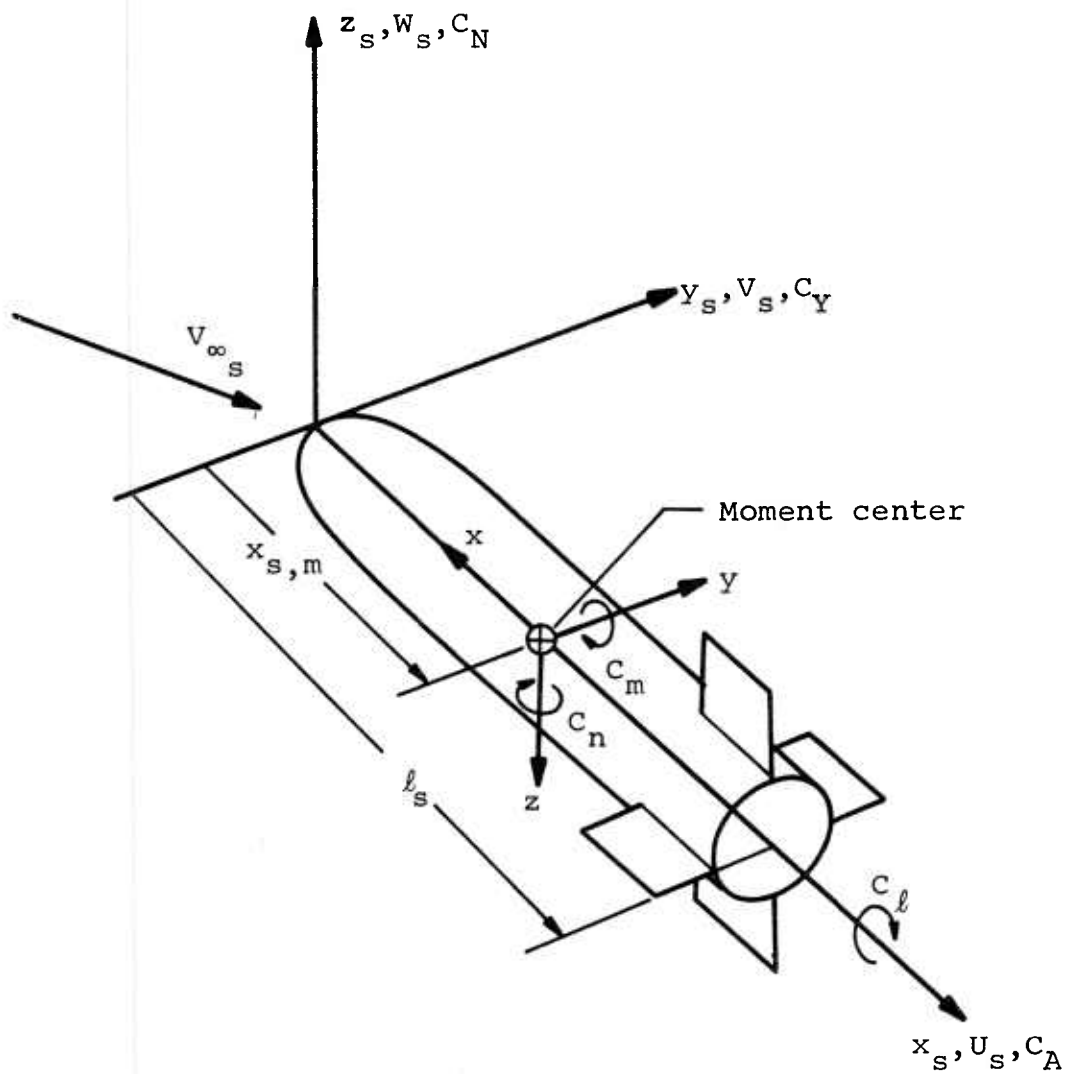


Figure 21.- Coordinate systems fixed in separated store and used in force and moment calculation.

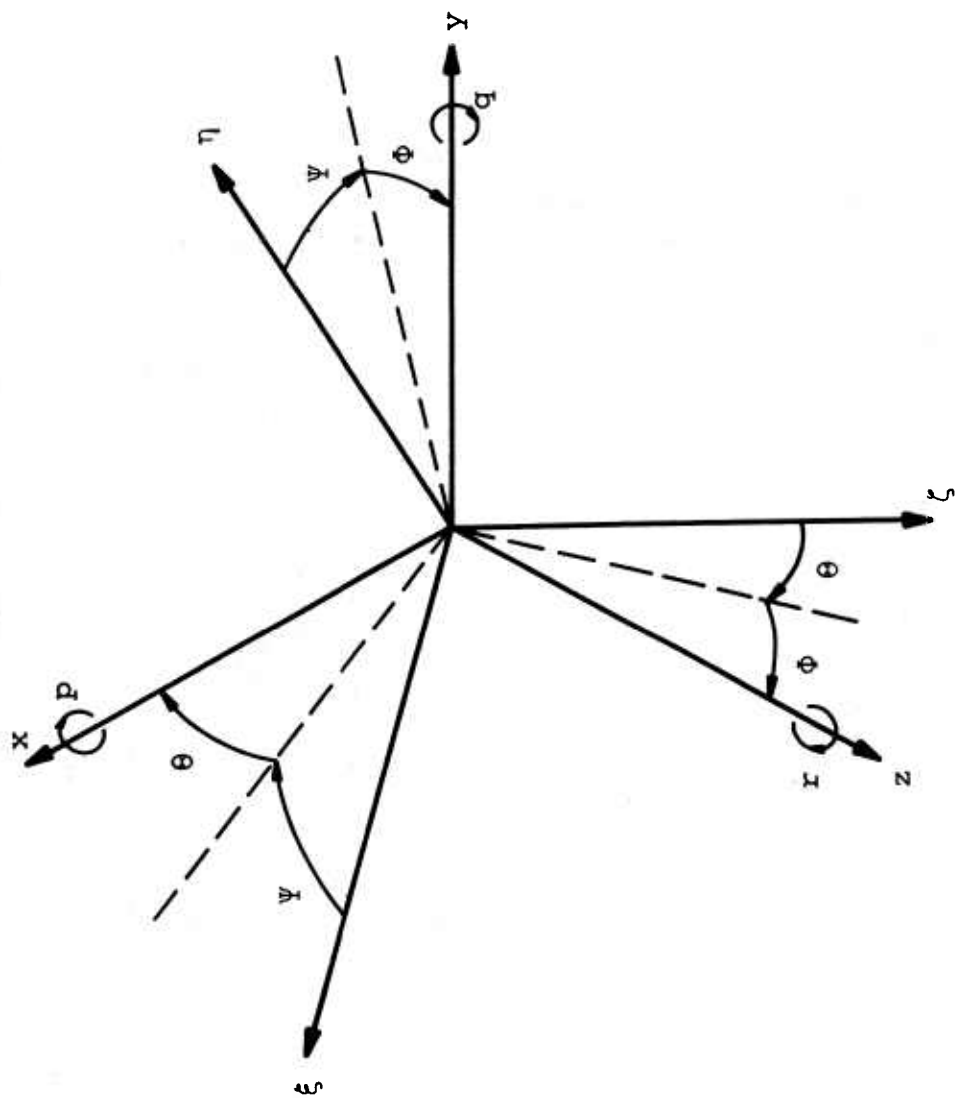


Figure 22.- Coordinate systems used in trajectory calculation.

SIX-DEGREE-OF-FREEDOM TRAJECTORY PROGRAM

SAMPLE TRAJECTORY CALCULATION NUMBER 2
 AIRCRAFT AND STORES ARE SCALED UP VERSIONS OF MODELS USED IN EXPERIMENTAL
 PROGRAM CONDUCTED IN CONJUNCTION WITH THIS WORK
 MODELS SCALED UP BY A FACTOR OF 20 TO APPROXIMATE A FULL SCALE AIRCRAFT
 THERE IS A SMALL FINLESS POINTEDED STORE AT THE 1/3 SEMISPAN LOCATION
 OF BOTH WING PANELS
 THERE ALSO ARE THREE FINLESS OGIVE-CYLINDER STORES GROUPED ON A
 TER-RACK/PYLON UNDER THE FUSELAGE
 THE BOTTOM STORE OF THE TER GROUPING IS THE STORE EJECTED WITH THE
 TRAJECTORY STARTING ONE RADIUS BELOW THE CARRIAGE POSITION
 IT IS A FREE-FLIGHT TRAJECTORY, NOT A CAPTIVE STORE TRAJECTORY
 DAMPING IS INCLUDED
 THE AIRCRAFT IS DIVING AT A FLIGHT PATH ANGLE OF -30 DEGREES

AIRCRAFT FLIGHT CONDITIONS
 ANGLE OF ATTACK = 6.00 DEGREES
 FLIGHT PATH ANGLE = -30.00 DEGREES
 MACH NUMBER = .40
 FREE STREAM MASS DENSITY = .0020482 SLUGS PER CUBIC FOOT
 FREE STREAM VELOCITY = 440.70 FEET PER SECOND

FUSELAGE INPUT DATA
 FUSELAGE LENGTH = 60.85000 FEET
 MAXIMUM RADIUS = 2.78340 FEET

INCOMPRESSIBLE SOURCE DISTRIBUTION

X/L	2.00000E-03	2.53000E-03	3.20060E-03	4.04870E-03	5.12060E-03	6.47450E-03	8.18310E-03	1.03370E-02
Q*(K)	6.01530E-06	-5.47820E-06	3.53980E-06	-2.17850E-06	1.61620E-06	-6.69620E-07	1.04450E-06	3.10400E-07
X/L	1.30480E-02	1.64560E-02	2.07290E-02	2.60720E-02	3.27300E-02	4.09330E-02	5.11920E-02	6.36970E-02
Q*(K)	1.37370E-06	1.60040E-06	2.87800E-06	4.22660E-06	6.64360E-06	9.93870E-06	1.48130E-05	2.14030E-05
X/L	7.89070E-02	9.72240E-02	1.19020E-01	1.44580E-01	1.74060E-01	2.07370E-01	2.44150E-01	2.83720E-01
Q*(K)	3.00830E-05	4.05820E-05	5.20730E-05	6.24870E-05	6.87670E-05	6.29460E-05	7.32610E-05	4.50690E-06
X/L	3.25080E-01	3.86960E-01	4.08850E-01	4.50730E-01	4.92620E-01	5.34500E-01	5.76390E-01	6.18270E-01
Q*(K)	-7.68290E-07	-1.27860E-05	9.99140E-06	-1.15010E-05	1.07170E-05	-1.10600E-05	1.10630E-05	-1.07030E-05
X/L	6.60160E-01	7.02040E-01	7.43930E-01	7.85810E-01	8.27450E-01	8.68050E-01	9.06870E-01	9.43260E-01
Q*(K)	1.15550E-05	-9.89930E-06	1.64960E-05	-1.32980E-05	3.14260E-05	-4.55380E-05	5.78350E-05	-5.64920E-05
X/L	5.76730E-01	1.00700E+00	1.03380E+00	1.05730E+00	1.07760E+00	1.09480E+00	1.10940E+00	1.12150E+00
Q*(K)	-5.39670E-05	-4.82290E-05	-4.03720E-05	-3.24970E-05	-2.47050E-05	-1.66520E-05	-1.30210E-05	-9.74060E-06
X/L	1.13160E+00	1.13990E+00	1.14670E+00	1.15220E+00	1.15670E+00	1.16030E+00	1.16320E+00	1.16560E+00
Q*(K)	-5.94580E-06	-5.11050E-06	-1.93940E-06	-3.36030E-06	7.12840E-07	-3.64580E-06	3.49100E-06	-6.00770E-06
X/L	1.1E750E+00	1.1E900E+00						
Q*(K)	8.06400E-06	-9.41390E-06						

(a) Page 1.

Figure 23.- Trajectory program output for sample case 2.

WING INPUT DATA

LOCATION OF WING ROOT CHORD LEADING EDGE RELATIVE TO FUSELAGE NOSE
 XF = -22.45000 FEET
 ZF = 0.00000 FEET

INCIDENCE ANGLE OF WING ROOT CHORD RELATIVE TO FUSELAGE AXIS
 IW = 0.00 DEGREES

LENGTH OF WING ROOT CHORD
 CRM = 15.41200 FEET

WING SEMISPAN
 SSFAN = 20.00000 FEET

40 VORTICES ARE TO BE LAID OUT ON EACH WING PANEL
 5 CHORDWISE ROWS WITH 8 IN EACH ROW

SPANWISE LOCATIONS OF TRAILING VORTEX LEGS AND SWEEP ANGLES AND
 DIHEDRAL ANGLE OF WING SECTION TO THE RIGHT

I	LOCATION	SPANWISE	LE SWEEP	TE SWEEP	DIHEDRAL
	FEET	DEGREES	DEGREES	DEGREES	DEGREES
1	0.00000	0.00000	0.00000	0.00000	0.00000
2	-3.33333	48.60000	30.75000	0.00000	0.00000
3	-6.66667	48.60000	30.75000	0.00000	0.00000
4	-10.00000	48.60000	30.75000	0.00000	0.00000
5	-15.00000	48.60000	30.75000	0.00000	0.00000
6	-20.00000	48.60000	30.75000	0.00000	0.00000

80 THICKNESS PANELS ARE TO BE LAID OUT ON EACH WING PANEL
 5 CHORDWISE ROWS WITH 16 IN EACH ROW
 THE CHORDWISE ROWS COINCIDE WITH THE USED
 IN THE VORTEX LATTICE

(b) Page 2.

Figure 23.- Continued.

PYLON INPUT DATA

LEADING EDGE OF PYLON ROOT CHORD IS AT X = -8.24583 FEET (MEASURED FROM LOCAL WING LEADING EDGE)
 SPANNWISE LOCATION IS Y = 0.00000 FEET
 ROOT CHORD = 3.73333 FEET
 HEIGHT = 1.45200 FEET
 LEADING EDGE SWEEP ANGLE = 0.00000 DEGREES
 TRAILING EDGE SWEEP ANGLE = 0.00000 DEGREES

4 VORTICES ARE TO BE LAID OUT ON THE PYLON
 2 CHORDWISE ROWS WITH 2 IN EACH ROW

SPANNWISE LOCATIONS OF TRAILING VORTEX LEGS

K	Z FEET
1	2.70340
2	3.60940
3	4.43540

120 THICKNESS PANELS ARE TO BE LAID OUT ON THE PYLON
 2 CHORDWISE ROWS WITH 60 IN EACH ROW
 THE CHORDWISE ROWS COINCIDE WITH THOSE USED
 IN THE VORTEX LATTICE

(c) Page 3.

Figure 23.- Continued.

VORTEX LATTICE CONTROL POINT COORDINATES AND
INPUT TWIST AND CAMBER DISTRIBUTION
AT THESE POINTS
(WING COORDINATE SYSTEM)

WING CONTROL POINTS		X, FT	Y, FT	Z, FT	SLOPE
ROW	VORTEX				
1	1	-2.25106	-1.66667	0.00000	0.00000
1	2	-5.06520	-1.66667	0.00000	0.00000
1	3	-6.87534	-1.66667	0.00000	0.00000
1	4	-8.69348	-1.66667	0.00000	0.00000
1	5	-10.50761	-1.66667	0.00000	0.00000
1	6	-12.32175	-1.66667	0.00000	0.00000
1	7	-14.13589	-1.66667	0.00000	0.00000
1	8	-15.95003	-1.66667	0.00000	0.00000
2	1	-8.66345	-5.00000	0.00000	0.00000
2	2	-8.45286	-5.00000	0.00000	0.00000
2	3	-10.04227	-5.00000	0.00000	0.00000
2	4	-11.63168	-5.00000	0.00000	0.00000
2	5	-13.22110	-5.00000	0.00000	0.00000
2	6	-14.81051	-5.00000	0.00000	0.00000
2	7	-16.39992	-5.00000	0.00000	0.00000
2	8	-17.98933	-5.00000	0.00000	0.00000
3	1	-10.47583	-8.33333	0.00000	0.00000
3	2	-11.84052	-8.33333	0.00000	0.00000
3	3	-13.20520	-8.33333	0.00000	0.00000
3	4	-14.56989	-8.33333	0.00000	0.00000
3	5	-15.93458	-8.33333	0.00000	0.00000
3	6	-17.29927	-8.33333	0.00000	0.00000
3	7	-18.66395	-8.33333	0.00000	0.00000
3	8	-20.02864	-8.33333	0.00000	0.00000
4	1	-14.99130	-12.50000	0.00000	0.00000
4	2	-16.07508	-12.50000	0.00000	0.00000
4	3	-17.15887	-12.50000	0.00000	0.00000
4	4	-18.24265	-12.50000	0.00000	0.00000
4	5	-19.32643	-12.50000	0.00000	0.00000
4	6	-20.41021	-12.50000	0.00000	0.00000
4	7	-21.49399	-12.50000	0.00000	0.00000
4	8	-22.57777	-12.50000	0.00000	0.00000
5	1	-20.40987	-17.50000	0.00000	0.00000
5	2	-21.15657	-17.50000	0.00000	0.00000
5	3	-21.90326	-17.50000	0.00000	0.00000
5	4	-22.64996	-17.50000	0.00000	0.00000
5	5	-23.39665	-17.50000	0.00000	0.00000
5	6	-24.14334	-17.50000	0.00000	0.00000
5	7	-24.89004	-17.50000	0.00000	0.00000
5	8	-25.63673	-17.50000	0.00000	0.00000

PYLON CONTROL POINTS		X, FT	Y, FT	Z, FT
ROW	VORTEX			
1	1	-9.49583	0.00000	3.19640
1	2	-11.16249	0.00000	3.19640
2	1	-9.49583	0.00000	4.02240
2	2	-11.16249	0.00000	4.02240

(d) Page 4.

Figure 23.- Continued.

INPUT VALUES OF THE LOCAL SURFACE SLOPE OF THE THICKNESS
DISTRIBUTION, FOR EACH CHORDWISE ROW THE FIRST VALUE
IS FOR THE PANEL NEAREST THE LEADING EDGE

WING THICKNESS DATA

ROW	SLOPES									
1	.18074	.05400	.06400	.04460	.02800	.01955	-.00122	-.01341		
	-.02561	-.03782	-.05005	-.06000	-.06600	-.06719	-.06719	-.06719		
2	.18074	.05400	.06400	.04460	.02800	.01955	-.00122	-.01341		
	-.02561	-.03782	-.05005	-.06000	-.06600	-.06719	-.06719	-.06719		
3	.18074	.05400	.06400	.04460	.02800	.01955	-.00122	-.01341		
	-.02561	-.03782	-.05005	-.06000	-.06600	-.06719	-.06719	-.06719		
4	.18074	.05400	.06400	.04460	.02800	.01955	-.00122	-.01341		
	-.02561	-.03782	-.05005	-.06000	-.06600	-.06719	-.06719	-.06719		
5	.18074	.05400	.06400	.04460	.02800	.01955	-.00122	-.01341		
	-.02561	-.03782	-.05005	-.06000	-.06600	-.06719	-.06719	-.06719		

PYLON THICKNESS DATA

ROW	SLOPES									
1	1.74060	.75020	.35360	.06686	0.00000	0.00000	0.00000	0.00000	0.00000	
	0.00000	0.00000	0.00000	0.00000	0.00000	0.00000	0.00000	0.00000	0.00000	
	0.00000	0.00000	0.00000	0.00000	0.00000	0.00000	0.00000	0.00000	0.00000	
	0.00000	0.00000	0.00000	0.00000	0.00000	0.00000	0.00000	0.00000	0.00000	
	0.00000	0.00000	0.00000	0.00000	0.00000	0.00000	0.00000	0.00000	0.00000	
	0.00000	0.00000	0.00000	0.00000	0.00000	0.00000	0.00000	0.00000	0.00000	
	0.00000	0.00000	0.00000	0.00000	0.00000	0.00000	0.00000	0.00000	0.00000	
	0.00000	0.00000	0.00000	0.00000	0.00000	0.00000	0.00000	0.00000	0.00000	
	0.00000	0.00000	0.00000	0.00000	0.00000	0.00000	0.00000	0.00000	0.00000	
2	1.74060	.75020	.35360	.06686	0.00000	0.00000	0.00000	0.00000	0.00000	
	0.00000	0.00000	0.00000	0.00000	0.00000	0.00000	0.00000	0.00000	0.00000	
	0.00000	0.00000	0.00000	0.00000	0.00000	0.00000	0.00000	0.00000	0.00000	
	0.00000	0.00000	0.00000	0.00000	0.00000	0.00000	0.00000	0.00000	0.00000	
	0.00000	0.00000	0.00000	0.00000	0.00000	0.00000	0.00000	0.00000	0.00000	
	0.00000	0.00000	0.00000	0.00000	0.00000	0.00000	0.00000	0.00000	0.00000	
	0.00000	0.00000	0.00000	0.00000	0.00000	0.00000	0.00000	0.00000	0.00000	
	0.00000	0.00000	0.00000	0.00000	0.00000	0.00000	0.00000	0.00000	0.00000	
	0.00000	0.00000	0.00000	0.00000	0.00000	0.00000	0.00000	0.00000	0.00000	
	0.00000	0.00000	0.00000	0.00000	0.00000	0.00000	0.00000	0.00000	0.00000	

(e) Page 5.

Figure 23.- Continued.

RACK INPUT DATA

RACK LENGTH = 5.56833 FEET
 MAXIMUM RADIUS = .31667 FEET
 LOCATION OF RACK NOSE RELATIVE TO LOCAL WING LEADING EDGE
 X = -7.12833 FEET
 Z = 4.75207 FEET
 RACK INCIDENCE ANGLE RELATIVE TO WING ROOT CHORD
 IR = 0.00000 DEGREES

INCOMPRESSIBLE SOURCE DISTRIBUTION

X/L	2.00000E-03	5.98370E-03	1.28790E-02	2.28990E-02	3.61190E-02	5.24850E-02	7.18530E-02	9.40060E-02
O*(K)	-5.66440E-07	2.04470E-05	5.21430E-05	6.60020E-05	8.00620E-05	8.86210E-05	9.26910E-05	9.08970E-05
X/L	1.18660E-01	1.45480E-01	1.74080E-01	2.04040E-01	2.34880E-01	2.66130E-01	2.97400E-01	3.28670E-01
O*(K)	8.20190E-05	7.57630E-05	1.78350E-05	1.20500E-04	-1.18400E-04	5.38280E-05	-5.13060E-05	4.57470E-05
X/L	3.59950E-01	3.91220E-01	4.22490E-01	4.53770E-01	4.85040E-01	5.16310E-01	5.47590E-01	5.78860E-01
O*(K)	-4.82800E-05	4.64540E-05	-4.78690E-05	4.68620E-05	-4.73570E-05	4.71190E-05	-4.71250E-05	4.73480E-05
X/L	6.10130E-01	6.41410E-01	6.72680E-01	7.03950E-01	7.35230E-01	7.66500E-01	7.97770E-01	8.29050E-01
O*(K)	-4.68770E-05	4.76410E-05	-4.65040E-05	4.81510E-05	-4.57760E-05	4.93870E-05	-4.45210E-05	5.80370E-05
X/L	8.60320E-01	8.91590E-01	9.22870E-01	9.52780E-01	9.78670E-01	9.98690E-01	1.01230E+00	
O*(K)	-7.46670E-05	2.81500E-04	-2.91260E-04	-3.08560E-04	-2.14530E-04	-7.91270E-05	-4.65230E-05	

(f) Page 6.

Figure 23.- Continued.

STORE INPUT DATA

STORE NO	SHAPE NO	LENGTH FT	MAXIMUM RADIUS FT	STORE LOCATION RELATIVE TO LOCAL WING CHORD LEADING EDGE	INCIDENCE ANGLE DEG
			X, FT Y, FT Z, FT		
10	5	7.38333	.4667	-1.02750 -6.66667 1.98612	0.00000
20	2	10.62500	.62500	-4.60000 0.00000 6.52167	0.00000
21	2	10.62500	.62500	-3.61720 -.86667 4.96333	0.00000
22	2	10.62500	.62500	-3.61720 .86667 4.96333	0.00000
30	5	7.38333	.4667	-1.02750 6.66667 1.98612	0.00000

SOURCE DISTRIBUTION FOR SHAPE NO 5

INCOMPRESSIBLE SOURCE DISTRIBUTION

X/L	2.00000E-03	2.86920E-03	4.10680E-03	5.86250E-03	8.33990E-03	1.18100E-02	1.66190E-02	2.31920E-02
Q*(K)	3.89500E-06	-2.94050E-06	1.89890E-06	5.60640E-07	2.62880E-06	4.79150E-06	9.73390E-06	1.84190E-05
X/L	3.20070E-02	4.35380E-02	5.81460E-02	9.71890E-02	1.21590E-01	1.48620E-01	1.77420E-01	
Q*(K)	3.24180E-05	5.36170E-05	5.64720E-05	9.35680E-05	8.97160E-05	9.58660E-05	5.88680E-05	1.34570E-04
X/L	2.07790E-01	2.39800E-01	2.73540E-01	3.09090E-01	3.46530E-01	3.88800E-01	4.26440E-01	4.67910E-01
Q*(K)	-2.04990E-05	1.29040E-04	1.05120E-05	1.34660E-04	9.01540E-05	2.61210E-05	1.27540E-04	1.06930E-04
X/L	5.09580E-01	5.50810E-01	5.90970E-01	6.29480E-01	6.65940E-01	6.99650E-01	7.30650E-01	7.58810E-01
Q*(K)	6.58560E-05	-1.74060E-04	3.10920E-05	-2.33650E-04	4.96120E-05	-2.86510E-04	8.20150E-05	-2.07990E-04
X/L	7.84920E-01	8.09700E-01	8.33720E-01	8.57460E-01	8.81190E-01	9.04930E-01	9.28670E-01	9.52410E-01
Q*(K)	1.68710E-04	-2.17830E-04	2.24930E-04	-2.10590E-04	2.13690E-04	-2.09990E-04	2.13800E-04	-2.05820E-04
X/L	9.76140E-01	9.95880E-01	1.02360E+00	1.04350E+00				
Q*(K)	1.94700E-04	2.26620E-05	-4.13870E-04	1.84640E-05				

SOURCE DISTRIBUTION FOR SHAPE NO 2

INCOMPRESSIBLE SOURCE DISTRIBUTION

X/L	2.00000E-03	2.64730E-03	3.51320E-03	4.67050E-03	6.21490E-03	8.27210E-03	1.10060E-02	1.46260E-02
Q*(K)	4.85130E-06	-4.32150E-06	2.44260E-06	-7.10540E-07	1.26380E-06	1.09350E-06	2.57490E-06	4.32910E-06
X/L	1.94000E-02	2.56610E-02	3.38100E-02	4.43160E-02	5.76990E-02	7.44850E-02	9.51450E-02	1.19990E-01
Q*(K)	7.80300E-06	1.35100E-05	2.30180E-05	3.79470E-05	5.99540E-05	8.95020E-05	1.22140E-04	1.54820E-04
X/L	1.49040E-01	1.81940E-01	2.17810E-01	2.55310E-01	2.93050E-01	3.30790E-01	3.68520E-01	4.06260E-01
Q*(K)	1.28200E-04	2.02610E-04	-5.04760E-05	-1.13980E-04	1.15940E-04	-1.24680E-04	1.20500E-04	-1.23260E-04
X/L	4.44000E-01	4.81730E-01	5.19470E-01	5.57210E-01	5.94940E-01	6.32680E-01	6.70420E-01	7.08150E-01
Q*(K)	1.21440E-04	-1.22660E-04	1.21850E-04	-1.22350E-04	1.22110E-04	-1.21330E-04	1.22330E-04	-1.21880E-04
X/L	7.45890E-01	7.82630E-01	8.21360E-01	8.59100E-01	8.96840E-01	9.34570E-01	9.722310E-01	1.01000E+00
Q*(K)	1.22630E-04	-1.21490E-04	1.23180E-04	-1.20630E-04	-1.174950E-04	1.39120E-04	-9.35870E-05	-5.42850E-05
X/L	1.04770E+00	1.08400E+00	1.11710E+00	1.14590E+00	1.16970E+00	1.18840E+00	1.20250E+00	1.21270E+00
Q*(K)	-2.99660E-05	-1.25300E-05	1.24500E-04	-1.16740E-04	1.16950E-04	1.14800E-05	-1.19240E-04	-1.072710E-04
X/L	1.22000E+00	1.22500E+00	1.22840E+00					
Q*(K)	-1.02270E-05	4.66400E-06	-1.17130E-05					

(g) Page 7.

Figure 23.- Continued.

VORTEX LATTICE CONTROL POINT COORDINATES
INTERFERENCE VELOCITIES INDUCED AT THESE POINTS
CALCULATED VORTEX STRENGTHS
(WING COORDINATE SYSTEM)

WING CONTROL POINTS		X, FT	Y, FT	Z, FT	U/VINF	V/VINF	W/VINF	GAMMA/VINF
1	1	-3.2510E	-1.66667	0.00000	.00327	-.00212	-.00732	.71284
1	2	-5.06520	-1.66667	0.00000	.00036	-.00282	-.01010	.37250
1	3	-6.87534	-1.66667	0.00000	.00000	-.00264	-.01113	.27577
1	4	-8.69348	-1.66667	0.00000	-.01025	-.00110	-.00113	.20999
1	5	-10.50761	-1.66667	0.00000	-.01227	-.00115	-.00080	.15959
1	6	-12.32175	-1.66667	0.00000	-.00959	-.00216	.00653	.12661
1	7	-14.13585	-1.66667	0.00000	-.00499	-.00208	.00507	.10260
1	8	-15.95003	-1.66667	0.00000	-.00062	-.00184	.00894	.07232
2	1	-6.86345	-5.00000	0.00000	-.00139	-.00223	-.00540	.77807
2	2	-8.45286	-5.00000	0.00000	-.00369	-.00118	-.00521	.37343
2	3	-10.04227	-5.00000	0.00000	-.00890	-.00384	-.00544	.25815
2	4	-11.63168	-5.00000	0.00000	-.01217	-.00259	.00127	.16770
2	5	-13.22110	-5.00000	0.00000	-.00661	-.00009	.00659	.14443
2	6	-14.81051	-5.00000	0.00000	-.00266	-.00020	.00776	.12187
2	7	-16.39992	-5.00000	0.00000	.00064	-.00030	.00592	.09810
2	8	-17.98933	-5.00000	0.00000	.00246	-.00186	.00473	.06563
3	1	-10.47583	-8.33333	0.00000	-.00717	-.00373	-.00445	.75377
3	2	-11.84052	-8.33333	0.00000	-.00950	-.00039	-.00401	.34811
3	3	-13.20520	-8.33333	0.00000	-.00685	-.00450	.00451	.23880
3	4	-14.56989	-8.33333	0.00000	-.00264	-.00545	.00539	.18661
3	5	-15.93458	-8.33333	0.00000	-.00034	-.00512	.00607	.15127
3	6	-17.29927	-8.33333	0.00000	.00142	-.00402	.00357	.12191
3	7	-18.66395	-8.33333	0.00000	.00162	-.00281	.00222	.09249
3	8	-20.02864	-8.33333	0.00000	-.00137	-.00209	.00151	.05813
4	1	-14.59130	-12.50000	0.00000	-.00089	-.00176	.00168	.67276
4	2	-16.07508	-12.50000	0.00000	-.00000	-.00178	.00066	.32134
4	3	-17.15887	-12.50000	0.00000	-.00048	-.00176	.00066	.22649
4	4	-18.24265	-12.50000	0.00000	-.00015	-.00165	.00064	.17369
4	5	-19.32643	-12.50000	0.00000	-.00008	-.00149	.00058	.12620
4	6	-20.41021	-12.50000	0.00000	.00023	-.00131	.00052	.10570
4	7	-21.49395	-12.50000	0.00000	.00032	-.00115	.00046	.07768
4	8	-22.57777	-12.50000	0.00000	.00038	-.00100	.00040	.04862
5	1	-20.40987	-17.50000	0.00000	-.00013	-.00063	.00017	.52053
5	2	-21.15557	-17.50000	0.00000	-.00008	-.00061	.00017	.24671
5	3	-21.90326	-17.50000	0.00000	-.00003	-.00059	.00016	.17188
5	4	-22.64996	-17.50000	0.00000	.00001	-.00056	.00015	.12958
5	5	-23.39665	-17.50000	0.00000	.00004	-.00054	.00015	.09911
5	6	-24.14334	-17.50000	0.00000	.00007	-.00051	.00014	.07449
5	7	-24.89004	-17.50000	0.00000	.00010	-.00048	.00013	.05295
5	8	-25.63673	-17.50000	0.00000	.00011	-.00045	.00012	.03176
PYLON CONTROL POINTS		X, FT	Y, FT	Z, FT	U/VINF	V/VINF	W/VINF	GAMMA/VINF
1	1	-9.49583	0.00000	3.19640		0.00000		0.00000
1	2	-11.16249	0.00000	3.19640		0.00000		0.00000
2	1	-9.49583	0.00000	4.02240		0.00000		0.00000
2	2	-11.16249	0.00000	4.02240		0.00000		0.00000

(h) Page 8.

Figure 23.- Continued.

STORF NUMBR 20 IS THE STORE EJECTED
 ADDITIONAL INPUT FOR THIS STORE
 STORE MASS = 15.53000 SLUGS
 MOMENTS AND PRODUCTS OF INERTIA, SLLG - SQ FT
 IXX = 8.00000
 IYY = 80.00000
 IZZ = 80.00000
 IYZ = -0.00000
 IXY = -0.00000
 IYZ = -0.00000
 STORE MOMENT CENTER IS -5.31250 FEET BEHIND NOSE
 STORE CENTER OF GRAVITY OFFSET FROM MOMENT CENTER, FEET
 XBAR = -0.00000
 YBAR = -0.00000
 ZBAR = -0.00000
 POLYNOMIALS SPECIFYING COMPRESSIBLE STORE SHAPE
 X/L OF END OF EACH SECTION
 SECTION X/L
 1 .23530
 2 1.10000
 COEFFICIENTS OF POLYNOMIALS DESCRIBING EACH SECTION
 SECTION C1 C2 C3 C4 C5 C6 C7
 1 -.44130 -1.00000 .47060 .19470 -0.00000 -0.00000 1.00000
 2 .05082 -0.00000 -0.00000 -0.00000 -0.00000 -0.00000 -0.00000
 SEPARATION ASSUMED 10.62500 FEET FROM NOSE
 AXIAL-FORCE COEFFICIENT IS .20000
 CROSSFLCN-DRAG COEFFICIENT IS 0.00000

(i) Page 9.

Figure 23.- Continued.

TIME = 0.00000 SECONDS

FORCE AND MOMENT COEFFICIENTS

	CLM	CLN	CLL
RUOYANCY	.06514	-.00000	
SLANDER BODY	.42576	-.00000	
CROSSFLOW	0.00000	0.00000	0.00000
EMPHENAGE	0.00000	0.00000	0.00000
TOTAL	.49092	-.00000	0.00000

LOAD AND VELOCITY DISTRIBUTIONS

X, FT	X/L	CCN/DX	OCY/DX	U/V/S	V/V/S	W/V/S
.26563	.02500	.03468	-.00000	.97498	-.00000	.06275
.79608	.07500	.04156	.00000	.98634	-.00000	.05091
1.32813	.12500	.06205	-.00000	1.00362	-.00000	.04728
1.85938	.17500	.10835	.00000	1.01971	-.00000	.05398
2.39063	.22500	.05988	.00000	1.02735	-.00000	.06626
2.92188	.27500	.07064	-.00000	1.02815	-.00000	.07713
3.45313	.32500	.05709	0.00000	1.02730	0.00000	.08541
3.98438	.37500	.04988	.00000	1.02629	-.00000	.09250
4.51563	.42500	.04264	-.00000	1.02510	-.00000	.09864
5.04688	.47500	.03727	0.00000	1.02406	-.00000	.10390
5.57813	.52500	.03519	0.00000	1.02342	-.00000	.10865
6.10938	.57500	.03619	-.00000	1.02317	0.00000	.11335
6.64063	.62500	.03977	-.00000	1.02318	-.00000	.11836
7.17188	.67500	.04409	0.00000	1.02308	0.00000	.12395
7.70313	.72500	.04350	-.00000	1.02225	0.00000	.12988
8.23438	.77500	.04369	.00000	1.02095	-.00000	.13550
8.76563	.82500	.05415	-.00000	1.01911	0.00000	.14195
9.29688	.87500	.04358	0.00000	1.01321	-.00000	.14917
9.82813	.92500	-.00334	-.00000	1.00229	0.00000	.15254
10.35937	.97500	-.04871	.00000	.99185	0.00000	.14839

LOCATION OF STORE IN FUSELAGE COORDINATE SYSTEM, DIMENSIONS OF FEET

	RELATIVE TO FUSELAGE NOSE			RELATIVE TO INITIAL POSITION		
	XF	YF	ZF	DEL XF	DEL YF	DEL ZF
NOSE	-27.06600	0.00000	6.52167	0.00000	0.00000	0.00000
XMOM	-32.37850	0.00000	6.52167	0.00000	0.00000	0.00000
BASE	-37.65100	0.00000	6.52167	0.00000	0.00000	0.00000

TRANSLATIONAL VELOCITIES AND ACCELERATIONS OF STORE IN FUSELAGE COORDINATE SYSTEM

RELATIVE VELOCITIES AND ACCELERATIONS OF STORE IN FUSELAGE						
RELATIVE TO FUSELAGE MOTION						
	DXF	DYF	DZF	D2XF	D2YF	D2ZF
	0.00000	0.00000	10.00000	9.92643	.00000	21.90089

ROTATIONAL VELOCITIES AND ACCELERATIONS OF STORE IN STORE COORDINATE SYSTEM

AL VELOCITIES AND ACCELERATIONS OF STORE IN STORE COORDINATES						
	P	Q	R	PDOT	QDOT	RDOT
	0.00000	0.00000	0.00000	0.00000	1.68211	-.00000

STORE ANGULAR ORIENTATION IN FUSELAGE COORDINATE SYSTEM AND RATES OF CHANGE OF THESE ANGLES

: ANGULAR ORIENTATION IN FUSELAGE COORDINATE SYSTEM AND RATES						
ANGLES IN DEGREES, RATES OF CHANGE IN RADIANS PER SECOND						
	PSI	THETA	PHI	DPSI	DTHETA	DPHI
0.00000	0.00000	0.00000	0.00000	0.00000	0.00000	0.000000

(J) Page 10.

Figure 23.- Continued.

TIME = .30000 SECONDS

FORC AND MOMENT COEFFICIENTS

	CN	CY	CLM	CLN	CLL
PURUANCY	.07764	-.00000	-.01707	-.00000	
SLENDER BODY	.55624	-.00000	1.54336	-.00000	
CROSSFLOW	0.00000	0.00000	0.00000	0.00000	
EXPENNAGE	0.00000	0.00000	0.00000	0.00000	0.00000
TOTAL	.63408	-.00000	1.56630	-.00000	0.00000

LOAD AND VELOCITY DISTRIBUTIONS

X, FT	Y/L	DCK/DX	OCY/DX	U/V/S	V/V/S	W/V/S
.26563	.02500	.14619	-.00000	.57259	-.00000	.23320
.79668	.07500	.28308	-.00000	.57360	-.00000	.23456
1.32813	.12500	.27862	-.00000	.57466	-.00000	.23623
1.85938	.17500	.18764	-.00000	.57568	-.00000	.23923
2.39063	.22500	.04934	-.00000	.57657	-.00000	.24049
2.92188	.27500	.01898	-.00000	.57727	-.00000	.24294
3.45313	.32500	.01960	-.00000	.57776	-.00000	.24551
3.98438	.37500	.01978	-.00000	.57805	-.00000	.24813
4.51563	.42500	.01965	-.00000	.57816	-.00000	.25076
5.04688	.47500	.01932	-.00000	.57811	-.00000	.25335
5.57813	.52500	.01884	-.00000	.57792	-.00000	.25588
6.10938	.57500	.01825	-.00000	.57761	-.00000	.25835
6.64063	.62500	.01757	-.00000	.57719	-.00000	.26073
7.17188	.67500	.01678	-.00000	.57668	-.00000	.26301
7.70313	.72500	.01589	-.00000	.57609	-.00000	.26518
8.23438	.77500	.01490	-.00000	.57544	-.00000	.26723
8.76563	.82500	.01385	-.00000	.57474	-.00000	.26914
9.29688	.87500	.01277	-.00000	.57402	-.00000	.27091
9.82813	.92500	.01173	-.00000	.57330	-.00000	.27253
10.35937	.97500	.01080	-.00000	.57263	-.00000	.27403

LOCATION OF STORF IN FUSELAGE COORDINATE SYSTEM, DIMENSIONS OF FEET

	XF	YF	ZF	DEL XF	DEL YF	DEL ZF
NOSE	-26.81643	-.00000	9.88946	.24957	-.00000	3.36779
XNOM	-32.08861	.00000	10.54276	.28989	.00000	4.02109
BASE	-37.36079	.00000	11.19606	.33021	.00000	4.67439

TRANSITIONAL VELOCITIES AND ACCELERATIONS OF STORE IN FUSELAGE COORDINATE SYSTEM

	OXF	OYF	OZF	O2XF	O2YF	O2ZF
1.05909	.00000	.00000	16.76721	-.8.52429	-.00000	20.84069

ROTATIONAL VELOCITIES AND ACCELERATIONS OF STORE IN STORE COORDINATE SYSTEM

P	Q	R	POOT	QOOT	ROOT
0.00000	1.02605	-.00000	0.00000	6.05830	-.00000

STORE ANGULAR ORIENTATION IN FUSELAGE COORDINATE SYSTEM AND RATES OF CHANGE OF THESE ANGLES

	PSI	THETA	PHI	DPSI	DTHETA	DPHI
-.00000	7.06378	-.00000	-.00000	1.02605	-.00000	-.00000

(k) Page 11.

Figure 23.- Continued.

TIME = .60000 SECONDS

FORCE AND MOMENT COEFFICIENTS

	CN	CY	CLM	CLN	CLL
BUOYANCY	.20715	-.00000	-.08336	.00000	
SLFNDER BODY	1.84408	-.00000	5.39251	-.00000	
CROSSFLOW	0.00000	0.00000	0.00000	0.00000	
EMENNAGE	0.00000	0.00000	0.00000	0.00000	
TOTAL	2.05123	-.00000	5.30915	-.00000	

LOAD AND VELOCITY DISTRIBUTIONS

X, FT	X/L	DCN/UX	DCY/DX	U/V/S	V/V/S	W/V/S
.26563	.02500	.50009	.00000	.53810	-.00000	.79856
.79688	.07500	.97125	-.00000	.53715	-.00000	.80264
1.32813	.12500	.95327	-.00000	.53627	-.00000	.80900
1.85938	.17500	.93356	-.00000	.53547	-.00000	.81506
2.39063	.22500	.91259	-.00000	.53473	-.00000	.82106
2.92188	.27500	.89047	-.00000	.53406	-.00000	.82699
3.45313	.32500	.86750	-.00000	.53345	-.00000	.83287
3.98438	.37500	.84387	-.00000	.53289	-.00000	.83872
4.51563	.42500	.81965	-.00000	.53238	-.00000	.84453
5.04688	.47500	.79500	-.00000	.53191	-.00000	.85032
5.57813	.52500	.77000	-.00000	.53149	-.00000	.85608
6.10938	.57500	.74500	-.00000	.53110	-.00000	.86183
6.64063	.62500	.72000	-.00000	.53074	-.00000	.86757
7.17188	.67500	.69500	-.00000	.53041	-.00000	.87330
7.70313	.72500	.67000	-.00000	.53011	-.00000	.87902
8.23438	.77500	.64500	-.00000	.52984	-.00000	.88474
8.76563	.82500	.62000	-.00000	.52958	-.00000	.89045
9.29688	.87500	.59500	-.00000	.52934	-.00000	.89616
9.82813	.92500	.57000	-.00000	.52912	-.00000	.90187
10.35937	.97500	.54500	-.00000	.52891	-.00000	.90757

LOCATION OF STORE IN FUSELAGE COORDINATE SYSTEM, DIMENSIONS OF FEET

RELATIVE TO NOSE	XF	YF	ZF	DEL XF	DEL YF	DEL ZF
NOSE	-29.65861	-.00000	12.02494	-2.63061	-.00000	5.50327
XCOM	-33.12118	-.00000	16.06634	-.74268	-.00000	9.56467
BASE	-36.54575	.00000	20.14774	1.14525	.00000	13.62607

TRANSLATIONAL VELOCITIES AND ACCELERATIONS OF STORE IN FUSELAGE COORDINATE SYSTEM

RELATIVE TO FUSELAGE MOTION	DXF	DYF	DZF	D2XF	D2YF	D2ZF
	-12.30185	-.00000	17.18356	-92.12330	-.00000	-45.24369

ROTATIONAL VELOCITIES AND ACCELERATIONS OF STORE IN STORE COORDINATE SYSTEM

	P	Q	R	PDOT	QDOT	RDOT
	0.00000	4.64840	-.00000	0.00000	19.33546	-.00000

STORE ANGULAR ORIENTATION IN FUSELAGE COORDINATE SYSTEM AND RATES OF CHANGE OF THESE ANGLES

ANGLES IN DEGREES, RATES OF CHANGE IN RADIANS PER SECOND	PSI	THETA	PHI	OPSI	OTHEA	OPHI
	-.00000	49.86243	-.00000	-.00000	4.64840	-.00000

(1) Page 12.

Figure 23.- Concluded.

APPENDIX I

DETAILS OF SOURCE DISTRIBUTION PROGRAM

I-1. INTRODUCTION

The purpose of this appendix is to provide more detailed information on the source distribution program which was described in section 3. A listing of the program was presented in figure 1 and a general flow chart in figure 2. This appendix will present more detailed flow charts and tables equating the program notation to the algebraic notation.

I-2. MAIN PROGRAM

The flow chart of the main program is presented in figure I-1 and the table equating the program notation and the algebraic notation is presented in Table I-1. Referring to figure I-1, the first section of the program reads and prints the input data. These data were discussed in detail in section 3.2.1. The next section determines the source locations. The first source is placed at $x/\ell = \text{XSFST}$, an input quantity. The location of source $j + 1$ is given by

$$\left(\frac{x}{\ell}\right)_{j+1} = \left(\frac{x}{\ell}\right)_j + \text{PERCR} \left[\beta \left(\frac{r}{\ell}\right)_j \right]$$

The quantity PERCR was input and $(r/\ell)_j$, as well as $(dr/dx)_j$, is calculated in subroutine SHAPE. They are the body radius and surface slope at the j^{th} source location and are calculated from the input polynomials specifying the body shape. After calculating this information for all source locations it is printed.

The values of r/ℓ and dr/dx at the $(\text{NSORC} - 2)$ points where the flow tangency boundary condition is to be applied are next determined. For a discussion of this, see section 4.1.2 of reference 2. These points are located midway between sources. Since this condition is to be imposed at $(\text{NSORC} - 2)$ points, one position must be eliminated since there are $(\text{NSORC} - 1)$ of these positions. The one eliminated is the third one ahead of the point where the maximum body radius is first reached, XRMAX which was input.

The next part of the program calculates the coefficient matrix and the right-hand side of the set of simultaneous equations which are to be solved in order to determine the source strengths. The set of simultaneous equations is given by equations (19), (20), and (21) of reference 2. Note that the right-hand side is put in the (NSORC + 1) column of the C array.

Subroutine INVERS is next called to solve the set of equations for the source strengths. Upon returning from the subroutine the solution is in the (NSORC + 1) column of the C array. This solution is transferred to the Q array and the x/l locations and the source strengths are printed.

The last section of the program calculates the body shape given by the source distribution using equation (14) of reference 2. On the body surface the value of the stream function, ψ^* , is zero. An iteration on r^* is performed to find the value which gives $\psi^* = 0$. This is done at points as specified by the input data.

I-3. SUBROUTINE INVERS

Subroutine INVERS solves a set of simultaneous linear algebraic equations by Gaussian elimination. This routine comes from reference 5 which contains a flow chart. Not all of the options shown in that flow chart are in the present routine. The quantities in the parameter list are

A	array containing coefficient matrix and right-hand sides
NSYS	number of right-hand sides
N	number of equations
NMAX	first dimension of A array in calling program
MMAX	second dimension of A array in calling program

I-4. SUBROUTINE SHAPE

The purpose of this subroutine is to calculate the body radius and surface slope at a specified axial station. The body shape is specified by a series of polynomials of the form of equation (1) of this report. A flow chart of subroutine SHAPE is presented in figure I-2 and a table equating the program notation and the algebraic notation is presented in Table I-2.

The quantities in the parameter list are:

X value of x/ℓ at which radius and surface slope are to
 be calculated

NS number of polynomials describing body shape

XE array containing values of x/ℓ for the end points of
 the NS polynomials

C array containing the coefficients of the NS polynomials

R calculated value of r/ℓ at $x/\ell = X$

DRDX calculated value of dr/dx at $x/\ell = X$

The calculation performed by this subroutine consists of two steps. The first step is to determine which of the NS polynomials describes the shape at the value of X where the radius and surface slope is required. Once this is determined, the appropriate set of coefficients is used in equation (1) to determine r/ℓ . The value of dr/dx is found by differentiating equation (1).

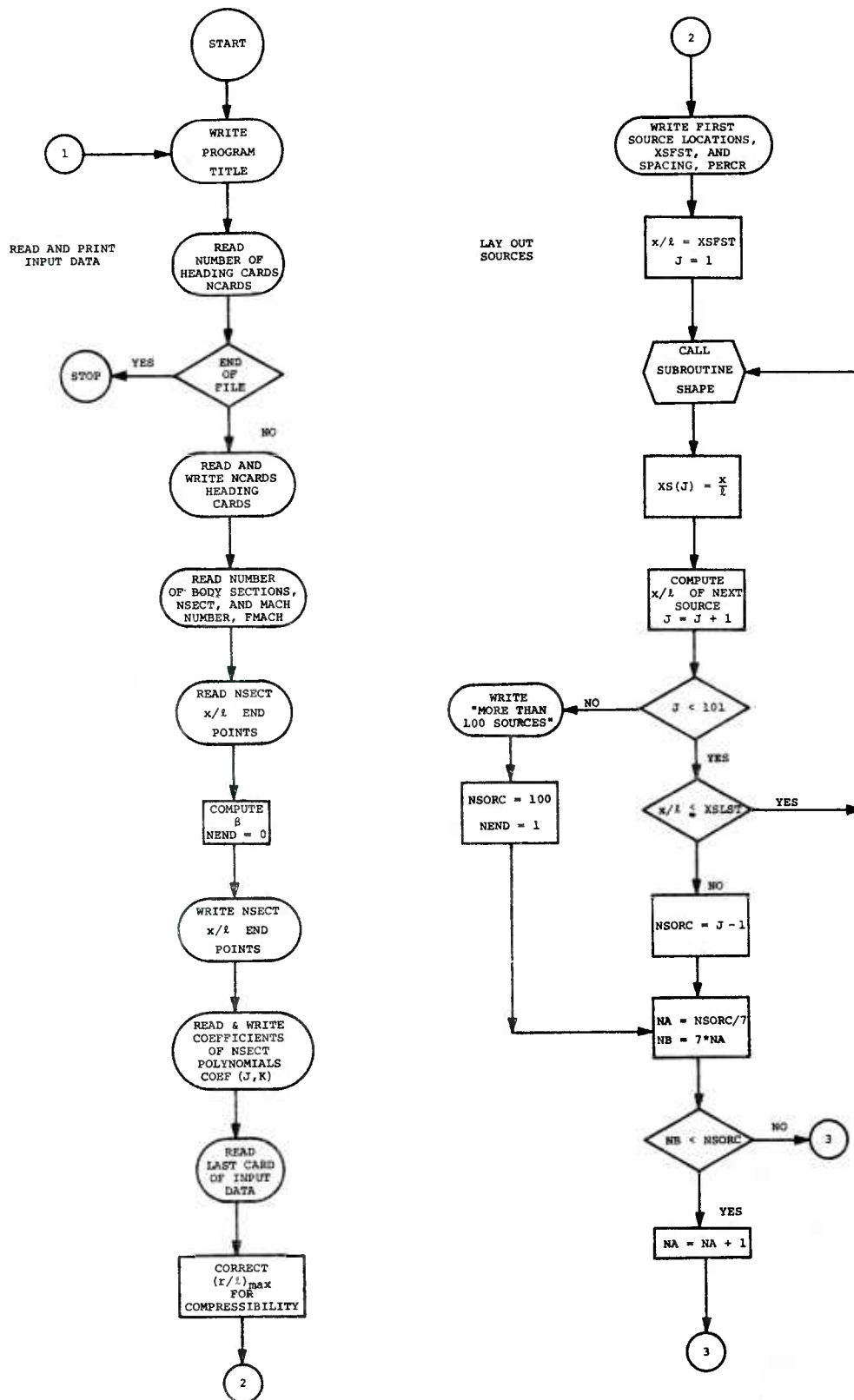
$$\frac{dr}{dx} = \frac{C_7}{2} \left[\frac{2C_2 \frac{x}{\ell} + C_3}{\sqrt{C_2 \left(\frac{x}{\ell}\right)^2 + C_3 \frac{x}{\ell} + C_4}} \right] + C_5 + 2C_6 \frac{x}{\ell}$$

TABLE I-1
 DICTIONARY OF NOTATION
 IN MAIN PROGRAM

<u>PROGRAM NOTATION</u>	<u>ALGEBRAIC NOTATION</u>
BETA	$\sqrt{1 - M_\infty^2}$
DRDX(K)	body surface slope, dr/dx , at location of k^{th} source
FMACH	M_∞
NSORC	number of sources
PSI	stream function, ψ^* (eq. (14), ref. 2)
Q(K)	strength of k^{th} source, Q_k^* (eqs. (14), (19), (20) and (21), ref. 2)
RA(J)	body radius at the j^{th} flow tangency boundary condition, r_j^* (eq. (19), ref. 2)
RL(K)	body radius at k^{th} source location, r_k^* (eqs. (14), (19) and (21), ref. 2)
TB(J)	body surface slope at j^{th} flow tangency boundary condition, $\tan \beta_j$ (eq. (19), ref. 2)
XC(J)	x/ℓ of j^{th} flow tangency boundary condition, x_j^* (eq. (19), ref. 2)
XS(K)	x/ℓ of k^{th} source, x_k^* (eqs. (14), (19) and (21), ref. 2)

TABLE I-2
 DICTIONARY OF NOTATION
 IN SUBROUTINE SHAPE

<u>PROGRAM NOTATION</u>	<u>ALGEBRAIC NOTATION</u>
$C(J,N)$ $J = 1, 2, \dots, 7$	C_1, C_2, \dots, C_7 of the n^{th} polynomial
DRDX	dr/dx
R	r/l
X	x/l

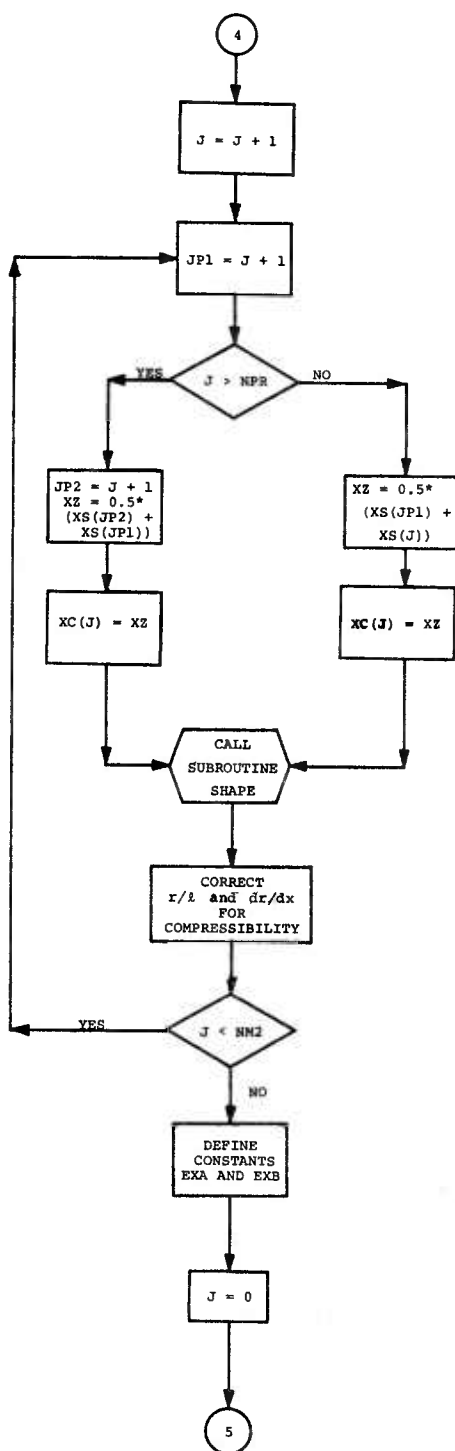
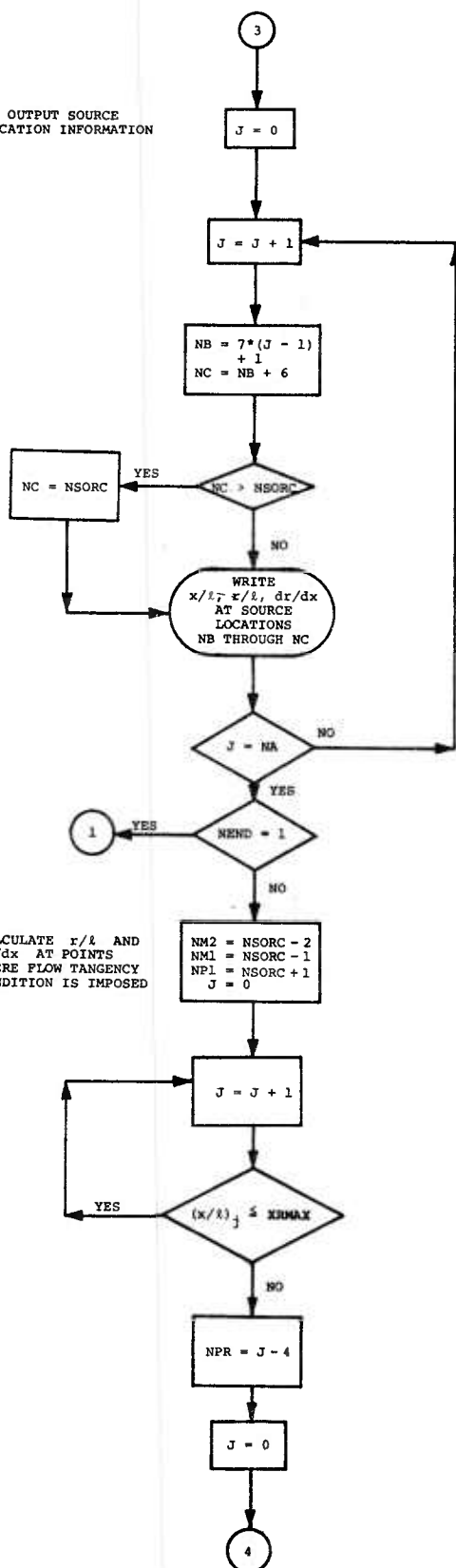


(a) Page 1.

Figure I-1.- Flow chart of source distribution program.

OUTPUT SOURCE
LOCATION INFORMATION

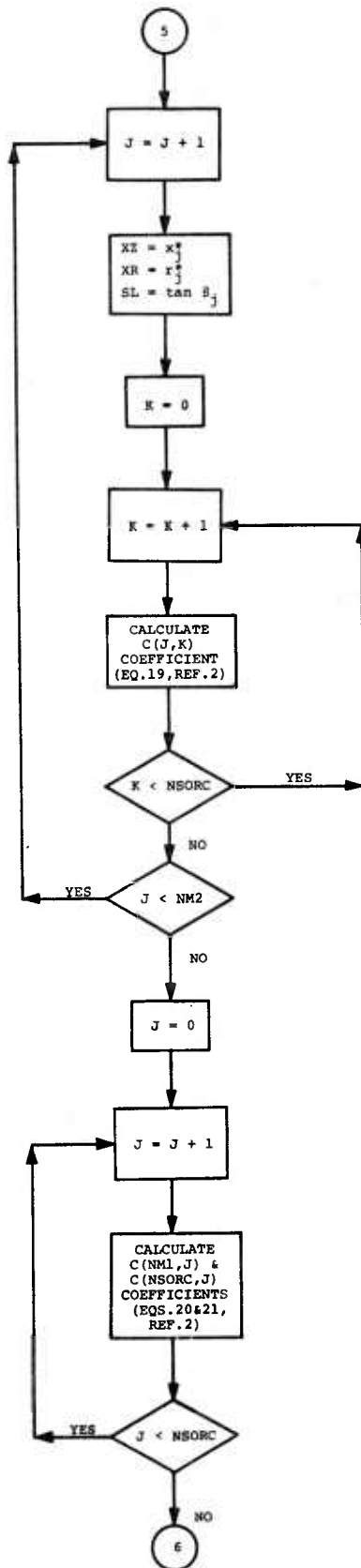
CALCULATE r/l AND
 dr/dx AT POINTS
WHERE FLOW TANGENCY
CONDITION IS IMPOSED



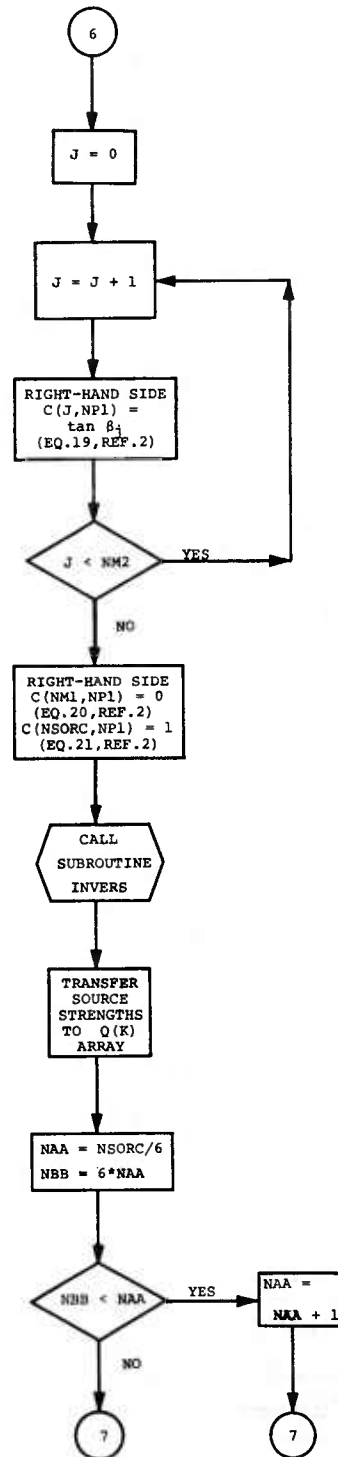
(b) Page 2.

Figure I-1.- Continued.

CALCULATE
COEFFICIENT
MATRIX



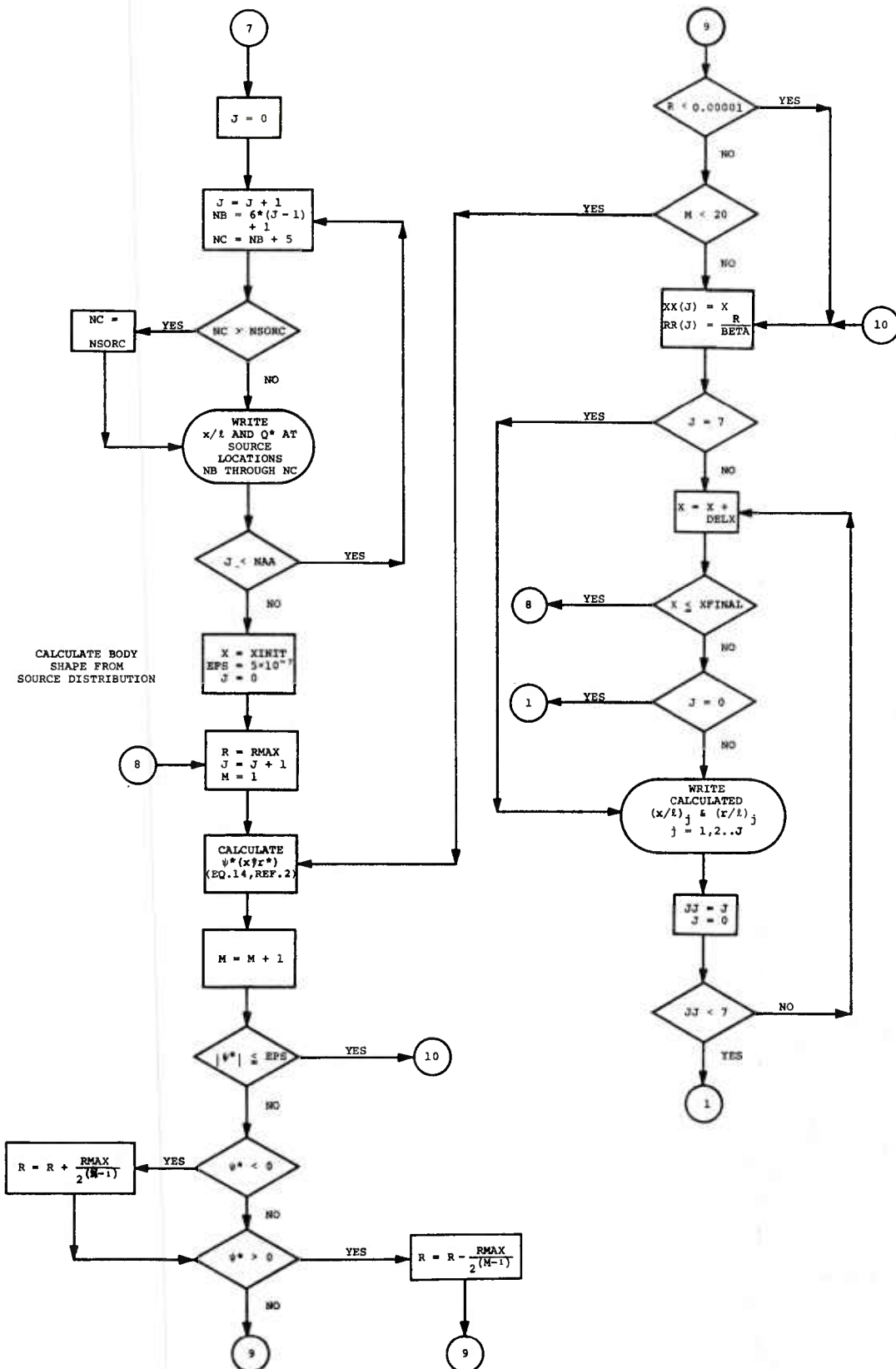
CALCULATE
RIGHT-HAND
SIDE



SOLVE FOR
SOURCE
STRENGTHS

(c) Page 3.

Figure I-1.- Continued.



(d) Page 4.

Figure I-1.- Concluded.

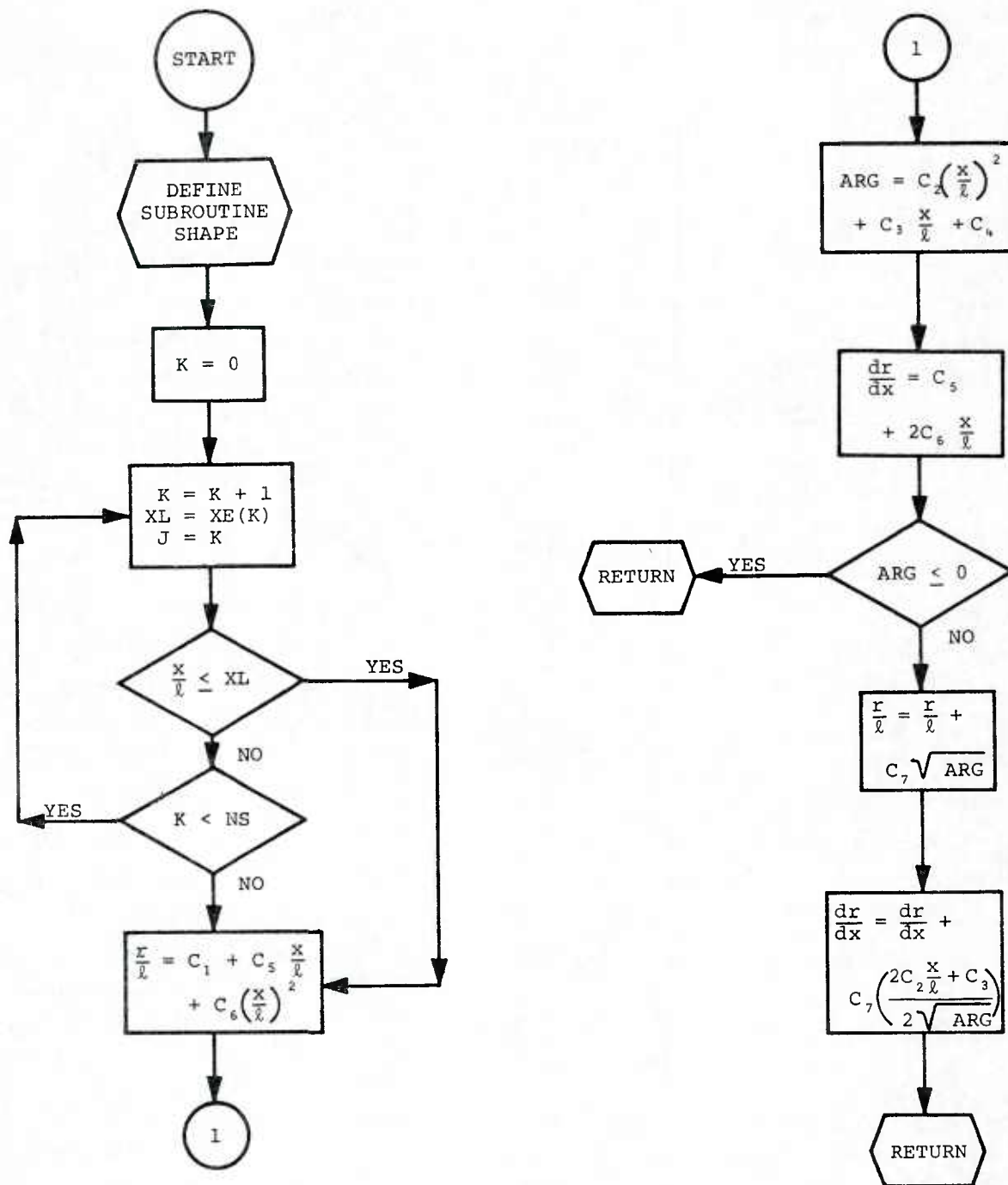


Figure I-2.- Flow chart of subroutine SHAPE.

APPENDIX II

DETAILS OF TRAJECTORY PROGRAM

II-1. INTRODUCTION

The purpose of this appendix is to provide more detailed information on the six-degree-of-freedom trajectory program which was described in section 4. A listing of the program was presented in figure 10 and a general flow chart in figure 11. This appendix will present more detailed flow charts and tables equating the program notation to the algebraic notation. The program consists of a main program and thirty-two subroutines. The main program will first be described and then the subroutines will be described in alphabetical order. The subroutines and their functions were listed in Table II.

II-2. MAIN PROGRAM

The first two pages of the flow chart which was presented in figure 11 are quite complete and will therefore not be expanded in this appendix. Using those pages, the description in section 4.1, the input data discussion in section 4.2.1, and the dictionary of notation in Table II-1, there should be sufficient information to understand the flow of the program.

The last page of the flow chart of figure 11 has been expanded and is presented in figure II-1. This portion of the program begins with card 6DA01419 on page 3 of the listing, figure 10(c), and is the integration loop of the program. The first step in the loop is to call subroutine FORCE to calculate the aerodynamic forces and moments acting on the store body. If the store has an empennage then subroutine EMPFOR is called to calculate the empennage forces and moments.

The next portion of the program solves for the translational and rotational accelerations. The set of six simultaneous equations which are solved are given in Appendix II of reference 1, equations (II-16) through (II-18) and (II-41) through (II-43). The coefficient matrix and right-hand side are stored in the FVN array. The first subscript of FVN is the equation number. The correspondence is

<u>Subscript Value</u>	<u>Equation Number</u>
1	II-16
2	II-17
3	II-18
4	II-41
5	II-42
6	II-43

The second subscript of FVN is the term in the equation. Here the correspondence is

<u>Subscript Value</u>	<u>Term</u>
1	$\ddot{\xi}$
2	$\ddot{\eta}$
3	$\ddot{\zeta}$
4	\dot{p}
5	\dot{q}
6	\dot{r}
7	Right-Hand Side

Thus, for example, FVN(3,5) is the coefficient of \dot{q} in equation (II-18). Certain parts of this section of the program are bypassed if the store center of gravity, c.g., lies on the store moment center. If this is the case, \bar{x}, \bar{y} and \bar{z} are zero and NASYM equals zero.

After calculating the coefficient matrix and right-hand side of the set of equations, subroutine INVERS is called to solve for the accelerations and the values are transferred to the DVAR array. The next steps of the program put the values of $\ddot{\xi}, \ddot{\eta}$, and $\ddot{\zeta}$ into the DVAR array and calculate the values of $\dot{\psi}, \dot{\theta}$, and $\dot{\phi}$, which are also put in the DVAR array. The DVAR array contains

DVAR(1)	$\ddot{\xi}$
DVAR(2)	$\ddot{\eta}$
DVAR(3)	$\ddot{\zeta}$
DVAR(4)	\dot{p}
DVAR(5)	\dot{q}
DVAR(6)	\dot{r}

DVAR(7)	$\dot{\xi}$
DVAR(8)	$\dot{\eta}$
DVAR(9)	$\dot{\zeta}$
DVAR(10)	$\dot{\psi}$
DVAR(11)	$\dot{\theta}$
DVAR(12)	$\dot{\phi}$

These are the derivatives of the twelve dependent variables.

The program next checks to see if the integration procedure has reached the end of an integration step. If it has $NOUT = 1$ and subroutine OUTPUT is called to print the output. Next a check is made to see if the end of the trajectory has been reached, that is, is the current value of the time equal to the final time which was input. If it is then the program transfers to the first input statement and attempts to read another set of input data. If the end has not been reached, then the integration routine, subroutine ADAMS, is called.

NDIFEQ is a control index used by subroutine ADAMS. If $NDIFEQ = 1$ upon returning to the main program, an error condition has been encountered in ADAMS, the calculation is to be terminated, and the next set of input data is to be read. If $2 \leq NDIFEQ \leq 7$, the program is at some intermediate point in the integration from one point to the next. When $NDIFEQ > 7$, the integration of one step has been completed and $NOUT$ is set equal to 1 so that the output subroutine will be called after the derivatives are calculated.

II-3. SUBROUTINE ADAMS

Subroutine ADAMS is the subroutine which integrates the set of differential equations. The subroutine will not be described in detail, however, an examination of the flow chart (fig. II-2) and the program listing (figs. 10(d) and 10(e)) will indicate how it functions. All returns from the subroutine are to the main program.

Consider the following set of n differential equations:

$$\begin{aligned}\dot{y}_1 &= f_1(t, y_1, y_2, \dots, y_n) \\ &\vdots \\ \dot{y}_n &= f_n(t, y_1, y_2, \dots, y_n)\end{aligned}$$

This subroutine uses a fourth-order Adams predictor-corrector method (ref. 6) to solve the above set of equations. To find the value of y_i at the $(j + 4)^{th}$ step, the following formula is used to predict the value

$$y_{i,j+4}^{(p)} = y_{i,j+3} + \frac{h}{24} (55\dot{y}_{i,j+3} - 59\dot{y}_{i,j+2} + 37\dot{y}_{i,j+1} - 9\dot{y}_{i,j}) \quad (II-1)$$

This assumes that all of the \dot{y}_i 's are known for the j , $(j + 1)$, $(j + 2)$, and $(j + 3)$ steps. The quantity h is the interval in the independent variable between these points. After the values of the $y_{i,j+4}^{(p)}$ have been found, the following equation is used to obtain the corrected values:

$$y_{i,j+4} = y_{i,j+3} + \frac{h}{24} (9\dot{y}_{i,j+4}^{(p)} + 19\dot{y}_{i,j+3} - 5\dot{y}_{i,j+2} + \dot{y}_{i,j+1}) \quad (II-2)$$

The use of the above equations require that four evenly spaced values of the dependent variables be known. These are found in this subroutine by means of a fourth-order Runge-Kutta method (ref. 6). To find the values of the y_i 's at the $(j + 1)^{th}$ step, the following equation is used:

$$y_{i,j+1} = y_{i,j} + \frac{1}{6} (k_{i,1} + 2k_{i,2} + 2k_{i,3} + k_{i,4}) \quad (II-3)$$

where

$$\left. \begin{aligned} k_{i,1} &= hf_i(t_j, x_{1,j}, x_{2,j}, \dots, x_{n,j}) \\ k_{i,2} &= hf_i(t_j + \frac{1}{2}h, x_{1,j} + \frac{1}{2}k_{1,1}, \dots, x_{n,j} + \frac{1}{2}k_{n,1}) \\ k_{i,3} &= hf_i(t_j + \frac{1}{2}h, x_{1,j} + \frac{1}{2}k_{1,2}, \dots, x_{n,j} + \frac{1}{2}k_{n,2}) \\ k_{i,4} &= hf_i(t_j + h, x_{1,j} + k_{1,3}, \dots, x_{n,j} + k_{n,3}) \end{aligned} \right\} \quad (II-4)$$

Thus, given initial values of the dependent variables, the y_i 's, the independent variable, t , and the integration interval size, h , the differential equations are integrated three steps using equations (II-3) and (II-4). At this point, the integration is continued using equations (II-1) and (II-2).

A discussion of both the Adams and Runge-Kutta methods is presented in reference 6. From this reference, the truncation error, Δy , at a given

step can be shown to be

$$\Delta y = \left(\frac{y_{i,j+4} - y_{i,j+4}^{(p)}}{14.2} \right) \quad (\text{II-5})$$

so that the absolute error is

$$\Delta y_{\text{ABS}} = |\Delta y|$$

and the relative error is

$$\Delta y_{\text{REL}} = \frac{\Delta y_{\text{ABS}}}{|y_{i,j+4}|} \quad (\text{II-6})$$

At the end of each integration step, error tests are made in the following manner.

An upper bound for the relative error is specified. Then, each step, the relative error is compared against this bound for each $y_{i,j+4}$, $i = 1, 2, \dots, n$. If the test fails for some i , there exists the possibility that the absolute error has become so small as to be insignificant. Hence, the absolute error for this $y_{i,j+4}$ is then compared against a specified absolute error bound. If for any $y_{i,j+4}$, both of the above tests fail, the increment h is cut to $(1/2)h$, and the calculation restarts using the Runge-Kutta method with t_{j+3} as t_0 .

If all error tests are "passed", the program tests whether the increment, h , being used is smaller than necessary. Since the error terms are roughly proportional to h^5 , doubling the interval should increase the error by approximately 32 times. However, doubling the increment if the error terms are all less than $1/32$ of their bounds would normally lead to oscillation in increment size and an inefficient program. In this program, if the relative error is less than $1/100$ of the relative-error bound (or less than $1/100$ of the absolute-error bound when the relative error test fails) for each $y_{i,j+4}$, the increment is doubled. The routine then restarts using the Runge-Kutta method with t_{j+4} as t_0 and $2h$ as the increment.

At the start of the program, a special error procedure is used, since the calculations are done using the Runge-Kutta method. The $y_{i,2}$ is calculated using the increment $2h$. Then, $y_{i,1}$ and $y_{i,2}$ are calculated using the increment h . The absolute error is given in this case by:

$$\left| \frac{y_{i,2}^{(h)} - y_{i,2}^{(2h)}}{14.2} \right|$$

The relative- and absolute-error tests are then made as described above. If they fail, the increment is cut in half and the cycle repeated. No attempt is made to double the increment during Runge-Kutta cycles. If the tests are passed, $y_{i,3}$ is calculated by Runge-Kutta using the increment h , and successive values are then calculated by the Adams method.

The quantities in the parameter list are:

H	current value of the integration interval
DS	initial guess at integration interval
Y	array containing current values of the dependent variables
DY	array containing current values of the derivatives of the dependent variables
NEQ	number of equations being integrated; routine dimensioned for a maximum of 12
NDIFEQ	control index
S	current value of independent variable

II-4. SUBROUTINE CEL1

Subroutine CEL1 calculates the complete elliptic integral of the first kind. This subroutine has been taken directly from reference 7. For a description of the routine that reference should be consulted. A listing of the routine is presented in figures 10(e) and 10(f). The comment cards give a brief explanation of the use of the routine.

II-5. SUBROUTINE CEL2

Subroutine CEL2 calculates the complete elliptic integral of the second kind. This subroutine has been taken directly from reference 7. For a description of the routine that reference should be consulted. A listing of the routine is presented in figures 10(f) and 10(g). The comment cards give a brief explanation of the use of the routine.

II-6. SUBROUTINE DIRCOS

Subroutine DIRCOS computes the direction cosines which relate the store body coordinate system to the inertial coordinate system. The direction cosines are given by equation (28) of reference 1. A listing of the routine is presented in figure 19(g). The three angles Ψ , θ , and ϕ are brought into the subroutine in A(10), A(11), and A(12), respectively and the direction cosines are returned in the D array.

II-7. SUBROUTINE ELI1

Subroutine ELI1 calculates the general elliptic integral of the first kind. This subroutine has been taken directly from reference 7. For a description of the routine that reference should be consulted. A listing of the routine is presented in figure 10(g). The comment cards give a brief explanation of the use of the routine.

II-8. SUBROUTINE ELI2

Subroutine ELI2 calculates the general elliptic integral of the second kind. This subroutine has been taken directly from reference 7. For a description of the routine that reference should be consulted. A listing of the routine is presented in figures 10(g) and 10(h). The comment cards give a brief explanation of the use of the routine.

II-9. SUBROUTINE EMPFOR

Subroutine EMPFOR calculates the empennage forces and moments by the method described in section 5.3 and Appendix I of reference 1. A listing of the subroutine is presented in figures 10(h) and 10(i), a flow chart in figure II-3, and a table equating the algebraic and program notation in Table II-2 of this report.

An examination of the flow chart shows that the first steps in the routine are to locate the point at which the empennage forces act relative to the store moment center and to set JMAX equal to 2 or 4 depending on whether the empennage is planar or cruciform.

The next part of the subroutine calculates the perturbation velocity field at the MSF control points on each of the JMAX fins. At this point these velocities are in the fuselage, or inertial coordinate system. The

free-stream components are now added and the resulting velocities resolved into the store body coordinate system by subroutine INTOST. These velocities are made dimensionless by the store free-stream velocity and the pitch and yaw damping terms are added if aerodynamic damping is being included. From these velocities the components normal to the fin surfaces are determined. Positive directions are shown in figure 10 of reference 1.

The remainder of the routine calculates the empennage forces and moments. First W_o and V_o shown in figure 10 of reference 1 are determined from the velocity field used in the store body force and moment calculation. Then the normal force, and the side force if the empennage is cruciform, are calculated using equations (I-13) and (I-18) of reference 1. The spanwise integrations are performed using Simpson's rule. It is to be noted that in the present program all four fins are assumed to have the same span, $s_h = s_v$. The pitching moment and yawing moment are calculated using equations (I-21) and (I-22).

These forces and moments are in the fin coordinate system. They are resolved into the body coordinate system using equations (58) through (61) of reference 1.

Finally, if rolling moment is to be calculated this is done using equation (I-30) or (I-52) of reference 1. Equation (I-30) is for a planar empennage and (I-52) is for a cruciform empennage.

II-10. SUBROUTINE EMPINI

Subroutine EMPINI initializes certain quantities which will be used repeatedly in the empennage force and moment calculation, subroutine EMPFOR. The equations programmed are given in Appendix I of reference 1. A listing of the subroutine is presented in figures 10(i) and 10(j), a flow chart in figure II-4, and a table equating the algebraic and program notation in Table II-3 of this report.

The flow chart indicates that the first calculation performed is to determine the radial distance outward from the body axis to the MSF fin control points. The first point is at the body-fin juncture, $r_f = a$ (see fig. 10, ref. 1), and the last is at $a = s_h = s_v$. The others are equally spaced in between these two points. Next, a check is made to determine that XTAIL was input as a negative quantity and then the angular orientation of the fins in the store-body coordinate system is determined.

Referring to figure 10 of reference 1, these angles are measured in the clockwise direction from the z_s axis.

JMAX is next set equal to 2 or 4 depending on whether the empennage is planar or cruciform and then the y_s and z_s coordinates of the control points on all of the fins are determined. Next, certain constants are calculated and then the values of $(cc_\ell)_s$ are calculated at the control points. They are the same for all panels since $s_h = s_v$ (see eqs. (I-14) and (I-19), ref. 1).

If rolling moment is not to be calculated, NROLL = 0, control is returned to the calling program. If rolling moment is to be calculated, and the empennage is planar, IPLNR = 1, $(cc_\ell)_s$ given by equation (I-29) of reference 1 is calculated at the control points. Note that in the program the following substitution is made

$$\cosh^{-1}(x) = \ln(x + \sqrt{x^2 + 1})$$

For a cruciform empennage, IPLNR = 0, equation (I-51) of reference 1 is used for the first control point where $y_f = a$. For the other control points equation (I-38) is used.

II-11. SUBROUTINE FORCE

Subroutine FORCE calculates the store-body forces and moments by the methods described in section 5.2 of reference 1. A listing of the subroutine is presented in figures 10(j) and 10(k), a flow chart in figure II-5, and a table equating the algebraic and program notation in Table II-4 of this report.

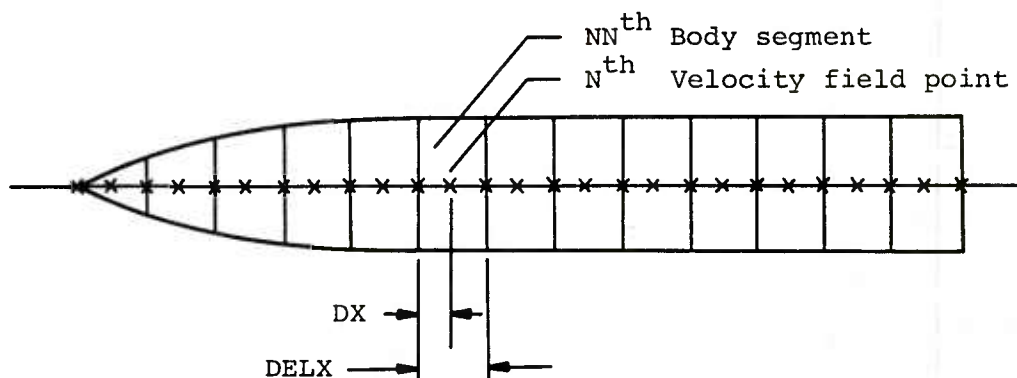
An examination of the flow chart shows that the first step in the routine is to check to see if the trajectory being calculated is to simulate a wind-tunnel captive-store trajectory. If it is, NGAM = 1, then the store attitude relative to the parent aircraft is changed. In wind-tunnel captive-store testing the yaw and pitch angles of the store are changed, only while measuring the aerodynamic forces and moments, to account for translational motion relative to the aircraft. The new angles are

$$\psi_{cs} = \psi_{ff} - \tan^{-1} \left(\frac{\dot{\eta}}{V_\infty \cos \alpha_f + \dot{\xi}} \right)$$

$$\theta_{cs} = \theta_{ff} + \tan^{-1} \left(\frac{\dot{\zeta}}{V_{\infty} \cos \alpha_f + \dot{\zeta}} \right)$$

The subscript cs refers to captive store and ff refers to free flight. The direction cosines between this new body coordinate system and the inertial or fuselage system are calculated in DIRCOS. If the trajectory is a free-flight case, the direction cosines between the true body coordinate system and the inertial system are calculated.

The next section of the program calculates the velocity field given by equation (40) of reference 1 at specified points along the separated store longitudinal axis. The store is removed from the flow field during this calculation. One of the input parameters was NSEG which is the number of equal length segments the body is to be broken into. These segments are of length DELX as shown in the following sketch



The velocities are calculated at the midpoint of each segment as well as at the two ends, the points indicated by x in the sketch. There are thus $NHSEG = 2 * NSEG + 1$ points. The perturbation velocity field is first calculated for all $NHSEG$ points. These velocities are the u, v , and w components given by equation (37) of reference 1. The free-stream velocity components are next determined and added to the perturbation velocities given by equation (38). At this time the velocities are made dimensionless by V_{∞} and written in the x_s, y_s, z_s coordinate system. If damping is being included the damping terms in equation (40) are added.

The routine next calculates the forces and moments. The buoyancy forces and moments are first determined. From equations (42) and (44) of reference 1 the normal force and the pitching moment can be approximated by

$$(C_N)_{BY} = \sum_{N=2,4\dots}^{NHSEG-1} DELX \left(\frac{dC_N}{dx_s} \right)_N = \frac{2\pi}{S_R} \sum_{N=2,4\dots}^{NHSEG-1} DELX \left[a_N^2 \frac{(W_{s_{N+1}}^* - W_{s_{N-1}}^*)}{DELX} \right]$$

$$(C_m)_{BY} = \frac{1}{\ell_R} \sum_{N=2,4\dots}^{NHSEG-1} DELX \left[(x_{s,m} - x_s) \left(\frac{dC_N}{dx_s} \right)_N \right]$$

These are the equations which are programmed. Similar equations can be written for the side force and yawing moment.

Next the slender-body forces and moments are calculated. Referring to equations (46) and (48) of reference 1, the normal force and pitching moment are approximated by

$$\begin{aligned} (C_N)_{SB} &= \sum_{N=2,4\dots}^{NHSEGO-1} DELX \left(\frac{dC_N}{dx_s} \right)_N = \frac{2\pi}{S_R} \sum_{N=2,4\dots}^{NHSEGO-1} DELX \frac{d}{dx_s} (a^2 W_s^*)_N \\ &= \frac{2\pi}{S_R} \left\{ \sum_{N=2,4\dots}^{NHSEGO-1} DELX \left[a_N^2 \frac{(W_{s_{N+1}}^* - W_{s_{N-1}}^*)}{DELX} \right] + \sum_{N=2,4\dots}^{NHSEGO-1} DELX \left(a_N \frac{da_N}{dx_s} W_{s_N}^* \right) \right\} \end{aligned}$$

$$(C_m)_{SB} = \frac{1}{\ell_R} \sum_{N=2,4\dots}^{NHSEGO-1} DELX \left[(x_{s,m} - x_s) \left(\frac{dC_N}{dx_s} \right)_N \right]$$

Here the summations are terminated at the assumed separation location as specified by NSEGXO of item 31 of the input data since $NHSEGO = 2 * NSEGXO + 1$. Note that the quantity in the first summation of $(C_N)_{SB}$ is the same as that in $(C_N)_{BY}$. Use has been made of this fact in the program. Similar expressions can be written for $(C_Y)_{SB}$ and $(C_n)_{SB}$.

If separation is assumed to occur ahead of the base of the store, $NHSEGO < NHSEG$, the viscous crossflow forces and moments in this region are calculated using equations (51) through (54) of reference 1. The normal force and pitching moment are approximated by

$$(C_N)_{CF} = \sum_{N=NHSEGO+1,+3..}^{NHSEG-1} DELX \left(\frac{dC_N}{dx_s} \right)_N = \frac{2c_{d_c}}{S_R} \sum_{N=NHSEGO+1,+3..}^{NHSEG-1} DELX \left(a_N^V c_N^* w_N^* \right)$$

$$(C_m)_{CF} = \frac{1}{\ell_R} \sum_{N=NHSEGO+1,+3..}^{NHSEG-1} DELX \left[(x_{s,m} - x_s) \left(\frac{dC_N}{dx_s} \right)_N \right]$$

II-12. SUBROUTINE INFWW

Subroutine INFWW calculates the influence coefficients of a horseshoe vortex as given by equations (10), (11), and (12) of section 4.2.2 of reference 1. The coordinate system and notation are shown in figure 2 of that reference. A listing of the subroutine is given in figures 10(k) and 10(l) of this report. A flow chart is not presented since the calculation is quite straightforward.

Referring to the listing and equations (10), (11), and (12)

$$F_u = FUI = FUONE$$

$$F_v = FVI = FVONE + FVTWO + FVTHRE$$

$$F_w = FWI = FWONE + FWTWO + FWTHRE$$

In terms of the notation in the equations and figure 2, the nine quantities in the subroutine parameter list are

PSII	$\tan \psi$
APHII	ϕ
XXX	x
YYY	y
ZZZ	z
SNN	s
FUI	F_u
FVI	F_v
FWI	F_w

II-13. SUBROUTINE INTOST

Subroutine INTOST (see fig. 10(1) for a listing) takes a vector with components specified in the inertial ξ, η, ζ coordinate system directions and transforms it into a vector with components in the store x, y, z coordinate system directions, see figure 9 of reference 1. That is,

$$\begin{bmatrix} s_x \\ s_y \\ s_z \end{bmatrix} = [A]' \begin{bmatrix} s_\xi \\ s_\eta \\ s_\zeta \end{bmatrix}$$

The matrix $[A]'$ is the transpose of the direction cosine matrix given by equation (II-2) of reference 1. The transpose is equal to the inverse since $[A]$ is orthogonal. The matrix $[A]$ was calculated in subroutine DIRCOS.

In terms of the above notation, the quantities in the parameter list of the subroutine are

XI	s_ξ
ETA	s_η
ZETA	s_ζ
X	s_x
Y	s_y
Z	s_z
DC	$[A]$

II-14. SUBROUTINE INVERS

For a discussion of subroutine INVERS see section I-3 of Appendix I of this report.

II-15. SUBROUTINE OUTPUT

Subroutine OUTPUT prints the output at the end of each integration step. A listing of the subroutine is presented in figures 10(1) and 10(m), a flow chart in figure II-6, and a table equating the algebraic and program notation in Table II-5 of this report.

The current value of the time is first printed and then the force and moment components calculated in subroutines FORCE and EMPFOR are summed up. The components and totals are then printed. Next the normal-force and side-force distributions and the velocity field along the store centerline are printed. The x_s locations are the midpoints of the body segments.

The next section of the subroutine locates the store nose, moment center, and base in the fuselage or inertial system. These points are located relative to the fuselage nose and also relative to where they would be had the store remained in the $t = 0$ position on the aircraft. These positions are printed.

The remainder of the subroutines prints the store moment center translational velocities and accelerations, the store rotational velocities and accelerations, and the store angular orientation and rates of change of these angles.

II-16. SUBROUTINE PTHIN

Subroutine PTHIN reads in the pylon thickness data and calculates certain quantities which characterize each of the pylon thickness source strips. The pylon thickness model is discussed in section 4.2.3 of reference 1 beginning at the bottom of page 17. The coordinate system and angle convention are shown in figure 6 of that reference. A listing of the subroutine is presented in figure 10(m), a flow chart in figure II-7, and a table equating the algebraic and program notation in Table II-6 of this report.

The number of strips in a chordwise row, NCPS, is first read in along with an index, NUNIP, which indicates whether the thickness distribution is similar at all spanwise stations. If it is similar, NUNIP = 1, the values of θ_p are read in for the first row and then the values of θ_p for the other rows are set equal to those of the first row. If the thickness distribution is not similar, NUNIP = 0, the values of θ_p for all rows are read in. The last step in this section of the subroutine applies the compressibility correction of section 3 of reference 1 to the values of θ_p .

The remainder of the subroutine calculates certain quantities associated with each thickness source strip which appear in equations (24)

through (26) of reference 1. These are

$$\Delta X_i, \tan \psi_i, x_{p_c}, \frac{\theta_p \Delta X_i \cos \psi_i}{2\pi}$$

The variables appearing in the subroutine parameter list are all defined in Table II-6.

II-17. SUBROUTINE PVLIN

Subroutine PVLIN reads in the pylon vortex-lattice data and calculates quantities from these data which locate and describe the horseshoe vortices. The vortex-lattice model is described in section 4.2.2 of reference 1. The coordinate system is shown in figure 2 of that reference. A listing of the subroutine is presented in figures 10(m) and 10(n), a flow chart in figure II-8, and a table equating the algebraic and program notation in Table II-7 of this report.

The first part of the subroutine reads data which are required to describe the pylon and to lay out the horseshoe vortices. It also applies the compressibility correction of section 3 of reference 1. The remainder of the subroutine calculates quantities associated with the horseshoe vortices and the control points. The bound leg of a vortex lies on the one-fourth-chord line of the area element. The X,Y,Z coordinates of the midspan of the bound leg are calculated as are the sweep of the bound leg and the semispan of the vortex. The control point lies at the midspan of the three-fourth-chord line of the area element. The X coordinate of this point is calculated as is the sweep of the three-fourth-chord line. The Y and Z coordinates of the control point are the same as for the bound-leg midpoint.

The variables appearing in the subroutine parameter list are all defined in Table II-7.

II-18. SUBROUTINE SHAPE

For a discussion of subroutine SHAPE see section I-4 of Appendix I of this report.

II-19. SUBROUTINE SIMSON

Subroutine SIMSON calculates the value of a definite integral using Simpson's rule. This can be found in any elementary numerical analysis book, for example, reference 8. As programmed here

$$I = \int_{x_0}^{x_0 + m\Delta x} f(x) dx \approx \frac{\Delta x}{3} \left[f(x_0) + 4f(x_0 + \Delta x) + 2f(x_0 + 2\Delta x) + 4f(x_0 + 3\Delta x) + 2f(x_0 + 4\Delta x) + \dots + 4f(x_0 + (m-1)\Delta x) + f(x_0 + m\Delta x) \right]$$

where m must be an even number and 4 or greater. The subroutine is listed in figure 10(n) of this report. Referring to the listing and the above equation, the quantities in the subroutine parameter list are

N	$m + 1$
F	$f(x)$
DX	Δx
SUM	I

II-20. SUBROUTINE SOROUT

Subroutine SOROUT prints a source distribution which has been read in for one of the axisymmetric bodies, the fuselage, rack, or a store. A listing of the subroutine is presented in figure 10(n). Eight x/l source locations are written followed by the source strengths for these locations. This is repeated until the entire distribution has been printed. The quantities in the subroutine parameter list are

N	number of sources
X	source locations
S	source strengths

II-21. SUBROUTINE STRIO

Subroutine STRIO reads and prints the input data which describe and locate all of the stores and calculates the locations of the tips of the noses in the wing coordinate system. A listing of the subroutine is presented in figures 10(n) and 10(o), a flow chart in figure II-9, and a table equating the algebraic and program notation in Table II-8 of this report. The wing coordinate system is shown in figure 2 of reference 1.

The first loop in the subroutine reads in data for each store including a shape number, NSHAPE(J), and applies the compressibility correction of section 3 of reference 1. The input data are then printed. The next main loop of the routine reads in the source distributions and assigns the appropriate one to each of the stores. At the end of this loop a check is made to see if the index NCOUNT is equal to the number of stores, NSTRS. If it is not, source distributions have not been input for all of the shape numbers in the NSHAPE array. This causes the message "source distributions not input for all stores" to be printed and the program stops. The last part of the subroutine locates all of the stores in the wing coordinate system. Use is made of a number of quantities calculated in subroutine WVLIN.

The variables appearing in the subroutine parameter list are all defined in Table II-8 except for XBWOI and ZBWO. These two variables are not used and could be omitted here and in card 6DA01256 of the main program, see figure 10(b).

II-22. SUBROUTINE STTOIN

Subroutine STTOIN (see fig. 10(o) for a listing) takes a vector with components specified in the store x, y, z coordinate system directions and transforms it into a vector with components in the inertial ξ, η, ζ coordinate system directions, see figure 9 of reference 1. That is,

$$\begin{bmatrix} s_{\xi} \\ s_{\eta} \\ s_{\zeta} \end{bmatrix} = [A] \begin{bmatrix} s_x \\ s_y \\ s_z \end{bmatrix}$$

The matrix $[A]$ is given by equation (II-2) of reference 1 and was calculated in subroutine DIRCOS.

In terms of the above notation, the quantities in the parameter list of the subroutine are

X	s_x
Y	s_y
Z	s_z
XI	s_ξ
ETA	s_η
ZETA	s_ζ
DC	[A]

II-23. SUBROUTINE THOUT

Subroutine THOUT prints the slopes of the wing and pylon thickness distributions which were read in as items 16 and 21 of the input data, see section 4.2.1. A listing of the subroutine is presented in figure 10(o). The variables in the parameter list of the subroutine are

MS	number of wing thickness panels
THETAL	array containing values of θ in incompressible space (see fig. 5, ref. 1)
BETA	$\beta = \sqrt{1 - M_\infty^2}$
NCWS	number of thickness panels in a chordwise row on the wing
NPY	index indicating whether a pylon is (NPY = 1) or is not (NPY = 0) present
MPS	number of pylon thickness panels
THETPL	array containing values of θ_p in incompressible space (see fig. 6, ref. 1)
NCPS	number of thickness panels in a chordwise row on the pylon

It is to be noted that the values of θ and θ_p brought into the subroutine are in incompressible space. Before printing, they are transformed to compressible space and after printing returned to incompressible space. A sample of the output from this subroutine is shown in figure 20(e).

II-24. SUBROUTINE THPVEL

Subroutine THPVEL calculates the velocities induced at a field point X, Y, Z by the pylon thickness distribution using equation (25) of reference 1. This equation is for one thickness source panel and, therefore, must be summed over all panels to obtain the total perturbation velocity due to pylon thickness. A listing of the subroutine is presented in figures 10(o) and 10(p), a flow chart in figure II-10, and a table equating the algebraic and program notation in Table II-9.

The first three quantities in the subroutine parameter list, XC , YC , and ZC , are the coordinates of the point X, Y, Z at which the velocities are to be calculated. The variables UP , VP , and WP are the u/V_∞ , v/V_∞ , and w/V_∞ perturbation velocities due to the wing-pylon vortex-lattice model and the wing and pylon thickness distributions. On entry into the subroutine they are the values excluding pylon thickness. Just before return to the calling program these velocities are added. The last quantity in the subroutine parameter list, JC , is not used.

The subroutine is basically a double loop which sums equation (25) of reference 1 over all of the thickness source strips. The outer loop sums over the span and the inner loop over the chord at a given spanwise location. The only part of the routine requiring explanation is that which begins with card 6DA23 31 and ends with card 6DA23 37. Figure 6 of reference 1 shows a line swept at an angle λ_{p_i} with respect to the Z direction. This line lies at the 50-percent chord of the source strip. If the point at which the velocities are to be calculated lies on the extension of this line then a limiting form of equation (25) must be used. This situation exists if

$$\frac{Z - Z_a}{F} \approx 1.0$$

where F is given by equation (26) of reference 1. The limiting form of equation (25) is

$$\frac{\Delta u}{V_\infty} = \frac{\theta}{2\pi} \frac{\Delta X_i}{\sin \psi_i} \cos \psi_i \left(\frac{1}{Z - Z_b} - \frac{1}{Z - Z_a} \right)$$

$$\frac{\Delta v}{V_{\infty}} = 0$$

$$\frac{\Delta w}{V_{\infty}} = \frac{\theta p \Delta X_i}{2\pi} \cos^2 \psi_i \left(\frac{1}{z - z_b} - \frac{1}{z - z_a} \right)$$

II-25. SUBROUTINE THWVEL

Subroutine THWVEL calculates the velocities induced at a field point X, Y, Z by the wing thickness distribution using equation (19) of reference 1. This equation is for one thickness source panel and, therefore, must be summed over all panels to obtain the total perturbation velocity due to wing thickness. A listing of the subroutine is presented in figure 10(p), a flow chart in figure II-11, and a table equating the algebraic and program notation in Table II-10.

The first three quantities in the subroutine parameter list, $XC, YC,$ and ZC , are the coordinates of the point X, Y, Z at which the velocities are to be calculated. The variables $UW, VW,$ and WW are the $u/V_{\infty}, v/V_{\infty},$ and w/V_{∞} perturbation velocities due to the wing-pylon vortex-lattice model and the wing thickness distribution. On entry into the subroutine they are the values excluding wing thickness. Just before return to the calling program these velocities are added. The last quantity in the subroutine parameter list, JC , is not used.

The subroutine is basically a double loop which sums equation (19) of reference 1 over all of the thickness source strips. The outer loop sums over the span and the inner loop over the chord at a given spanwise location. Inside this loop is another loop with the index $LSIDE$. When $LSIDE = 1$, the velocities due to the i^{th} source strip on the left wing panel are calculated. When $LSIDE = 2$, the velocities due to the corresponding strip on the right wing panel are calculated. Since all of the quantities describing the strips are for the left panel, the signs on $Y_a, Y_b, \tan \psi_i,$ and $\cos \psi_i$ are changed for the right panel, see section 4.2.3 of reference 1 for a further discussion of this. Upon exiting from the $LSIDE$ loop the signs are returned to their original condition.

II-26. SUBROUTINE VELFLD

Subroutine VELFLD, along with other subroutines which it calls, calculates the perturbation velocities at a point on the separated store due to all the other aircraft components. A listing of the subroutine is presented in figures 10(p) and 10(q), a flow chart in figure II-12, and a table equating the algebraic and program notation in Table II-11 of this report. The quantities in the parameter list of the subroutine are defined in this table.

If there is a fuselage ($NFU = 1$) the subroutine calls subroutine VELOC to calculate the perturbation velocities produced by the source distribution which models the fuselage volume. Next, two checks are made. The first determines whether the wing is near the bottom of the fuselage and the second determines whether the y_B coordinate of the field point is greater than the fuselage radius. If either of these tests are passed control transfers to the wing-pylon flow field calculation. If both fail, the fuselage angle-of-attack induced velocity is calculated using equation (39) of reference 1 and if there is no pylon ($NPY = 0$) or the pylon is not under the fuselage centerline the wing-pylon calculation is bypassed. If there is a pylon under the centerline $NCON$ is set equal to 2.

The next section of the subroutine calculates the wing-pylon induced velocities. The field point at which the velocities are to be calculated is located in the wing coordinate system, the X,Y,Z system of figure 5 of reference 1, and then subroutine VLIVEL is called to calculate the wing-pylon induced velocities. Upon return from the subroutine the perturbation velocities UF , VF , and WF are in directions parallel to X , Y , and Z . These velocities are resolved into the fuselage coordinate system and added to the fuselage induced perturbation velocities.

In a similar manner the perturbation velocities due to the rack, if one is present, and all other stores present, if any, are added in. In all cases the field point is first located in the coordinate system of the body in question, the velocities calculated in subroutine VELOC, and then resolved into the fuselage system as they are added up.

The perturbation velocities have been summed up in the fuselage system since this is the coordinate system to which the compressibility correction was applied, see section 3 of reference 1. The velocities are

now transformed to the compressible fuselage coordinate system using equation (2) of that reference. Subroutine INTOST is called to resolve the velocities into the separated store coordinate system, the x,y,z system shown in figures 8 and 9 of reference 1. The fuselage system is the ξ,η,ζ system shown in figure 9.

II-27. SUBROUTINE VELOC

Subroutine VELOC calculates the perturbation velocities induced at a field point of an axisymmetric body by the source distribution which represents its volume. A listing of the subroutine is presented in figure 10(q) and a flow chart in figure II-13 of this report. The coordinate system is shown in figure 1 of reference 1. The algebraic notation is defined in the list of symbols of that reference.

The quantities in the subroutine parameter list are:

X,Y,Z	x,y,z coordinates of the field point
XS	array containing the x_k locations of the N sources
SS	array containing the strengths, $Q_k/4\pi V_\infty$, of the N sources
NS	N, number of sources
U,V,W	$u/V_\infty, v/V_\infty$, and w/V_∞ perturbation velocities; positive in the $\bar{x}, \bar{y}, \bar{z}$ directions, respectively
RMAX	maximum radius of axisymmetric body

At the beginning of the subroutine the radial location, r , of the field point measured perpendicular to the x axis is calculated and the u/V_∞ perturbation velocity is set to zero. If the number of sources, NS, is zero, v/V_∞ and w/V_∞ are set to zero and control returns to the calling program. If this is not the case the radial perturbation velocity, v_r/V_∞ , is set to zero and r is compared with RMAX. If r is less than or equal to RMAX, the possibility exists that the field point lies inside the body. To determine whether or not this is the case, the value of the stream function ψ/V_∞ (called PSI in the subroutine) is calculated using the following equation

$$\frac{\psi(x,r)}{V_\infty} = \frac{1}{2} r^2 - \sum_{k=1}^N \frac{Q_k}{4\pi V_\infty} \left\{ 1 - \frac{(x - x_k)}{[(x - x_k)^2 + r^2]^{1/2}} \right\}$$

If the value of ψ/V_∞ is negative then the field point is inside the body and if $\psi/V_\infty = 0$ then the point lies on the body surface. For either of these situations v/V_∞ and w/V_∞ are set to zero and control returns to the calling program.

If the field point lies outside the body, the u/V_∞ and v_r/V_∞ perturbation velocities are calculated using the following equations

$$\frac{u(x,r)}{V_\infty} = \sum_{k=1}^N \frac{Q_k}{4\pi V_\infty} \frac{(x - x_k)}{[(x - x_k)^2 + r^2]^{3/2}}$$

$$\frac{v_r(x,r)}{V_\infty} = \sum_{k=1}^N \frac{Q_k}{4\pi V_\infty} \frac{r}{[(x - x_k)^2 + r^2]^{3/2}}$$

The remainder of the subroutine resolves v_r/V_∞ into components in the y and z directions. In doing this the signs of v/V_∞ and w/V_∞ are adjusted to reflect the quadrant of the y-z plane in which the field point is located.

II-28. SUBROUTINE VLCOEF

Subroutine VLCOEF calculates the coefficient matrix of the set of simultaneous equations which are to be solved to determine the strengths of the vortices in the wing-pylon vortex-lattice model, see section 4.2.2 of reference 1. These coefficients are the multipliers of $\Gamma_n/4\pi V_\infty$ in equations (6) and (7) of reference 1. A listing of the subroutine is presented in figures 10(q) and 10(r), a flow chart in figure II-14, and a table equating the algebraic and program notation in Table II-12 of this report. The quantities in the parameter list of the subroutine are defined in this table.

The subroutine consists of four double DO loops. The first double loop, the 212 loop, calculates the coefficients of the first summation on the left-hand side of equation (6). The second loop, the 312 loop,

calculates the coefficients of the second summation. The remaining two loops, 412 and 512, calculate the coefficients of the two summations in equation (7). If there is no pylon (NPY = 0) or if the pylon is under the fuselage centerline (IP = 1), the last three loops are bypassed.

All four loops calculate the coefficients in the same manner. The v^{th} control point is first located with respect to the coordinate system of the n^{th} vortex on the left wing panel or pylon and also with respect to the coordinate system of the image vortex on the right wing panel or pylon. Then subroutine INFWW is called twice to calculate the values of F_u , F_v , and F_w due to these two vortices. Prior to calling INFWW the second time the signs of the sweep and dihedral angles are changed for the reasons discussed on page 14 of reference 1. After this second calculation the signs are returned to the original condition. With these values of F_u , F_v , and F_w determined, the coefficient is then calculated.

II-29. SUBROUTINE VLIVEL

Subroutine VLIVEL calculates the perturbation velocities at a field point due to the wing-pylon vortex-lattice model and wing and pylon thickness. The methods used are described in sections 4.2.2 and 4.2.3 of reference 1. A listing of the subroutine is presented in figure 10(r), a flow chart in figure II-15, and a table equating the algebraic and program notation in Table II-13 of this report. The quantities in the parameter list of the subroutine are defined in this table.

At the beginning of the subroutine the three variables, UI, VI, and WI, which return the incompressible wing-pylon perturbation velocities to the calling program, are set to zero. A check is next made on the value of the index NCON. If it is equal to two only pylon thickness velocities are to be calculated. Subroutine THPVEL is called for this purpose.

If NCON is not equal to two, the velocities induced at the field point by the wing vortex lattice are first calculated. These velocities are given by equations (8) through (14) in reference 1. The field point is first located with respect to the coordinate system of the n^{th} vortex on the left wing panel and also with respect to the coordinate system of the image vortex on the right wing panel. Then subroutine INFWW is called twice to calculate the values of F_u , F_v , and F_w due to these two vortices. Prior to calling INFWW the second time the signs of the sweep

and dihedral angles are changed for the reasons discussed on page 14 of reference 1. After this second calculation the signs are returned to the original condition. With these values of F_u , F_v , and F_w determined, the velocities are calculated using equation (8). The value of Γ_n/V_∞ is contained in the CIR array. These velocities are calculated and summed up for all M wing vortices.

The next loop in the program calculates the velocities due to the pylon vortex lattice in an identical manner. This calculation is not performed when NCP equals zero. This is the case when there is no pylon.

The remainder of the subroutine calls subroutines THWVEL and THPVEL to calculate the velocities induced by the wing and pylon thickness distributions. If NCP equals zero the pylon calculation is bypassed since there is no pylon.

II-30. SUBROUTINE VLOUT

Subroutine VLOUT prints the coordinates of the wing-pylon vortex-lattice control points and the wing twist and camber distribution which was read in. These quantities are for the actual wing-pylon combination, not the equivalent incompressible one, and are in the wing coordinate system shown in figure 14 of this report. A sample of the output produced by this subroutine is shown in figure 20(d). A listing of the subroutine is presented in figure 10(s).

The variables in the subroutine parameter list are:

M	number of wing vortices
NCW	number of wing vortices in a chordwise row; input, item 11
BETA	$\beta = \sqrt{1 - M_\infty^2}$
PCX,PVY, PVZ	arrays containing the x,y,z coordinates of the wing control points in incompressible space in wing coordinate system
ALPHAL	array containing the input twist and camber distribution; input, item 14
NPY	index indicating whether a pylon is (NPY = 1) or is not (NPY = 0) present; input, item 4
MP1	$M + 1$

MMP	M + MP where MP is the number of pylon vortices
NCP	number of pylon vortices in a chordwise row; input, item 18
PCPX,PVPY, PVPZ	arrays containing the x,y,z coordinates of the pylon control points in incompressible space in wing coordinate system

It is noted that the x coordinates of the control points are transformed to compressible space, using equation (1) of reference 1, before printing.

II-31. SUBROUTINE VLRHS

Subroutine VLRHS calculates the right-hand-side vector of the set of simultaneous equations, equations (6) and (7) of reference 1, which are to be solved to determine the strengths of the vortices in the wing-pylon vortex-lattice model, see section 4.2.2 of reference 1. A listing of the subroutine is presented in figures 10(s) and 10(t), a flow chart in figure II-16, and a table equating the algebraic and program notation in Table II-14 of this report. The quantities in the parameter list of the subroutine are defined in this table.

The major portion of this routine is devoted to evaluating the externally induced perturbation velocities, $u_{i,v}$, $v_{i,v}$, and $w_{i,v}$, at all of the wing-pylon control points.

The first section calculates the fuselage induced velocities if a fuselage is present (NFU = 1). The velocities induced at the wing control points are not calculated if the wing lies in the fuselage x-y plane. If the velocities are to be calculated, the control point associated with an area element is located in the fuselage coordinate system (see fig. 13) and subroutine VELOC is called to calculate the velocities at this point. These velocities are next resolved into the wing coordinate system and added to the UEI, VEI, and WEI arrays. This is repeated for all M control points. If there is a pylon, NPY = 1, and the pylon is not under the fuselage centerline, IP > 1, the same procedure is followed for the MP pylon control points. If the pylon is below the fuselage centerline, the calculation is not performed since only the lateral, v_i , velocity appears in the boundary condition (see eq. (7), ref. 1). In the y_B equal zero plane v_i due to the fuselage is zero.

The next loop in the subroutine repeats the calculation for the ejector rack if one is present, NRACK = 1. Only velocities induced by the rack at the wing control points are calculated. The rack is assumed to be immediately below the pylon and thus induces no lateral velocity at the pylon control points.

The perturbation velocities induced by all of the stores are next calculated in the same manner as for the fuselage and rack. In this calculation, velocities induced by the stores at the pylon control points are not calculated when the pylon is located below the fuselage centerline, IP = 1. The fuselage $x_B - z_B$ plane is a vertical plane of symmetry and thus any stores on one side of this plane are assumed to have images on the other side of the plane. The lateral velocities induced would thus be equal and opposite in sign and cancel each other.

If a pylon is present, NPY = 1, its thickness distribution produces perturbation velocities at the wing control points. Subroutine THPVEL is next called for each of the M wing control points for the purpose of calculating these velocities and adding them to the UEI, VEI, and WEI arrays. Similarly, subroutine THWVEL is called to calculate the wing thickness perturbation velocities at the MP pylon control points. This calculation is bypassed when the pylon is below the fuselage centerline since the net lateral velocity due to the two wing panels is zero in the $x_B - z_B$ plane.

The last two loops in the subroutine calculate the right-hand sides of equations (6) and (7) of reference 1. Note that these equations have been multiplied by 4π , thus the factor 12.566371 in the subroutine.

II-32. SUBROUTINE VSTOUT

Subroutine VSTOUT prints the coordinates of the wing-pylon vortex-lattice control points, the perturbation velocities induced at these points by all of the other aircraft components (these were calculated in subroutine VLRHS), and the vortex strengths which were determined by solving the set of simultaneous equations given by equations (6) and (7) of reference 1. The quantities brought into the subroutine are in incompressible space. Therefore, the compressibility correction of section 3 of reference 1 is applied just before printing so that the compressible values are tabulated. A sample of the output produced by this subroutine

is shown in figure 20(g) of this report. The wing coordinate system is shown in figure 14 and a listing of the subroutine is presented in figure 10(t).

The variables in the subroutine parameter list are:

M	number of wing vortices
NCW	number of wing vortices in a chordwise row; input, item 11
BETA	$\beta = \sqrt{1 - M_\infty^2}$
BETASQ	β^2
UEI,VEI, WEI	arrays containing incompressible perturbation velocities at the wing-pylon vortex-lattice control points; u_i/V_∞ , v_i/V_∞ , and w_i/V_∞ appearing in equations (6) and (7) of reference 1
CIR	array containing the incompressible vortex strengths; Γ_n/V_∞ in equations (6) and (7) of reference 1
PCX,PVY, PVZ	arrays containing the x,y,z coordinates of the wing control points in incompressible space in wing coordinate system
NPY	index indicating whether a pylon is (NPY = 1) or is not (NPY = 0) present; input, item 4
MP1	M + 1
MMP	M + MP where MP is the number of pylon vortices
NCP	number of pylon vortices in a chordwise row; input, item 18
PCPX,PVPY, PVPZ	arrays containing the x,y,z coordinates of the pylon control points in incompressible space in wing coordinate system

II-33. SUBROUTINE WTHIN

Subroutine WTHIN reads in the wing thickness data and calculates certain quantities which characterize each of the wing thickness source strips. The wing thickness model is discussed in section 4.2.3 of reference 1. The coordinate system and angle convention are shown in figure 5 of that reference. A listing of the subroutine is presented in figure 10(t), a flow chart in figure II-17, and a table equating the algebraic and program notation in Table II-15 of this report.

The number of strips in a chordwise row, NCWS, is first read in along with an index, NUNIS, which indicates whether the thickness distribution is similar at all spanwise stations. If it is similar, NUNIS = 1, the values of θ are read in for the first row and then the values of θ for the other rows are set equal to those of the first row. If the thickness distribution is not similar, NUNIS = 0, the values of θ for all rows are read in. The last step in this section of the subroutine applies the compressibility correction of section 3 of reference 1 to the values of θ .

The remainder of the subroutine calculates certain quantities associated with each thickness source strip which appear in equations (18) through (20) of reference 1. These are

$$\Delta X_i, \tan \psi_i, X_c, Z_1, \frac{\theta \Delta X_i \cos \psi_i}{2\pi}$$

The variables appearing in the subroutine parameter list are all defined in Table II-15.

II-34. SUBROUTINE WVLIN

Subroutine WVLIN reads in the wing vortex-lattice data and calculates quantities from these data which locate and describe the horseshoe vortices. The vortex-lattice model is described in section 4.2.2 of reference 1. The coordinate system is shown in figure 2 of that reference. A listing of the subroutine is presented in figure 10(u), a flow chart in figure II-18, and a table equating the algebraic and program notation in Table II-16 of this report. All of the quantities appearing in the subroutine parameter list are defined in this table.

The first part of the subroutine reads data which are required to describe the wing and to lay out the horseshoe vortices. Next the wing twist and camber distribution, if any, is read. Two indices, NTAC and NUNI, are first input. If NTAC = 0 there is no twist and camber. The index NUNI indicates whether the twist and camber distribution is similar at all spanwise stations. If it is similar, NUNI = 1, the values of $\tan \alpha_\ell$ are read in for the first row and then the values of $\tan \alpha_\ell$ for the other rows are set equal to those of the first row. If the thickness distribution is not similar, NUNI = 0, the values of $\tan \alpha_\ell$ for all rows are read in. Following this the compressibility correction of section 3

of reference 1 is applied to the wing root chord, leading- and trailing-edge sweep angles, and twist and camber distribution.

The remainder of the subroutine calculates quantities which describe the wing segments, the horseshoe vortices, and the control points. This is done in a double DO loop. The quantities associated with the wing segment are calculated in the outer loop and are the X,Y,Z coordinates, the dihedral angle, and the local chord at the midspan and the left-hand side. In the inner loop, quantities describing each wing area element and associated horseshoe vortex are calculated. The first quantities calculated are the planform plane sweep angles of the $1/4$ and $3/4$ chord lines of the area element, the dihedral angle, the chordal plane $1/4$ chord sweep angle, and the chordal plane semispan. The bound leg of a vortex lies on the $1/4$ chord line of the area element. The X,Y,Z coordinates of the midspan of the bound leg are next calculated. The control point lies at the midspan of the $3/4$ chord line of the area element. The X coordinate of this point is calculated. The Y and Z coordinates of the control point are the same as for the bound-leg midpoint. The last three quantities calculated in the loop are the X,Y,Z coordinates of the intersection of the $3/4$ chord line with the left, or outboard side, of the area element.

Just before returning to the calling program, the span and average chord of the incompressible wing are calculated.

TABLE II-1

DICTIONARY OF NOTATION IN MAIN PROGRAM

The following list presents most of the variable names used in the main program. Those which appear in parameter lists of subroutines but are not used in the main program are not included. Where possible a variable name is identified by a symbol in the list of symbols or an equation number in reference 1. Where a variable is an input quantity, it is so identified and section 4.2.1 of this report should be referred to for the definition. Primes associated with the algebraic notation indicate incompressible space (see section 3 of ref. 1). The x_B, y_B, z_B coordinate system is shown in figure 13 of this report.

<u>PROGRAM NOTATION</u>	<u>ALGEBRAIC NOTATION</u>
ACCG	g , 32.174 feet/second
ALFAC	α_f , degrees; input, item 3
ALFACR	α_f , radians
ALFAI	α'_f , degrees
ALFAIR	α'_f , radians
ALFWIR	angle of attack of wing in incompressible space, rad.
BETA	β
CA	C_A ; input, item 36
CAPG	$\cos(\alpha_f + \gamma_f)$
CDC	c_{d_c} ; input, item 36
CIR(N)	Γ'_n/V_∞
CLALPH	lift-curve slope of tail panels; input, item 38
CLLEM	$(C_\ell)_E$, equations (62) and (I-30) or equations (63) and (I-52)
CLMBY	$(C_m)_{BY}$, equation (44)
CLMCF	$(C_m)_{CF}$, equation (53)

Table II-1.- Continued.

CLMEM	$(C_m)_E$, equation (60)
CLMSB	$(C_m)_{SB}$, equation (48)
CLNBY	$(C_n)_{BY}$, equation (45)
CLNCF	$(C_n)_{CF}$, equation (54)
CLNEM	$(C_n)_E$, equation (61)
CLNSB	$(C_n)_{SB}$, equation (49)
CNBY	$(C_N)_{BY}$, equation (42)
CNCF	$(C_N)_{CF}$, equation (51)
CNEM	$(C_N)_E$, equation (58)
CNORM	total C_N
CNSB	$(C_N)_{SB}$, equation (46)
COEF(I,J)	coefficients of polynomials specifying separated store shape; input, item 35
COSSPS(I)	$\cos \psi_i$ for a pylon thickness panel
COSSWS(I)	$\cos \psi_i$ for a wing thickness panel
CPITCH	total C_m
CRIIR	$\cos(RIIR)$
CROLL	total C_ℓ
CSIBCR(N)	$\cos(SIBCR(N))$
CSIBIR(N)	$\cos(SIBIR(N))$
CSIDE	total C_Y
CSIIR(N)	$\cos(SIIR(N))$
CWICR	$\cos(WICR)$
CWIIR	$\cos(WIIR)$
CYAW	total C_n
CYBY	$(C_Y)_{BY}$, equation (43)
CYCF	$(C_Y)_{CF}$, equation (52)

Table II-1.- Continued.

CYEM	$(C_Y)_E$, equation (59)
CYSB	$(C_Y)_{SB}$, equation (47)
DC(I,J)	[A], equation (28)
DDTIME	input value of integration interval; set equal to DTIME of item 40
DELX	length of body segment used in force calculation
DELXI	DELX in incompressible space
DTIME	current value of integration interval
DTR	degrees to radians conversion factor, 1/57.29578
DVAR(N), N = 1,2,...12	$\ddot{\xi}, \ddot{\eta}, \ddot{\zeta}, \dot{p}, \dot{q}, \dot{r}, \dot{\xi}, \dot{\eta}, \dot{\zeta}, \dot{\psi}, \dot{\theta}, \dot{\phi}$ respectively
EDRDX(I).	da/dx_s at the midpoint of the i^{th} segment of the separated store
ERAD(I)	a at the midpoint of the i^{th} segment of the separated store
ESTLGC	l_s of separated store
ESTLGI	l'_s of separated store
ESTRMX	a_{max} of separated store
EXST(I)	x_s location of the i^{th} half segment on the separated store
FINSS	tail fin semispan; input, item 38
FIXX	I_{xx}
FIXY	I_{xy}
FIXZ	I_{xz}
FIYY	I_{yy}
FIYZ	I_{yz}
FIZZ	I_{zz}
FLTHC	fuselage length; input, item 5
FLTHI	fuselage length in incompressible space

Table II-1.- Continued.

FMACH	M_∞ ; input, item 3
FRMAX	fuselage maximum radius; input, item 5
FSOR(N)	array containing the strengths of the fuselage source distribution
FXL(N)	array containing the x'_B positions of the fuselage sources
GAMF	fuselage flight path angle, γ_f ; input, item 3
GXX,GYY,GZZ	g_x, g_y, g_z , equation (67)
IP	pylon location specification; input, item 17
IPLNR	empennage type; input, item 37
M	number of vortices on wing, $M = NCW*MSW$
MMP	$M + MP$
MP	number of vortices on pylon, $MP = NCP*MSP$
MPS	number of pylon thickness panels, $MPS = NCPS*MSP$
MPL	$M + 1$
MS	number of wing thickness panels, $MS = NCWS*MSW$
MSF	input, item 37
MSP	input, item 18
MSW	input, item 11
NCP	input, item 18
NCPS	input, item 20
NCW	input, item 11
NCWS	input, item 15
NDAMP	input, item 31
NDIFEQ	control index used in subroutine ADAMS
NEJECT	number of store being separated; input, item 31
NEJSTR	subscript associated with separated store, $1 \leq NEJSTR \leq NSTRS$

Table II-1.- Continued.

NEMP	input, item 31
NEQ	number of differential equations being integrated by subroutine ADAMS; NEQ = 12
NFSOR	number of fuselage sources; input, item 6
NFU	input, item 4
NGAM	input, item 31
NHSEG	number of points along store axis where velocity field is to be calculated; NHSEG = 2*NSEG + 1
NHSEGO	number of points along store axis ahead of separation point where velocity field is to be calculated; NHSEGO = 2*NSEGXO + 1
NPOLY	input, item 31
NPY	input, item 4
NRACK	input, item 4
NROLL	input, item 31
NRSOR	number of rack sources; input, item 23
NSEG	input, item 31
NSEGXO	input, item 31
NSTRS	input, item 4
NUMSTR(I)	number associated with i^{th} store; input, item 26
PI	π , 3.1415927
PHIROL	fin orientation; input, item 38
QSREF	$q_{\infty S} S_R$
QSREFL	$q_{\infty S} S_R \ell_R$
QSTORE	$q_{\infty S}$, equation (69)
RAD	radians to degrees conversion factor, 57.29578
RADAV	average body radius in fin region; input, item 38
REFL	ℓ_R , equation (72)

Table II-1.- Continued.

RHO	ρ_{∞} ; input, item 3
RIC	rack incidence angle; input, item 22
RII	rack incidence angle in incompressible space, degrees
RIIR	rack incidence angle in incompressible space, radians
RLTHC	rack length; input, item 22
RLTHI	rack length in incompressible space
RRMAX	maximum rack radius; input, item 22
RSOR(N)	array containing the strengths of the rack source distribution
RXL(N)	array containing the axial locations of the rack sources
SAPG	$\sin(\alpha_f + \gamma_f)$
SIBCR(I)	incidence angle of i^{th} store relative to fuselage axis, radians; $(WIC + SIC(I)) * DTR$
SIBIR(I)	incidence angle of i^{th} store relative to fuselage axis in incompressible space; radians; $WIIR + SIIR(I)$
SIC(I)	incidence angle of the i^{th} store; input, item 26
SII(I)	incidence angle of i^{th} store relative to wing root-chord in incompressible space, degrees
SIIR(I)	incidence angle of i^{th} store relative to wing root-chord in incompressible space, radians
SINSPS(I)	$\sin \psi_i$ for a pylon thickness panel
SINSWS(I)	$\sin \psi_i$ for a wing thickness panel
SLTHC(I)	length of i^{th} store; input, item 26
SLTHI(I)	length of i^{th} store in incompressible space
SMASS	m, mass of separated store; input, item 32
SREF	S_R , equation (70)
SRMAX(I)	maximum radius of i^{th} store
SSIBCR(I)	$\sin(SIBCR(I))$
SSIBIR(I)	$\sin(SIBIR(I))$

Table II-1.- Continued.

SSIIR(I)	$\sin(\text{SIIR}(I))$
SWICR	$\sin(\text{WICR})$
SWIIR	$\sin(\text{WIIR})$
TIME	t, current value of time
TIMEF	final time; input, item 40
TIMEI	initial time; input, item 40
UU	\dot{x}_O
VAR(N), N = 1,2,...12	$\xi, \eta, \zeta, p, q, r, \xi, \eta, \zeta, \psi, \theta, \phi$ respectively
VINF	V_∞ ; input, item 3
VSTORE	$V_{\infty S}$, equation (41)
VZERO	input, item 39
WIC	wing incidence angle, degrees; input, item 9
WICR	wing incidence angle, radians
WII	wing incidence angle in incompressible space, degrees
WIIR	wing incidence angle in incompressible space, radians
WW	\dot{z}_O
XBAR	\bar{x} ; input, item 33
XBASEI	ξ coordinate of separated store base at $t = 0$
XBPO	x_B coordinate of leading edge of pylon root chord
XBPOI	x'_B coordinate of leading edge of pylon root chord
XBRO	x_B coordinate of tip of rack nose
XBROI	x'_B coordinate of tip of rack nose
XBSO(I)	x_B coordinate of tip of nose of i^{th} store
XBSOI(I)	x'_B coordinate of tip of nose of i^{th} store
XBWOC	x_B coordinate of wing root-chord leading edge; input, item 9

Table II-1.- Continued.

XBWOI	x'_B coordinate of wing root-chord leading edge
XCGI	ξ coordinate of separated store moment center at $t = 0$
XEND(N)	end points of polynomials specifying separated store shape; input, item 34
XLEL(I)	x' coordinate of local wing-chord leading edge measured relative to root-chord leading edge
XMOM	$x_{s,m}$; input, item 33
XNOSEI	ξ coordinate of tip of separated store nose at $t = 0$
XP	x' coordinate of pylon root-chord leading edge measured relative to wing root-chord leading edge
XPC	x coordinate of pylon root-chord leading edge measured relative to wing root-chord leading edge
XRNC	input, item 22
XRNI	value of XRNC in incompressible space
XSEP	$x_{s,o}$
XTAIL	input, item 38
XWRO	x coordinate of tip of rack nose measured from wing root-chord leading edge
XWROI	value of XWRO in incompressible space
XWSO(I)	x coordinate of tip of nose of i^{th} store measured from wing root-chord leading edge
XWSOI(I)	value of XWSO(I) in incompressible space
YBAR	\bar{y} ; input, item 33
YBASEI	η coordinate of separated store base at $t = 0$
YBPO	y_B coordinate of pylon
YBRO	y_B coordinate of rack
YBSO(I)	y_B coordinate of i^{th} store
YCGI	η coordinate of separated store moment center at $t = 0$
YNOSEI	η coordinate of tip of separated store nose at $t = 0$
YWRO	y location of rack in wing coordinate system

Table II-1.- Concluded.

Z(I)	input, item 19
ZBAR	\bar{z} ; input, item 33
ZBASEI	ζ coordinate of separated store base at $t = 0$
ZBPO	z_B coordinate of pylon root-chord leading edge
ZBRO	z_B coordinate of tip of rack nose
ZBSO(I)	z_B coordinate of tip of nose of i^{th} store
ZBWO	$z_{B_{\text{item 9}}}$ coordinate of wing root-chord leading edge; input, item 9
ZCGI	ζ coordinate of separated store moment center at $t = 0$
ZLEL(I)	z coordinate of local wing-chord leading edge measured relative to root-chord leading edge
ZNOSEI	ζ coordinate of tip of separated store nose at $t = 0$
ZP	z coordinate of pylon root-chord leading edge measured relative to wing root-chord leading edge
ZRN	input, item 22
ZWRO	z location of tip of rack nose measured relative to wing root-chord leading edge

TABLE II-2

DICTIONARY OF NOTATION IN SUBROUTINE EMPFOR

The following list presents most of the variable names used in subroutine EMPFOR. Where possible a variable name is identified by a symbol in the list of symbols or an equation number in reference 1. Symbols in figures 8 and 10 of that reference are also used. Where a variable is an input quantity, it is so identified and section 4.2.1 of this report should be referred to for the definition. The x_B, y_B, z_B coordinate system is shown in figure 13 of this report.

<u>PROGRAM NOTATION</u>	<u>ALGEBRAIC NOTATION</u>
ABU	$\alpha_u + \beta_u$, equations (I-28) and (I-37)
ALFACR	α_f , radians
ANG	ϕ_f , radians (fig. 10)
AS	α_s , equation (I-16)
BETA	β
BS	β_s , equation (I-20)
CCL3(K)	$(cc_\ell)_3$ and $(cc_\ell)_4$, equations (I-14) and (I-19); equal since $s_h = s_v$
CCL5(K)	$(cc_\ell)_5$ if planar empennage, equation (I-29); $(cc_\ell)_6$ if cruciform empennage, equations (I-38) and (I-51)
CCLEM	$(C_\ell)_E$, equations (62) and (I-30) or equations (63) and (I-52)
CLMEM	$(C_m)_E$, equation (60)
CLNEM	$(C_n)_E$, equation (61)
CNEM	$(C_N)_E$, equation (58)
CYEM	$(C_Y)_E$, equation (59)
DTR	degrees to radians conversion factor, $1/57.29578$
FCONA	$(dC_L/d\alpha)_H/\pi(s_h - a)^2$
FCONB	$FCONA/\ell_R$

Table II-2.- Continued.

FCONC	$l_f - x_{s,m}$, figure 8
FROLE(K)	$\phi_f + 90^\circ$ for fin 1, $\phi_f + 270^\circ$ for fin 2, $\phi_f + 180^\circ$ for fin 3, ϕ_f for fin 4; radians; see figure 10
IPLNR	empennage type; input, item 37
IT	body segment number at which the empennage forces act
JMAX	number of tail fins
MSF	input, item 37
NDAMP	input, item 31
NGAM	input, item 31
NHSEG	number of points along store axis where velocity field was calculated
NROLL	input, item 31
PHIROL	ϕ_f ; input, item 38
RADAV	average body radius in fin region; input, item 38
RFIN(K)	$a + \left(\frac{K-1}{MSF-1} \right) (s_h - a)$ or $a + \left(\frac{K-1}{MSF-1} \right) (s_v - a)$; figure 10 with $s_h = s_v$
UTL(K,J)	U_s^* at the k^{th} control point on the j^{th} fin
VAR(N) N = 1, 2, ... 12	$\xi, \eta, \zeta, p, q, r, \xi, \eta, \zeta, \psi, \theta, \phi$, respectively
VINF	V_∞ ; input, item 3
VN(K,J)	velocity normal to the surface of the j^{th} fin at the k^{th} control point
VO	$V_o/V_{\infty s}$, see figure 10
VRATIO	$V_\infty/V_{\infty s}$
VSO	V_s^* in the y_s direction of figure 10
VSTORE	$V_{\infty s}$, equation (41)
VTL(K,J)	V_s^* at the k^{th} control point on the j^{th} fin
WO	$W_o/V_{\infty s}$, see figure 10

Table II-2.- Concluded.

WSO	W_s^* in the z_s direction of figure 10
WTL(K,J)	W_s^* at the k^{th} control point on the j^{th} fin
XB	x_B' coordinate of a fin control point in incompressible space
XMOM	$x_{s,m}$; input, item 33, positive quantity
XTAIL	input, item 38
YB	y_B coordinate of a fin control point
YTAIL(K,J)	$y_{s_{fin}}$ coordinate of the k^{th} control point on the j^{th}
ZB	z_B coordinate of a fin control point
ZTAIL(K,J)	$z_{s_{fin}}$ coordinate of the k^{th} control point on the j^{th}

TABLE II-3

DICTIONARY OF NOTATION IN SUBROUTINE EMPINI

The following list presents most of the variable names used in subroutine EMPINI. Where possible a variable name is identified by a symbol in the list of symbols or an equation number in reference 1. Symbols in figures 8 and 10 of that reference are also used. Where a variable is an input quantity, it is so identified and section 4.2.1 of this report should be referred to for the definition.

<u>PROGRAM NOTATION</u>	<u>ALGEBRAIC NOTATION</u>
AKK1	$K(k_1)$, equation (I-43)
AK1	k_1 , equation (I-42)
ARG3	A_1 , equation (I-44)
A2	a^2 , figure 10
A4	a^4 , figure 10
BETA	β
CAPRSQ	R^2 , equation (I-39)
CCL3(K)	$(cc_\ell)_3$ and $(cc_\ell)_4$, equations (I-14) and (I-19); equal since $s_h = s_v$
CCL5(K)	$(cc_\ell)_5$ if planar empennage, equation (I-29); $(cc_\ell)_6$ if cruciform empennage, equations (I-38) and (I-51)
CK	$\sqrt{1 - AK1*AK1} = \sqrt{1 - k_1^2}$
CKCK	$1 - k_1^2$
CTWGAM	$\cos 2\gamma$, equation (I-41)
CTWTHE	$\cos 2\theta$, equation (I-40)
DTR	degrees to radians conversion factor, 1/57.29578
EAK	$E(A_1, k_1)$, equation (I-49)
EPIO2K	$E(\pi/2, k_1)$, equation (I-48)
FAK	$F(A_1, k_1)$, equation (I-47)

Table II-3.- Concluded.

FCONA	$(dC_L/d\alpha)_H/\pi(s_h - a)^2$
FCONB	$FCONA/\ell_R$
FCONC	$\ell_f - x_{s,m}$, figure 8
FINSS	tail fin semispan; input, item 38
FROLE(K)	$\phi_f + 90^\circ$ for fin 1, $\phi_f + 270^\circ$ for fin 2, $\phi_f + 180^\circ$ for fin 3, ϕ_f for fin 4; radians; see figure 10
IPLNR	empennage type; input, item 37
JMAX	number of tail fins
MSF	input, item 37
NROLL	input, item 31
PHIROL	ϕ_f ; input, item 38
RADAV	average body radius in fin region; input, item 38
RFIN(K)	$a + \left(\frac{K-1}{MSF-1}\right)(s_h - a)$ or $a + \left(\frac{K-1}{MSF-1}\right)(s_v - a)$; figure 10 with $s_h = s_v$
SHS	s_h^2
STWGAM	$\sin 2\gamma$, equations (I-41) and (I-42)
TOVPI	$2/\pi$
TTWGAM	$\tan 2\gamma$, equations (I-41) and (I-42)
TWOTHE	2θ , equation (I-40)
XTAIL	input, item 38
XTAILI	XTAIL in incompressible space
YTAIL(K,J)	y_s coordinate of the k^{th} control point on the j^{th} fin
ZTAIL(K,J)	z_s coordinate of the k^{th} control point on the j^{th} fin

TABLE II-4

DICTIONARY OF NOTATION IN SUBROUTINE FORCE

The following list presents most of the variable names used in subroutine FORCE. Where possible a variable name is identified by a symbol in the list of symbols or an equation number in reference 1. Where a variable is an input quantity, it is so identified and section 4.2.1 of this report should be referred to for the definition. Primes associated with the algebraic notation indicate incompressible space (see section 3 of ref. 1). The x_B, y_B, z_B coordinate system is shown in figure 13 of this report.

<u>PROGRAM NOTATION</u>	<u>ALGEBRAIC NOTATION</u>
ALFACR	α_f , radians
BETA	β
CDC	c_{d_c} ; input, item 36
CLMBY	$(C_m)_{BY}$, equation (44)
CLMCF	$(C_m)_{CF}$, equation (53)
CLMSB	$(C_m)_{SB}$, equation (48)
CLNBY	$(C_n)_{BY}$, equation (45)
CLNCF	$(C_n)_{CF}$, equation (54)
CLNSB	$(C_n)_{SB}$, equation (49)
CNBY	$(C_N)_{BY}$, equation (42)
CNCF	$(C_N)_{CF}$, equation (51)
CNSB	$(C_N)_{SB}$, equation (46)
CNX (NN)	total dC_N/dx_s at the midpoint of the NN^{th} body segment
CONA	$2/a_{max}^2$
CONB	$2c_{d_c}/\pi a_{max}^2$

Table II-4.- Continued.

CRIFI	cosine of the angle between the rack longitudinal axis and the fuselage longitudinal axis in incompressible space; measured in x'_B, z_B plane
CYBY	$(C_Y)_{BY}$, equation (43)
CYCF	$(C_Y)_{CF}$, equation (52)
CYSB	$(C_Y)_{SB}$, equation (47)
CYX(NN)	total dC_Y/dx_s at the midpoint of the NN^{th} body segment
DC(I,J)	$[A]$, equation (28)
DCN	dC_N/dx_s
DCY	dC_Y/dx_s
DELX	length of a body segment; store length divided by NSEG which was input in item 31
DX	$DELX/2$
EDRDX(I)	da/dx_s at the midpoint of the i^{th} segment of the separated store
ERAD(I)	a at the midpoint of the i^{th} segment of the separated store
ESTRMX	a_{max} of separated store
ETA	η coordinate of point on store axis measured relative to store moment center
NDAMP	input, item 31
NGAM	input, item 31
NHSEG	number of points along store axis where velocity field is to be calculated; $NHSEG = 2*NSEG + 1$
NHSEGO	number of points along store axis ahead of separation point where velocity field is to be calculated; $NHSEGO = 2*NSEGXO + 1$
NRACK	input, item 4
NSEG	input, item 31
NSEGXO	input, item 31
RIIR	rack incidence angle in incompressible space, radians

Table II-4.- Concluded.

SRIFI	sine of the angle between the rack longitudinal axis and the fuselage longitudinal axis in incompressible space; measured in x'_B, z_B plane
UT(N)	U_S^* at the N^{th} point along body, equation (40)
VAR(N), N = 1, 2, ..., 12	$\dot{\xi}, \dot{\eta}, \dot{\zeta}, p, q, r, \xi, \eta, \zeta, \psi, \theta, \phi$ respectively
VC	V_C^* , equation (55)
VETA	η component of the store free-stream velocity vector, equation (32)
VINF	V_∞ ; input, item 3
VRATIO	$V_\infty/V_{\infty S}$
VSTORE	$V_{\infty S}$, equation (41)
VT(N)	V_S^* at the N^{th} point along body, equation (40)
VX	$U_{\infty S, x_S}$ equation (35)
VXI	ξ component of the store free-stream velocity vector, equation (32)
VY	$-V_{\infty S, y_S}$ equation (35)
VZ	$W_{\infty S, z_S}$ equation (35)
VZETA	ζ component of the store free-stream velocity vector, equation (32)
WIIR	wing incidence angle in incompressible space, radians
WT(N)	W_S^* at the N^{th} point along body, equation (40)
XB	x'_B coordinate of a point along store body axis
XI	ξ coordinate of a point on store axis measured relative to store moment center
XMOM	$x_{S, m}$; input, item 33
XSTOR	x_S coordinate of point on store axis
XXX	x coordinate of point on store axis
YB	y_B coordinate of a point along store body axis
ZB	z_B coordinate of a point along store body axis
ZETA	ζ coordinate of a point on store axis measured relative to store moment center

TABLE II-5

DICTIONARY OF NOTATION IN SUBROUTINE OUTPUT

The following list presents most of the variable names used in subroutine OUTPUT. Where possible a variable name is identified by a symbol in the list of symbols or an equation number in reference 1. The x_B, y_B, z_B coordinate system is shown in figure 13 of this report.

<u>PROGRAM NOTATION</u>	<u>ALGEBRAIC NOTATION</u>
CLLEM	$(C_\ell)_E$, equations (62) and (I-30) or equations (63) and (I-52)
CLLT	total C_ℓ
CLMBY	$(C_m)_{BY}$, equation (44)
CLMCF	$(C_m)_{CF}$, equation (53)
CLMEM	$(C_m)_E$, equation (60)
CLMSB	$(C_m)_{SB}$, equation (48)
CLMT	total C_m
CLNBY	$(C_n)_{BY}$, equation (45)
CLNCF	$(C_n)_{CF}$, equation (54)
CLNEM	$(C_n)_E$, equation (61)
CLNSB	$(C_n)_{SB}$, equation (49)
CLNT	total C_n
CNBY	$(C_N)_{BY}$, equation (42)
CNCF	$(C_N)_{CF}$, equation (51)
CNEM	$(C_N)_E$, equation (58)
CNSB	$(C_N)_{SB}$, equation (46)
CNT	total C_N
CNX(K)	total dC_N/dx_s at the midpoint of the K^{th} body segment
CYBY	$(C_Y)_{BY}$, equation (43)

Table II-5.- Continued.

CYCF	$(C_Y)_{CF}$, equation (52)
CYEM	$(C_Y)_E$, equation (59)
CYSB	$(C_Y)_{SB}$, equation (47)
CYT	total C_Y
CYX(K)	total dC_Y/dx_s at the midpoint of the K^{th} body segment
DC(I,J)	$[A]$, equation (28)
DVAR(N), N = 1,2,...12	$\ddot{\xi}, \ddot{\eta}, \ddot{\zeta}, \dot{p}, \dot{q}, \dot{r}, \dot{\xi}, \dot{\eta}, \dot{\zeta}, \dot{\psi}, \dot{\theta}, \dot{\phi}$ respectively
DXB	ξ coordinate of the store base at time t relative to where it would have been had it remained in the $t = 0$ position on the aircraft
DXCG	ξ coordinate of the store moment center at time t relative to where it would have been had it remained in the $t = 0$ position on the aircraft
DXN	ξ coordinate of the store nose at time t relative to where it would have been had it remained in the $t = 0$ position on the aircraft
DYB	η coordinate of the store base at time t relative to where it would have been had it remained in the $t = 0$ position on the aircraft
DYCG	η coordinate of the store moment center at time t relative to where it would have been had it remained in the $t = 0$ position on the aircraft
DYN	η coordinate of the store nose at time t relative to where it would have been had it remained in the $t = 0$ position on the aircraft
DZB	ζ coordinate of the store base at time t relative to where it would have been had it remained in the $t = 0$ position on the aircraft
DZCG	ζ coordinate of the store moment center at time t relative to where it would have been had it remained in the $t = 0$ position on the aircraft
DZN	ζ coordinate of the store nose at time t relative to where it would have been had it remained in the $t = 0$ position on the aircraft
ESTLGC	ℓ_s of separated store

Table II-5.- Continued.

ETA	η coordinate of point on store axis measured relative to store moment center
EXST(J)	x_s at the J^{th} point along store axis
PHI	Φ , degrees
PSI	Ψ , degrees
SLTHC(NEJSTR)	l_s of separated store
THA	θ , degrees
TIME	t
UT(J)	U_s^* at J^{th} point along store axis
VAR(N), N = 1,2,...12	$\dot{\xi}, \dot{\eta}, \dot{\zeta}, p, q, r, \xi, \eta, \zeta, \Psi, \theta, \Phi$ respectively
VT(J)	V_s^* at J^{th} point along store axis
WT(J)	W_s^* at J^{th} point along store axis
XBASE	ξ coordinate of separated store base at time t
XBASEI	ξ coordinate of separated store base at $t = 0$
XCGI	ξ coordinate of separated store moment center at $t = 0$
XI	ξ coordinate of point on store axis measured relative to store moment center
XL	x_s/l_s
XMOM	$x_{s,m}$
XNOSE	ξ coordinate of separated store nose at time t
XNOSEI	ξ coordinate of separated store nose at $t = 0$
XXX	x coordinate of point on store axis
YBASE	η coordinate of separated store base at time t
YBASEI	η coordinate of separated store base at $t = 0$
YCGI	η coordinate of separated store moment center at $t = 0$
YNOSE	η coordinate of separated store nose at time t
YNOSEI	η coordinate of separated store nose at $t = 0$

Table II-5.- Concluded.

ZBASE	ζ coordinate of separated store base at time t
ZBASEI	ζ coordinate of separated store base at $t = 0$
ZCGI	ζ coordinate of separated store moment center at $t = 0$
ZETA	ζ coordinate of point on store axis measured relative to store moment center
ZNOSE	ζ coordinate of separated store nose at time t
ZNOSEI	ζ coordinate of separated store nose at $t = 0$

TABLE II-6

DICTIONARY OF NOTATION IN SUBROUTINE PTHIN

The following list presents most of the variable names used in subroutine PTHIN. Where possible a variable name is identified by a symbol in the list of symbols or an equation number in reference 1. Symbols in figure 6 of that reference are also used. Where a variable is an input quantity, it is so identified and section 4.2.1 of this report should be referred to for the definition.

<u>PROGRAM NOTATION</u>	<u>ALGEBRAIC NOTATION</u>
BETA	β
CRP	length of pylon root chord; input, item 17
CRPI	length of pylon root chord in incompressible space; CRP/BETA
DELTPX(I)	ΔX_i ; equals $X_a - X_b$ of figure 6 of reference 1
FACTOP(I)	$\theta_p \Delta X_i \cos \psi_i / 2\pi$ of i^{th} pylon thickness source strip
KMAX	MSP + 1
MPS	number of pylon thickness source strips; MPS = NCPS*MSP
MSP	input, item 18
NCPS	input, item 20
NUNIP	input, item 20
SWPPCS(I)	$\tan \psi_i$
SWPPLI	tangent of pylon leading-edge sweep angle in incompressible space
SWPPTI	tangent of pylon trailing-edge sweep angle in incompressible space
THETPL(I)	θ_p of the i^{th} pylon thickness source strip
TWOPI	2π
XP	x' coordinate of pylon root-chord leading edge measured relative to wing root-chord leading edge

Table II-6.- Concluded.

XPRC(I)	x_{Pc} of i^{th} pylon thickness source strip; see figure 6 of reference 1
Z(K)	input, item 19

TABLE II-7

DICTIONARY OF NOTATION IN SUBROUTINE PVLIN

The following list presents most of the variable names used in subroutine PVLIN. Where possible a variable name is identified by a symbol in the list of symbols or an equation number in reference 1. Symbols in figure 2 of that reference are also used. Where a variable is an input quantity, it is so identified and section 4.2.1 of this report should be referred to for the definition.

<u>PROGRAM NOTATION</u>	<u>ALGEBRAIC NOTATION</u>
BETA	β
CRP	length of pylon root chord; input, item 17
CRPI	length of pylon root chord in incompressible space
DTR	degrees to radians conversion factor, $1/57.29578$
H	pylon height; input, item 17
IP	input, item 17
KMAX	$MSP + 1$
M	number of vortices on wing
MMP	$M + MP$
MP	number of vortices on pylon
MP1	$M + 1$
MSP	input, item 18
NCP	input, item 18
PCPX(I)	X coordinate of the control point associated with the i^{th} vortex on the pylon
PHIP	angle between the pylon and wing planform planes, $-\pi/2$
PSIPLE	sweep angle of pylon leading edge; input, item 17
PSIPTE	sweep angle of pylon trailing edge; input, item 17

Table II-7.- Concluded.

PVPX(I)	X coordinate of the bound-leg midpoint of the i^{th} pylon vortex
PVPY(I)	Y coordinate of the bound-leg midpoint of the i^{th} pylon vortex
PVPZ(I)	Z coordinate of the bound-leg midpoint of the i^{th} pylon vortex
SP(I)	semispan, s , of the i^{th} pylon vortex
SWPCR(I)	tangent of the sweep angle of the 3/4-chord line of the area element associated with the i^{th} pylon vortex
SWPPLE	$\tan(\text{PSIPLE})$
SWPPLI	$\tan(\text{PSIPLE})$ in incompressible space
SWPPTE	$\tan(\text{PSIPTE})$
SWPPTI	$\tan(\text{PSIPTE})$ in incompressible space
SWPVP(I)	$\tan \psi$ of the i^{th} pylon vortex
XLEL(IP)	X coordinate of the wing leading edge at the pylon location
XP	X coordinate of the pylon root-chord leading edge
XPLE	location of pylon root-chord leading edge relative to local wing-chord leading edge; input, item 17
XPLEI	location of pylon root-chord leading edge relative to local wing-chord leading edge in incompressible space
Y(IP)	Y location of pylon
YP	Y(IP)
Z(K)	input, item 19
ZLEL(IP)	Z coordinate of wing leading edge at pylon location
ZP	ZLEL(IP)

TABLE II-8

DICTIONARY OF NOTATION IN SUBROUTINE STRIO

The following list presents most of the variable names used in subroutine STRIO. Where possible a variable name is identified by a symbol in the list of symbols in reference 1. Where a variable is an input quantity, it is so identified and section 4.2.1 of this report should be referred to for the definition.

<u>PROGRAM NOTATION</u>	<u>ALGEBRAIC NOTATION</u>
BETA	β
DUMQ(J)	input, item 30
DUMX(J)	input, item 29
MSHAPE	input, item 28
MSOR	input, item 28
NSHAPE(J)	input, item 26
NSHPT	input, item 27
NSSOR(K)	number of sources in the source distribution representing the volume of the k^{th} store
NSTRS	input, item 4
NUMSTR(J)	input, item 26
RAD	radians to degrees conversion factor, 57.29578
SIC(J)	input, item 26
SII(J)	value of SIC(J) in incompressible space
SLTHC(J)	input, item 26
SLTHI(J)	value of SLTHC(J) in incompressible space
SRMAX(J)	input, item 26
SSOR(K,J)	array containing the k values of $Q_k/4\pi V_\infty$ for the j^{th} store

Table II-8.- Concluded.

SXL(K,J)	array containing the k values of x' at which the sources are located for the j th store; negative and measured from the tip of the nose
XLEL(I)	X coordinate of wing leading edge at Y = Y(I)
XSNC(J)	input, item 26
XSNI(J)	value of XSNC(J) in incompressible space
XWSOI(J)	X coordinate of tip of nose of j th store
Y(I)	input, item 12
YWSO(J)	Y coordinate of tip of nose of j th store, input
YSN(J)	input, item 26
ZLEL(I)	Z coordinate of wing leading edge at Y = Y(I)
ZSN(J)	input, item 26
ZWSO(J)	Z coordinate of tip of nose of j th store

TABLE II-9

DICTIONARY OF NOTATION IN SUBROUTINE THPVEL

The following list presents most of the variable names used in subroutine THPVEL. Where possible a variable name is identified by a symbol in the list of symbols or an equation number in reference 1. Symbols in figure 6 of that reference are also used. Where a variable is an input quantity, it is so identified and section 4.2.1 of this report should be referred to for the definition.

<u>PROGRAM NOTATION</u>	<u>ALBEGRAIC NOTATION</u>
COSSPS(I)	$\cos \psi_i$
COSSWP	$\cos \psi_i$
DZ	$Z - Z_a$
DZB	$Z - Z_b$
E	E, equation (26)
F	F, equation (26)
FACTOP(I)	$\theta_p \Delta X_i \cos \psi_i / 2\pi$
G	G, equation (26)
GD	FACTOP(I)
H	H, equation (26)
JPS	i
KMAX	MSP + 1
MSP	input, item 18
NCPS	input, item 20
SINSPS(I)	$\sin \psi_i$
SINSWP	$\sin \psi_i$
SWPPCS(I)	$\tan \psi_i$

Table II-9.- Concluded.

U	$\sum_i \left(\frac{\Delta u}{V_\infty} \right)_i$, equation (25)
UP	total wing-pylon u/V_∞ perturbation velocity at point X,Y,Z
V	$\sum_i \left(\frac{\Delta v}{V_\infty} \right)_i$, equation (25)
VP	total wing-pylon v/V_∞ perturbation velocity at point X,Y,Z
W	$\sum_i \left(\frac{\Delta w}{V_\infty} \right)_i$, equation (25)
WP	total wing-pylon w/V_∞ perturbation velocity at point X,Y,Z
XC	X coordinate of field point
XPRC(I)	x_{pc} of i^{th} pylon thickness source strip
Y(IP)	y_p location of pylon
YC	Y coordinate of field point
Z(K)	input, item 19
ZC	Z coordinate of field point
ZLEL(IP)	Z coordinate of wing leading edge at pylon location

TABLE II-10

DICTIONARY OF NOTATION IN SUBROUTINE THWVEL

The following list presents most of the variable names used in subroutine THWVEL. Where possible a variable name is identified by a symbol in the list of symbols or an equation number in reference 1. Symbols in figure 5 of that reference are also used. Where a variable is an input quantity, it is so identified and section 4.2.1 of this report should be referred to for the definition.

<u>PROGRAM NOTATION</u>	<u>ALGEBRAIC NOTATION</u>
A	A, equation (20)
B	B, equation (20)
C	C, equation (20)
COSSWP	$\cos \psi_i$
COSSWS(I)	$\cos \psi_i$
D	D, equation (20)
F	± 1
FACTOR(I)	$\theta \Delta X_i \cos \psi_i / 2\pi$
IMAX	$MSW + 1$
MSW	input, item 11
NCWS	input, item 15
SINSWP	$\sin \psi_i$
SINSWS(I)	$\sin \psi_i$
SWPCS(I)	$\tan \psi_i$
U	$\sum_i \left(\frac{\Delta u}{V_\infty} \right)_i$, equation (19)
UW	u/V_∞ perturbation velocity due to wing-pylon vortex lattice and wing thickness

Table II-10.- Concluded.

V	$\sum_i \left(\frac{\Delta v}{V_\infty} \right)_i$, equation (19)
VW	v/V_∞ perturbation velocity due to wing-pylon vortex lattice and wing thickness
W	$\sum_i \left(\frac{\Delta w}{V_\infty} \right)_i$, equation (19)
WW	w/V_∞ perturbation velocity due to wing-pylon vortex lattice and wing thickness
XC	X coordinate of field point
XRC(I)	x_c of i^{th} wing thickness source strip
Y(I)	input, item 12
YC	Y coordinate of field point
ZC	Z coordinate of field point
Z1(I)	Z coordinate of i^{th} wing thickness source strip

TABLE II-11

DICTIONARY OF NOTATION IN SUBROUTINE VELFLD

The following list presents most of the variable names used in subroutine VELFLD. Where possible a variable name is identified by a symbol in the list of symbols or an equation number in reference 1. Where a variable is an input quantity, it is so identified and section 4.2.1 of this report should be referred to for the definition. Primes associated with the algebraic notation indicate incompressible space (see section 3 of ref. 1). The x_B, y_B, z_B coordinate system is shown in figure 13 of this report.

<u>PROGRAM NOTATION</u>	<u>ALGEBRAIC NOTATION</u>
ALFACR	α_f , radians
BETA	β
BETASQ	β^2
CRIFI	cosine of the angle between the rack longitudinal axis and the fuselage longitudinal axis in incompressible space, measured in x'_B, z_B plane
CSIBIR(J)	cosine of the angle between the longitudinal axis of the j^{th} store and the fuselage longitudinal axis in incompressible space, measured in x'_B, z_B plane
CWIIR	cosine of the angle between the wing root chord and the fuselage longitudinal axis in incompressible space, measured in x'_B, z_B plane
DC(I,J)	[A], equation (28)
FRMAX	fuselage maximum radius; input, item 5
FSOR(N)	array containing the strengths of the fuselage source distribution
FXL(N)	array containing the x'_B positions of the fuselage sources
IP	pylon location specification; input, item 17
NCON	control index used in subroutine VLIVEL
NEJSTR	subscript associated with separated store, $1 \leq \text{NEJSTR} \leq \text{NSTRS}$

Table II-11.- Continued.

NFSOR	number of fuselage sources; input, item 6
NFU	input, item 4
NPY	input, item 4
NRACK	input, item 4
NRSOR	number of rack sources; input, item 23
NSSOR(J)	number of sources in the source distribution representing the volume of the J^{th} store
NSTRS	input, item 4
RRMAX	rack maximum radius; input, item 22
RSOR(N)	array containing the strengths of the rack source distribution
RXL(N)	array containing the axial locations of the rack sources
SALF	$\sin \alpha_f'$
SRIFI	sine of the angle between the rack longitudinal axis and the fuselage longitudinal axis in incompressible space, measured in x_B', z_B plane
SRMAX(J)	maximum radius of J^{th} store
SSIBIR(J)	sine of the angle between the longitudinal axis of the J^{th} store and the fuselage longitudinal axis in incompressible space, measured in x_B', z_B plane
SSOR(K,J)	array containing the K values of the source strengths of the source distribution for the J^{th} store
SWIIR	sine of the angle between the wing root chord and the fuselage longitudinal axis in incompressible space, measured in x_B', z_B plane
SXL(K,J)	array containing the K axial locations of the sources for the J^{th} store
UF	u/V_∞ perturbation velocity due to a component of the parent aircraft
UTU	during calculation, sum of u/V_∞ perturbation velocities due to parent aircraft in incompressible fuselage coordinate system; upon return to calling program, sum of u/V_∞ perturbation velocities in compressible space in separated store x,y,z coordinate system

Table II-11.- Continued.

VF	v/V_∞ perturbation velocity due to a component of the parent aircraft
VTV	during calculation, sum of v/V_∞ perturbation velocities due to parent aircraft in incompressible fuselage coordinate system; upon return to calling program, sum of v/V_∞ perturbation velocities in compressible space in separated store, x,y,z coordinate system
WF	w/V_∞ perturbation velocity due to a component of the parent aircraft
WTW	during calculation, sum of w/V_∞ perturbation velocities due to parent aircraft in incompressible fuselage coordinate system; upon return to calling program, sum of w/V_∞ perturbation velocities in compressible space in separated store, x,y,z coordinate system
XB	x'_B coordinate of point where velocity field is to be calculated
XBROI	x'_B coordinate of tip of rack nose
XBSOI(J)	x'_B coordinate of tip of nose of J^{th} store
XBWOI	x'_B coordinate of wing root-chord leading edge
XR	x' coordinate of point where velocity field is to be calculated measured in rack coordinate system
XS	x' coordinate of point where velocity field is to be calculated measured in J^{th} store coordinate system
XW	x' coordinate of point where velocity field is to be calculated measured in wing coordinate system
YB	y'_B coordinate of point where velocity field is to be calculated
YBRO	y'_B coordinate of rack
YBSO(J)	y'_B coordinate of J^{th} store
YR	y coordinate of point where velocity field is to be calculated measured in rack coordinate system
YS	y coordinate of point where velocity field is to be calculated measured in J^{th} store coordinate system
YW	y coordinate of point where velocity field is to be calculated measured in wing coordinate system

Table II-11.- Concluded.

ZB	z_B coordinate of point where velocity field is to be calculated
ZBRO	z_B coordinate of tip of rack nose
ZBSO(J)	z_B coordinate of tip of nose of J^{th} store
ZBWO	z_B coordinate of wing root-chord leading edge
ZR	z coordinate of point where velocity field is to be calculated measured in rack coordinate system
ZS	z coordinate of point where velocity field is to be calculated measured in J^{th} store coordinate system
ZW	z coordinate of point where velocity field is to be calculated measured in wing coordinate system

TABLE II-12

DICTIONARY OF NOTATION IN SUBROUTINE VLCOEF

The following list presents most of the variable names used in subroutine VLCOEF. Where possible a variable name is identified by a symbol in the list of symbols or in section 4.2.2 of reference 1. Symbols in figure 2 of that reference are also used. Where a variable is an input quantity, it is so identified and section 4.2.1 of this report should be referred to for the definition. Certain of the variable names appearing in the following list are marked with an asterisk, *. These variables are dimensioned for two (2) in the subroutine. The subscript one (1) pertains to the left wing panel or pylon while the subscript two (2) pertains to the image vortex on the right wing panel or pylon.

<u>PROGRAM NOTATION</u>	<u>ALGEBRAIC NOTATION</u>
COSPHI(JC)	$\cos \phi_v$, equation (6)
FUP*	$F_{u_n^{th}}$ at the v^{th} wing or pylon control point due to the pylon vortex
FUW*	$F_{u_n^{th}}$ at the v^{th} wing or pylon control point due to the wing vortex
FVN(JC,JV)	coefficient in equation (6) or (7) of $\Gamma_n/4\pi V_\infty$ in the v^{th} equation; JC = v, JV = n
FVP*	$F_{v_n^{th}}$ at the v^{th} wing or pylon control point due to the pylon vortex
FVW*	$F_{v_n^{th}}$ at the v^{th} wing or pylon control point due to the wing vortex
FWP*	$F_{w_n^{th}}$ at the v^{th} wing or pylon control point due to the pylon vortex
FWW*	$F_{w_n^{th}}$ at the v^{th} wing or pylon control point due to the wing vortex
IP	pylon location specification; input, item 17 (IP = 1 under fuselage centerline)
JC	control point index v in equation (6) or (7)
JCP	index of the i^{th} pylon control point, JCP = 1,2,... MP

Table II-12.- Continued.

JV	vortex index n in equation (6) or (7)
JVP	index of the i^{th} pylon vortex, $JVP = 1, 2, \dots, MP$
M	number of vortices on wing
MMP	$M + MP$
MP	number of vortices on pylon
MP1	$M + 1$
NPY	input, item 4; $NPY = 0$, no pylon
PCPX(I)	X coordinate of the control point associated with the i^{th} vortex on the pylon
PCX(I)	X coordinate of the control point associated with the i^{th} vortex on the wing
PHI(I)	dihedral angle, ϕ_i , associated with the i^{th} vortex on the wing
PHIP	angle between the pylon and wing planform planes, $-\pi/2$
PVPX(I)	X coordinate of the bound-leg midpoint of the i^{th} pylon vortex
PVPY(I)	Y coordinate of the bound-leg midpoint of the i^{th} pylon vortex
PVPZ(I)	Z coordinate of the bound-leg midpoint of the i^{th} pylon vortex
PVX(I)	X coordinate of the bound-leg midpoint of the i^{th} wing vortex
PVY(I)	Y coordinate of the bound-leg midpoint of the i^{th} wing vortex
PVZ(I)	Z coordinate of the bound-leg midpoint of the i^{th} wing vortex
SINPHI(JC)	$\sin \phi_v$, equation (6)
SP(I)	semispan, s , of the i^{th} pylon vortex
SW(I)	semispan, s , of the i^{th} wing vortex
SWPVP(I)	$\tan \psi$ of the i^{th} pylon vortex
SWPVV(I)	$\tan \psi$ of the i^{th} wing vortex

Table II-12.- Concluded.

XPP	x location of the v^{th} pylon control point relative to the n^{th} pylon vortex
XPW	x location of the v^{th} pylon control point relative to the n^{th} wing vortex
XWP	x location of the v^{th} wing control point relative to the n^{th} pylon vortex
XWW	x location of the v^{th} wing control point relative to the n^{th} wing vortex
YPP*	y location of the v^{th} pylon control point relative to the n^{th} pylon vortex
YPW*	y location of the v^{th} pylon control point relative to the n^{th} wing vortex
YWP*	y location of the v^{th} wing control point relative to the n^{th} pylon vortex
YWW*	y location of the v^{th} wing control point relative to the n^{th} wing vortex
ZPP	z location of the v^{th} pylon control point relative to the n^{th} pylon vortex
ZPW	z location of the v^{th} pylon control point relative to the n^{th} wing vortex
ZWP	z location of the v^{th} wing control point relative to the n^{th} pylon vortex
ZWW	z location of the v^{th} wing control point relative to the n^{th} wing vortex

TABLE II-13

DICTIONARY OF NOTATION IN SUBROUTINE VLIVEL

The following list presents most of the variable names used in subroutine VLIVEL. Where possible a variable name is identified by a symbol in the list of symbols or in section 4.2.2 of reference 1. Symbols in figure 2 of that reference are also used. Where a variable is an input quantity, it is so identified and section 4.2.1 of this report should be referred to for the definition. Certain of the variable names appearing in the following list are marked with an asterisk, *. These variables are dimensioned for two (2) in the subroutine. The subscript one (1) pertains to the left wing panel or pylon while the subscript two (2) pertains to the image vortex on the right wing panel or pylon.

<u>PROGRAM NOTATION</u>	<u>ALGEBRAIC NOTATION</u>
CIR(JV)	Γ_n/V_∞ of the n^{th} wing or pylon vortex; $JV = n$
FUP*	F_u at the field point due to the n^{th} pylon vortex
FUW*	F_u at the field point due to the n^{th} wing vortex
FVP*	F_v at the field point due to the n^{th} pylon vortex
FVW*	F_v at the field point due to the n^{th} wing vortex
FWP*	F_w at the field point due to the n^{th} pylon vortex
FWW*	F_w at the field point due to the n^{th} wing vortex
JV	vortex index n in equation (6) or (7)
JVP	index of the i^{th} pylon vortex, $JVP = 1, 2, \dots, MP$
M	number of vortices on wing
MMP	$M + MP$
MP	number of vortices on pylon
MP1	$M + 1$
NCON	control index set in subroutine VELFLD; if $NCON = 2$ only pylon thickness velocities are to be calculated
NCP	input, item 18

Table II-13.- Continued.

PHI(I)	dihedral angle, ϕ_i , associated with the i^{th} vortex on the wing
PHIP	angle between the pylon and wing planform planes, $-\pi/2$
PMX	X coordinate of field point
PMY	Y coordinate of field point
PMZ	Z coordinate of field point
PVPX(I)	X coordinate of the bound-leg midpoint of the i^{th} pylon vortex
PVPY(I)	Y coordinate of the bound-leg midpoint of the i^{th} pylon vortex
PVPZ(I)	Z coordinate of the bound-leg midpoint of the i^{th} pylon vortex
PVX(I)	X coordinate of the bound-leg midpoint of the i^{th} wing vortex
PVY(I)	Y coordinate of the bound-leg midpoint of the i^{th} wing vortex
PVZ(I)	Z coordinate of the bound-leg midpoint of the i^{th} wing vortex
SP(I)	semispan, s , of the i^{th} pylon vortex
SW(I)	semispan, s , of the i^{th} wing vortex
SWPVP(I)	$\tan \psi$ of the i^{th} pylon vortex
SWPVV(I)	$\tan \psi$ of the i^{th} wing vortex
UI	u/V_∞ perturbation velocity at field point in incompressible space
VI	v/V_∞ perturbation velocity at field point in incompressible space
WI	w/V_∞ perturbation velocity at field point in incompressible space
XPM	x location of field point relative to the i^{th} pylon vortex
XWM	x location of field point relative to the i^{th} wing vortex

Table II-13.- Concluded.

YPM*	y location of field point relative to the i^{th} pylon vortex
YWM*	y location of field point relative to the i^{th} wing vortex
ZPM	z location of field point relative to the i^{th} pylon vortex
ZWM	z location of field point relative to the i^{th} wing vortex

TABLE II-14

DICTIONARY OF NOTATION IN SUBROUTINE VLRHS

The following list presents most of the variable names used in subroutine VLRHS. Where possible a variable name is identified by a symbol in the list of symbols or an equation number in reference 1. Where a variable is an input quantity, it is so identified and section 4.2.1 of this report should be referred to for the definition. Primes associated with the algebraic notation indicate incompressible space (see section 3 of ref. 1). The x_B, y_B, z_B fuselage coordinate system is shown in figure 13 of this report. Each of the other axisymmetric bodies has a coordinate system associated with it as is shown in figure 1 of reference 1. The X, Y, Z wing-pylon coordinate system is shown in figure 2 of that reference.

<u>PROGRAM NOTATION</u>	<u>ALGEBRAIC NOTATION</u>
ALFAIR	α'_f , radians
ALPHLI(N)	α_ℓ in incompressible space; $\tan \alpha_\ell$ in compressible space was input as item 14
CIR(N)	array containing the right-hand sides of equations (6) and (7) of reference 1
COSPHI(I)	$\cos \phi_i$ of the i^{th} wing vortex
CRIIR	cosine of the rack incidence angle in incompressible space; compressible incidence angle was input in item 22
CSIIR(N)	cosine of the N^{th} store incidence angle in incompressible space; compressible incidence angle was input in item 26
CWIIR	cosine of the wing incidence angle in incompressible space; compressible incidence angle was input in item 9
IP	pylon location specification; input, item 17
M	number of vortices on wing
MMP	$M + MP$
MP	number of vortices on pylon

Table II-14.- Continued.

MP1	$M + 1$
NFU	input, item 4
NPY	input, item 4
NRACK	input, item 4
NSTRS	input, item 4
PCPX(J)	X coordinate of the control point associated with the j^{th} pylon vortex
PCX(J)	X coordinate of the control point associated with the j^{th} wing vortex
PVPY(J)	Y coordinate of the bound-leg midpoint and control point of the j^{th} pylon vortex
PVPZ(J)	Z coordinate of the bound-leg midpoint and control point of the j^{th} pylon vortex
PVY(J)	Y coordinate of the bound-leg midpoint and control point of the j^{th} wing vortex
PVZ(J)	Z coordinate of the bound-leg midpoint and control point of the j^{th} wing vortex
SINPHI(I)	$\sin \phi_i$ of the i^{th} wing vortex
SRIIR	sine of the rack incidence angle in incompressible space; compressible incidence angle was input in item 22
SSIIR(N)	sine of the N^{th} store incidence angle in incompressible space; compressible incidence angle was input in item 26
SWIIR	sine of the wing incidence angle in incompressible space; compressible incidence angle was input in item 9
UEI(NV)	u_i/V_∞ at the control point of the v^{th} vortex
UI	u'/V_∞ perturbation velocity at a vortex control point due to an aircraft component
VEI(NV)	v_i/V_∞ at the control point of the v^{th} vortex
VI	v'/V_∞ perturbation velocity at a vortex control point due to an aircraft component

Table II-14.- Continued.

WEI(NV)	w_1/V_∞ at the control point of the v^{th} vortex
WI	w'/V_∞ perturbation velocity at a vortex control point due to an aircraft component
WIIR	wing incidence angle in incompressible space; compressible value was input in item 9
XBP	x'_B coordinate of a pylon control point
XBW	x'_B coordinate of a wing control point
XBWOI	x'_B coordinate of wing root-chord leading edge
XRW	x' coordinate of a wing control point in the rack coordinate system
XSP	x' coordinate of a pylon control point in the N^{th} store coordinate system
XSW	x' coordinate of a wing control point in the N^{th} store coordinate system
XWROI	X coordinate of tip of rack nose
XWSOI(N)	X coordinate of tip of nose of N^{th} store
YBP	y_B coordinate of a pylon control point
YBW	y_B coordinate of a wing control point
YRW	y coordinate of a wing control point in the rack coordinate system
YSP	y coordinate of a pylon control point in the N^{th} store coordinate system
YSW	y coordinate of a wing control point in the N^{th} store coordinate system
YWRO	Y coordinate of tip of rack nose
YWSO(N)	Y coordinate of tip of nose of N^{th} store
ZBP	z_B coordinate of a pylon control point
ZBW	z_B coordinate of a wing control point
ZBWO	z_B coordinate of wing root-chord leading edge
ZRW	z coordinate of a wing control point in the rack coordinate system

Table II-14.- Concluded.

ZSP	z coordinate of a pylon control point in the N^{th} store coordinate system
ZSW	z coordinate of a wing control point in the N^{th} store coordinate system
ZWRO	Z coordinate of tip of rack nose
ZWSO(N)	Z coordinate of tip of nose of N^{th} store

TABLE II-15

DICTIONARY OF NOTATION IN SUBROUTINE WTHIN

The following list presents most of the variable names used in subroutine WTHIN. Where possible a variable name is identified by a symbol in the list of symbols or an equation number in reference 1. Symbols in figure 5 of that reference are also used. Where a variable is an input quantity, it is so identified and section 4.2.1 of this report should be referred to for the definition.

<u>PROGRAM NOTATION</u>	<u>ALGEBRAIC NOTATION</u>
BETA	β
CHLOCB(I)	local incompressible wing chord at the midspan of the (I - 1) th wing segment
CHLOCL(I)	local incompressible wing chord at the left or outboard side of the (I - 1) th wing segment
DELTX(I)	ΔX_i ; equals $X_a - X_b$ of figure 5 of reference 1
FACTOR(I)	$\theta \Delta X_i \cos \psi_i / 2\pi$ of the i th wing thickness source strip
IMAX	MSW + 1
MS	number of wing thickness source strips; MS = NCWS*MSW
MSW	input, item 11
NCWS	input, item 15
NUNIS	input, item 15
SWPCS(I)	$\tan \psi_i$ of the i th thickness source strip
SWPWLI(I)	tangent of the leading-edge sweep angle in incompressible space of the (I - 1) th wing segment
SWPWTI(I)	tangent of the trailing-edge sweep angle in incompressible space of the (I - 1) th wing segment
TANPHI(I)	$\tan \phi_i$ of the (I - 1) th wing segment
THETAL(I)	θ of the i th thickness source strip; input in item 16 and then transformed to incompressible space
TWOPI	2π

Table II-15.- Concluded.

XRC(I)	X _c of the i th thickness source strip; see figure 5 of reference 1
XLEL(I)	X coordinate of wing leading edge at Y = Y(I)
Y(I)	input, item 12
ZLEL(I)	Z coordinate of wing leading edge at Y = Y(I)
Zl(I)	Z coordinate of i th wing thickness source strip

TABLE II-16

DICTIONARY OF NOTATION IN SUBROUTINE WVLIN

The following list presents most of the variable names used in subroutine WVLIN. Where possible a variable name is identified by a symbol in the list of symbols or an equation number in reference 1. Symbols in figure 2 of that reference are also used. Where a variable is an input quantity, it is so identified and section 4.2.1 of this report should be referred to for the definition.

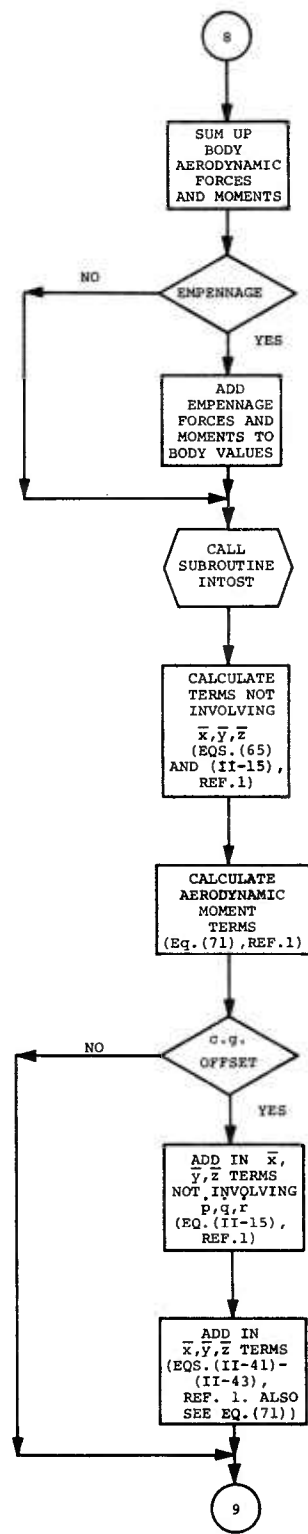
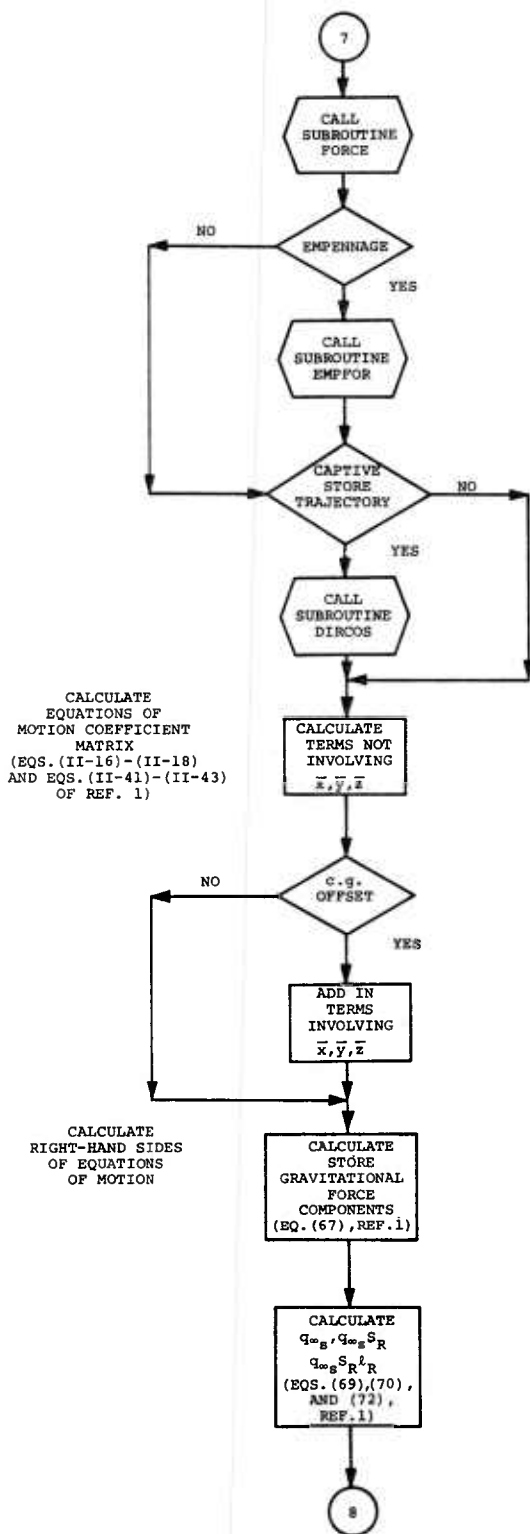
<u>PROGRAM NOTATION</u>	<u>ALGEBRAIC NOTATION</u>
ALPHAL(I)	$\tan \alpha_l$; input, item 14
ALPHLI(I)	$\tan \alpha_l$ in incompressible space
BETA	β
CAVE	average wing chord in incompressible space
CHLOCB(I)	local incompressible wing chord at the midspan of the (I - 1) th wing segment
CHLOCL(I)	local incompressible wing chord at the left or outboard side of the (I - 1) th wing segment
COSPHI(I)	$\cos \phi_i$ of the i th wing vortex
CRW	length of wing root chord; input, item 10
CRWI	length of wing root chord in incompressible space
DTR	degrees to radians conversion factor, 1/57.29578
IMAX	MSW + 1
M	number of vortices on wing; $M = NCW * MSW$
MSW	input, item 11
NCW	input, item 11
NTAC	input, item 13
NUNI	input, item 13

Table II-16.- Continued.

PCX(I)	X coordinate of the control point associated with the i^{th} vortex on the wing
PHI(I)	dihedral angle, ϕ_i , in radians associated with the i^{th} vortex on the wing
PHID(I)	input, item 12
PSIWLE(I)	input, item 12
PSIWTE(I)	input, item 12
PTLX(I)	X coordinate of the 3/4 chord of the left side of the area element associated with the i^{th} vortex on the wing
PTLY(I)	Y coordinate of the 3/4 chord of the left side of the area element associated with the i^{th} vortex on the wing
PTLZ(I)	Z coordinate of the 3/4 chord of the left side of the area element associated with the i^{th} vortex on the wing
PVX(I)	X coordinate of the bound-leg midpoint of the i^{th} wing vortex
PVY(I)	Y coordinate of the bound-leg midpoint of the i^{th} wing vortex
PVZ(I)	Z coordinate of the bound-leg midpoint of the i^{th} wing vortex
SINPHI(I)	$\sin \phi_i$ of the i^{th} wing vortex
SPAN	wing span
SREF	area of incompressible wing
SSPAN	semispan of wing; input, item 10
SUMY(I)	Y location of the midspan of the $(I - 1)^{\text{th}}$ wing segment
SW(I)	semispan, s , of the i^{th} wing vortex
SWPC(I)	tangent of the sweep angle of the 3/4 chord line of the area element associated with the i^{th} wing vortex measured in the planform plane
SWPV(I)	$\tan \psi_p$ of the i^{th} wing vortex

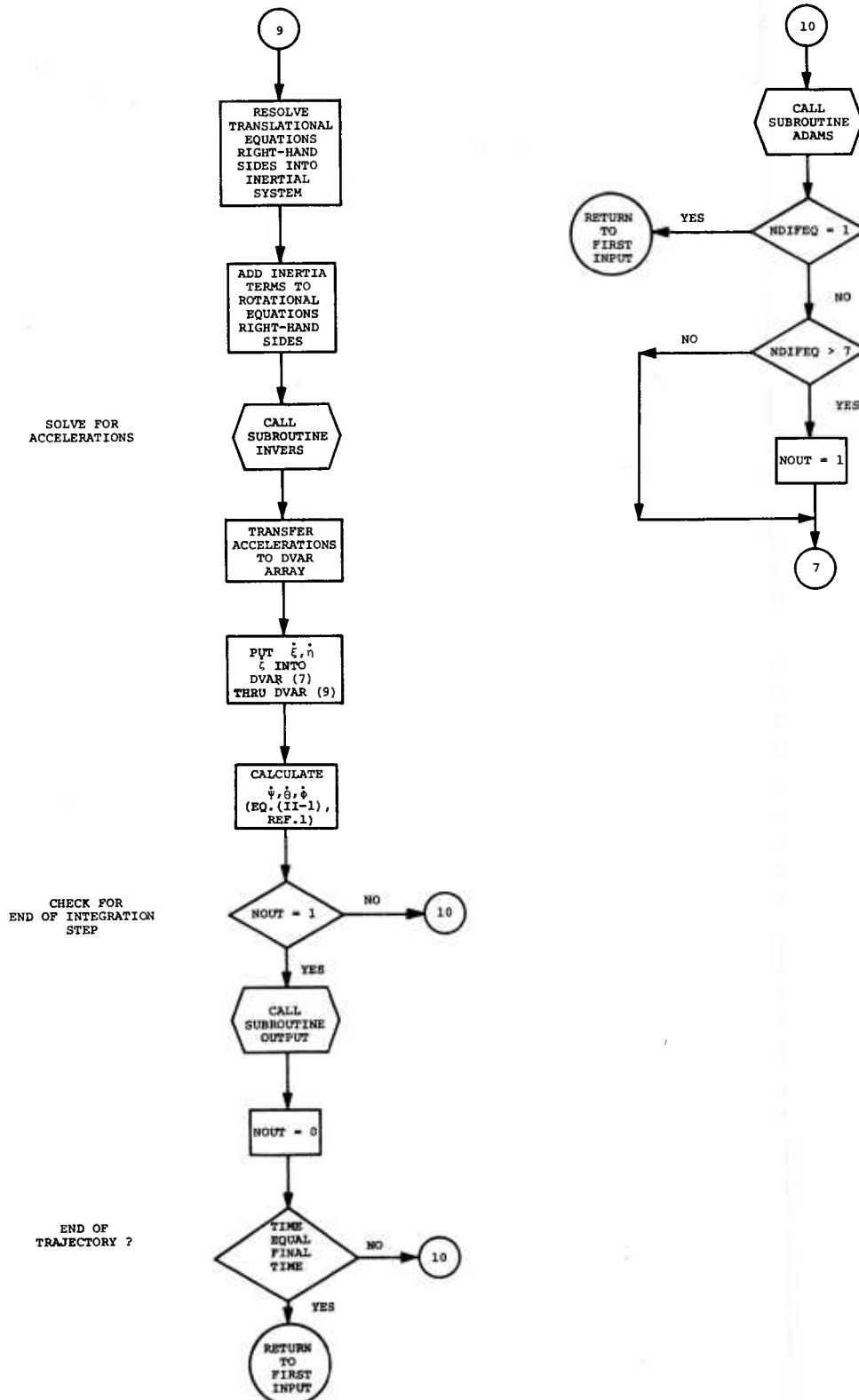
Table II-16.- Concluded.

SWPVV(I)	$\tan \psi$ of the i^{th} wing vortex
SWPWL(I)	tangent of the leading-edge sweep angle in incompressible space of the $(I - 1)^{\text{th}}$ wing segment
SWPWT(I)	tangent of the trailing-edge sweep angle in incompressible space of the $(I - 1)^{\text{th}}$ wing segment
TANPHI(I)	$\tan \phi_i$ of the $(I - 1)^{\text{th}}$ wing segment
XLEL(I)	X coordinate of wing leading edge at $Y = Y(I)$
Y(I)	input, item 12
YLOC(I)	SUMY(I)/SSPAN
ZLEL(I)	Z coordinate of wing leading edge at $Y = Y(I)$

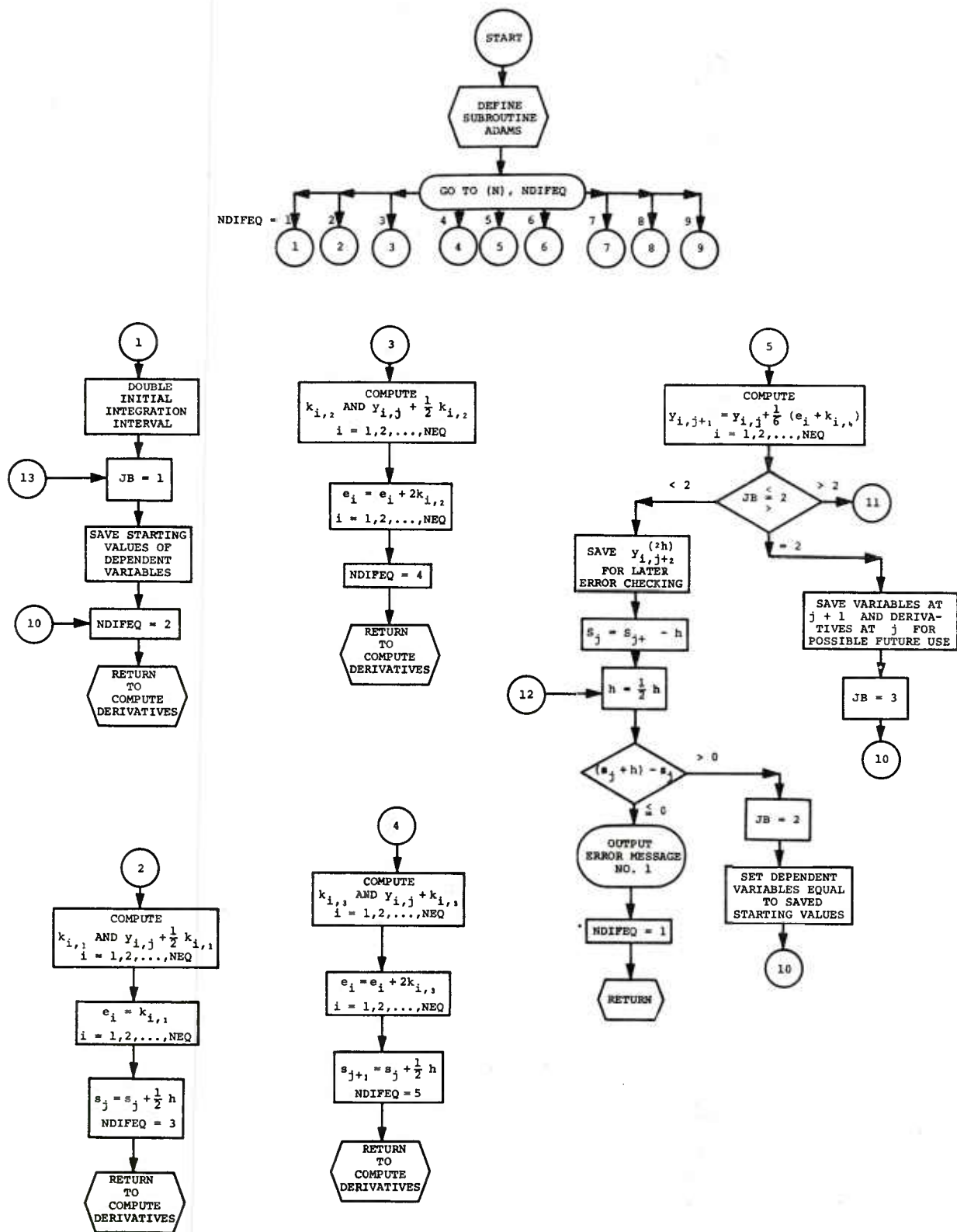


(a) Page 1.

Figure II-1.- Flow chart of integration loop of main program.

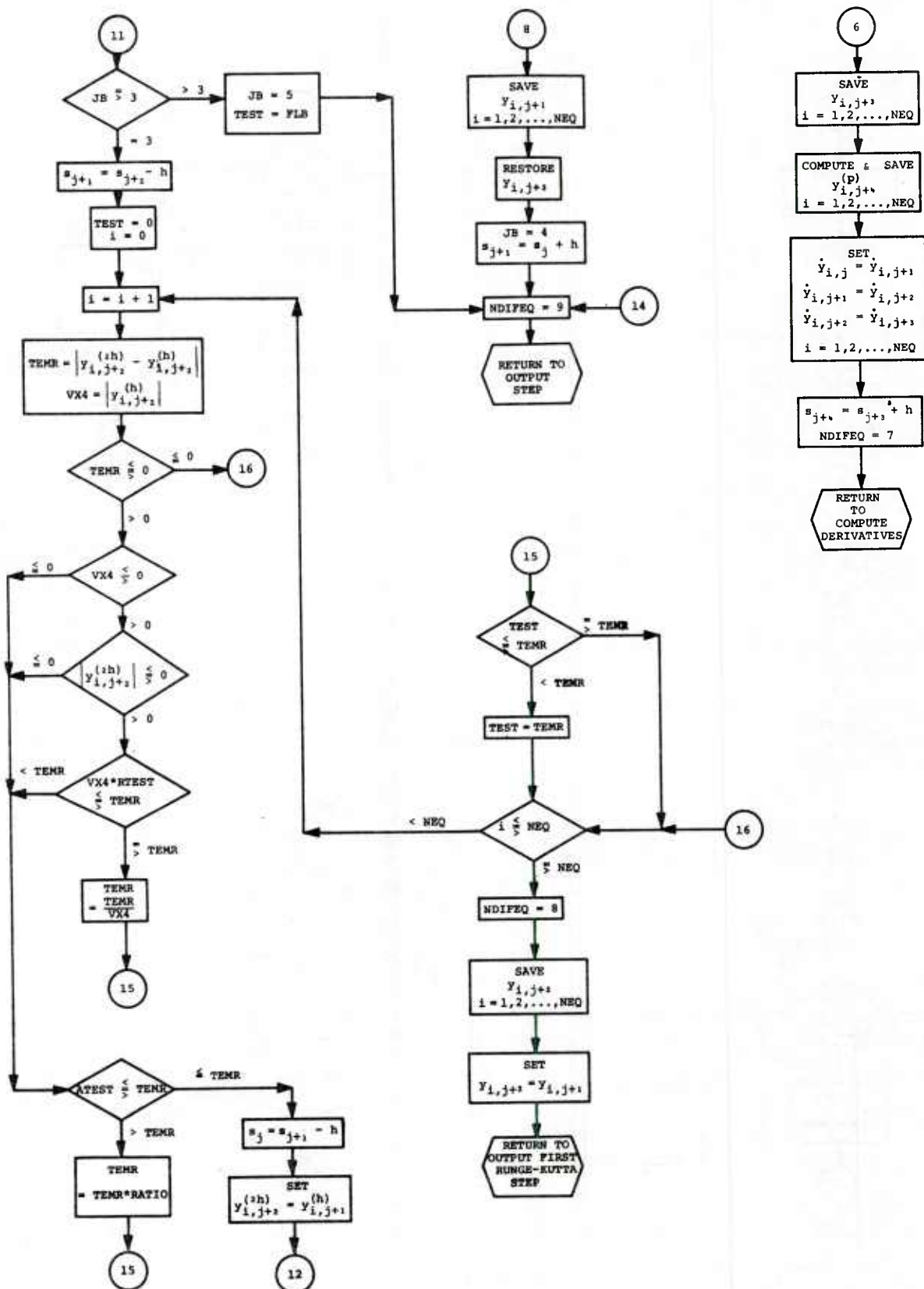


(b) Page 2.
Figure II-1.- Concluded.



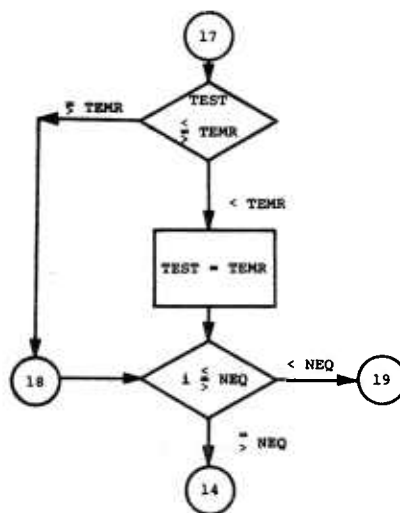
(a) Page 1.

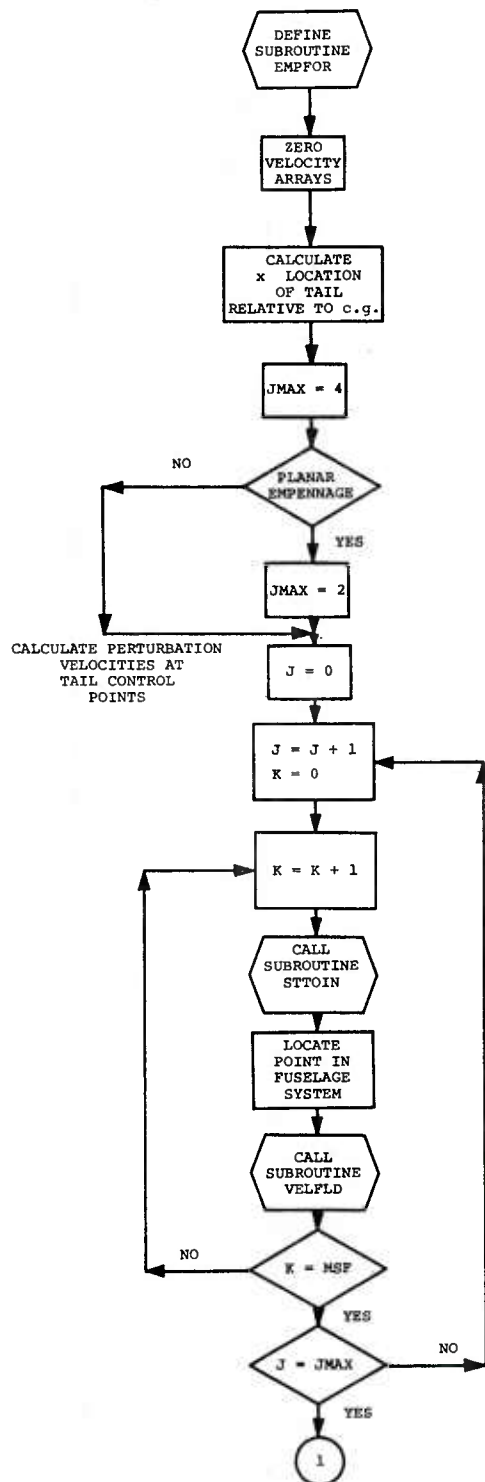
Figure II-2.- Flow chart of subroutine ADAMS.



(b) Page 2.

Figure II-2.- Continued.

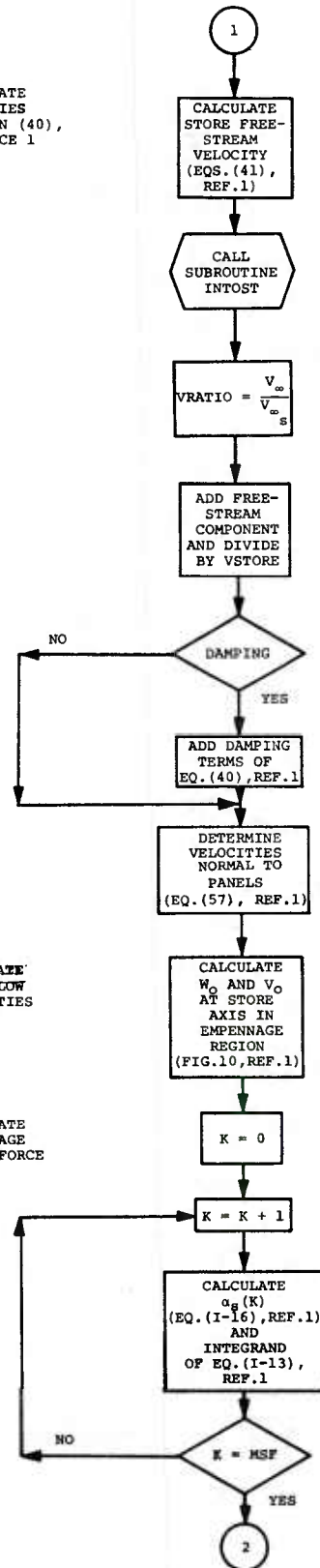




CALCULATE VELOCITIES OF EQUATION (40), REFERENCE 1

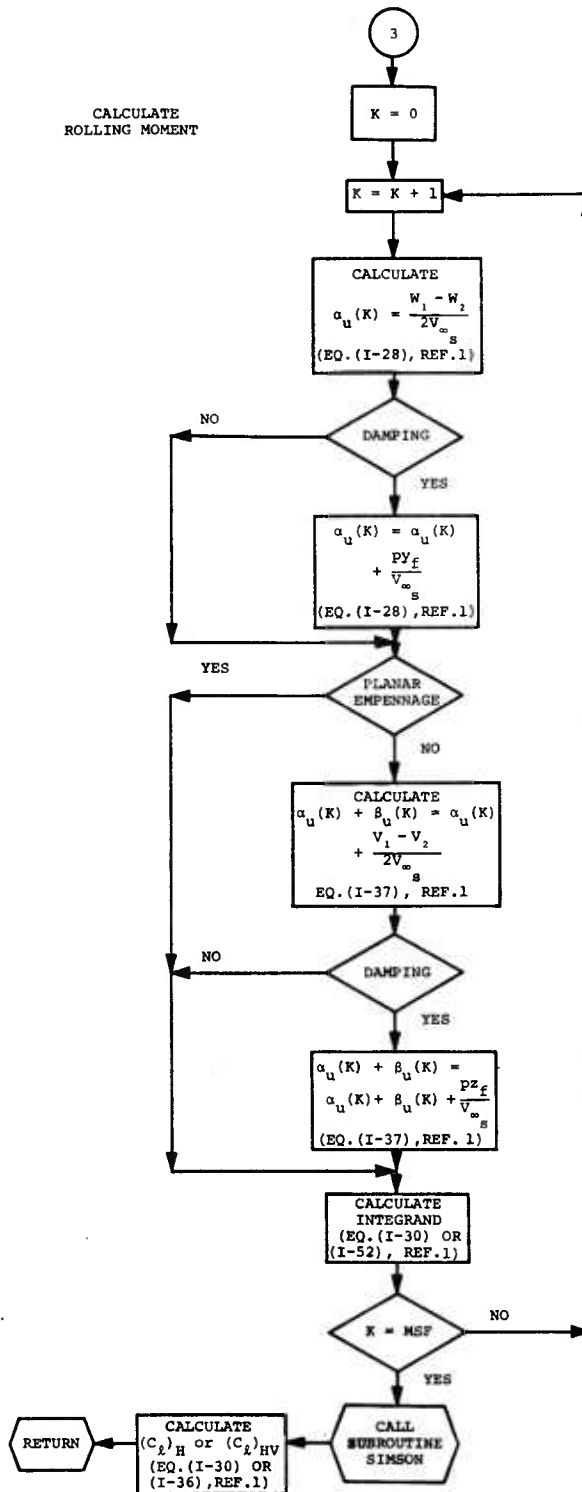
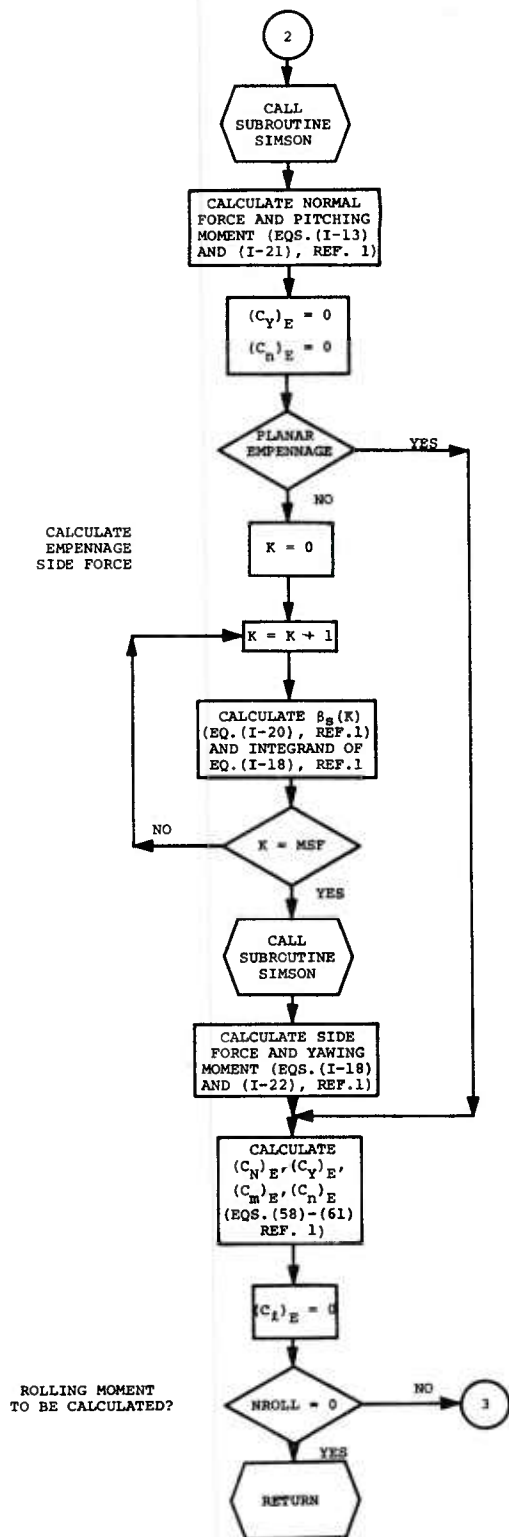
CALCULATE CROSSFLOW VELOCITIES

CALCULATE EMPENNAGE NORMAL FORCE



(a) Page 1.

Figure II-3.- Flow chart of subroutine EMPFOR.



(b) Page 2.

Figure II-3.- Concluded.

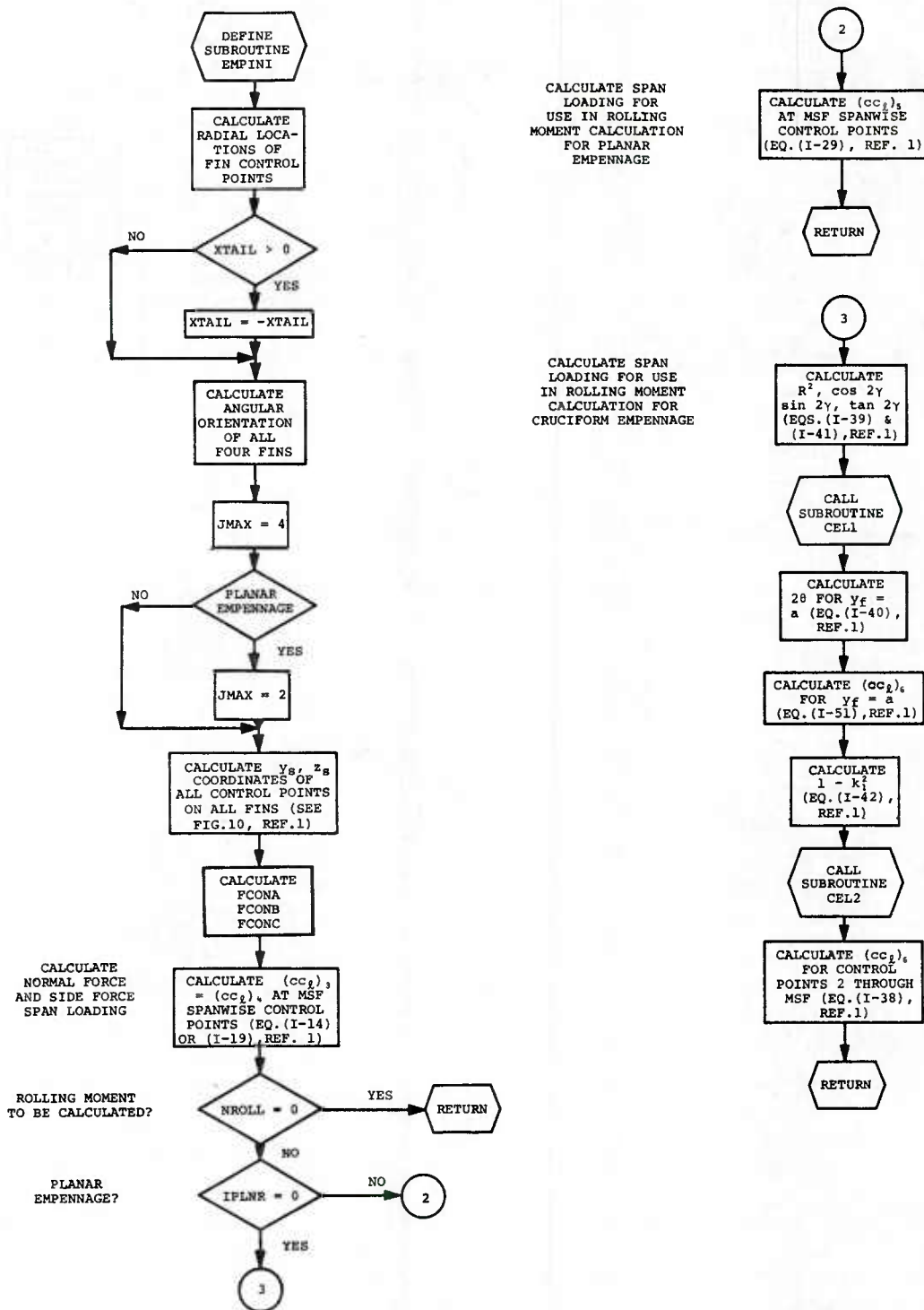
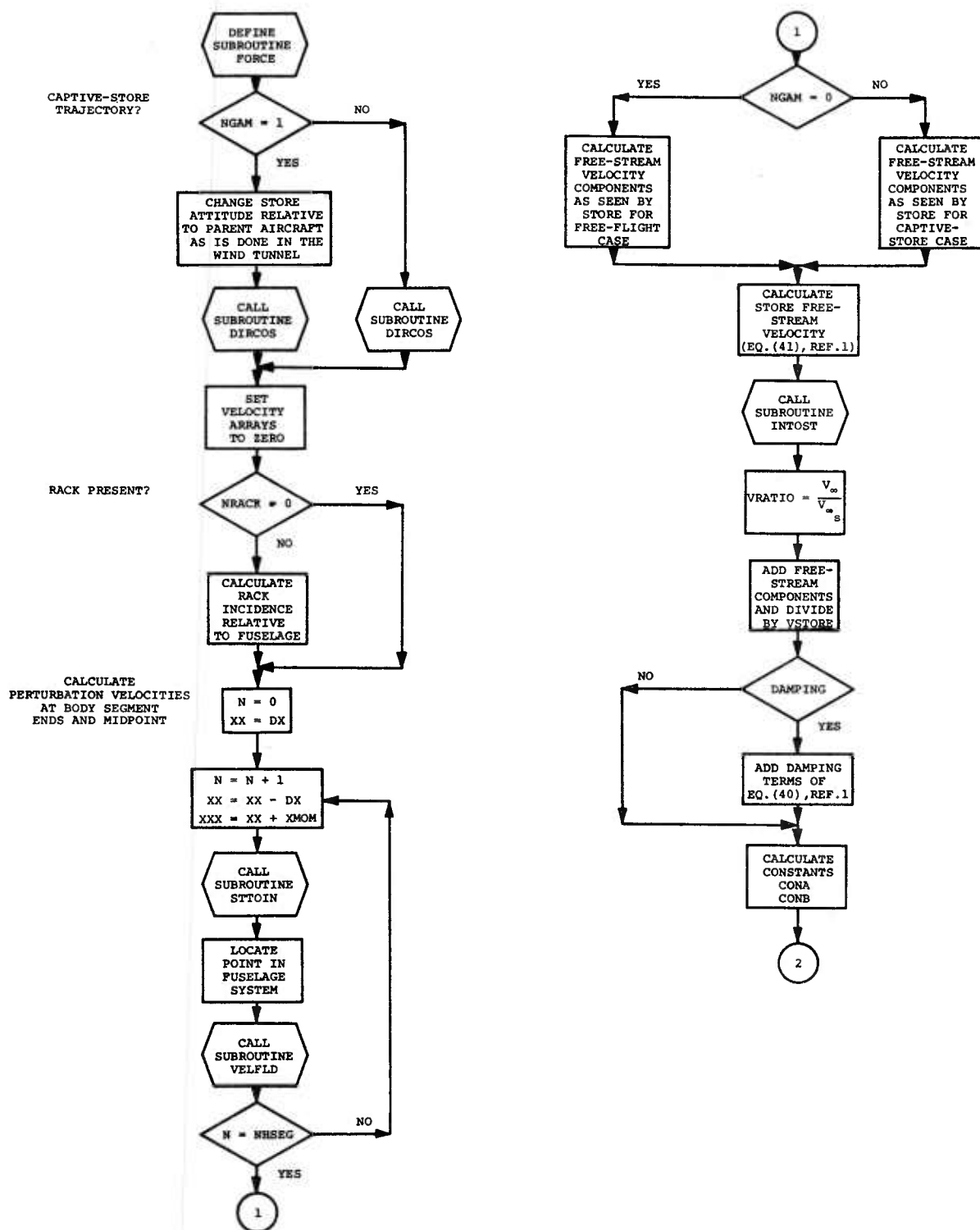


Figure II-4.- Flow chart of subroutine EMPINI.



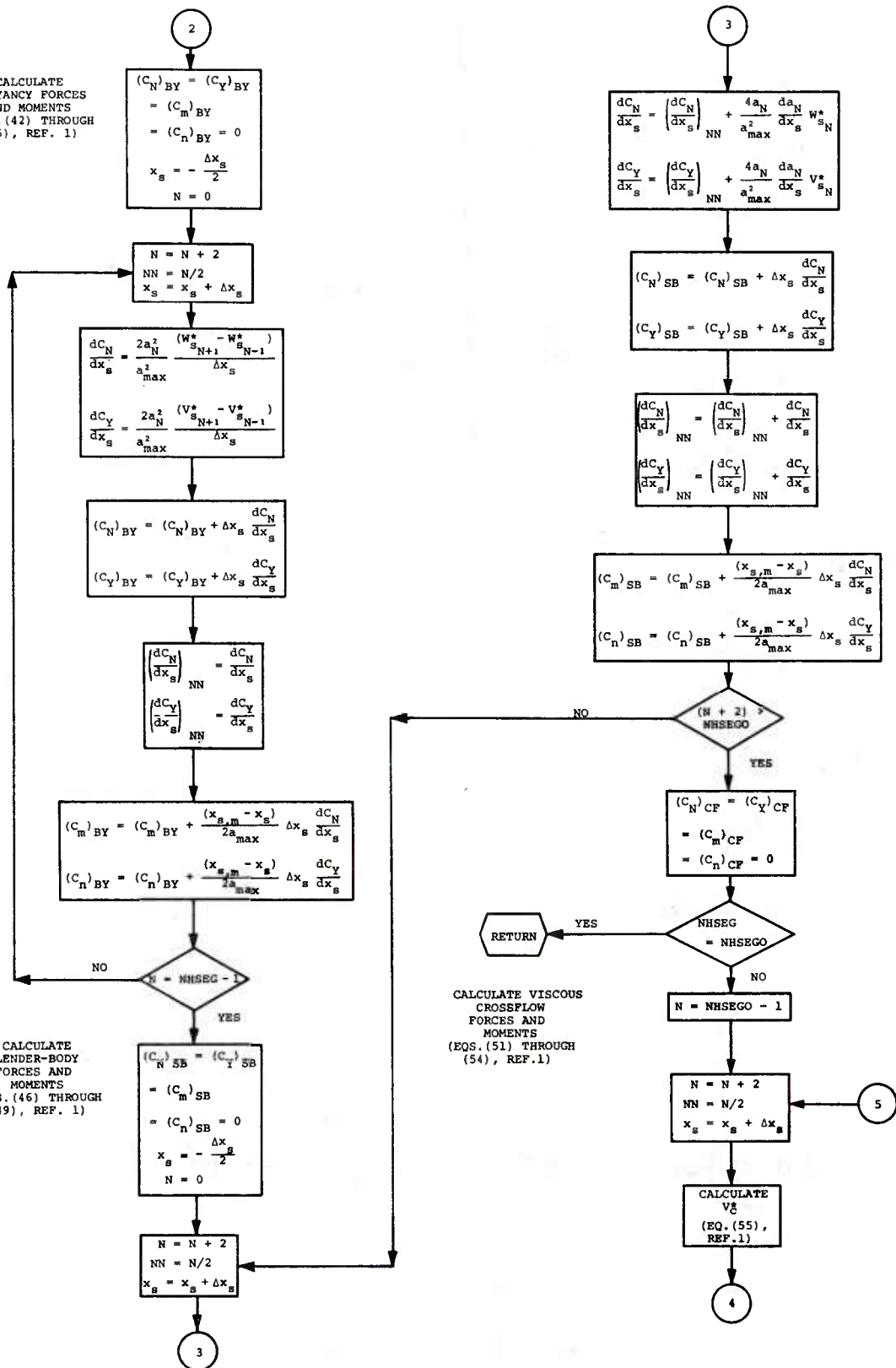
(a) Page 1.

Figure II-5.- Flow chart of subroutine FORCE.

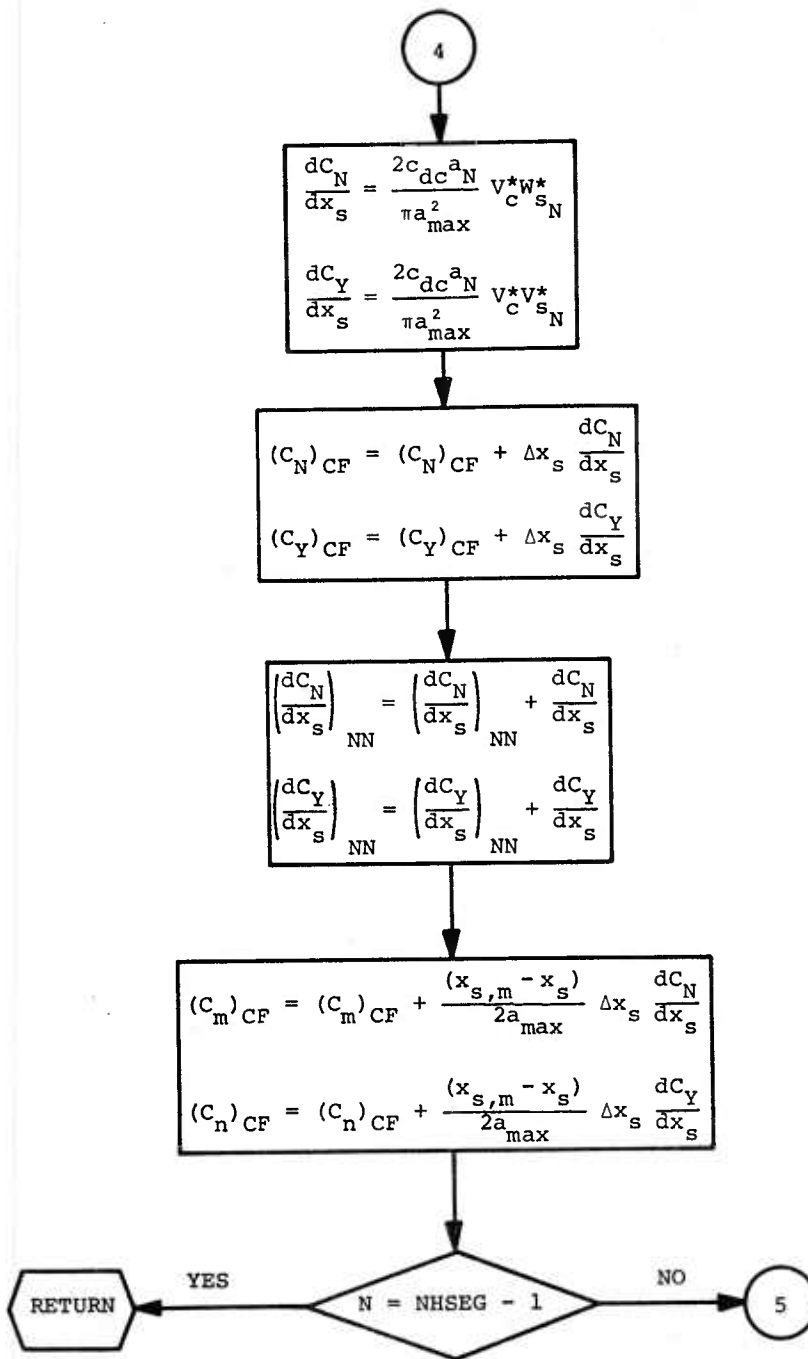
CALCULATE
BUOYANCY FORCES
AND MOMENTS
(EQS. (42) THROUGH
(45), REF. 1)

CALCULATE
SLENDER-BODY
FORCES AND
MOMENTS
(EQS. (46) THROUGH
(49), REF. 1)

CALCULATE VISCOUS
CROSSFLOW
FORCES AND
MOMENTS
(EQS. (51) THROUGH
(54), REF. 1)



(b) Page 2.
Figure II-5.- Continued.



(c) Page 3.

Figure II-5.- Concluded.

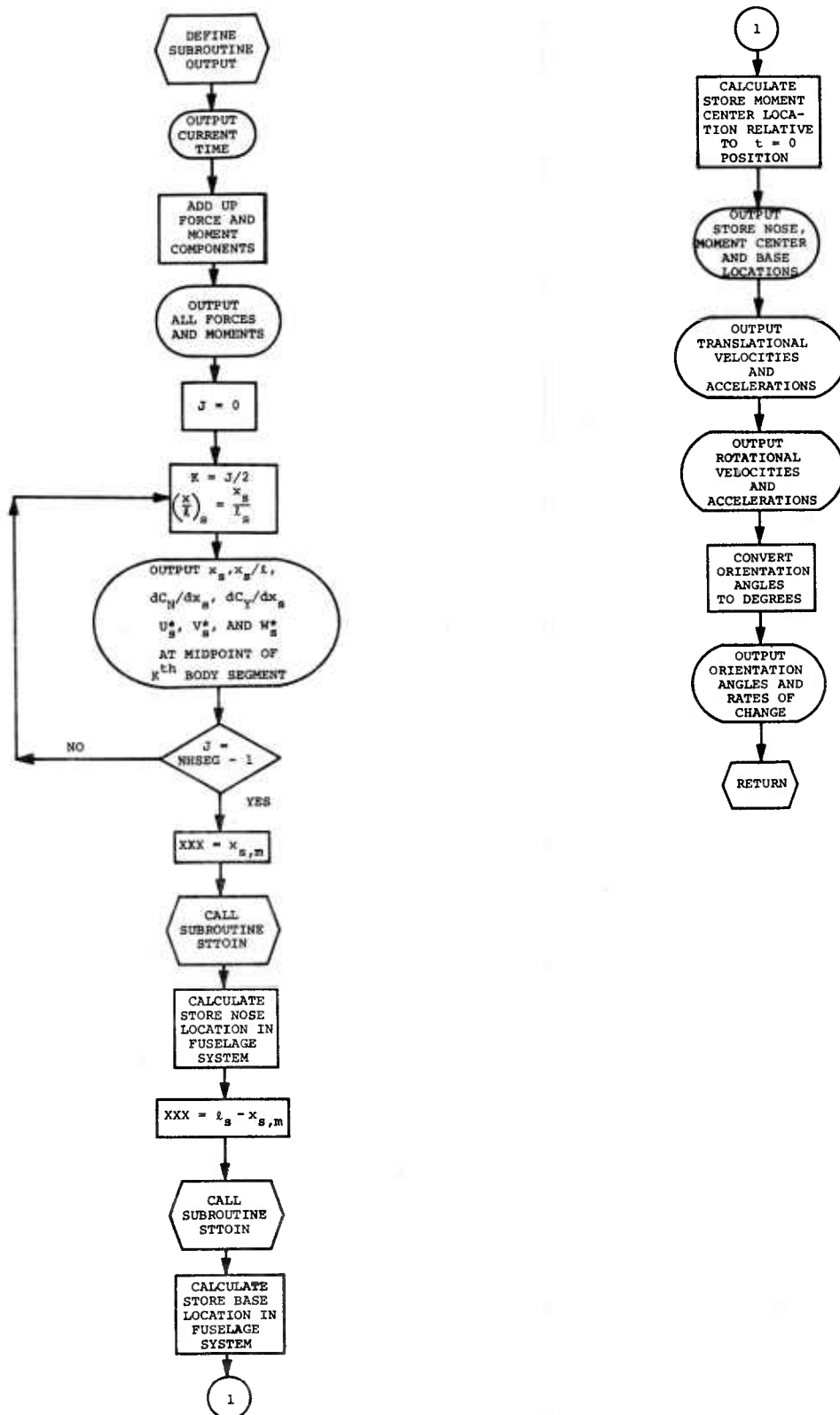


Figure II-6.- Flow chart of subroutine OUTPUT.

SIMILAR THICKNESS
DISTRIBUTION
FOR ALL
CHORDWISE
ROWS?

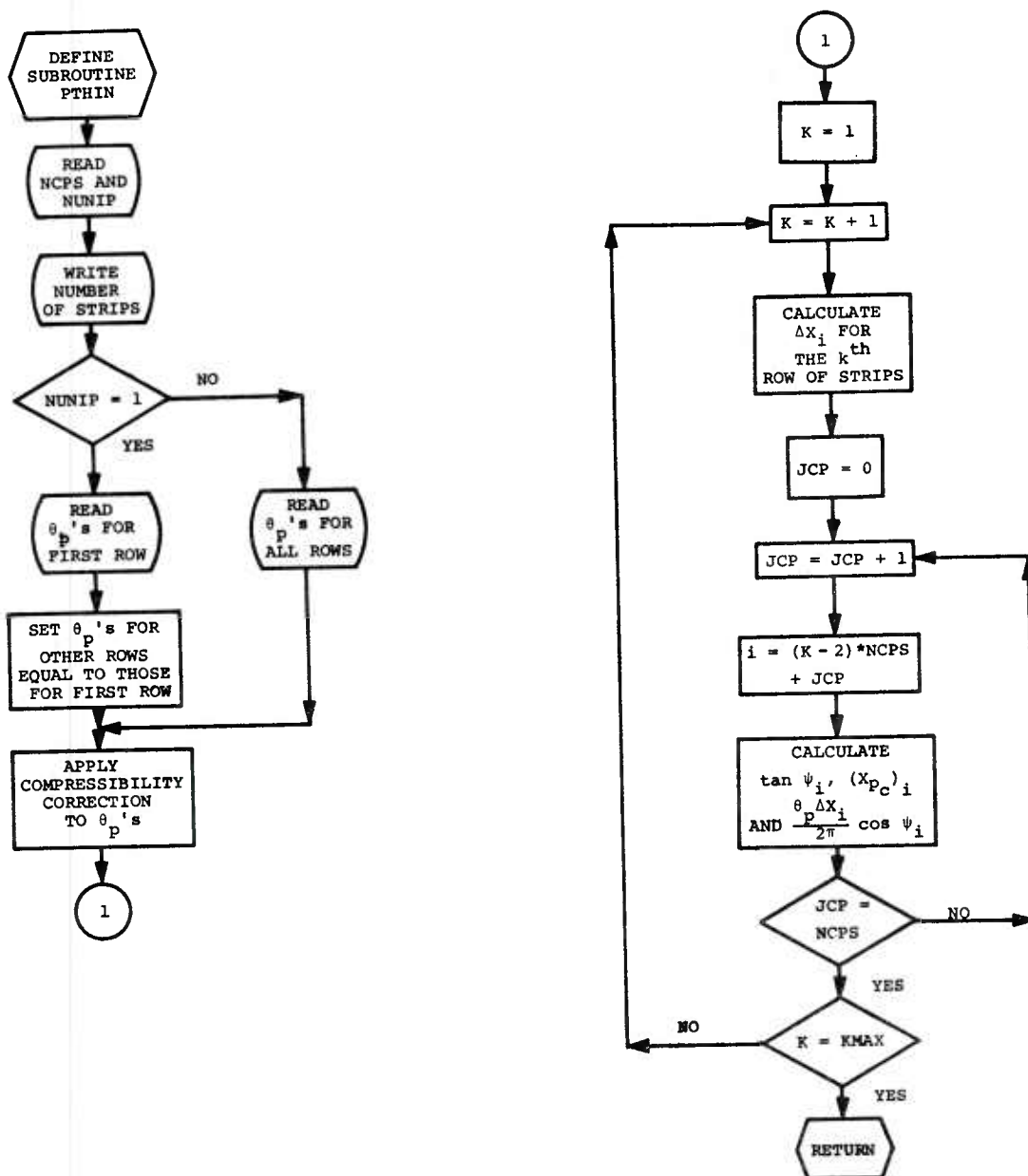


Figure II-7.- Flow chart of subroutine PTHIN.

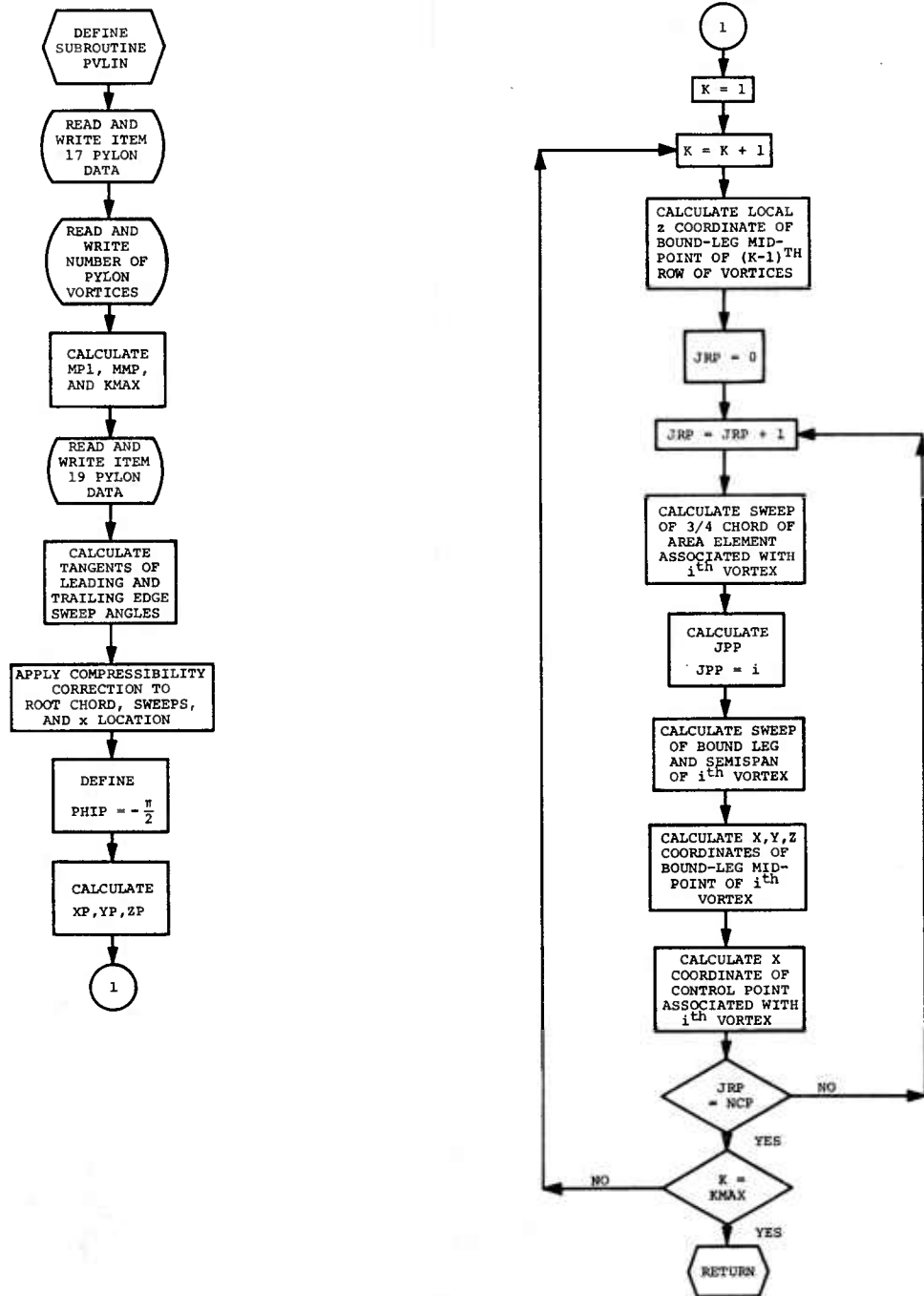


Figure II-8.- Flow chart of subroutine PVLIN.

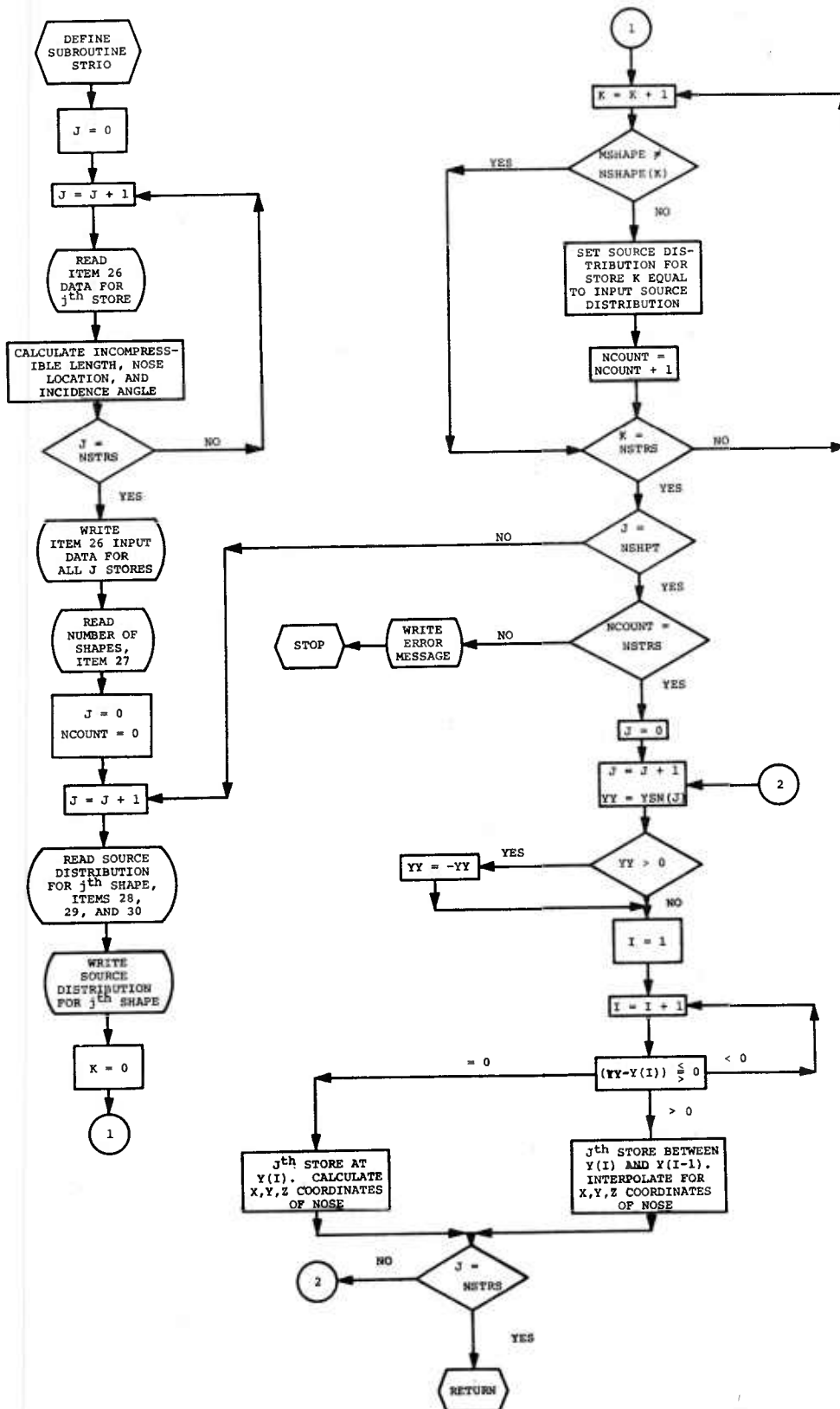


Figure II-9.- Flow chart of subroutine STRIO.

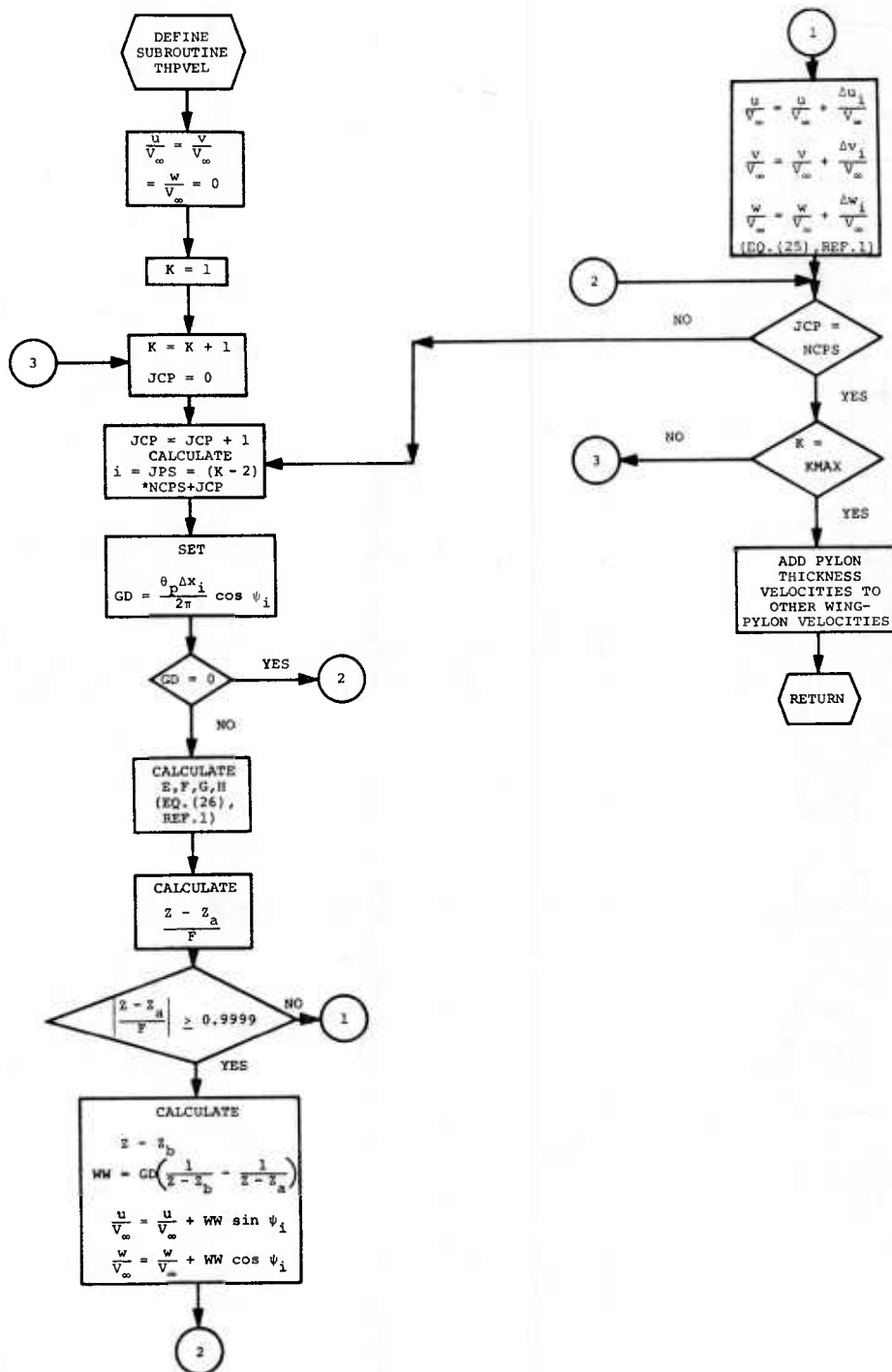


Figure II-10.- Flow chart of subroutine THPVEL.

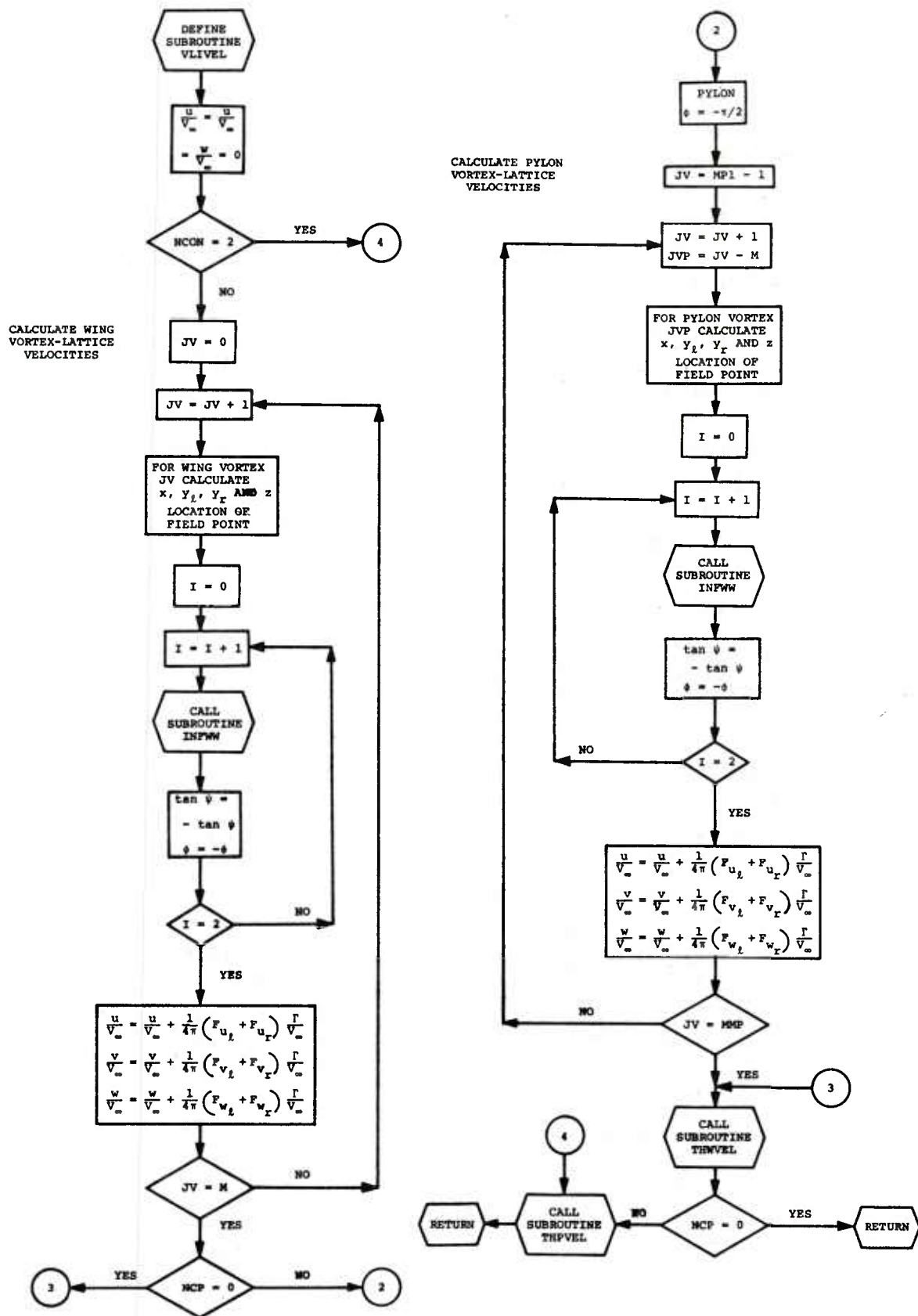
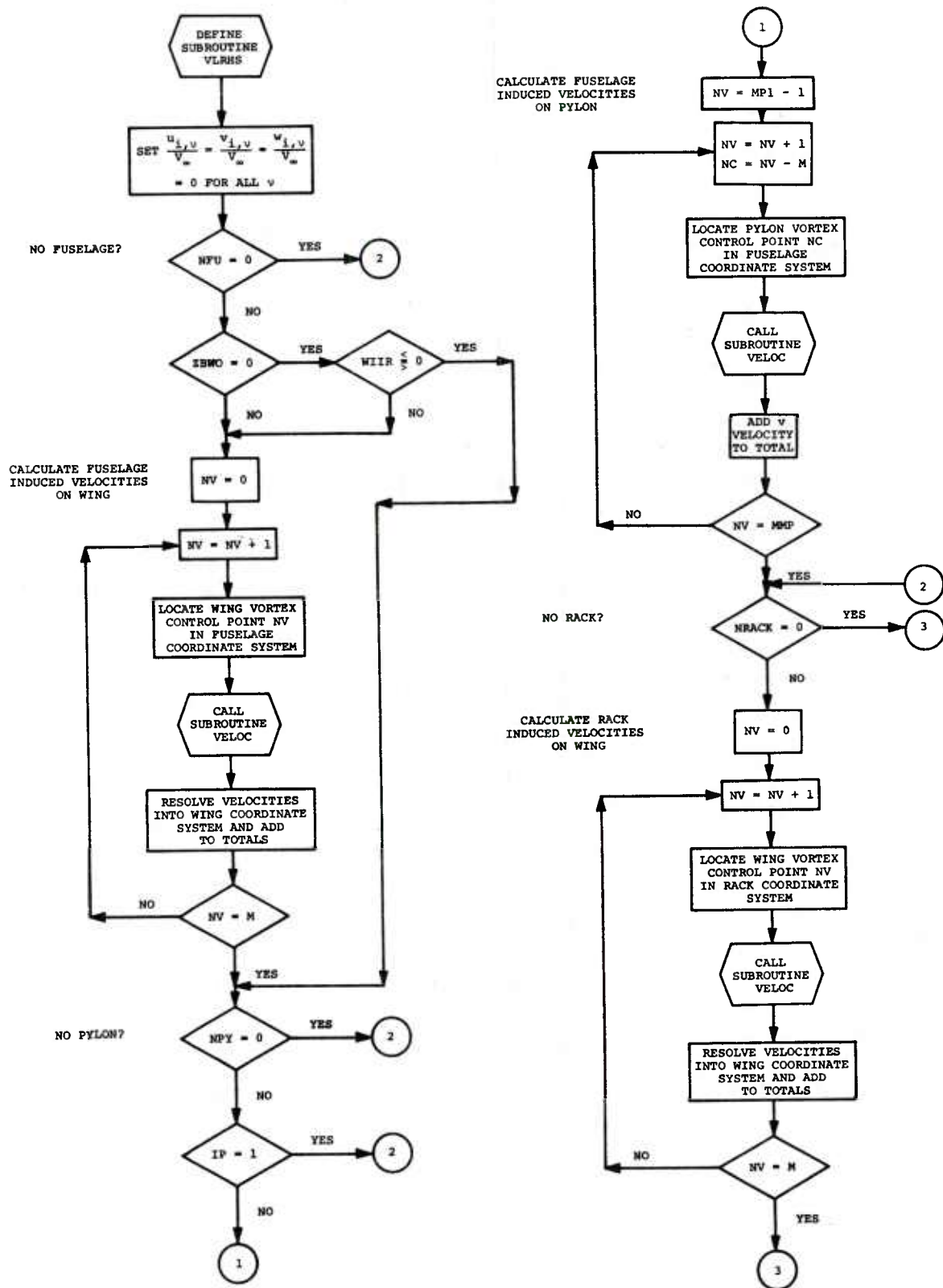
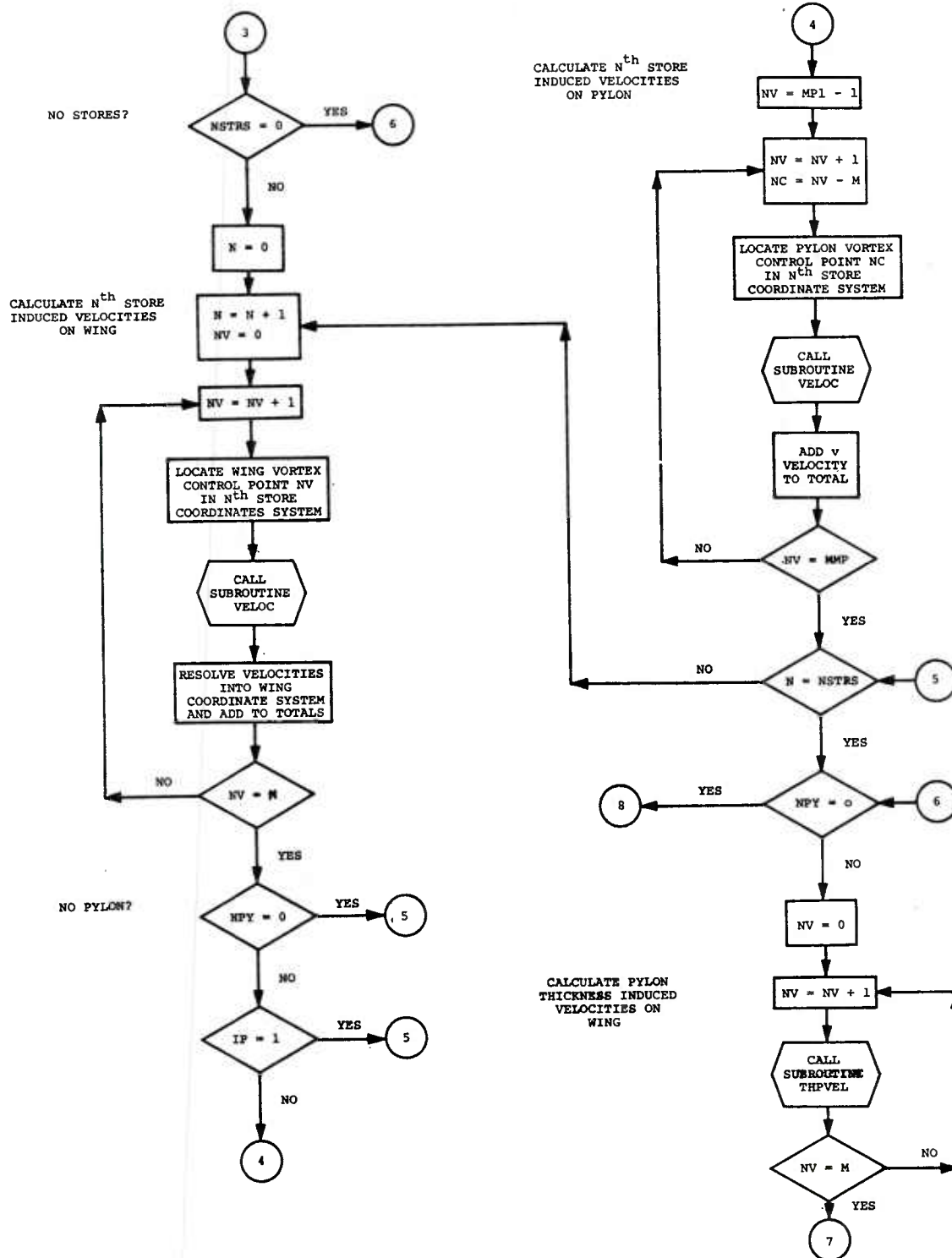


Figure II-15.- Flow chart of subroutine VLIVEL.



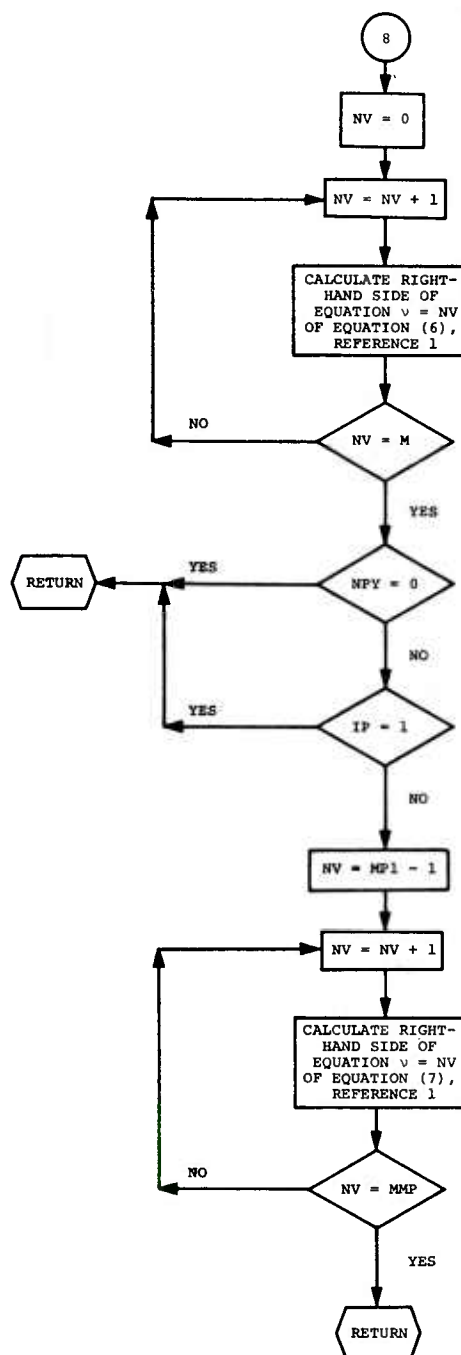
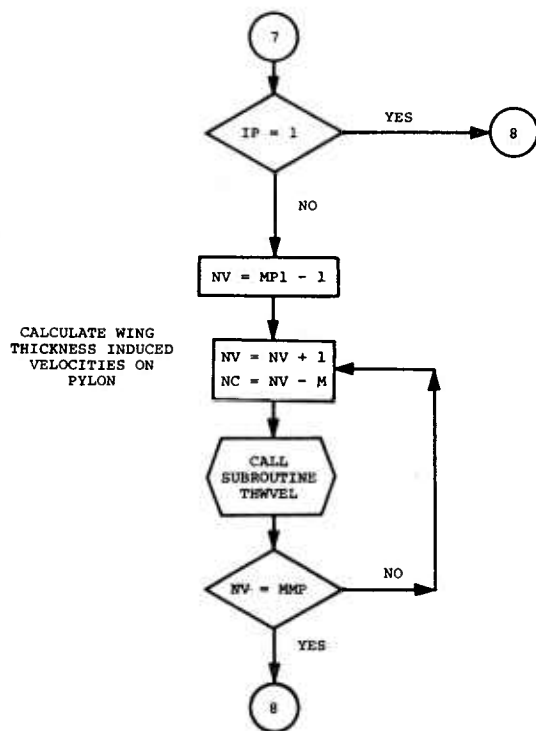
(a) Page 1.

Figure II-16.- Flow chart of subroutine VLHRS.



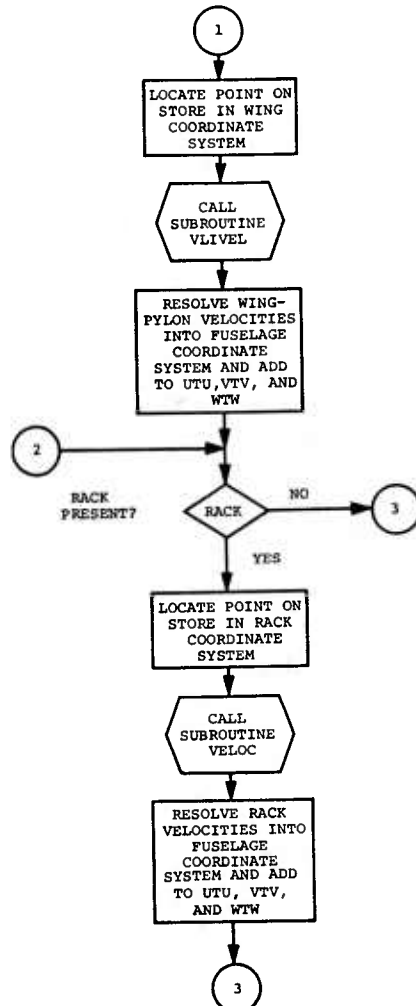
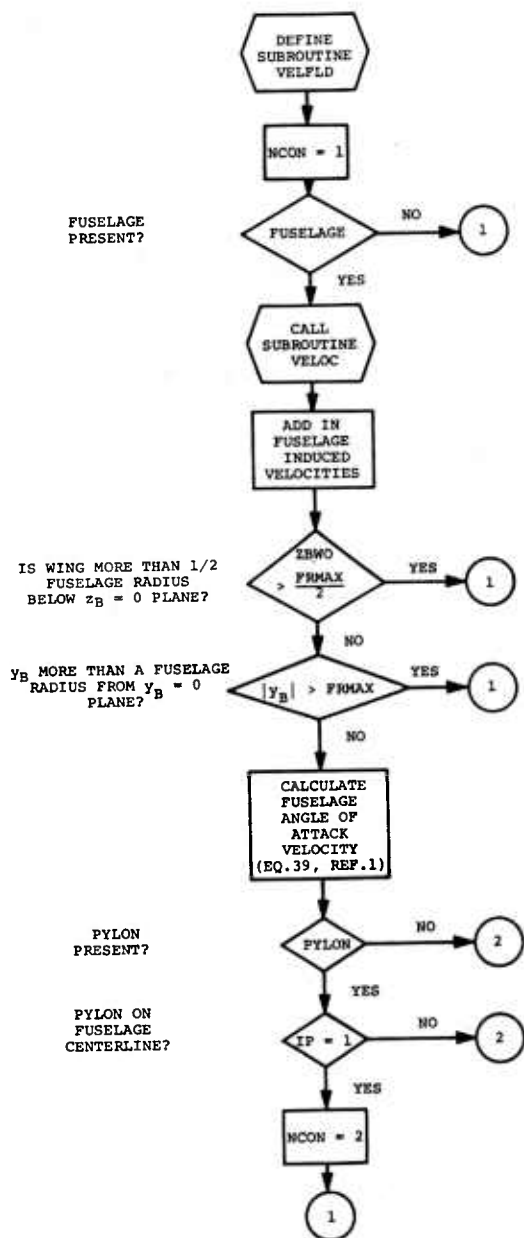
(b) Page 2.

Figure II-16.- Continued.



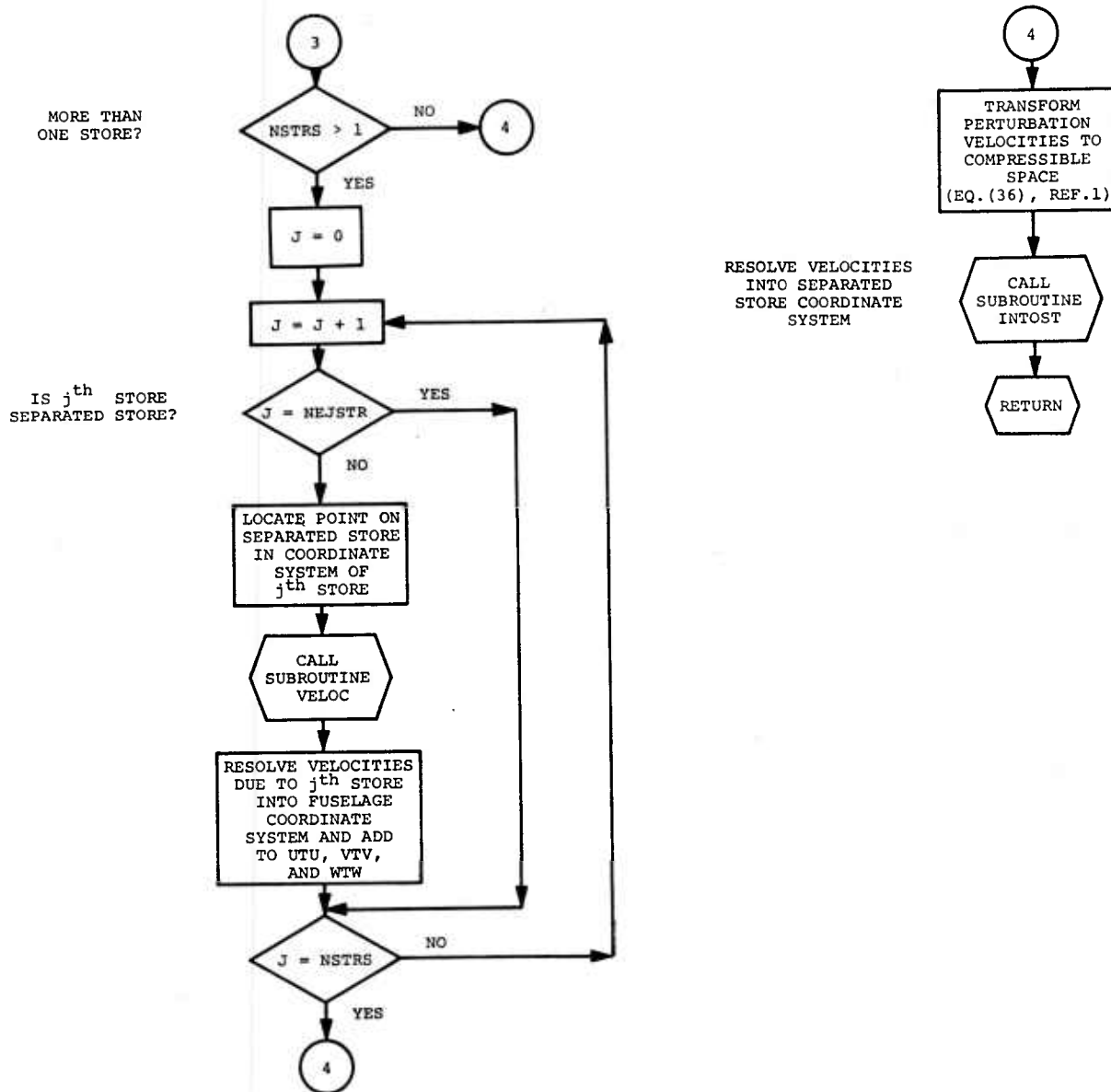
(c) Page 3.

Figure II-16.- Concluded.



(a) Page 1.

Figure II-12.- Flow chart of subroutine VELFLD.



(b) Page 2.

Figure II-12.- Concluded.

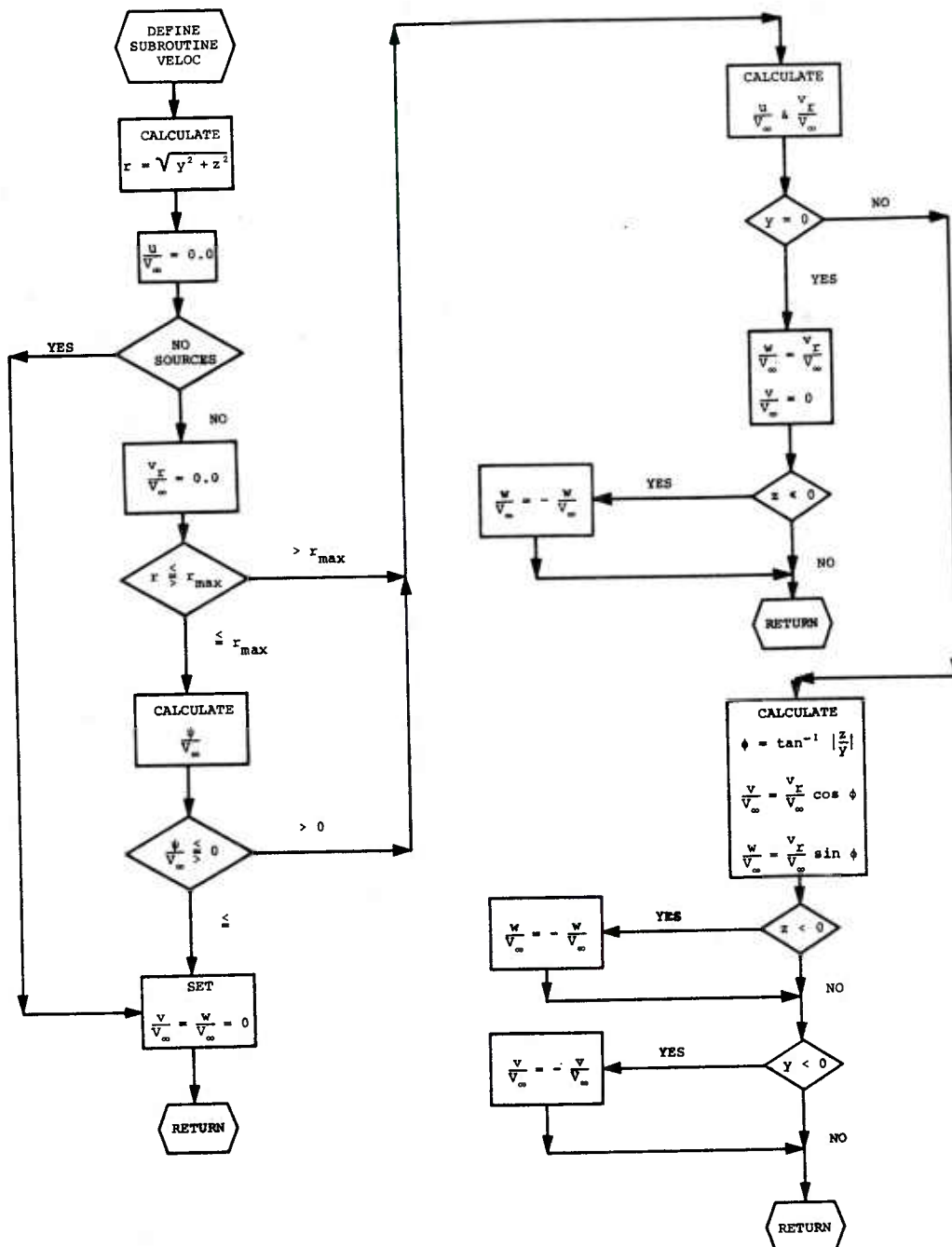
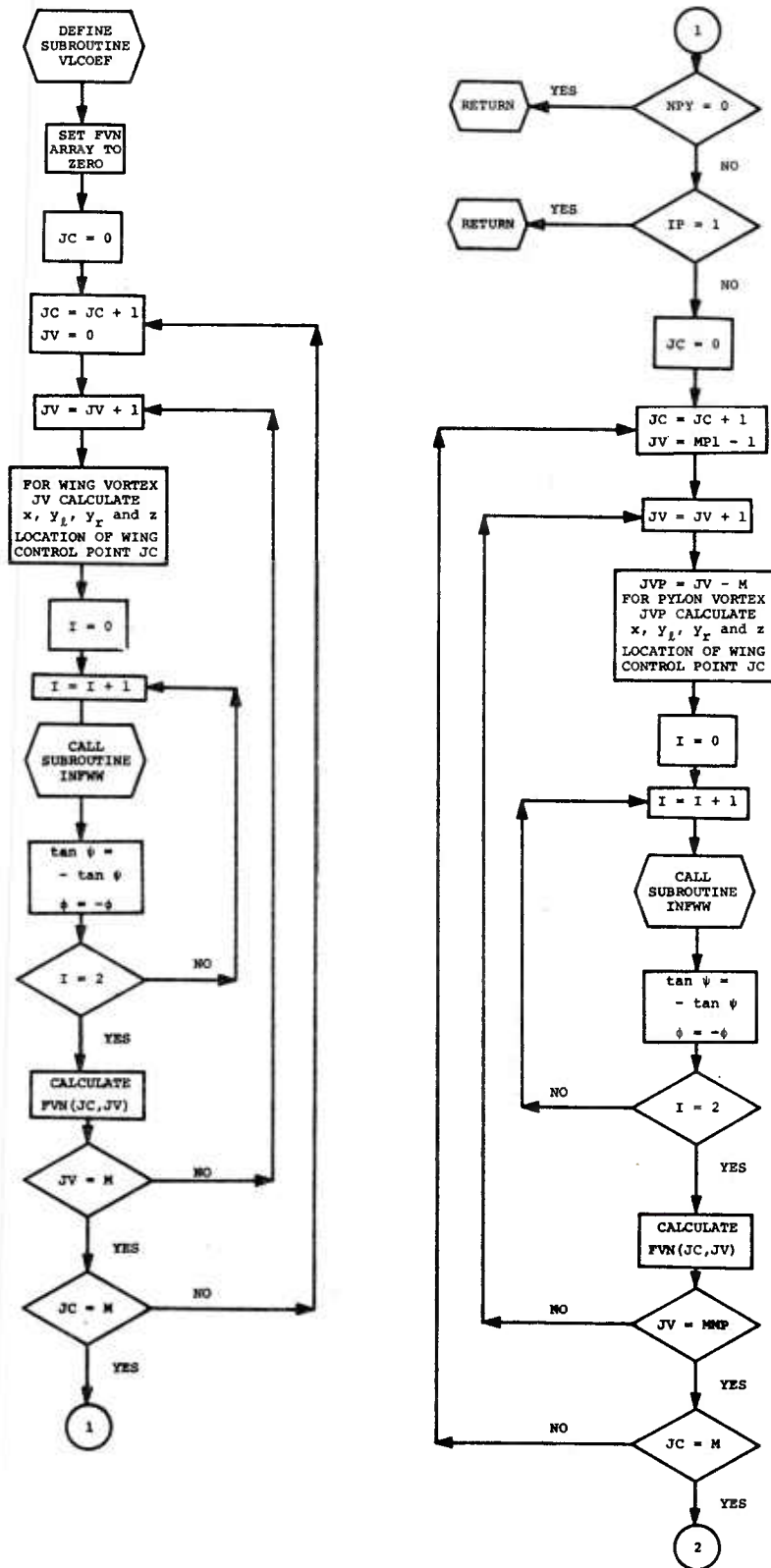
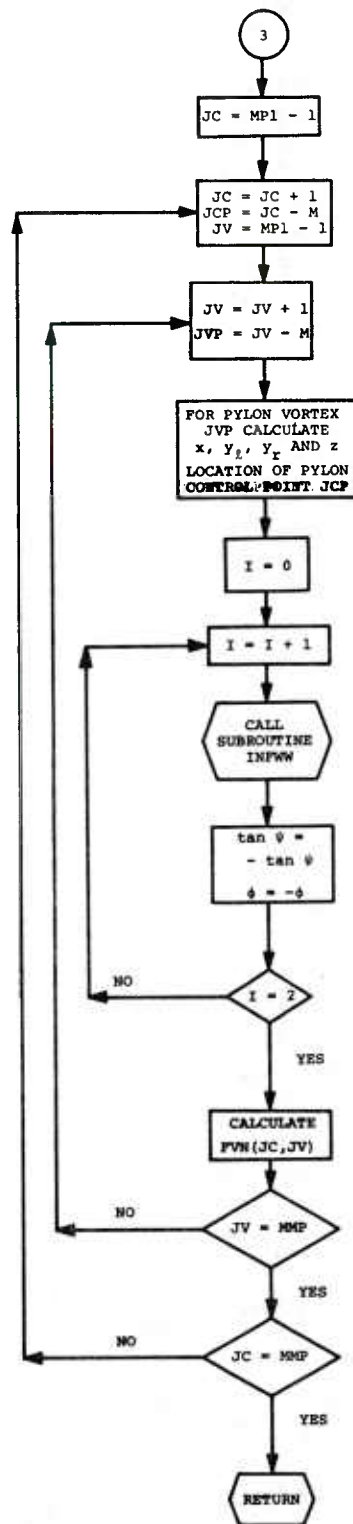
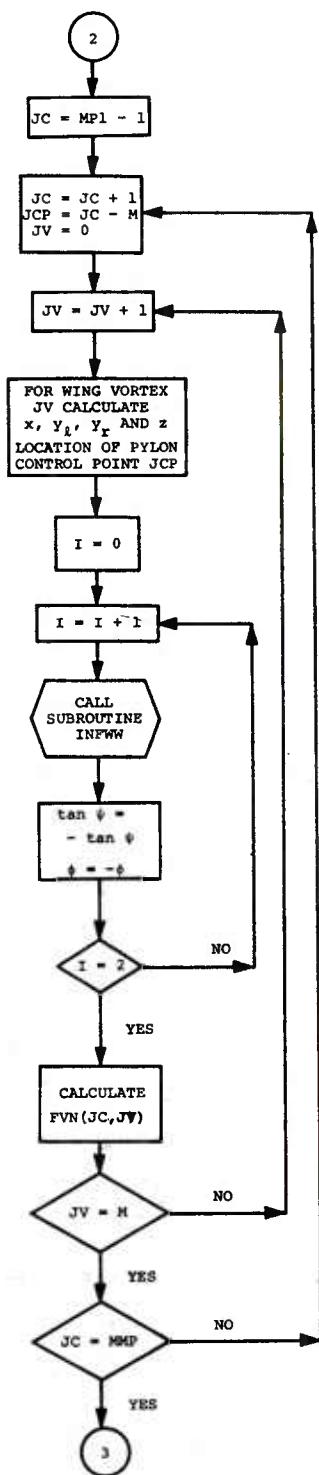


Figure II-13.- Flow chart of subroutine VELOC.



(a) Page 1.

Figure II-14.- Flow chart of subroutine VLCOEF.



(b) Page 2.

Figure II-14.- Concluded.

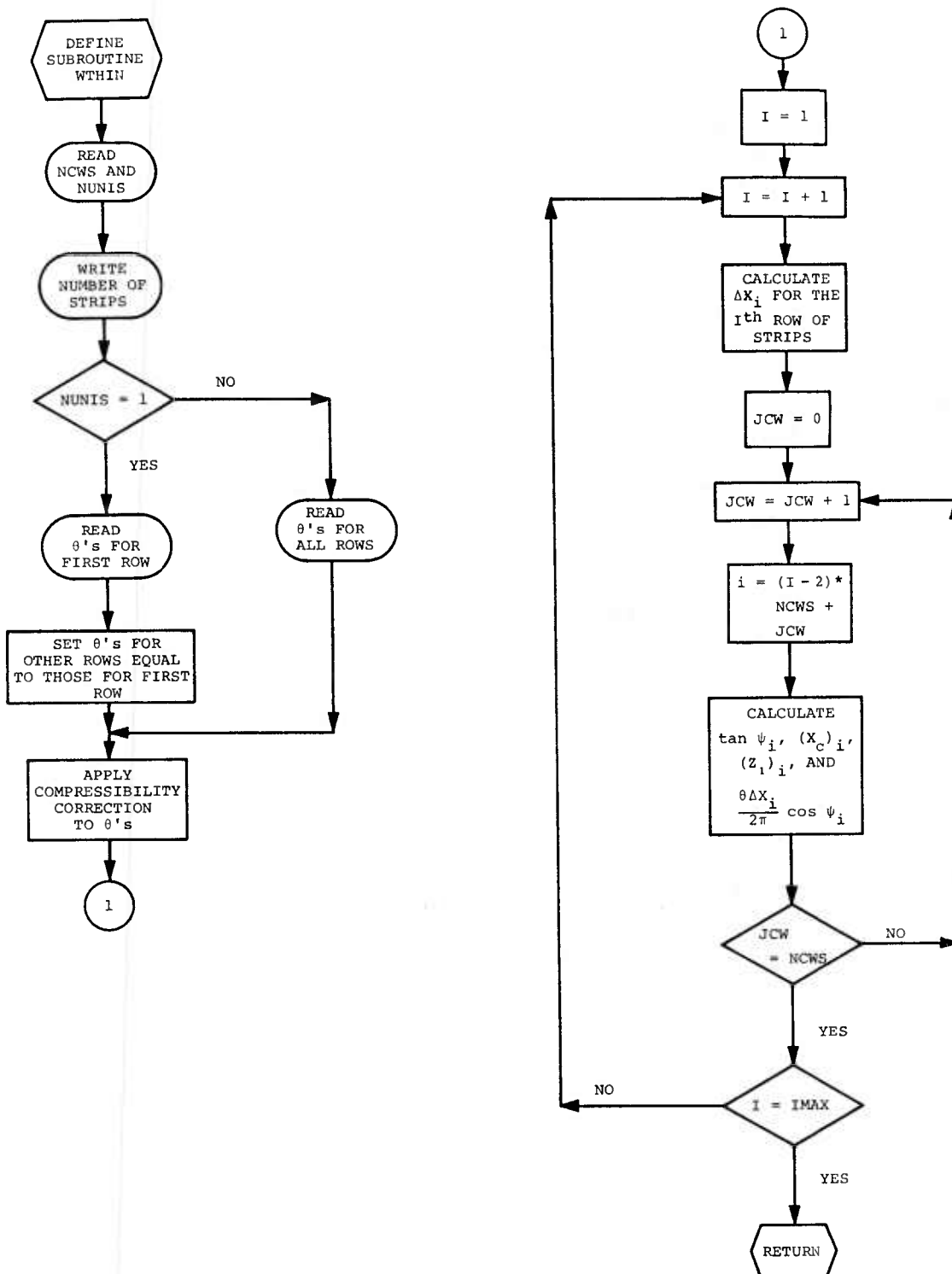
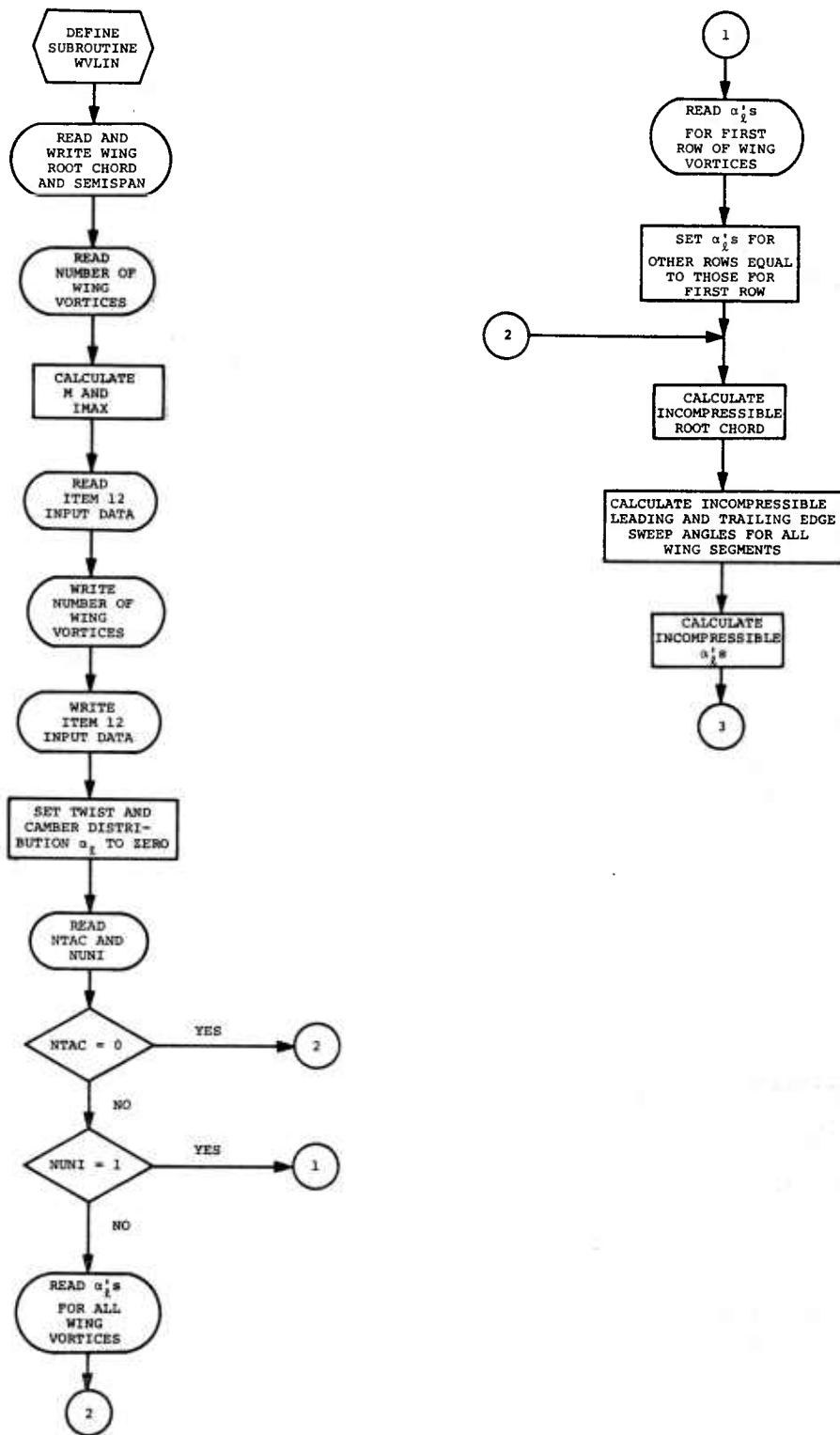
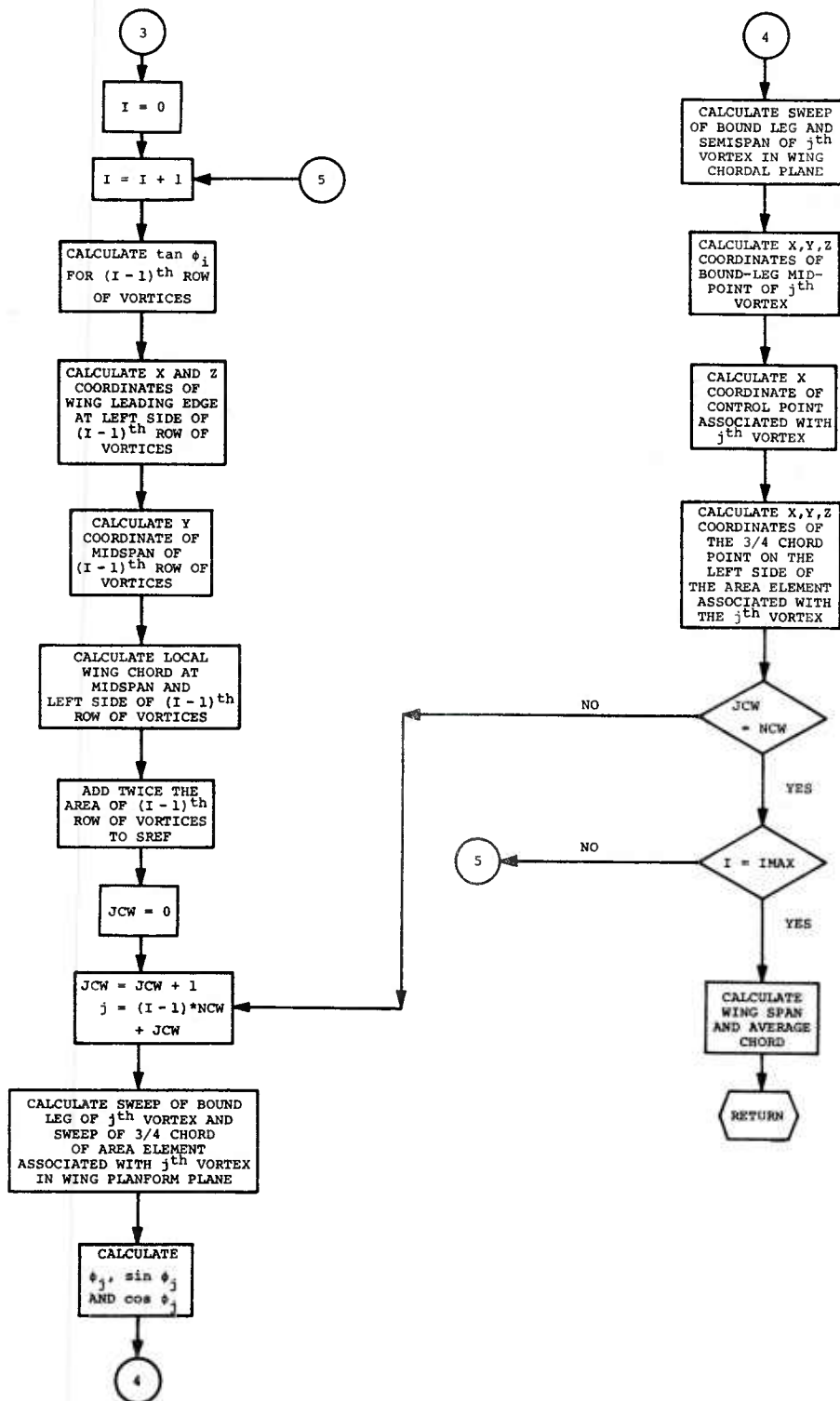


Figure II-17.- Flow chart of subroutine WTHIN.



(a) Page 1.

Figure II-18.- Flow chart of subroutine WVLIN.



(b) Page 2.

Figure II-18.- Concluded.

REFERENCES

1. Goodwin, F. K., Dillenius, M. F. E., and Nielsen, J. N.: Prediction of Six-Degree-of-Freedom Store Separation Trajectories at Speeds up to the Critical Speed. Vol. I.- Theoretical Methods and Comparisons with Experiment. Technical Report AFFDL-TR-72-83, Vol. I., 1972.
2. Goodwin, F. K., Nielsen, J. N., and Dillenius, M. F. E.: A Method for Predicting Three-Degree-of-Freedom Store Separation Trajectories at Speeds up to the Critical Speed. Technical Report AFFDL-TR-71-81, July 1971.
3. Hopkins, E. J.: A Semiempirical Method for Calculating the Pitching Moment of Bodies of Revolution at Low Mach Numbers. NACA RM A51C14, May 1951.
4. DeYoung, J. and Harper, C. W.: Theoretical Symmetric Span Loading at Subsonic Speeds for Wings Having Arbitrary Plan Form. NACA Report 921, 1948.
5. Conte, S. D.: Elementary Numerical Analysis. McGraw-Hill Book Co., Inc., New York, NY, 1965, pp. 174-176.
6. Hildebrand, F. B.: Introduction to Numerical Analysis. McGraw-Hill Book Co., Inc., New York, NY, 1956, Chapter 6.
7. IBM System/360 Scientific Subroutine Package, Version III, Programmers Manual. IBM Corp., GH20-0205-4, August 1970, pp. 372-381.
8. Scarborough, J. B.: Numerical Mathematical Analysis. John Hopkins Press, Baltimore, 1966, p. 137.

UNCLASSIFIED

Security Classification

DOCUMENT CONTROL DATA - R & D

(Security classification of title, body of abstract and indexing annotation must be entered when the overall report is classified)

1. ORIGINATING ACTIVITY (Corporate author) Nielsen Engineering & Research, Inc. 510 Clyde Avenue Mountain View, CA 94043		2a. REPORT SECURITY CLASSIFICATION Unclassified	
		2b. GROUP N/A	
3. REPORT TITLE PREDICTION OF SIX-DEGREE-OF-FREEDOM STORE SEPARATION TRAJECTORIES AT SPEEDS UP TO THE CRITICAL SPEED. Volume II - Users Manual for the Computer Programs			
4. DESCRIPTIVE NOTES (Type of report and inclusive dates) Final Technical Report - December 1970 to June 1972			
5. AUTHOR(S) (First name, middle initial, last name) Frederick K. Goodwin and Marnix F. E. Dillenius			
6. REPORT DATE October 1974		7a. TOTAL NO. OF PAGES 254	7b. NO. OF REFS 8
8a. CONTRACT OR GRANT NO. F33615-71-C-1116		9a. ORIGINATOR'S REPORT NUMBER(S) NEAR Report TR 41	
b. PROJECT NO. 8219		9b. OTHER REPORT NO(S) (Any other numbers that may be assigned this report) AFFDL-TR-72-83, Volume II	
c. Task No. 821902			
10. DISTRIBUTION STATEMENT Approved for public release; distribution unlimited			
11. SUPPLEMENTARY NOTES None		12. SPONSORING MILITARY ACTIVITY Air Force Flight Dynamics Lab. Wright-Patterson Air Force Base Ohio 45433	
13. ABSTRACT Detailed instructions are presented for using two computer programs which calculate the six-degree-of-freedom trajectories of external stores which are separated from fighter-bomber type aircraft at speeds up to the critical speed. Single and multiple store configurations can be handled by the programs. The first program calculates the source distributions which represent the volume distributions of the fuselage, store(s), and ejector rack if one is present. The second program uses a lifting surface theory to determine a vorticity distribution which represents the wing and pylon loading and calculates the trajectory of the ejected store. This report describes the two programs, presents instructions for preparing input for the programs, describes the output from each program, and presents sample cases.			

UNCLASSIFIED

Security Classification

14.	KEY WORDS	LINK A		LINK B		LINK C	
		ROLE	WT	ROLE	WT	ROLE	WT
	External stores Aerodynamic interference Subsonic flow Aerodynamic loads Flow fields Store separation						

UNCLASSIFIED

Security Classification